Simultaneous Delivery of FGF-2 and BMP-7 Enhances Bone Regeneration on Novel Biomimetic Scaffolds

by

Kunal Jethalal Rambhia

A dissertation submitted in partial fulfillment
of the requirements for the degree of
Doctor of Philosophy
(Biomedical Engineering)
in the University of Michigan
2019

Doctoral Committee

Professor Peter X. Ma, Chair
Professor Renny Franceschi
Professor William V. Giannobile
Associate Professor Kenneth Kozloff
Professor Yuji Mishina

Kunal Jethalal Rambhia

krambhia@umich.edu

ORCID iD: 0000-0003-0248-1437

© Kunal Jethalal Rambhia

2019

Dedication

This work is dedicated to the memory of
Ratanshi Shah and Meghbai & Lakamshi Rambhia.

This work is also dedicated to all the animals
that are used for biomedical research - the goats, cows, horses, donkeys, rabbits, mice, rats, dogs, and sheep, whose lives are used for the benefit of humans. I hope one day, there is a better way.
Michami Dukadam

Acknowledgements

Thank you to **Dr. Peter X. Ma** for your support and guidance over the past six years. You have allowed me to develop my scientific skills, pushed me into new areas of research, and supported me each step of the way. I am thankful to have had the opportunities to work to advance the field of bone tissue engineering under your leadership – and to develop skills in managing lab inventory, working with vendors for purchasing, training and mentoring new students, and writing grants and manuscripts.

I also would like to thank **Dr. Yuji Mishina, Dr. William V. Giannobile, Dr. Renny Franceschi, and Dr. Ken Kozloff**, who faithfully served as members of my dissertation committee. Your honest and thorough feedback has continually strengthened the quality of my work and I appreciate the time and effort you have given. In particular, my collaborations with Dr. Mishina over the past three years have been invaluable. I appreciate your patience and direct feedback as I learned to probe and understand molecular signaling pathways.

To all the members – past and present – of the Ma Lab, thank you for your continuous support as colleagues and collaborators. In particular, I was lucky to have been trained by **Zhongning Liu and Thomas W. Eyster**, who helped me early on to establish the technical skills I would need to complete my research. Thank you to my collaborators within the lab, **Yasmine Doleyres, Zhen Zhang**, and **Renato Navarro;** I would not have been able to be successful without your help, time, encouragement, and friendship. I have been fortunate to work with so many people of different backgrounds and disciplines in the Ma Lab, and I enjoyed getting to know you all. Thanks to **Melanie Gupte, Jeremy Holzwarth, Jun Wang, Ruonan**

Dong, Laura Saunders, Kelly Wang, Jiang Hu, Xiaobing Jin, Chao Zhao, Ganjun Feng, Ting Gong, and Raha Kannan.

One of the best and most rewarding aspects of my time at Michigan was being able to mentor fantastic undergraduate and graduate researchers. Thanks to **Mikayla Doepker, Tyler Powell, Gowri Viswanathan, JT Felix, and Yao Yao** for working with me and supporting this endeavor.

I would like to acknowledge and thank **Haichun Pan and Maiko Omi** for helping me to master the art of Western blotting and for providing all the calvarial osteoblasts we used in our signaling pathway experiments. I would also like to thank **Dr. Bo Yang and Dr. Jiao Jiao** for providing the human iPSC-MSCs that we used for this research. Thanks to **Michelle Lynch** of the MicroCT core, **Theresa Cody and Chris Strayhorn** of the UM School of Dentistry Histology Core, **Taocong Jin** of the Molecular Biology Core, **Bonne Nolan** at BSRB, **Erin Semmens** in the BMS office, and all of the delivery, janitorial and support staff at the School of Dentistry. I appreciate all of your help and hard work. I would also like to thank **Doug Noll** – it was a pleasure to work with you as your GSI and I learned a great deal about teaching and grading from you.

To the BME department, BME basketball group, BME Graduate Student Council, and in particular to Grad Coordinator **Maria Steele**, thank you! It has been fun to be a part of a dynamic and motivated group of people. Thanks to **Lonnie Shea, Tim Bruns, and Joan Greve**, for their support over the years. Thanks also to **Stewart Thornhill and Michael Johnson** at the UM Ross School of Business for their mentorship during my time as a member of the Zell Lurie Commercialization Fund, and to all the amazing members of this group. To my teammates at the

Ann Arbor Ice Cube and **Vet's Ice Arena**, especially the **Ice-o-Topes**, **Puckings**, **Warriors**, and **Twin Eagle Brewing**, thanks for letting me skate with you all!

To my friends and family, I appreciate you sticking with me through this journey and being a constant source of support and encouragement. Thanks especially to **Tom Schneider, Eric Lockhart, Nick Jimenez, Philip Taff, Howard Locker, Neha Kaushal, Sibu Kuruvilla, Biming Wu, Cameron Yamanishi, Sarah O'Connor, Adam Stinchcombe, Crystal Watson, Matt Watson, Gigi Gronvall, Amesh Adalja, Yuliya Seldina, and Leanna Foster**.

To my grandmother, **Maniben Shah**, thanks for being the moral compass of our family and teaching us to do right and to work hard. To my parents, **Alka and Jethalal Rambhia**, you have supported me unconditionally from day one and I am forever grateful for that. My brother, **Arun Rambhia**, thanks for always pushing me to be better and achieve more. To my second parents, **Rashmi and Bipin Turakhia**, my brother and sister-in-law **Jay and Jessica Turakhia**, you all have been a source of strength and positivity, and I am so thankful to have you as a part of my life. I'd be remiss if I didn't also thank **Princess**, my pit bull companion who greatly enriched my life in Michigan with her love and affection.

Last, and certainly not least, thanks to the love of my life, **Milly Rambhia**. You have supported me through thick and thin, and I am blessed to have you by my side. I am forever grateful for your fierce loyalty, sense of humor, spirit for adventure, friendship, kindness, and love. I truly would not have reached this point without you.

Funding Sources:

I would like to acknowledge the financial support I have received from the Rackham Merit Fellowship, Rackham Graduate Student Research Grant & Travel Grant, and the Ruth L. Kirschstein-NRSA T32 Predoctoral Training Grant from the Center for Organogenesis (NIH T32

HD007505). I also acknowledge additional support from NIH R01 DE022327, NIH R01 DE027662, NIH R01DE017689, NIH R01 DE015384, DOD W81XWH-12-2-0008, NSF DMR-1206575

Table of Contents

Dedication ii

Acknowledgements iii

List of Tables x

List of Figures xi

Abstract xiii

Chapter 1. Introduction and Thesis Outline 1

Chapter 2. Biomineralization and Bone Regeneration 4

2.1. Development and fracture of bone 4
2.1.1. Bone development 4
2.1.2. Fracture healing 5

2.2. Principles of bone tissue engineering 6

2.3. Stem cells in bone tissue engineering 7
2.3.1. Mesenchymal stem cells (MSCs) 7
2.3.2. Adipose derived stem cells (ADSCs) 8
2.3.3. Embryonic stem cells (ESCs) 8
2.3.4. Induced pluripotent stem cells (iPSCs) 9

2.4. Scaffolds for bone tissue engineering 10
2.4.1. Scaffolding design criteria 10
2.4.2. Porous and highly interconnected scaffolds 11
2.4.3. Nanofibrous scaffolds for bone tissue engineering 12
2.4.4. Composite materials for bone tissue engineering scaffolds 13
2.4.5. Injectable scaffolds 14
2.4.6. Surface modification and functionalization of scaffolds for bone regeneration 16
2.4.7. 3D Printed Scaffolds 17

2.5. Growth and differentiation factors in bone tissue engineering 17
2.5.1. Bone morphogenetic proteins (BMPs) 18
2.5.2. Alternative factors and their combinations 20

Chapter 3. Controlled Drug Release for Tissue Engineering 23

3.1. Introduction 23

3.2. Microspheres designed for controlled release 25

3.3. New hydrogel approaches that improve controlled release 26
3.3.1. Efforts to reduce the burst release effect in hydrogels 27
3.3.2. Composite hydrogel – microsphere delivery systems used to deliver multiple GFs 28

3.4. Porous scaffolds made of natural materials with controlled release capacity 30
3.4.1. Reducing burst release effect 30
3.4.2. Sustaining release for extended treatment time period 31
3.5. Synthetic polymer scaffolds allow for precise control of release kinetics 32
3.5.1. Polymer scaffolds and microspheres with nanofibrous architecture 34
3.5.2. Composite scaffold-microsphere delivery systems 35
3.6. Modifications to controlled release polymers 39
3.6.1. Heparin based delivery systems with natural scaffold materials 40
3.6.2. Other affinity-based controlled release systems 41
3.7. Other novel/unique approaches to controlled release 42
3.7.1. Multiphasic devices allow pulsatile or sequential delivery 42
3.7.2. Magnetic molecularly imprinted polymer controlled release systems 43
3.8. Areas of need for improving controlled release platforms 44
3.8.1. Sequential or simultaneous delivery of multiple drugs 44
3.9. Conclusion and perspectives 46
Chapter 4. Controlled Release of BMP-7 and FGF-2 from 3D PLLA Scaffolds Enhances Ectopic Osteogenesis in Mice 48
4.1. Introduction 48
4.1.1. Limitations of autologous bone grafts for treating critical size defects 48
4.1.2. Polymeric scaffolds combined with drug delivery systems have the potential to improve bone tissue engineering 48
4.1.3. FGF-2 is an attractive growth factor for bone tissue engineering applications 50
4.2. Materials and Methods: 51
4.2.1. Preparation of nanospheres immobilized on nanofibrous scaffolds and *in vitro* release study. 51
4.2.2. Cell isolation, expansion, migration, proliferation, and differentiation *in vitro*. 52
4.2.3. Subcutaneous implantation and specimen analysis. 54
4.2.4. RNA extraction and real-time PCR. 55
4.2.5. Statistical analysis. 56
4.3. Results 56
4.3.1. Effects of FGF-2 on BMSC proliferation and differentiation *in vitro* 56
4.3.2. Effects of FGF-2 on maturing BMSCs or mature primary osteoblasts 58
4.3.3. Dual-release of BMP-7 and FGF-2 on 3D PLLA nanofibrous scaffolds. 59
4.3.4. Stimulation of BMP-7-induced bone formation by controlled release of FGF-2. 60
4.3.5. Stem cell recruitment and angiogenesis regulated by FGF-2 during the early stage of endochondral ossification. 62
4.4. Discussion 64
4.5. Conclusion 67
Chapter 5. Dual Delivery of FGF-2 and BMP-7 from Nanofibrous Spongy Microspheres Platform Enhances Repair of Critical Size Bone Defect 77
5.1. Introduction 77
5.1.1. Scaffolds for bone tissue engineering 77
5.1.2. Simultaneous growth factor delivery 78
5.2. Materials and methods 80
5.2.1. NF-SMS fabrication 80
5.2.2. Smooth microsphere fabrication 80
5.2.3. Encapsulation of BMP-7 and FGF-2 and incorporation of PLGA-NS into NF-SMS 80

5.2.4. Cell Culture and osteogenic differentiation 81
5.2.5. 3D culture of hiPSCs on NF-SMS 82
5.2.6. Calcium quantification 82
5.2.7. Confocal Imaging 82
5.2.8. RNA extraction and RT-qPCR 83
5.2.9. Calvarial bone-defect repair model construction 84
5.2.10. Micro CT analysis 84
5.2.11. Histological analysis 84
5.2.12. Statistical Analyses 85

5.3 Results 85
5.3.1. Fabrication and characterization of NF-SMS 85
5.3.2. *In vitro* 2D evaluation of dose, length, and timing of FGF-2 85
5.3.3. Osteogenic gene expression by qRT-PCR analysis of RUNX2 87
5.3.4. Evaluation of nanofibrous spongy microsphere platform 87
5.3.5. *In vitro* osteogenic differentiation of hiPSC-MSCs on NF-SMS 89
5.3.6. Controlled release of FGF-2 and BMP-7 from PLGA nanospheres 90
5.3.7. *In vivo* repair of calvarial defects with NF-SMS and drug-loaded PLGA-NS 90
5.3.8. Radiographic analysis to screen for heterotopic or ectopic bone formation 91

5.4. Discussion 91

5.5. Conclusion 95

Chapter 6. FGF-2 enhances ACVR1 dependent canonical BMP signaling in mouse calvarial osteoblasts 104

6.1. Introduction 104
6.1.1. Canonical BMP signaling 104
6.1.2. Receptor and ligand specificity 105
6.1.3. FGF-2 expression during bone development 105
6.1.4. Crosstalk between BMP and FGF signaling pathways 106

6.2. Materials and Methods 107
6.2.1. Cell Isolation and Culture 107
6.2.2. Induction and inhibition of BMP and FGF signaling 108
6.2.3. Protein isolation and western blot analysis 108
6.2.4. Immunohistochemical analysis 109

6.3. Results 110
6.3.1. Activation of canonical BMP and FGF signaling in mouse osteoblasts 110
6.3.2. Pharmacologic suppression of BMP receptor activity 111
6.3.3. ACVR1 and BMPR1A receptor deficient cells 112
6.3.4. Inhibition of FGF receptor and ERK1/2 signaling results in corresponding reduction of p-Smad1/5/9 113
6.3.5. Non-canonical BMP signaling is unaffected by FGF-2 114
6.3.6. Increased LDN-19 concentration eliminates FGF-2 induced Smad phosphorylation 114
6.3.7. FGF-2 does not affect Smad1 synthesis or p-Smad degradation 116
6.3.8. BMP and FGF signaling overlap in BMSCs and Suture Cells 117

6.4. Discussion 117

6.5. Conclusion 120

Chapter 7. Conclusions 128

Chapter 8. Future Work 132

Appendix A. Diagrams of BMP and FGF signaling pathways 136

Bibliography 143

List of Tables

Table 2.1. Markers of Osteogenic Differentiation 21
Table 6.1. Antibody Concentrations 120
Table 6.2. Inhibitor Doses and Treatment Times 121

List of Figures

Figure 2.1. Nanofibrous scaffolds for bone tissue engineering 22
Figure 3.1: SEM images of solid walled (SW)-PLLA and NF-PLLA scaffolds. 33
Figure 3.2. Nanofibrous scaffolds with PDGF microspheres promote vasculogenesis *in vivo*. 36
Figure 3.3. Characterization of PLGA50–64K nanospheres (NS) and nanosphere incorporated PLLA nano-fibrous scaffolds (NS-scaffolds). 38
Figure 4.1. FGF-2 and BMP-7 regulation of rabbit BMSC proliferation and differentiation. 68
Figure 4.2. Effect of FGF-2 on maturing BMSCs or primary osteoblasts. 70
Figure 4.3. Dual-release of BMP-7 and FGF-2 on 3D PLLA nanofibrous scaffolds. 71
Figure 4.4. Ectopic bone regeneration controlled by dual-release of BMP-7 and FGF-2 on 3D PLLA nanofibrous scaffolds. 73
Figure 4.5. Stem cells recruitment and angiogenesis regulated by delivery of FGF-2 during the early stage of BMP-7-induced endochondral ossification. 76
Figure 5.1. Synthesis of nanofibrous spongy microspheres. 96
Figure 5.2. FGF-2 and BMP-7 regulation of hiPSC-MSC proliferation and differentiation. 97
Figure 5.3. Effect of FGF-2 on maturing hiPSC-MSCs. 98
Figure 5.4. FGF-2 and BMP-7 regulation of RUNX2 expression. 99
Figure 5.5. *In vitro* evaluation of NF-SMS compared with S-MS. 101
Figure 5.6. Combinatorial effect of FGF-2 and BMP-7 on *in vitro* differentiation of hiPSC-MSCs on NFSMS. 101
Figure 5.7. Controlled release of FGF-2 and BMP-7 and surgical implantation of NF-SMS in cranial defect. 102
Figure 5.8. µCT and histological characterization of calvarial defect repair after 8 weeks. 103
Figure 5.9. Radiological imaging of mouse carcasses for ectopic/heterotopic bone. 103
Figure 6.1. Activation of canonical BMP and FGF signaling by BMP-7 and FGF-2 122
Figure 6.2. Selective inhibition and conditional knockout of ACVR1 and BMPR1A receptor kinases 124
Figure 6.3. Selective inhibition of FGF receptor and MEK/ERK signaling 125
Figure 6.4. Evaluation of non-canonical BMP signaling pathway 126
Figure 6.5. Increased LDN-19 concentration inhibits Smad1/5/9 phosphorylation induced by FGF-2 126
Figure 6.6. Evaluation of FGF-2 effect on Smad1 degradation 127
Figure 6.7. Comparison of p-Smad1/5/9 and p-ERK1/2 in murine suture cells and BMSCs 127
Figure A.1. Overview of BMP and FGF signaling pathways. 136
Figure A.2. Selective inhibition of BMP receptor kinase activity. 137

Figure A.3. BMP ligand and receptor specificity. 138
Figure A.4. Induction of mutant BMPR1A or ACVR1 deficient phenotype by Tamoxifen activation of *Cre.* 138
Figure A.5. Pharmacological inhibition of FGF receptor kinase activity. 139
Figure A.6. Selective inhibition of p-ERK1/2 with pharmacological inhibitors. 140
..... 140
Figure A.7. Inhibition of non-canonical BMP signaling pathway. 140
Figure A.8. Common regulatory mechanisms of Smad-dependent signaling. 141
Figure A.9. Inhibition of translation and proteasomal degradation of Smad and p-Smad proteins. 141
Figure A.10. Possible mechanisms for p-ERK1/2 targeting of ACVR1. 142

Abstract

Every year, more than one million Americans experience nonhealing, large volume bone injuries caused by trauma, infection, surgical resection, or disease.[1,2] Current clinical treatment options include surgical fixation, bone grafting, and administration of osteogenic growth factors. However, there are drawbacks and inefficiencies to each of these methods. Surgical methods are invasive and increase risk of infection. Autografts result in donor site morbidity and are inherently limited in shape, size, and amount of bone available for transplant. Allografts and xenografts introduce a risk of immunogenic response or disease transmission.[3,4] The half-lives of osteogenic growth factors such as bone morphogenetic proteins (BMPs) are brief *in vivo,* and current therapies cannot support sustained delivery of growth factors over a sustained amount of time. Supraphysiological high dose treatments of growth factors are required to compensate for these limitations, which can have unwanted and potentially harmful side effects including nonspecific bone growth or tumor development. [5] Regeneration of bone through tissue engineering is therefore a desired solution to large volume bone defects.

We develop a biomimetic synthetic polymer scaffold and composite drug delivery system to enhance bone regeneration. In **Part 1**, we employ a 3D disc shaped PLLA scaffold and PLGA drug delivery system for the co-delivery of bone morphogenetic protein 7 (BMP-7) and basic fibroblast growth factor (FGF-2) for ectopic bone regeneration. We demonstrate that there is a

dose dependent increase in RUNX2 expression in BMSCs treated with FGF-2, and that 25ng/ml FGF-2 + BMP-7 increases RUNX2 expression nearly 2-fold compared with BMP-7 alone after 2 weeks of osteogenic induction. Induction of BMSCs with BMP-7 and 3 days of 25 ng/ml FGF-2 increased their calcium deposition by 2-fold compared with BMSCs induced with BMP-7 alone. Mineralization by BMSCs was diminished as the duration of FGF-2 was increased from 3 days to 14 days, from 6 mg/dl (3 days FGF-2) to less than 2 mg/dl (14 days FGF-2). Based on our *in vitro* assays, we developed a PLGA drug delivery system to encapsulate FGF-2 in low molecular weight PLGA nanoparticles to achieve ~75% release within the first 2 weeks. We encapsulated BMP-7 in high molecular weight PLGA nanoparticles to achieve long term release, with a diminished burst release of only ~20%. Compared with BMP-7 alone, we found that FGF-2 and BMP-7, released from PLGA nanoparticles conjugated to a NF-PLLA scaffold, produce an additive effect on ectopic bone formation in a subcutaneous mouse model, increasing calcium deposition in the 10ng/scaffold (slow release FGF-2) and 100ng/scaffold (fast release FGF-2) by 84% and 74%, respectively, after 6 weeks of *in vivo* implantation. New bone volume in the 10ng/scaffold (slow release FGF-2) group was increased by 2.5-fold compared with BMP-7 alone. Expression of pro-angiogenic factors was increased by 2-fold (CD146), 10-fold (VWF), and by 50% (CD31) in groups treated with FGF-2 + BMP-7 compared with controls, emphasizing the importance of FGF-2 directed angiogenesis during bone formation.

In **Part 2,** we employ injectable nanofibrous spongy microspheres (NF-SMS) and combine them with our PLGA drug delivery system for BMP-7 and FGF-2 to repair a critical size calvarial bone defect in mice. We observed that 2ng/ml of FGF-2 for 3 days does not significantly enhance or reduce mineralization of human iPSC-MSCs after 2 weeks or 4 weeks in monolayer culture. Increasing the duration of FGF-2 treatment to 28 days reduced calcium

deposition by ~25%. No significant differences in mineralization were observed when FGF-2 treatment was delayed by 2 weeks during BMP-7 induced osteogenic differentiation. RUNX2 expression was enhanced by ~25% in human iPSC-MSCs treated with FGF-2 for 3 days in combination with BMP-7, when compared to BMP-7 treatment alone. Extending FGF-2 treatment to 9 days produced a synergistic increase in RUNX2 expression, increasing over 3-fold compared with BMP-7 alone. When iPSC-MSCs were seeded onto NF-SMS *in vitro* and induced with BMP-7 and/or FGF-2 in 3D spinner culture, we observed that a 3 day treatment with FGF-2 combined with BMP-7 increased mineralization and expression of RUNX2 by more than 2-fold. Osteocalcin gene expression was also increased by ~20%. We therefore constructed a PLGA drug delivery system similar to system used in Part 1, using low molecular weight PLGA to encapsulate 10ng or 100ng of FGF-2, and high molecular weight PLGA to encapsulate BMP-7 and the resulting nanoparticles were conjugated to NF-SMS and applied to a cranial defect in mice. We observed increased new bone volume in groups treated with low dose (10ng/defect) FGF-2 and BMP-7 (3.5 mm^3), compared with BMP-7 alone (2.7 mm^3).

In **Part 3**, we explore crosstalk between BMP and FGF signaling pathways in mouse calvarial osteoblasts to improve our understanding of the regulatory mechanisms for these pathways. At baseline, FGF-2 increases BMP-7 induced Smad1/5/9 phosphorylation by 20% compared with BMP-7 alone, while no additive effect was observed when osteoblasts were treated with FGF-2 and BMP-2 or BMP-4. In cells pre-treated with LDN-193189, all BMP-7 induced Smad1/5/9 phosphorylation was inhibited, while abundant p-Smad1/5/9 was observed in cells induced with both BMP-7 and FGF-2. We found that Activin A receptor, type I (ACVR1) deficient cells were incapable of BMP-7 induced Smad1/5/9 phosphorylation, whether or not FGF-2 was present, emphasizing the importance of the receptor's kinase activity. When FGFR

activity was inhibited by SU5402, there was a corresponding 70% decrease in Smad1/5/9 phosphorylation when cells were treated with FGF-2 and BMP-7. Inhibition of ERK signaling pathway with PD184352 and U0126 decreased Smad1/5/9 phosphorylation by approximately 70% and 30%, respectively, suggesting the importance of ERK signaling in BMP and FGF signaling crosstalk. We further observed a complete elimination of Smad1/5/9 phosphorylation as LDN-193189 dose was increased from 100nM to 3000nM. Based on this finding we propose a competitive relationship between p-ERK1/2 and LDN-193189 and further propose that p-ERK1/2 targets ACVR1 as a substrate, and thus activating its Smad phosphorylation activity.

This thesis provides insights into the utility of simultaneous drug delivery for tissue regeneration and its potential for clinical translation to improve treatment of large volume bone defects.

Chapter 1. Introduction and Thesis Outline

The purpose of this dissertation is to advance the development of a drug-loaded polymeric scaffold for bone tissue engineering as a promising synthetic substitute for autologous bone grafts. While still considered the reference standard for treatment of large volume bone injuries, autologous grafts are limited in their clinical applications by donor site morbidity, limited tissue availability, and potential for graft failure.[6,7] The clinical use of bone morphogenetic proteins (BMP) as bone graft substitutes has resulted in serious adverse effects due in part to the supraphysiologic dose of BMP required for adequate healing.[8] New approaches to treating these large volume injuries are needed. Our proposed strategy utilizes tissue engineering and drug delivery concepts to develop synthetic drug-loaded biomimetic scaffolds for bone regeneration.

Chapter 2 introduces the basic biological processes that govern bone formation during normal development and compare those with the biological processes activated during fracture healing. We describe the principles of bone tissue engineering, along with the cell types, scaffolds, and growth factors used in various tissue engineering platforms. This chapter is adapted from the publication: Rambhia KJ, Ma PX. Biomineralization and Bone Regeneration. In: Atala A, Lanza R, Mikos AG, Nerem R, editors. Princ. Regen. Med. 3rd ed. Academic Press; 2018. p. 853–66.

In **Chapter 3**, we review the literature pertaining to the use of controlled release drug delivery systems for bone tissue engineering. We describe the use of microspheres and hydrogels made from synthetic or natural polymers for drug delivery. We discuss efforts to reduce burst release, the use of composite scaffolds, and the controlled release of multiple factors to enhance tissue regeneration. This chapter is adapted from the publication: Rambhia KJ, Ma PX. Controlled drug release for tissue engineering. *J. Control. Release*. 2015 Aug;219:119–28.

Chapter 4 describes on our efforts to enhance the osteogenic potential of synthetic poly(l-lactic acid) (PLLA) scaffolds by simultaneously delivering two growth factors: recombinant human BMP-7 and recombinant human basic fibroblast growth factor (rhFGF-2). We first established an *in vitro* cell culture model using rabbit mesenchymal stem cells to evaluate and optimize the dose and duration of FGF-2 treatment in combination with BMP-7 as a basis for our *in vivo* studies. We subsequently encapsulated the growth factors in poly (lactic-co-glycolic acid) (PLGA) nanospheres with tailored release patterns for each factor. Low molecular weight PLGA was used to encapsulate FGF-2 in fast releasing nanospheres while high molecular weight PLGA was used to encapsulate BMP-7 in slow releasing nanospheres. After seeding drug-loaded nanospheres onto PLLA scaffolds and implanting them in a subcutaneous mouse model, we found that FGF-2 augmented BMP-7 stimulated ectopic bone formation, and that their combined effect observed was dependent on the dose and duration of FGF-2 treatment. We also found that FGF-2 may contribute to enhanced bone formation due to its effects on cell migration and proliferation, as well as its angiogenic and osteogenic effects.

Chapter 5 details the adaptation of the PLGA drug delivery system developed in Chapter 4 to be combined with a novel, injectable nanofibrous spongy microsphere scaffold (NF-SMS). We established an *in vitro* model to evaluate induced pluripotent cell-derived human

mesenchymal stem cells in 2D monolayer and 3D culture on NF-SMS. We used a similar approach to control the release kinetics of FGF-2 and BMP-7 by encapsulating these factors in varying molecular weight of PLGA nanospheres and subsequently conjugating drug-loaded PLGA nanospheres to the injectable NF-SMS scaffold. In a murine critical size cranial defect model, we found that BMP-7 with low dose FGF-2 enhanced bone regeneration over BMP-7 alone.

Lastly, in **Chapter 6**, we sought to better understand the crosstalk between the FGF-2 and BMP-7 signaling pathways through a series of experiments to measure the effect of FGF-2 on canonical Smad signaling in mouse calvarial osteoblasts. We identified a potential new link between these signaling pathways and propose a new mechanism by which FGF-2 signaling modulates BMP receptor activity, enhancing the phosphorylation of R-Smad1/5/9 proteins.

This research elucidates the criteria for achieving an additive/synergistic effect of BMP-7 and FGF-2 through relevant *in vitro* and *in vivo* models. We discuss the conclusions from this work in **Chapter 7**. This work provides guidelines for future development of composite scaffolds designed to provide a favorable microenvironment and architecture for cell invasion, as well as multiple relevant biological cues to stimulate healing and tissue regeneration. **Chapter 8** discusses future directions for research that will build upon the work presented in this dissertation.

Chapter 2. Biomineralization and Bone Regeneration

2.1. Development and fracture of bone

2.1.1. Bone development

Normal bone formation takes place by two different processes, namely endochondral ossification and intramembranous ossification. The endochondral ossification process features a sequential formation and degradation of cartilaginous tissue. By contrast, intramembranous ossification occurs by direct differentiation of precursor cells into mature osteoblasts.[9]

Limbs of the body undergo endochondral ossification while the flat bones in the skull are formed by intramembranous ossification. While these two processes are regulated by many of the same signaling molecules, the means by which cells differentiate and form bone are vastly different. In intramembranous ossification, precursor cranial neural crest cells differentiate into osteoblasts, which are bone-forming cells.[10,11] By contrast, mesenchymal stem cells establish a cartilage template, which is subsequently mineralized to form cortical bone during endochondral ossificiation.[12] During embryonic development, specific embryologic zones are defined for the formation of precisely defined structures of cartilage and bone. These early processes are regulated by several signals including soluble growth and differentiation factors, as well as cell-cell and cell-extracellular matrix (ECM) interactions. During an initial commitment phase, cells that will form bone are committed in a defined time and space. After initial

commitment, cells are then differentiated into the terminal and mature cell phenotypes that are needed to construct bone.

2.1.2. Fracture healing

In some ways, bone fracture healing is similar to the process of initial bone development as described above.[13] It involves the establishment of an environment that drives the differentiation of precursor cells to repair and replenish the tissue at the site of the injury. Fracture healing has several distinct features. After a fracture occurs, there is an immediate inflammatory response that recruits activated macrophages and polymorphonuclear neutrophils (PMNs) to the site of injury. The macrophages release multiple factors that stimulate the formation of a hematoma. Granulation tissue fibroblasts then proliferate to form a blastema. Osteoprogenitor cells are then recruited from the periosteum, surrounding soft tissue, and bone marrow to the site of the fracture. These cells differentiate into chondrocytes and osteoblasts to repair the fracture. Several soluble growth and differentiation factors influence this process. Mitogenic growth factors stimulate proliferation of precursor cells. They include fibroblast growth factors (FGFs), insulin-like growth factors (IGFs), and platelet-derived growth factors (PDGFs). Previous research indicates that FGF-2 expression is activated at post-fracture day 1, and subsequently declines by Day 14, though still elevated compared with the pre-fracture expression.[14] Differentiation factors such as BMPs induce differentiation of precursors into osteoblasts and chondrocytes. Typically, differentiation follows a proliferative phase, so BMPs are often found in higher concentrations later in the healing process. Their expression at post fracture day 1 is significantly increased, and continues to increase by day 14 and remains high throughout fracture healing.[14]

2.2. Principles of bone tissue engineering

For fractures to be healed successfully a sufficient number of precursor cells must be present at the site of injury and they must be directed towards osteogenic differentiation. Cells can be recruited *in vivo* or implanted directly. Expression of signaling factors can be up regulated or they too can be applied directly. The signals must be given in appropriate time course and quantity to stimulate cell growth and differentiation in a controlled manner.

While fractures can heal naturally without intervention, larger defects require clinical interventions to repair or regenerate bone. These are referred to as critical size defects.[15] The reference standard treatment of these injuries is autologous bone grafting, a process by which donor bone tissue removed from the patient's hip is shaped according to the site of injury, and surgically implanted into the defect site. These grafts contain viable cells, signaling factors, and a matrix that can support healing. However, the success of these grafts is variable, the surgical intervention has associated risks, and donor site morbidity has been reported as a complication of this treatment.

In this chapter, we provide an updated overview of the state of bone tissue engineering as a means for treating bone defects and disease.[16] Bone tissue engineering provides an alternative method to regenerate bone while eliminating some of the limitations associated with grafts. In tissue engineering, a precisely engineered scaffold can be combined with an appropriate osteoprogenitor cell type and relevant growth and differentiation factors.[17] Damaged tissue sites that reach critical sizes can have limited self-healing potential in terms of availability of precursor cells, concentration of growth and differentiation factors, as well as by scarring or inflammation. Thus, delivery of cells and growth factors can boost the efficacy of

bioengineered scaffolds for bone regeneration in these cases. Nucleotide and gene delivery[18] and immune modulation[19] are also being pursued in bone and bone regeneration research.

2.3. Stem cells in bone tissue engineering

Stem cells are defined cell populations with the capacity for self-renewal and the potential for differentiation to multiple cell fates.[20] In bone tissue engineering, adult mesenchymal stem cells (MSCs), often derived from bone marrow, are the most common cell type used to regenerate bone. Other cell types frequently used in the field include embryonic stem cells (ESCs), induced pluripotent stem cells (iPSCs), and adipose derived stem cells (ADSCs).

2.3.1. Mesenchymal stem cells (MSCs)

MSCs are a common cell source for bone regeneration therapies because they are easily obtained and amplified. They are a multipotent cell type and have low immunogenicity. *In vivo*, MSCs give rise to cells that make up bone, cartilage and fat. MSCs have been isolated from fetal blood, liver, and umbilical cord, but they are most frequently derived from bone marrow. In culture, they exhibit fibroblastic morphology. They easily adhere to plastic dishes and flasks and can be expanded in culture for several passages without loss of phenotype.

Osteogenic differentiation of MSCs can be stimulated *in vitro* by an induction media supplemented with dexamethasone, ascorbic acid (vitamin C), and beta-gylcerophosphate. Exposure to osteogenic media causes up-regulation of alkaline phosphatase (ALP) activity and expression of two transcription factors that direct osteogenic differentiation, runt-related transcription factor 2 (RUNX2) and osterix (OSX) in MSCs during early stages of differentiation. During later stages, expression of matrix proteins including osteocalcin,

osteopontin, and bone sialoprotein can be observed. Deposition of calcium within the extracellular matrix (ECM) is also observed as osteogenic differentiation progresses. [Table 2.1]

2.3.2. Adipose derived stem cells (ADSCs)

Like bone marrow, white adipose tissue is mesodermally derived, and contains endothelial cells, smooth muscle cells, and MSCs. The MSCs can be isolated from adipose tissue and expanded in culture. These cells, ADSCs, behave similarly in culture to MSCs obtained from bone marrow. They are multipotent, highly proliferative, and can be obtained in large numbers with minimal invasiveness. ADSCs can be directed towards osteogenic differentiation with the same induction media used for MSCs. Given their similarities to bone marrow-derived MSCs, ADSCs are a clinically relevant cell source with potential for use in bone tissue engineering. However, when compared to MSCs from other sources, the efficiency of osteogenic differentiation of ADSCs is low, in both *in vitro* and *in vivo* studies.[21–23] Many researchers have therefore designed studies that aim to increase osteogenic differentiation of ADSCs by treating cells with osteogenic growth factors or introducing osteoconductive scaffolds. [23]

2.3.3. Embryonic stem cells (ESCs)

ESCs are derived from fertilized embryos, typically donated from embryos that are not used following *in vitro* fertilization. These cells are grown in a plastic dish on a layer of feeder cells that help maintain ESCs in their undifferentiated, pluripotent state. To differentiate ESCs, the cells are allowed to clump, forming embryoid bodies, which can then be subjected to distinct culture conditions and give rise to all three primordial germ layers. Direct differentiation of ESCs or differentiation of ESCs to an intermediate MSC stage can be used in tissue engineering applications.[24] Culture of committed cells is conducted in monolayer and supplemented with

lineage-specific media conditions. Osteogenic differentiation media used to differentiate ESCs is the same combination of exogenous factors used for MSC differentiation. While ESCs have greater capacity for self-renewal and can give rise to more tissue types when compared to MSCs, ethical issues and complex culture requirements complicate their clinical and research use.

Nonetheless, human ESCs or hESC-derived mesenchymal progenitor cells have been seeded onto an osteoconductive nanofibrous scaffold and subsequently treated with osteogenic factors. These culture conditions guide the osteogenic differentiation of hESC-derived cells in 3D and demonstrate the potential role of hESCs in bone tissue engineering.[24,25]

2.3.4. Induced pluripotent stem cells (iPSCs)

As an alternative to the controversial use of ESCs, iPSCs were developed to have the same capacity for self-renewal and pluripotency as ESCs. These cells are adult cells that have been reprogrammed to behave like ESCs. When iPSCs were initially described in 2006, researchers exposed mouse embryonic or adult fibroblasts to four factors under culture conditions used to maintain ESCs. The resulting cells had the same morphology, growth properties, and gene expression as ESCs and formed tumors of all three germ layers.[26] These cells were referred to as iPSCs.

The innovation of iPSCs was revolutionary to the field of stem cell biology, as it opened new areas of research on cell fate determination. It also opened the door to the use of iPSCs in tissue engineering. Several studies have combined iPSCs or iPSC-derived cells with tissue engineering constructs to regenerate bone. In tissue engineering, one of the most appealing characteristics of iPSCs is that they originate from a patient with a tissue defect. The ability to isolate and proliferate a patient-specific cell source would alleviate the risks in tissue engineering of allogenic graft rejection or disease transmission.

Several methods and several adult cell types are now being used to generate iPSCs. The most common of these methods are exposure of cells to exogenous factors, genetic modification by viruses, and other methods of genetic alteration.[27,28] Currently researchers are pursuing methods that increase the efficiency of reprogramming and reduce risk of tumor formation.[27,29–32] As methods to reprogram adult somatic cells improve, so does the variety of cell types that can be reprogrammed to iPSCs. In humans, dermal fibroblasts are among the most common cells used for iPSC generation. Other cell types that have been reprogrammed include dental and oral cells, cord blood cells, and peripheral blood cells.[33]

Human and murine iPSCs show promise for osteogenic differentiation[34,35] and in bone tissue engineering.[36–41] Like other cell types, human iPSCs and cells derived from iPSCs can be seeded onto scaffolds and differentiated bone-forming osteoblasts.

2.4. Scaffolds for bone tissue engineering

2.4.1. Scaffolding design criteria

Scaffolds engineered for bone regeneration are designed to support cell adhesion, migration, proliferation, and differentiation.[17,42–44] Key features of a supportive architecture for bone tissue engineering scaffold include a controlled porous microstructure, high interconnectivity between pores, mechanical stability, a controlled degradation rate, and osteoconductive interaction with cells. The porous microstructure facilitates the ingrowth of cells and enhances regeneration of tissue. Interconnectivity of pores allows for uniform cell seeding and nutrient exchange. Scaffolds are designed to degrade at controlled rates to match the rate of formation of new tissue. Finally, the structure and microenvironment of scaffolds are conducive to differentiation of precursor cells into osteoblasts and to support functional activities of

osteoblasts in bone regeneration. In addition, it was found that a fibrous nanostructure could enhance osteoconductive characteristics of scaffolds for bone tissue engineering.[45] Nanofibers mimic the native extracellular matrix of bone and nanofibrous scaffolds support enhanced osteogenic differentiation when compared to non-nanofibrous scaffolds. Nanofibrous scaffolds were shown to enhance osteogenic differentiation *in vitro* and better heal critical size calvarial defects in a rat model when compared to solid walled scaffolds.[46,47]

To fabricate porous, three dimensional (3D) scaffolds and microspheres for bone regeneration, a variety of processing techniques have been developed. These include, solvent casting/particulate leaching[48,49], gas foaming[50,51], emulsion freeze-drying[52], electrospinning[53,54], rapid prototyping[55,56], and thermally induced phase separation (TIPS) [57–59]. Each of these methods have advantages and disadvantages that are discussed at length in several review papers[45,60–63]. This chapter will not provide an exhaustive description of processing techniques. It will instead focus on how scaffolding design can be used to improve bone tissue engineering with respect to porosity, interconnectivity, mechanical strength, elastic modulus, morphology, and surface properties.

2.4.2. Porous and highly interconnected scaffolds

The porosity and interconnectivity of pores in scaffolds are important for uniform distribution of cells when seeded on a scaffold. A classical method to obtain porous scaffolds is the solvent casting/salt leaching method.[48] The process involves the casting of a mixture of polymer solution and salt (NaCl) into a mold. Subsequent drying of the mixture and leaching of the salt with water results in a porous structure. The pore size and porosity of the scaffolds fabricated using this method can be controlled by the particle size of the added salt and the salt-

to-polymer ratio. This method produces scaffolds with limited inter-pore connectivity, limiting its value in tissue engineering.

To create a scaffold with highly interconnected pores and a spherical pore shape, paraffin and sugar spheres were used a porogen.[64,65] The interconnectivity of the scaffold was finely tuned by changing the heat treatment time to bond the paraffin spheres. Meanwhile, changing the concentration of polymer solution, size of paraffin spheres, and number of casting steps controlled porosity and pore size. Together, this approach allowed for the creation of porous scaffolds with high interconnectivity, which is critical to the uniformity of cell seeding and tissue ingrowth on the scaffold.

2.4.3. Nanofibrous scaffolds for bone tissue engineering

It is well established that the ECM plays a critical role in regulating cell behavior.[66] As previously noted, one of the key design features in bone tissue engineering has been the development of scaffolds with fibrous nanostructures that mimic native ECM and support cellular attachment, differentiation and proliferation. Therefore, scaffolds were designed with nanofibrous structures that resembled the collagen fibers present in native ECM.[67] Collagen nanofibers were shown to play an integral role in cell adhesion, proliferation, and differentiation as early as the 1980s. To create PLLA scaffolds with nanofibers that resembled collagen fibers, a liquid-liquid phase separation technique was developed by integrating sugar sphere template leaching with phase separation.[68] The resulting nanofibrous PLLA (NF-PLLA) matrix featured fibers with diameters ranging from 50-500nm, or within the same range of collagen fibers.[59,64,69,70] **[Figure 2.1]**

The combination of techniques to make pores and techniques to make nanofibrous materials produced scaffolds with biomimetic nanostructures and porous microstructures, which

incorporate the advantages of both synthetic materials and natural structures for bone tissue engineering.

Nanofibrous materials have been successfully fabricated using electrospinning for applications in bone tissue engineering. Electrospinning uses an electric field to overcome surface tension of polymer solutions. This causes the polymer to be ejected out of a needle to a conductive collector, resulting in fibers on the nano to sub-micro scale. [45] Early electrospinning scaffolds for bone tissue engineering were made of PCL as the biodegradable polymer of choice.[71–73] Today, electrospun scaffolds are made from a variety of synthetic and natural polymers and can also be combined into composite scaffolds as described in the next section. Several different electrospun scaffolds for bone tissue engineering have been described, including one method that used PLLA nanofibrous scaffolds that were produce by both TIPS and electrospinning, and enhanced by surface calcium phosphate deposition, for bone tissue engineering.[74,75]

2.4.4. Composite materials for bone tissue engineering scaffolds

The makeup of natural bone extracellular matrix is a combination of fibrous proteins, primarily collagen, upon which mineralized calcium is deposited.[66] In bone regeneration, researchers often attempt to replicate the natural ECM by synthesizing polymers from natural or synthetic building blocks. Due to intrinsic limitations of individual polymers, it is challenging to create a tissue engineering scaffold using a single material source that incorporates the fibrous microstructure of native ECM and supports sufficient mineralization. There are key limitations to each individual material, as no “perfect” single material exists for bone tissue engineering. Researchers therefore combine materials in various ways to form composite scaffolds that possess the advantageous qualities of each component material and better support the physical

and biochemical requirements of bone regeneration. Integration of a mineral component into a fibrous scaffold can contribute to both the structural integrity and osteoconductive activity of the scaffold.[45]

A variety of synthetic materials have been developed for bone tissue engineering, including PLLA, PLGA, Poly glycolic acid (PGA), and others. Similarly, collagen, hydroxyapatite (HAP), decalcified bone matrix, chitosan, and other natural materials have been used in bone regeneration applications. The goal of composite scaffolds for bone regeneration is to have a biocompatible, osteoconductive matrix with suitable mechanical properties.

One early composite matrix was made from combining synthetic polymer with ceramic through thermally induced phase separation (TIPS). These scaffolds, made from highly porous poly(α-hydroxy acids)/HAP, had significantly improved physical properties (compressive modulus and yield strength) when compared to pure polymer scaffolds. They also improved cellular ingrowth, increased osteoblast survival rate, and enhanced bone-specific gene expression.[70,76,77] Alternatively, coating a polymeric scaffold with apatite particles can produce a composite scaffold with improved ability to deposit calcium in bone regeneration.[77,78]

Other composites have been developed in an effort to combine the advantageous qualities of different synthetic and natural materials. [79–81]

2.4.5. Injectable scaffolds

Concurrent with the development of implantable 3D scaffolds for tissue engineering, researchers have sought to develop injectable scaffolds in the form of hydrogels, microspheres, or nanospheres.

Microspheres

An effort to fabricate microspheres with the same porosity and interconnectivity of 3D scaffolds yielded two new tissue engineering scaffolds. These particles retain the favorable characteristics of their implantable counterparts while having the potential for noninvasive treatment. The nanofibrous hollow microsphere (single pore) (NF-HMS) and the nanofibrous spongy microsphere (multiple pores) (NF-SMS) were created to mimic the physical characteristics of a 3D scaffold in an injectable format. Nanofibrous microspheres made from linear poly(L-lactic acid) (PLLA) create solid nanofibrous microspheres. By substituting linear PLLA with star-shaped PLLA in a surfactant-free emulsification technique, a hollow microsphere, with a single pore was developed.[82] By changing the number of arms on the star-shaped PLLA and by altering its hydroxyl density, additional pores could be introduced, forming the NF-SMS.[83] These two novel microsphere scaffolds have shown promise for cartilage and dental tissue regeneration. [82,84]

Other microsphere-based systems are used as cell carriers and/or drug carriers, and are composed of synthetic, natural, or composite polymers.[85–89] These can be porous or nonporous and used independently as tissue engineering platforms, or in combination with a 3D scaffold or hydrogel.[90,91]

Hydrogels

Considerable research has been conducted on the use of hydrogels for bone regeneration. Hydrogels are polymer networks made of natural or synthetic components that are hydrophilic in nature and form viscous gels due to three-dimensional interactions between the polymer chains. These interactions can be either physical or chemical crosslinks between polymer chains. In bone tissue engineering, a number of hydrogels have been used to serve as a scaffold or for delivery of

osteogenic drugs. An ideal hydrogel should be injectable so that it can be used to treat a bone defect noninvasively and fill abnormally shaped tissue defects. It should also be biocompatible and be able to release osteogenic drugs over an extended period of time.[92] Controlled drug release remains a challenge for hydrogels, as they are often prone to a burst release of drug within the first 24-48 hours of treatment.

Hydrogels are often combined with other materials to form composite scaffolds for bone regeneration. PLLA/poly ε-caprolactone (PCL) nanoyarns were suspended in a collagen hydrogel to make a composite scaffold that showed benefits for *in vitro* differentiation of human mesenchymal stem cells.[93] In another study, 45S5 bioglass was introduced into aliginate, forming a composite hydrogel that demonstrated enhanced osteogenic potential with MC3T3-E1 osteoblast precursor cells.[94] A third study used a nanohydroxyapatite-reinforced chitosan hydrogel to stimulate osteogenic differentiation *in vitro* and bone regeneration *in vivo*.[95] These represent a small sampling of the many composite hydrogels being evaluated for bone tissue engineering.

2.4.6. Surface modification and functionalization of scaffolds for bone regeneration

In an effort to increase the effectiveness of tissue engineering scaffolds, biologically active molecules can be attached to the surface or integrated within the scaffold. A specific molecule or peptide can be chosen to promote cell attachment and proliferation or to direct cell differentiation.[68,96,97] For example, modification of poly(alpha-hydroxy acids) scaffold with gelatin enhanced osteoblast attachment, proliferation, and deposition of collagen.[98] Surface modification of a PLLA scaffold with calcium phosphate by electrodeposition enhanced osteogenic differentiation of MC3T3-E1 cells when compared to cells attached to a control PLLA scaffold.[75] PEG hydrogels that are functionalized with integrin-specific peptides can

enhance bone formation and vascularization when also treated with VEGF.[99] Scaffolds can also be functionalized by deposition of diamond nanoparticles. The addition of nanoparticles to a conventional scaffold can change the physical and chemical characteristics of the scaffold and enhance cell attachment and differentiation to support better bone formation.[100] Various additional methods and strategies for surface modification of scaffolds are being pursued.[96,101]

2.4.7. 3D Printed Scaffolds

3D printing technology is becoming increasingly capable of designing microenvironments and developing novel tissue engineering platforms. Many 3D printed scaffolds for bone regeneration have been developed, using many of the same natural, synthetic, and composite polymers discussed previously.[102] One approach to 3D printing scaffolds for bone tissue engineering is to print scaffolds that can be used to make vascularized bone grafts.[103] By varying internal porosity of the scaffold or adding osteogenic and angiogenic factors like zinc and silicon, researchers have attempted to increase neovascularization of regenerated bone and simultaneously enhancing osteogenic differentiation of progenitor cells.[104–106] The successes and challenges of current strategies, descriptions of 3D printing methodologies, and the clinical progress of 3D printing for bone tissue engineering are covered in depth in relevant reviews in the literature.[107–109]

2.5. Growth and differentiation factors in bone tissue engineering

Bioactive molecules, hormones (e.g. PTH), and nucleic acids (e.g. miRNA) can be used to enhance growth and differentiation of cells. The effective combination of these factors with tissue engineering constructs and drug delivery systems can improve regeneration of bone both *in vitro* and *in vivo*.

2.5.1. Bone morphogenetic proteins (BMPs)

A group of proteins within the transforming growth factor-β (TGF-β) super family, known as BMPs, play various roles in bone development, as well as the development of a multitude of tissues within the human body. While 15 BMPs have been identified, BMP-2 and BMP-7 show the most robust activity to induce bone formation.[110] Both BMP-2 and BMP-7 have been used clinically in FDA-approved devices to treat a narrow range of severe bone defects.

BMPs act on bone-forming osteoblasts, preosteoblasts, and other precursor cells, including MSCs, ADSCs, iPSCs, and ESCs. Typically, BMPs form homodimers and bind with known BMP receptors to activate a cascade of signaling pathways that initiate differentiation and mineralization of cells and tissue. Some evidence of BMP 2/7 heterodimers having a stronger osteogenic effect than the respective homodimers has been published.[111,112] BMP-2 and BMP-7 act to stimulate osteogenic differentiation through intracellular phosphorylation of the Smad1/5/9 proteins. Upon phosphorylation, p-Smad1/5/9 proteins translocate to the nucleus and upregulates runt-related transcription factor-2 (RUNX2). BMPs can also activate other pathways in parallel, including Wnt signaling.[113] BMP-related signaling is generally divided into either Smad-dependent or Smad-independent pathways.

The clinical use of BMP-2 began after its approval by the FDA in 2002 for the treatment of anterior lumbar interbody fusion (ALIF) within a threaded titanium tapered cage.[114] The scope of its use expanded in 2004 to include tibial nonunions and in 2007 for oral maxillofacial reconstruction. Following the expanded use of BMP-2 for these clinical and other off label applications, a number of serious side effects were observed and reported.[8] Inflammatory

complications, including swelling of the cervical spine[115], radiculopathy[116], ectopic bone formation[117,118], osteoclast activation[119,120], urogenital events[121], and wound complications were reported.[8]

The clinical side effects observed with BMP products is attributed in large part due to the supraphysiological doses used in the Sryker OP-1 and Medtronic BMP-Infuse Bone Graft. Stryker OP-1 product incorporates 1.75-3.5 mg of BMP-7 within a bovine collagen sponge for the treatment of delayed union, persistent nonunion, and lumbar spinal fusion surgery.[122,123] The Medtronic BMP-Infuse product incorporates 1.5-12 mg BMP-2 into an absorbable collagen sponge of variable size.[124]

The OP-1 and Infuse Bone Graft products use collagen sponge materials to trap BMPs within the collagen matrix. The rapid diffusion of protein from these systems and the short half-life of BMPs *in vivo* necessitates the use of high doses of drug of BMPs to induce sufficient bone formation. To overcome this limitation, researchers have pursued the development of drug delivery system can provide local, clinically relevant doses that can be sustained. This is often accomplished by encapsulating BMPs in a delivery vehicle such as a biocompatible polymer microsphere or hydrogel. Our lab previously demonstrated that controlled release of 5µg rhBMP-7 in a PLGA nanosphere delivery system enhanced a bone tissue engineering scaffold in a subcutaneous mouse model.[125] An orthotopic calvarial defect model used PLGA/PEG scaffolds to deliver 1µg BMP-2 over 3 weeks in mice. After 6 weeks, partial healing of calvaria was observed in BMP-2 treated mice, while no substantial healing occurred in empty defects.[126] In a 5mm rat calvarial defect, the delivery of 5µg BMP-2 from a PLA/PGA scaffold partially healed the defect after 45 days.[127] These studies, along with our previous subcutaneous models, serve as a guideline for the appropriate dose of BMP to use in tissue

engineering platforms, as well as the completeness of healing to be expected in a rodent calvarial defect model.

2.5.2. Alternative factors and their combinations

In addition to BMPs, other proteins including TGF-β, Vascular Endothelial Growth Factor (VEGF), Platelet Derived Growth Factor (PDGF), Fibroblast Growth Factor (FGF), and to a lesser extent Endothelial Growth Factor (EGF) and Insulin-like Growth Factor (IGF) have been used to promote bone regeneration. These growth factors have been shown to contribute to osteogenesis by supporting development of new blood vessels, stimulating cell migration, recruitment and proliferation, and directing differentiation of progenitor cells to osteogenic fate. [128]

Of particular interest is the combinatorial effect of pro-angiogenic and pro-osteogenic factors as new blood vessel formation is essential to bone healing and survival of bone grafts.[129] Delivery of multiple factors as part of a tissue engineering construct provides endogenous cells with a scaffold to grow with the added benefit of providing relevant biological cues to stimulate healing. Combinations of PDGF and BMP[130], VEGF and BMP[131], and FGF-2 and BMP[132] have all shown potential for enhanced bone regeneration.

In this dissertation, we focus on the combinatorial effect of controlled release of FGF-2 and BMP-7 from a novel tissue engineering construct. Previous *in vitro* and *in vivo* studies have evaluated the co-delivery of FGF-2 with BMP-2, -4, or -7 and revealed inconclusive and sometimes contradictory results.[132–137] Published studies vary greatly with respect to the dose of FGF-2 administered, the length of FGF-2 treatment, the animal or *in vitro* model used, and types of scaffolds or drug delivery systems. We explore the dose and duration of FGF-2 required to achieve an additive effect with BMP-7, the mechanism for crosstalk in their

respective signaling pathways, and evaluate the co-delivery of these factors from novel biomimetic tissue engineering scaffolds in relevant animal models.

While FGF-2 has been employed on its own to stimulate bone regeneration[138,139], its use in combination with BMPs has resulted in contradictory findings. It is important to consider the many potential roles of FGF-2 on osteogenesis, angiogenesis, mitogenesis, as well as its role as a competence factor[140–142] and in maintaining stemness of progenitor cells[143,144]. In kidney development, both BMP-7 and FGF-2 are thought to have a role in maintaining competence of mesenchymal cells to induction factors.[145] Studies that pre-incubate progenitor cells with FGF-2 have shown an increase in osteogenic potential of those cells as a result.[146,147] As a competence factor, FGF-2 could potentially enhance the sensitivity of MSCs to BMP-7. By contrast, the role of FGF-2 in maintaining stemness of progenitor cells highlights the importance of the timing of FGF-2 treatment during osteogenic induction.

Table 2.1. Markers of Osteogenic Differentiation

Marker of Osteogenic differentiation	Highest expression during stages of osteogenic differentiation	Function
Alkaline phosphatase (ALP)	Early	The function of ALP is not well described, however it is thought to have a role in promoting calcification of tissue.[148]
Runt related transcription factor 2 (RUNX2)	Early	RUNX2 is a transcription factor that activates osteogenic genes and plays a role in cell fate determination of MSCs to osteoprogenitor cells.[149]
Osterix (OSX)	Early	Osterix is a transcription factor that acts downstream of RUNX2 to direct osteogenic differentiation[150]
Osteocalcin (OCN)	Late	Osteocalcin is the most abundant non-collagenous protein in bone extracellular matrix. It serves as a metabolic regulator of bone.[151]

Bone sialoprotein (BSP)	Late	Extracellular matrix protein of bone that regulates the microenvironment of osteoblasts, hypertrophic chondrocytes, and osteoclasts. Regulates bone formation, mineralization and turn over.[152]
Osteopontin (OPN)	Late	Similar to BSP, osteopontin is an extracellular matrix protein that regulates mineralization and bone matrix quality.[153]

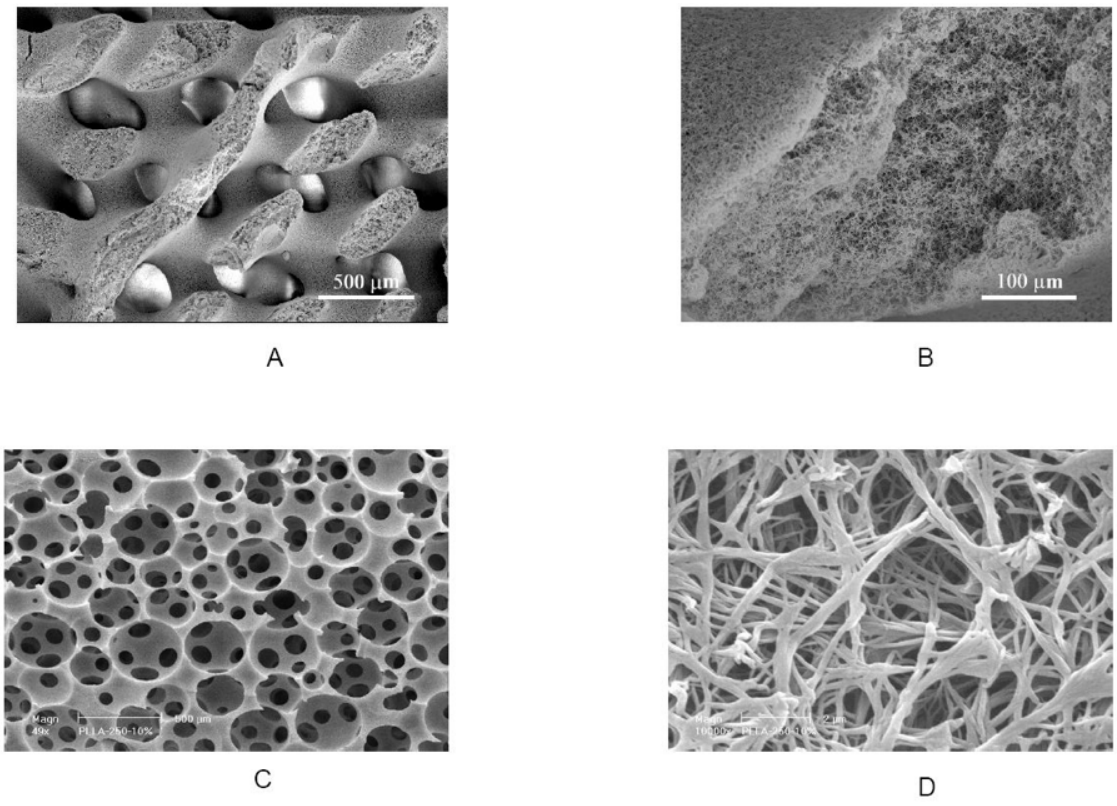


Figure 2.1. Nanofibrous scaffolds for bone tissue engineering
(A, B) Scanning electron micrographs of scaffolds fabricated using a spherical porogen (paraffin sphere) leaching technique: (A) poly-l-lactic acid (PLLA), (B) poly(lactic-co-glycolic acid) (85/15), and (C, D) PLLA scaffolds fabricated using a thermally induced solid ± liquid phase separation technique in dioxane (C) or benzene (D).

(A, B) From Ma PX, Choi J-W. Biodegradable polymer scaffolds with well-defined interconnected spherical pore network. Tissue Eng 2001;7(1):23–33; (C, D) From Ma PX, Zhang R. Microtubular architecture of biodegradable polymer scaffolds. J Biomed Mater Res 2001;56(4):469–77; Ma PX, Zhang R, Xiao G, Franceschi R. Engineering new bone tissue in vitro on highly porous poly(alpha-hydroxyl acids)/hydroxyapatite composite scaffolds. J Biomed Mater Res (United States) February 2001;54(2):284–93.

Chapter 3. Controlled Drug Release for Tissue Engineering

3.1. Introduction

Tissue regeneration can be facilitated by the use of biomimetic materials that create a suitable microenvironment for the recruitment, adhesion, proliferation, and differentiation of cells. This process can be further stimulated by the addition of drugs that have an influence on cellular function and tissue regeneration. For the purpose of this chapter, the term "drug" will be used to refer to small molecule chemicals, peptides, proteins, growth factors, cytokines, and other bioactive molecules used to support or stimulate cellular activities and new tissue regeneration.

Advanced tissue engineering systems often combine one or more of these three integral components: biomaterial matrices, living cells, and bioactive drugs. Researchers increasingly recognize the need for more spatiotemporal control over the release of drugs that directly or indirectly affect cellular signaling or tissue regeneration. Specifically, there is a growing desire to mimic the inherent complexity of natural tissue by delivering multiple drugs simultaneously, sequentially, or in multiphasic patterns. Researchers hypothesize that having fine control over the delivery of multiple stimuli over time will enhance the speed, quantity, and quality of tissue regeneration.

Tissue engineering scaffolds are being designed to serve as the 3D template and matrix microenvironment with respect to cell adhesion, proliferation, and differentiation. Incorporating a tunable drug delivery mechanism into such scaffolds may further stimulate the growth of new

tissue and the repair of injury. Controlled drug delivery can be accomplished by physically or chemically adsorbing the drug onto the surface[101] of the material matrix (scaffold), encapsulating the drug directly within the scaffold, or by incorporating drug delivery systems on the scaffold. The subsequent release of the drug occurs by diffusion or due to degradation of the scaffold or encapsulating material. The quantity and duration of drug released can be controlled by altering the composition of the material, the delivery system, or the methods of drug integration. Drug release kinetics and duration can further be tuned by changing the dose of the drug added or by coating the material with a substrate (e.g. heparin) that specifically or nonspecifically binds cells or drugs.

In tissue engineering, controlled release of drugs from a scaffold can accelerate the local regenerative process and circumvent the concerns over the potential undesired systemic effects of a drug in the body. Drugs must meet a minimum threshold to be effective, but due to their short half-lives *in vivo*, it is challenging to achieve a relevant dose at the site of injury for an extended period of time without causing unwanted side effects of over-exposure of cells and tissue that could occur when drugs are delivered systemically. Controlled release of drugs from tissue engineering scaffolds can help establish localized, clinically relevant drug concentrations for extended periods of time. The challenges in the field of controlled release lie in the ability to finely tune the release of the drug without negatively affecting the mechanical or structural properties of the scaffold and without damaging or quickly eluting the drug itself.[154]

A number of different types of materials have been employed to deliver drugs in a controlled manner, including porous materials and hydrogels made from frequently used natural and synthetic polymers. Composite materials that combine natural and synthetic materials or combine hydrogel and porous materials are also commonly used in controlled release.

The extent to which these new drug delivery systems have been tested varies from studies that only examine the basic biocompatibility, material characteristics and drug release kinetics, studies that evaluate the potential of drug delivery systems *in vitro*, and those that have been evaluated *in vivo*. These systems further differ based on whether they involve the delivery of a single drug, the simultaneous delivery of multiple drugs, the sequential delivery of multiple drugs, and the co-delivery of cells and single or multiple drugs.

This review examines the advances in controlled release of drugs for the purpose of tissue engineering, with an emphasis on recent studies within the past a few years. This article will cover advances in material synthesis that improve the ability to tune the release kinetics of drugs from various natural and synthetic material types, covering microspheres, hydrogels, porous scaffolds, nanofibrous scaffolds, and composite material systems. It will also describe scaffold surface modifications, strategies used to deliver multiple drugs, and other novel advances. Finally, this review suggests areas in which additional research is needed to further the field of controlled release for tissue engineering.

3.2. Microspheres designed for controlled release

Microspheres and nanospheres are commonly used in controlled release of drugs across many clinical disciplines, including cancer treatment, infection control, inflammation control, and tissue regeneration. In tissue engineering, drugs are adsorbed to the surface of or encapsulated within the core of microspheres. Drug release from the micro/nanosphere matrix usually features a burst release associated with smaller quantities of drug attached to the surface of the microsphere, followed by a sustained release, which is associated with degradation of the polymer and release of encapsulated drug. Microspheres can be made from natural or synthetic polymers and can be made as hydrogels, solid, porous, and nanofibrous microspheres. PLGA and

chitosan microspheres are two of the most common synthetic and natural polymers used in the fabrication of microspheres for tunable drug delivery.[155] When delivered *in vivo*, microspheres are sometimes susceptible to being cleared out of the animal and/or migrating away from the defect/implantation site. To maintain local treatment, microspheres are often combined with scaffolds or hydrogels in composite delivery systems. For this review, microspheres will be discussed in the context of their use in composite systems.

3.3. New hydrogel approaches that improve controlled release

Hydrogels are defined as a network of polymer chains that are hydrophilic by nature and swell in the presence of water. Increasing the crosslinking density between polymer chains or changing the polymer content can alter their physical characteristics and degradation rates, which in turn can affect their use in drug delivery. Hydrogels are attractive matrices for drug delivery and tissue engineering because they are easy to assemble from both natural and synthetic polymers and tend to be biocompatible. They are also adaptable to an injectable cell delivery system that is desirable to produce a minimally invasive treatment. However, hydrogel-based drug delivery systems usually exhibit a strong burst release of drug for a short period of time,[156–158] from a few minutes up to 48 hours while total release of drugs from hydrogels may hardly extend beyond 1 week. Additionally, hydrogels are typically not adhesive for cells and proteins and they do not allow penetration by cells; instead hydrogel-based delivery systems require that cells be pre-loaded into the matrix prior to delivery. Due to these constraints, hydrogels are usually unsuitable for long-term controlled release. However, efforts are being made to adapt these materials to reduce the burst release effect and extend the length of time that a drug can be released from the material.

3.3.1. Efforts to reduce the burst release effect in hydrogels

The release of drugs from a hydrogel matrix occurs primarily through diffusion. A major effort in hydrogel drug delivery systems is to control the rate at which biomolecules are released from a hydrogel matrix. A conventional method for extending the duration and reducing burst effect from hydrogels is to increase the crosslinking density of the polymers. A matrix-metalloprotease (MMP)–sensitive hyaluronic acid-based hydrogel was made with varying degrees of crosslinking, which generally showed that gel degradation rate decreased as crosslink density increased.[159]

Effort has been made in controlling burst release through the development of a multifunctional interpenetrating polymer network.[160] For example, hydrogels are synthesized from poly(ethylene glycol) methacrylate, *N*-isopropylacrylamide, and methacrylated alginate using ammonium persulfate and *N,N,N',N'*-tetramethylethylenediamine (TEDMED) as a redox initiator system. Alginate was chosen because its high number of carboxyl groups makes it sensitive to pH and therefore attractive for oral drug delivery. The redox initiator system was selected to overcome the limits of common photopolymerization methods that use a toxic photoinitiator or result in inconsistent drug delivery. These gels have been evaluated using model drugs for 24 hours at low pH (i.e., simulating gastric environment) and have not yet been tested for tissue engineering applications, which would likely require long-term sustained release.

Colloidal gelatin hydrogels assembled from oppositely charged gelatin nanospheres were used to deliver BMP-2 and basic fibroblast growth factor (bFGF or FGF-2). The release kinetics from this delivery system depends more on the crosslinking density of the gel than the type of gelatin used.[137] When evaluated *in vitro*, gels with high crosslinking density showed a sustained release of growth factor from the gel over a 30-day period, while also showing a

minimal burst effect in BMP-2 release. The release profile of FGF-2 showed a stronger burst effect. This study represented an attempt to co-deliver multiple growth factors with independent release rates using a colloidal gel. The *in vivo* analysis of this dual delivery system did not produce conclusive evidence of a combined effect and additional studies to optimize this co-delivery system are needed.

The self-assembling peptide nanofiber scaffold consisting of ionic self-complimentary peptides with 16 amino acids (RADA16) was tested as a slow release hydrogel.[161] The release kinetics of five model drugs were studied using diffusion experiments *in vitro* and mathematical models. While slow release was accomplished, it was only measured for seven days. Additional studies on RADA16-I nanofiber scaffolds involved the release of active cytokines from the hydrogel and testing their activity *in vitro*. The release kinetics of FGF-2, VEGF, and brain-derived neurotrophic factor (BDNF) were tested by diffusion experiments; FGF-2 was subsequently released from the peptide scaffold in a neural stem cell (NSC) proliferation experiment. Significant stimulation of NSC proliferation was observed for up to three weeks.[162] Peptide scaffolds were also used to deliver FGF-2 and growth differentiation factor-5 (GDF-5) for *in vivo* treatment of medial collateral ligament (MCL) injury.[163]

3.3.2. Composite hydrogel – microsphere delivery systems used to deliver multiple GFs

Due to the challenges in altering the physical characteristics of hydrogels themselves to extend and control the release rate of drugs, researchers have turned to first encapsulating or adsorbing drugs in polymeric microspheres before incorporating them into the gel matrix. In these systems, the microspheres serve to control the release of the drug while the hydrogel is primarily a scaffold to retain cells in a 3D structure.

Early work using this approach involved the encapsulation of IGF-1 and TGF-β in poly(D, L-lactic-*co*-glycolic acid) (PLGA) microspheres and then loading these drug-containing microspheres into poly(ethylene oxide) (PEO)-based hydrogels.[164] In this cartilage tissue engineering study, two growth factors were released over 15 days, stimulating chondrocyte proliferation *in vitro*. This study set an early example for the potential of hydrogel-microsphere composite delivery systems but also highlighted the challenges of adapting these systems to tissue engineering, including the need for dose control, loading efficiency, and optimizing growth factor release characteristics.

In a similar approach, researchers encapsulated IGF-1 and hepatocyte growth factor (HGF) in PLGA microspheres and integrated these microspheres along with human ADSCs into a hydrogel made of a tri-block copolymer of polypropylene glycol and polyethylene glycol for cardiac tissue engineering.[165] The encapsulation of growth factors into microspheres muted the burst release and allowed for a sustained release over 21 days. The release of growth factors from the PLGA microspheres was attributed to the slow degradation of the polymer over time.

A more recent study used the same principle to deliver FGF-2 and BMP-7 loaded in chitosan (CS) nanoparticles in a gellan xanthan gel matrix. This study showed significant improvements in alkaline phosphatase activity and calcium deposition when compared to single growth factor delivery, suggesting that the dual delivery of growth factors supported better osteogenic differentiation.[166] The release kinetics over 21 days showed a burst release on the first day for the hydrogel-microsphere system but demonstrated a more sustained release of BMP-7 thereafter.

These studies represent dual growth factor release from composite hydrogel systems that reduce the burst release typically associated with hydrogels, enhancing the regeneration of

various tissue types. These systems are worth to be further evaluated *in vivo,* and efforts are needed to achieve distinct release kinetics for each factor when dual or multiple release is involved.

3.4. Porous scaffolds made of natural materials with controlled release capacity

Porous scaffolds are solid, three-dimensional physical structures with a porous architecture that allows infiltration, attachment, and proliferation of cells and tissue regeneration. A number of natural polymer materials have been employed as porous scaffolds for controlled release of drugs for the purposes of tissue regeneration. These include hyaluronic acid (HA), chitosan, alginate, collagen, fibrin, and others. These natural materials offer some potential advantages for tissue engineering. For example, collagen makes up a major portion of the natural extracellular matrix (ECM) of bone and other structural tissues and is therefore an attractive scaffolding material for tissue regeneration. Many efforts to use natural materials for controlled release in the form of hydrogels, as previously discussed, and porous scaffolds/microparticles are ongoing. One approach is to modify the surface of natural polymers with affinitive substrates, such as heparin, that can help control the release of drugs from the scaffold.

3.4.1. Reducing burst release effect

Similar to hydrogel-based delivery, there is a perceived need to reduce the burst effect and extend the length of time natural materials can be used to deliver drugs in a spatiotemporally controlled manner.

To better control the release of TGF-β3 for chondrogenic differentiation of human mesenchymal stem cells, researchers used hollow hyaluronan (HA) microspheres prepared by a previously described method involving the removal of a polystyrene core. TGF-β3 was incorporated into the microspheres by diffusion loading.[167] These HA microspheres were

compared to collagen microspheres for *in vitro* chondrogenic differentiation. The release kinetics of the HA microspheres showed a 20% burst release on the first day followed by sustained release over 6 days. The *in vitro* results showed positive markers for chondrogenesis, as suggested by significant increases in collagen II and aggrecan expression as well as a significant decrease of collagen X expression. The authors argue that the burst release is advantageous to this application due to the need for early commitment of MSCs during chondrogenic differentiation. This system may be suitable for chondrogenic regeneration but remains to be evaluated for its potential for long-term release and for regeneration of other tissue types.

3.4.2. Sustaining release for extended treatment time period

Long-term sustained release of dexamethasone from CS nanoparticles for osteogenic differentiation was achieved when the nanoparticles were synthesized using a microfluidic device.[168] Despite a moderate burst release, sustained intracellular delivery of dexamethasone was observed for up to 21 days. Significant increases in ALP activity, osteocalcin expression, and calcium deposition were observed.

Sustained long-term release of recombinant human BMP-2 (rhBMP-2) was achieved from a collagen-hydroxyapatite scaffold for 21 days. In this bone tissue regeneration study, the burst release was controlled to a minor burst in the first four hours, followed by sustained release for 21 days.[169] After 7 days, the controlled release system significantly increased ALP activity and after 14 days showed significantly higher calcium concentration when cultured with MC3T3 cells. An 8-week *in vivo* implantation of the scaffold in a rat calvarial defect showed improved healing when compared to scaffold only (no drug) or empty defect control, with significantly greater area of new bone formed when measured by quantitative histomorphometric analysis.

While natural scaffolds offer certain advantages, they also have some specific drawbacks. In particular, natural polymers are subject to inconsistent degradation rates and many of them have limited mechanical strength.[170] Natural scaffolds sometimes lead to unwanted host inflammatory responses, although ways to harness and/or reduce the inflammatory responses caused by natural materials are being studied.[171–174] Alternatively, synthetic materials may overcome some of these limitations in natural materials.

3.5. Synthetic polymer scaffolds allow for precise control of release kinetics

As alternatives to natural scaffolds, researchers sought to create novel synthetic polymer scaffolds that could provide the 3D microenvironment for tissue engineering while overcoming issues such as low mechanical strength and variable degradation rates.[175] Many synthetic polymers, each with different structural, biological, and mechanical characteristics, have been used for this purpose. The most commonly used synthetic polymers include PLLA, poly(glycolic acid) (PGA), PLGA, and poly(caprolactone) (PCL). Scaffolds made from these polymers form porous structures. The size of macro-pores and the interpore connectivity of the 3D structure affect the surface area and therefore the drug release kinetics. Furthermore, the porosity and interpore connectivity affect the ability of cells to penetrate and proliferate in and on the surface of the scaffold **[Figure 3.1.A,B].**[176]

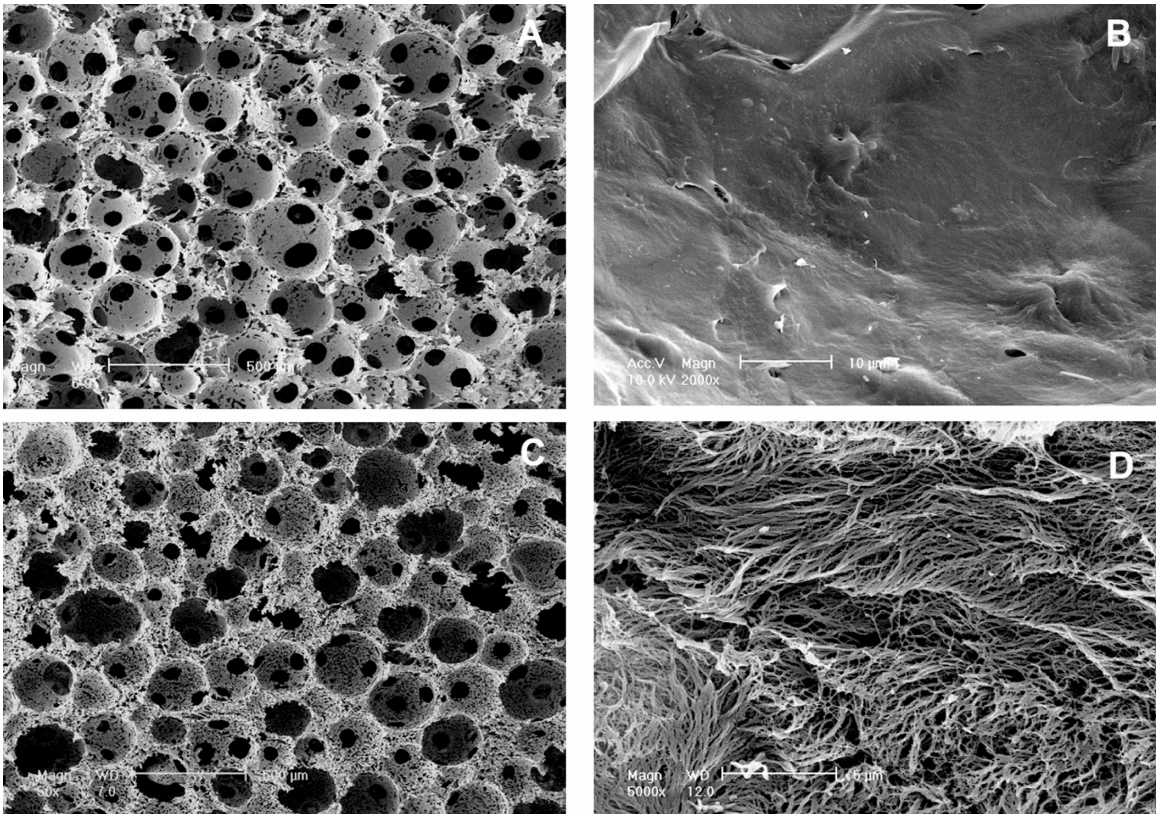


Figure 3.1: SEM images of solid walled (SW)-PLLA and NF-PLLA scaffolds.
(A) Macroporous structure of SW-PLLA scaffolds at low magnification; (B) Solid-walled architecture of SW-PLLA scaffolds at high magnification; (C) Macroporous structure of NF-PLLA scaffolds at low magnification; and (D) Nanofibrous architecture of NF-PLLA scaffolds at high magnification.

Reprinted from Biomaterials, 32(31), Jing Wang, Haiyun Ma, Xiaobing Jin, et al. The effect of scaffold architecture on odontogenic differentiation of human dental pulp stem cells. 7822–7830. (2011) with permission from Elsevier.

These synthetic polymers and copolymers are used in tissue engineering and controlled release through three methods. When drugs are incorporated into matrix of the scaffold, degradation of the polymer dictates release kinetics of the drug. The scaffold walls are impregnated with drug and as the polymer degrades, drug is released. When scaffold surfaces are coated with polymer/drug layer, the release is controlled by diffusion and degradation of the coating polymer.[177] The integration of microspheres into scaffolds offer a third mechanism to control the release of drugs in tissue engineering applications similar to the composite hydrogel-

microsphere delivery systems. Approaches include, for example, the delivery of model drugs from a synthetic composite scaffold using polystyrene microspheres[178] or the delivery of FGF-2 encapsulated gelatin microspheres that are seeded onto a PCL-PLLA scaffold to support osteoblast proliferation and adhesion.[179]

3.5.1. Polymer scaffolds and microspheres with nanofibrous architecture

Synthetic polymer porous scaffolds and microspheres with nanofibrous (NF) architecture have gained increased popularity for the purposes of tissue engineering because they create a 3D microenvironment similar to the nanofibrous collagen found in extracellular matrix of native tissue.[65] While solid walled porous scaffold have been studied for controlled release, there is evidence that nanofibrous scaffolds for tissue engineering are superior due to their biomimetic architecture.[176,180] Several excellent review articles cover the methods used to synthesize NF scaffolds and their applications for drug delivery in tissue engineering.[154,181–188] In short, there are three major methods to synthesize NF scaffolds including self-assembly, electrospinning, and thermally induced phase separation. Controlled release can be accomplished by the same three methods as non-nanofibrous scaffolds. The technique of electrospinning allows researchers to directionally align fibers, which are otherwise randomly oriented. Alignment of nanofibers is advantageous for neural[189] or vascular tissue regeneration.

Nanofibrous scaffolds made from natural materials[190–192] or synthetic/natural blends have also been developed. A NF scaffold made from a PLLA-PCL and silk fibroin composite was used to deliver curcumin for skin regeneration. [193] VEGF was delivered from a NF scaffold made from a PLLA-PCL and gelatin blend for cardiac tissue regeneration.[194] A blend of PCL and gelatin was used to delivery antibiotic for bone regeneration.[195] A core sheath

PCL and silk fibroin blend was investigated *in vitro* for delivery of model drugs and shows potential for tissue engineering and drug delivery.[196]

3.5.2. Composite scaffold-microsphere delivery systems

PLGA microspheres and nanospheres (NS) have been used frequently as drug and cell carriers[82]. Distinct release profiles can be achieved by changing the lactic acid (LA) to glycolic acid (GA) ratio or altering the molecular weight of the polymers. Microspheres have also been used in combination with 3D scaffolds to modulate the microenvironment through drug release. A NF PLLA scaffold could be seeded with microspheres encapsulating PDGF[197] or nanospheres encapsulating rhBMP-7[198]. In these two studies, the NF scaffold-micro/nanosphere combination demonstrated the *in vivo* capability of this system to promote soft tissue and hard tissue regeneration.

PLGA microspheres with varying molecular weights were fabricated using established double emulsion techniques. Doses ranging from 2.5μg to 25μg of PDGF were encapsulated in the microspheres and immobilized onto the NF scaffold, which was subcutaneously implanted in a rat wound model. The *in vivo* performance was measured at 3, 7, 14, and 21 days.[199] The higher molecular weight microspheres were associated with a longer-term release of rhPDGF-BB and showed enhanced cell migration and vasculogenesis **[Figure 3.2]**.[200] Enhanced expression of several chemokines was found to be behind such effects.

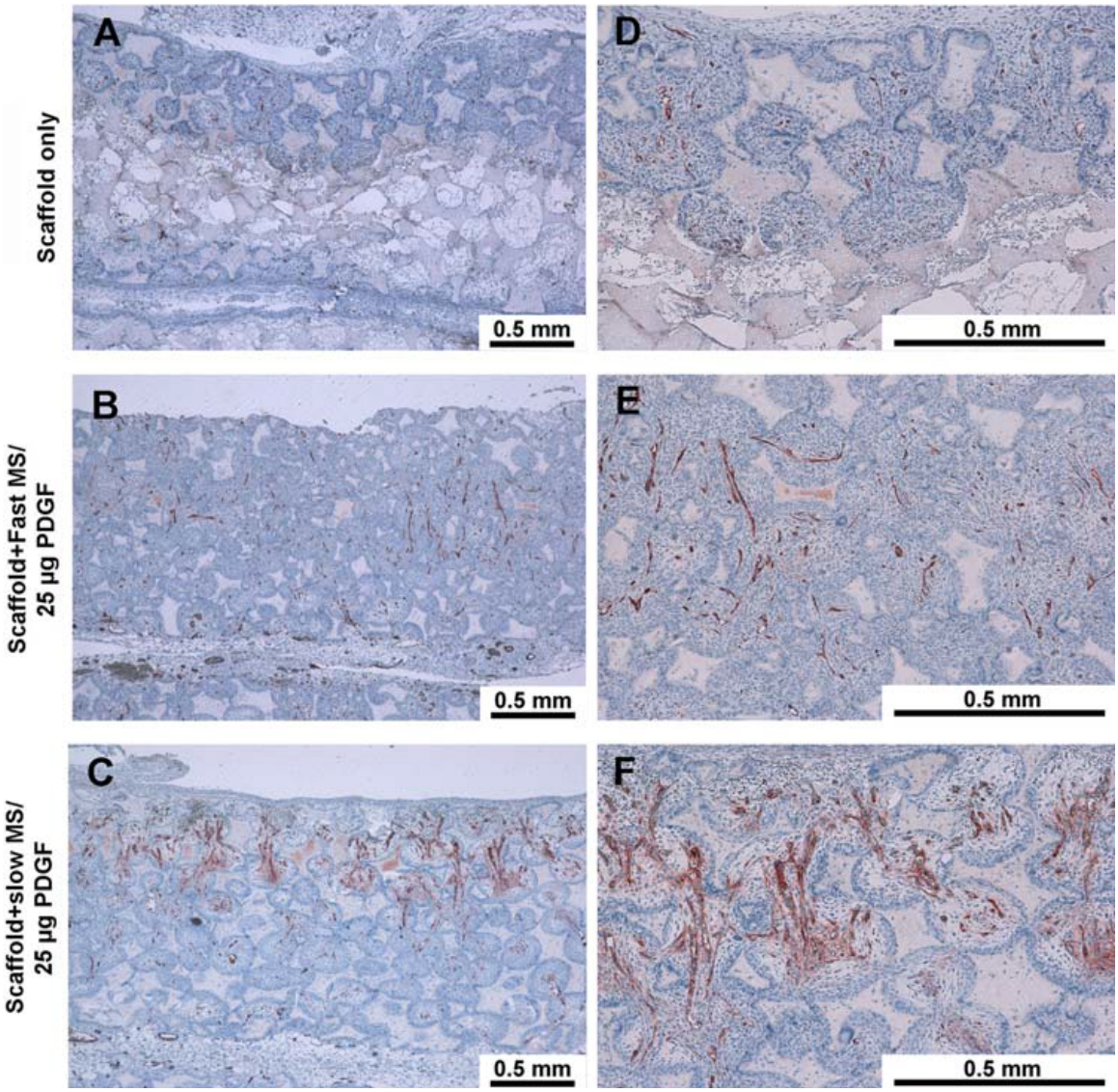


Figure 3.2. Nanofibrous scaffolds with PDGF microspheres promote vasculogenesis *in vivo*. *Left panel is low magnification (10X), right panel is high magnification (40X). Positive Factor VIII stained blood vessels were located in the central regions of the pores within penetrated tissues. The blood vessels also permeated through the inter-openings between each pore. The group with 25 mg PDGF encapsulated in slow release PLGA microspheres had measurably more vascularization.*

Reprinted from PLoS One, 3(3), Qiming Jin, Guabao Wei, Zhao Lin, et. al. Nanofibrous Scaffolds Incorporating PDGF-BB Microspheres Induce Chemokine Expression and Tissue Neogenesis In Vivo. e1729 (2008), under Creative Commons Attribution license

Nanospheres with an average diameter around 300nm were prepared using the double emulsion technique. The release of rhBMP-7 from nanospheres immobilized onto an NF scaffold (Figure 3) was evaluated for bone regeneration in a subcutaneous implantation rat model.[198] The incorporation of rhBMP-7 nanospheres significantly increased new bone formation at 3 weeks and 6 weeks after implantation. At 6 weeks, the NF scaffold/rhBMP-7 nanosphere complex generated more tissue than a scaffold with directly adsorbed rhBMP-7 based on radiographic analysis. Hematoxylin and eosin (H&E) staining and von Kossa staining confirmed the superior bone regeneration of the composite scaffold-nanosphere complex to control scaffolds. The *in vitro* release kinetics showed a moderate burst release followed by sustained release for more than 70 days. Delivery of the antibiotic drug doxycycline was also achieved by a NF scaffold-nanosphere composite system.[201] Antibiotic delivery may play an important role in tissue regeneration as to protect the site of injury from infection. This combination of NF PLLA scaffolds and PLGA micro/nanospheres offers long-term delivery not attainable by other approaches. This controlled release system has the unique abilities to moderate the burst release, extend the treatment time, and provide a superior 3D microenvironment for tissue engineering.

[Figure 3.3]

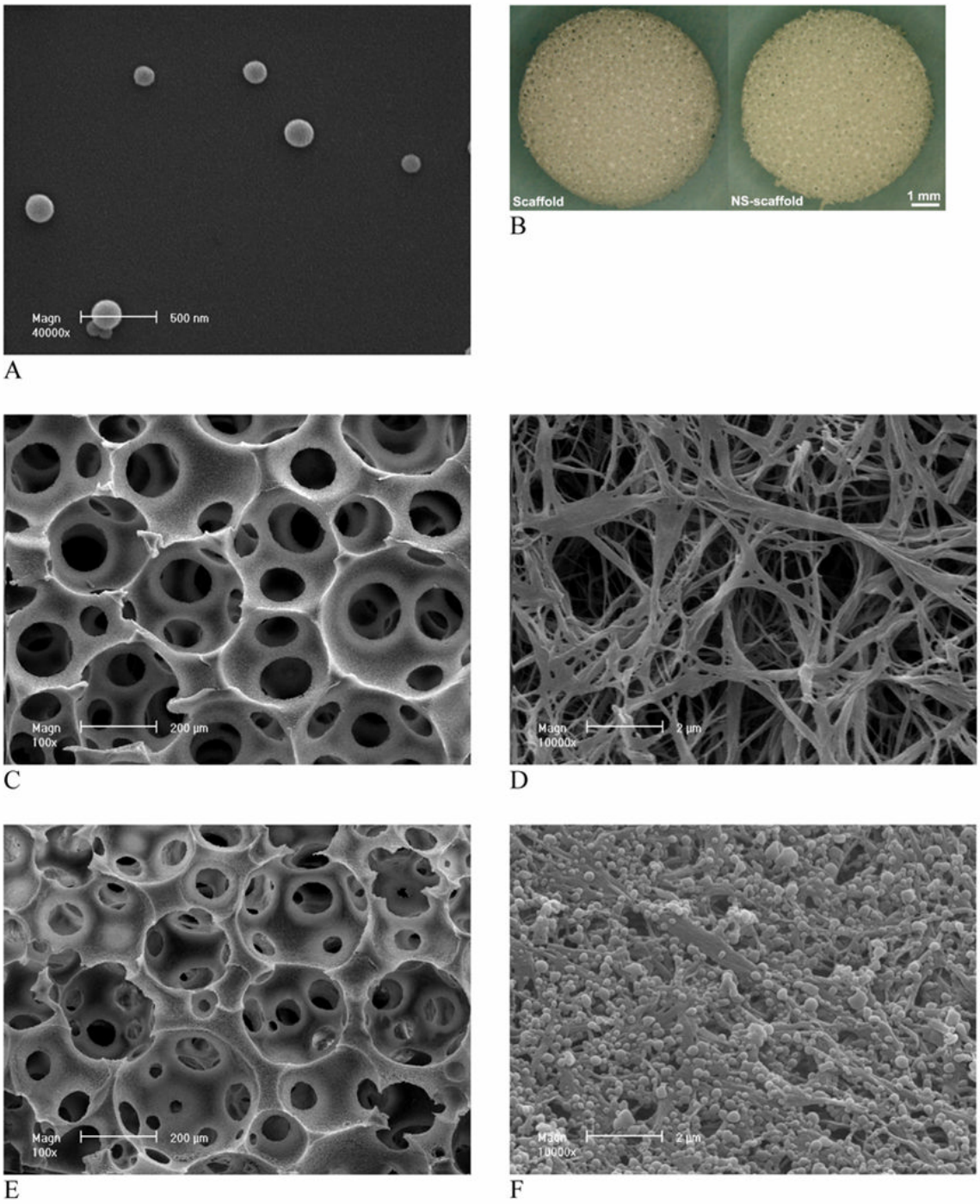


Figure 3.3. Characterization of PLGA50–64K nanospheres (NS) and nanosphere incorporated PLLA nano-fibrous scaffolds (NS-scaffolds).

(A) Scanning electron micrograph of rhBMP-7 containing PLGA50–64K nanospheres; (B) Macroscopic photographs of PLLA scaffolds before (left) and after (right) nanosphere incorporation; (C, D) Scanning electron micrographs of PLLA nano-fibrous scaffolds before nanosphere incorporation at 100x (C) and 10,000x (D); (E, F) Scanning electron micrographs of PLLA nano-fibrous scaffolds after PLGA50–64K nanosphere incorporation at 100x (E) and 10,000x (F).

Reprinted from Biomaterials, 28(12), Guobao Wei, Qiming Jin, William V. Giannobile, Peter X. Ma The enhancement of osteogenesis by nano-fibrous scaffolds incorporating rhBMP-7 nanospheres. 2087-2096. (2007) with permission from Elsevier.

3.6. Modifications to controlled release polymers

One common approach to changing the release kinetics of scaffold-based delivery systems is to modify the surface of the material with a substrate that binds selectively or non-selectively with drugs and other bioactive molecules. Surface modification has been used in tissue engineering approaches generally to improve the hydrophilicity, mechanical properties, and biocompatibility of a polymer scaffold. Biocompatibility is improved by increasing the ability of cells to attach, spread, proliferate, and differentiate throughout the scaffold. Frequently used surface modifiers include extracellular matrix proteins or peptides such as collagen[202–204], fibronectin,[205] laminin[205], and gelatin[203,206]. Growth factors[207], synthetic chemicals[208], and compounds such as graphene[209] have also been used to modify the surface of a scaffold matrix. Various peptides[210–212], often short amino acid sequences of ECM proteins, are also used to increase biocompatibility of scaffold surfaces. Other approaches such as argon plasma[213], phosphonate groups[214], or cold atmospheric plasma[215] modifications have also improved adhesion and cellular infiltration and proliferation on scaffolds.

While these modifications aid in improving biocompatibility of scaffold for regeneration of various tissue types, few actually have been designed to improve controlled release of drugs. In one case, modification of a PLGA scaffold with 2-N, 6-O sulfated chitosan increased adsorption of rhBMP-2 onto the scaffold and prolonged its release.[216] In another example, bFGF modification of a PCL nanofibrous matrix increased cellular proliferation and attachment, and bFGF was also released over two weeks from a scaffold mineralized with hydroxyapatite and a non-mineralized scaffold.[207]

The addition of substrates with affinity to specific drugs, such as heparin, may help reduce the burst effect and extend and sustain drug release from a polymer scaffold.[217]

3.6.1. Heparin based delivery systems with natural scaffold materials

Heparin is a glycosaminoglycan (GAG) known to specifically bind with many enzymes, cytokines, growth factors (including FGF-2 and VEGF), and other proteins. It is a highly sulfated and a highly anionic linear polysaccharide[218] that has varying levels of binding affinity for peptides and proteins. Controlled release of a drug from a heparin based delivery system (HBDS) is dependent on the heparin binding affinity of the drug being released. Researchers developed porous scaffolds made from collagen/hydroxyapatite nanocomposite, which were then modified with heparin and used to deliver VEGF for bone tissue engineering.[218] Using an *in situ* or a post scaffold fabrication modification approach, heparin was incorporated into the scaffold matrix or coated the scaffold surface. VEGF was loaded onto the heparin-modified scaffolds by physical adsorption. Varying amounts of heparin were incorporated into scaffolds and each was tested in an *in vitro* cell proliferation study. The release kinetics of the growth factor from the scaffold was examined for 7 days and showed a reduction in burst release for scaffolds with both types of heparin modification. However, growth factor bioactivity was reduced in comparison to control levels. This study showed improved cell proliferation in the scaffolds prepared with heparin *in situ* but differentiation studies may further determine the potential of this approach. Furthermore, *in vivo* testing and long-term release experiments have yet to be undertaken.

A heparin-containing fibrin-based matrix was developed to deliver nerve growth factor in a controlled manner, as the authors hypothesized that providing a high molar excess of heparin sites would slow diffusion-based growth factor release.[219] Release experiments and *in vitro* cellular assays conducted over 15 days showed a burst release followed by sustained release of

growth factor. Neurite extension was observed in the dorsal root ganglia studies in response to the biphasic release.

Heparin has also been used in combination with fibrin to deliver TGF-β3 in an *in vivo* tendon-to-bone healing model.[220] The *in vitro* release studies showed that the incorporation of the HBDS into the fibrin matrix reduced the burst release showed potential for sustained, long-term release. The delivery system was evaluated *in vivo* using a rat model up to 56 days. While growth factor delivery led to significant improvements in mechanical and structural properties, scar tissue reduction was not observed. Further optimization of this delivery system and increased understanding of the *in vivo* release kinetics are needed.

3.6.2. Other affinity-based controlled release systems

Heparin is frequently used to functionalize a 3D matrix for controlled release because it has affinity to many proteins. In addition to the use of heparin as a surface modifier, hydrogels and scaffold have been modified in several other ways to achieve affinity-based controlled release. These examples are covered in more detail in recent reviews of affinity-based delivery systems[221,222], and include use of cyclodextrins, DNA aptamers, protein-protein interactions, ionic interactions, and others. Cyclodextrins, which are cyclic oligosaccharides, can be fabricated as hydrogels or can be used to coat devices, scaffolds, or prostheses. They have been effectively applied to deliver antibiotics while reducing burst effect and extending length of treatment.[223] DNA aptamers are single stranded oligonucleotides that have high affinity for specific targets. They have been used to deliver PDGF-BB for up to 25 days in modified composite hydrogel-microparticle delivery system[222] and both PDGF-BB and VEGF in a functionalized polystyrene microparticles for 10 days.[224] Protein-protein interactions take advantage of peptides with specific affinity to growth factors in delivery systems to help control their release.

For example, a PEG hydrogel was modified with various peptides to modulate and tune the release of bFGF for more than 30 days.[225] Similarly, a peptide derived from the VEGF receptor was used to modify PEG hydrogel microspheres and regulate VEGF delivery for up to 30 days.[226]

3.7. Other novel/unique approaches to controlled release

Other approaches to controlled release are being explored for various tissue engineering applications. The spatiotemporal control of drug delivery is governed by the individual needs of a specific tissue type or mechanism of action of a drug. For example, the pulsatile treatment of parathyroid hormone (PTH) stimulates osteogenesis while a sustained delivery of the same hormone results in resorption of existing bone.[227] As previously mentioned, some tissue engineering systems take advantage of a burst release to deliver a higher dose of a drug that promotes early cell differentiation. A number of highly specialized drug delivery systems are therefore being developed and some of these are highlighted below.

3.7.1. Multiphasic devices allow pulsatile or sequential delivery

A multiphasic device physically separates a bioactive molecule with a material film and allows the sustained, pulsatile delivery of a drug over an extended period of time. Pulsatile release of PTH is achieved in a device made of polyanhydride isolation layers and PTH-loaded alginate drug layers in a PLLA cylinder.[228] Four sequential doses of PTH were released with 24 hours of separation between each pulse. This delivery system offers the additional flexibility to deliver multiple drugs and additional studies that incorporate this device into a scaffold for *in vitro* and *in vivo* tissue regeneration are ongoing.

In another approach, researchers used multilayered self-assembled polymer-based biomimetic implant to deliver rhBMP-2 and gentamicin for healing bone defects and for

treatment of orthopedic implant surfaces.[229] This device takes advantage of a laponite clay barrier between drug layers that prevents interlayer diffusion and allows for sustained release. In this system, antibiotic is released early in the treatment, while rhBMP-2 is released for up to 55 days. The system showed positive antibacterial activity and increased ALP activity over a 5-week study. Testing of this device *in vivo* and incorporation of different drugs and growth factors are needed to demonstrate the value of this approach. The addition of more layers may increase concern about the size of the device for surgical implantation.

In wound dressing, regeneration of epidermal tissue is stimulated by exposure to growth factors or other bioactive agents. A multilayered hydrogel was designed[230,231] with an internal layer comprised of a gelatin and hyaluronic acid film crosslinked with genipin and loaded with proadrenomedullin N-terminal 20 peptide (PAMP), which is a natural peptide that has a proangiogenic and antimicrobial effect. An external layer comprised of biodegradable polyurethane was loaded with nanoparticles of bemiparin, which promotes the activation of VEGF and FGF. The internal layer slowly releases PAMP and the external layer provides mechanical stability and releases bemiparin. This device was tested in two *in vivo* models for 14 days and produced promising results.

3.7.2. Magnetic molecularly imprinted polymer controlled release systems

Molecularly imprinted polymer (MIP) nanoparticles are created with binding sites that have specific affinity for a target molecule. Magnetic MIPs, or MMIPs, are made by a new technique that involves encapsulating an inorganic magnetic particle with molecularly imprinted polymers. MIPs have unique chemical and physical properties, including large surface area, which make them useful for drug delivery. The introduction of an inorganic magnetic particle helps resolve inefficiencies and reduce the time in separating MIPs from solution.[232] A new

method of synthesizing MMIPs involves the use of a cross-linker *N,N* –bis methacryloyl ethylenediamine, which was used to prepare nanoparticles that could deliver meloxicam, a non steroidal anti-inflammatory drug, in a controlled manner. During *in vitro* release testing, MMIPs were exposed to simulated gastric, intestinal, and biological fluids by varying pH from 1 to 6.8 to 7.4, respectively. The release experiments were carried out for 36 hours and showed a burst release in the first 5 hours followed by a sustained release for the remainder of the experiment in gastric and intestinal simulated fluids. At a biological pH of 7.4, the burst release extended to the first 10 hours and was followed by a sustained release for up to 40 hours. This novel material may prove to be useful but release times must be extended and additional *in vivo* release studies are needed.

3.8. Areas of need for improving controlled release platforms

3.8.1. Sequential or simultaneous delivery of multiple drugs

Complex tissues are often responsive to multiple factors at different points in time. Much of what we know about new tissue formation is learned from our understanding of pre-natal and post-natal tissue growth and formation. It is becoming increasingly clear that the ability to finely control the release of drugs and growth factors from 3D scaffolds can enhance tissue engineering and reduce healing time of injury and defects. Sequential delivery of two drugs has been explored using scaffolds, composite scaffold/hydrogel-microsphere systems, core-shell polymer matrices, and hydrogels. Several studies have examined the effect of sequential delivery of VEGF followed by PDGF for vascular tissue regeneration, including those designed to recover heart function following myocardial infarction.[233–238] Other drug combinations have also been explored for sequential delivery in vascular tissue engineering.[239–242] Additional systems have been designed to sequentially deliver BMPs, simvastatin, FGFs, VEGF, and other

drugs in different combinations for bone/dental tissue regeneration.[137,243–254] Few sequential delivery systems have been designed that target regeneration of other tissue types, such as neural tissue[255,256] or cartilage[257]. Some sequential delivery systems have only been tested using model proteins or drugs.[258,259] Multiphasic delivery of drugs from composite polymer systems[198,260–267] allow for the delivery of more than two drugs[268] or two doses of a drug. These devices can be designed as core-shell structures or multilayered devices in which drugs are separated by barrier layers.

For sequential delivery systems, considerable work has been done in the areas of vascular and bone tissue engineering. While the combination of PDGF-BB and VEGF shows promise, additional drug combinations may also enhance vascular tissue regeneration. Similarly, many combinations of drugs have been used for sequential delivery, but no single combination of drug, dose, and temporal delivery has been identified as superior to others. Optimization of these systems is needed, as is the ability to deliver more than two drugs. As controlled release systems increase in complexity, optimization of these systems will be challenging. Understanding the underlying mechanisms by which drug combination act over time is important to optimizing delivery systems. Improvements in the ability to control the temporal delivery of drugs will improve the ongoing research that supports multiple growth factor/drug release.

The types and combinations of materials used for controlled release in tissue engineering are numerous. However, many still lack the ability to extend release of drugs past 1 or 2 weeks. Surface modifications and functionalization of delivery systems provide a means for extending treatment. Heparin-based systems are most commonly used, but newer approaches have been developed. Most of these systems, however, have only been designed and evaluated for the delivery of a single drug.

Determining *in vitro* release kinetics is insufficient in understanding the effects of drugs released from a scaffold *in vivo*. Few studies, if any, examine the *in vivo* release kinetics, which are important to understanding the spatiotemporal control that a delivery system has. Furthermore, additional studies are needed to evaluate tissue engineering constructs with *in vivo* defect models. While subcutaneous implantation models provide useful data, fewer studies have tested the viability of healing injuries or critical defects within the appropriate *in vivo* microenvironment. Given the limitations of small animal models, studies involving large animals and human clinical trials are important to optimization of scaffolds and devices. These areas of focus are needed in future *in vivo* controlled release studies.

3.9. Conclusion and perspectives

Controlled release for tissue engineering is a growing field that is seeking new ways to improve the 3D microenvironment provided by material scaffolds and to stimulate molecular signaling of cells within these microenvironments. Increased understanding of molecular signaling is being used to develop delivery systems that finely control the spatiotemporal release of multiple drugs and enhance new tissue growth. New materials and new combinations of materials are being synthesized to achieve different release kinetics that better support regeneration of various tissue types. Material combinations, for example those that combine nanofibrous matrices with micro/nanospheres is intended to offer the control factor release and 3D microenvironment suitable for tissue engineering.

Clinical applications for these new controlled release systems are being developed across many tissue types, including bone, cartilage, blood vessels, epidermal, cardiac, neural, and others. Porous scaffolds and hydrogels are also amenable to the development of patient-specific regenerative treatments utilizing the potential of iPSCs.[269] Advances on all three fronts of

tissue engineering – material matrix design, drug delivery, and regenerative cells – will help to push the field into clinical use in the near future.

Chapter 4. Controlled Release of BMP-7 and FGF-2 from 3D PLLA Scaffolds Enhances Ectopic Osteogenesis in Mice

4.1. Introduction

4.1.1. Limitations of autologous bone grafts for treating critical size defects

More than 500,000 large volume bone injuries each year are treated with bone grafts or synthetic bone graft substitutes. There is a high medical cost, estimated at $2.5 billion, associated with the invasive interventions used to treat these injuries.[270] Despite the widespread use of autologous bone grafts as the reference standard treatment, there are limitations to this approach. Namely, autologous bone grafts require donor tissue to be harvested, typically from the iliac crest of the hip or from bone near the site of injury. Donor site morbidity, including inflammation and infection, has been reported.[7] For repair of large defects where more graft material is needed, availability of donor site bone is often limiting.[271] At the injury site, shaping the autologous bone to the geometry of the injury or defect is also a significant limitation. The use of allografts or xenografts, where tissue is taken from human donors or animals, is further complicated by potential immune rejection by the graft recipient[272] and disease transmission from the donor[273].

4.1.2. Polymeric scaffolds combined with drug delivery systems have the potential to improve bone tissue engineering

To overcome these limitations, bone tissue engineering approaches have been developed over the past 20 years. In particular, polymeric scaffolds with biomimetic features have shown

great promise in repair of critical size bone defects, thereby avoiding the need to harvest donor tissue.[45] Scaffolds with sufficient porosity allow cells to penetrate and attach throughout the interior of the scaffold. Interconnected pores also allow blood vessel in-growth, supporting cell survival and tissue regeneration.[62,183] We previously demonstrated that scaffolds with nanofibrous architecture, whose fibers mimic collagen fibers found in native extracellular matrix, are advantageous for bone tissue engineering.[25,274]

To further enhance the regenerative properties of biomimetic scaffolds, one strategy has been to deliver growth factors to the site of injury and, thereby, initiate repair by promoting infiltration of the scaffolds by surrounding progenitor cells[275]. BMPs are the most commonly used growth factors in bone regeneration. BMP-2, BMP-4 and BMP-7 have all been shown to induce bone formation[276]. However, despite significant evidence of their potential benefit in bone repair and regeneration in animal and preclinical studies, the clinical uses of BMPs are limited to a few FDA-approved indications. One of the main drawbacks of commercially available BMP products is their reliance on supraphysiological BMP concentrations to obtain desired clinical outcomes. This not only increases cost, but also leads to more frequent complications in certain applications, particularly those associated with off-label use[277,278]. After a number of serious side effects were reported, the FDA published a notice regarding the off-label use of BMP products that diminished their use in the clinic.[8]

These disappointing results emphasize the need for new BMP delivery strategies if the full clinical promise of BMP products is to be realized. Possible strategies to improve the efficacy of BMP-induced bone healing include 1) long-term controlled release of BMP at physiologically-relevant doses, 2) the delivery of BMP together with other growth factors using distinct dosages

and release kinetics, or 3) the provision of higher numbers of responding cells/stem cells at the site of implantation in the host [279–281].

As a first step to enhance BMP regenerative activity, we developed a controlled release system for BMP delivery and showed that localized, sustained delivery of recombinant human BMP-7 (rhBMP-7) from PLGA nanospheres immobilized on PLLA nanofibrous scaffolds induced significant bone formation, compared to passive adsorption of rhBMP-7 onto the scaffold. The latter strategy was ineffective due to either the loss of rhBMP-7 biological function or insufficient duration of treatment[125]. In the present study, we investigate the use of this controlled release system to deliver BMP together with a potent bone-related growth factor, FGF-2.

4.1.3. FGF-2 is an attractive growth factor for bone tissue engineering applications

Basic fibroblast growth factor (bFGF, also known as FGF-2) has multiple functions in tissue growth and regeneration. FGF-2 can stimulate the proliferation of a variety of cells, including fibroblasts, vascular endothelial cells, chondrocytes, osteoblasts[282] and BMSCs[147,283]. FGF-2 can also enhance the migration of rabbit and human BMSCs. It is reasoned that FGF-2 benefits bone regeneration at least partially through its role in promoting stem cell recruitment and proliferation.

Both autologous bone grafts and tissue engineering constructs are subject to failure when implanted *in vivo*, partially due to the lack of sufficient vascularization in the newly formed bone.[284] Vascularization of bone is necessary for transport of nutrients, oxygen, and biological signals[285]. FGF-2 is a potent stimulator of new blood vessel formation[282] and, as studies have suggested, improves bone repair via angiogenic stimulation[286,287].

Based on these properties, researchers have attempted to use FGF-2 to improve BMP-induced bone regeneration. However, this strategy yielded contradictory results[135,288–290].

Promising results indicate that low doses of FGF-2 can promote BMP-directed osteogenic differentiation *in vitro*[291] and *in vivo*[132,292], though there may be an age-related component to their combined efficacy. In one study, BMP-2 and FGF-2 were simply adsorbed onto the surface of a collagen-containing tissue engineering scaffold [135]. Surface adsorption of proteins to a scaffold results in rapid release of nearly all the growth factor in a matter of hours. *In vivo*, this leads to the rapid elimination of the growth factors from the body[293] thereby preventing sustained effects. A controlled release system that has ability to locally deliver growth factors at different doses and with tunable release kinetics is needed to advance these tissue engineering platforms.

In the current study, we describe a new approach for regulated delivery of BMP-7 and FGF-2 using nanofibrous PLLA scaffolds and PLGA nanospheres to tune the delivery of both growth factors in an ectopic murine bone formation model. We also describe studies designed to elucidate the role of FGF-2 in bone formation with the help of the controlled release system.

4.2. Materials and Methods:

4.2.1. Preparation of nanospheres immobilized on nanofibrous scaffolds and *in vitro* release study.

PLGA copolymers with LA/GA ratio of 50:50 (Medisor®, PLGA50-6.5K, M_w =6.5 kDa; PLGA50-64K, M_w =64 kDa) were purchased from Alkermes Inc. (Wilmington, OH). Poly (L-lactic acid) (PLLA) with inherent viscosity of 1.6dL/g was purchased from Boehringer Ingelheim (Ingelheim, Germany). PLLA nanofibrous scaffolds were fabricated using an established phase separation and sugar sphere leaching technique[125]. The scaffolds used in the current study were cut into a disc-like shape with a height of 2mm and a diameter of 7.2mm. BMP-7 (kindly provided by Stryker Biotech, Hopkinton, MA) and FGF-2 (kindly provided by Shenandoah Biotech,

Warwick, PA) were encapsulated into PLGA nanospheres using an established double emulsion technique[125]. Two different PLGA formulations (PLGA50-6.5K referred to as fast release, PLGA50-64K referred to as slow release) were used for encapsulation of FGF-2 at each dosage outlined below. BMP-7 was encapsulated in PLGA50-64K nanospheres. The structure of the scaffolds after nanosphere immobilization was examined using scanning electron microscopy (SEM, Philips XL30 FEG). 10ng, 100ng and 1000ng doses of FGF-2/scaffold was used for *in vivo* implantation. BMP-7 was loaded at a dosage of 5μg/scaffold. FGF-2 and BMP-7 PLGA nanospheres were added to scaffolds separately using a post seeding method[125]. Release profiles from PLGA nanospheres-immobilized PLLA scaffolds were determined *in vitro* by radioactivity detection. The radio-labeled ^{125}I-FGF-2 (PerkinElmer, Shelton, CT) and ^{125}I-BMP-7 (Department of Epidemiology, the University of Michigan) were added as a tracer respectively (^{125}I-FGF-2: unlabeled FGF-2=1:100, ^{125}I-BMP-7: unlabeledBMP-7=1:100). Scaffolds loaded with PLGA nanospheres were placed in 1.0mL PBS (10mM, pH=7.4 with 0.1% BSA) at 37°C under orbital shaking at 60rpm. Release medium was collected at the designated time points: 1, 3, 5, 7, 10, 14, 21, 28, 35, 42, 49, 56, 63 days and equal amount of fresh medium was added. The radioactivity of collected media was analyzed using a gamma counter (Gamma 5500, Beckman) and converted to calculate the amount of released protein. Scaffolds with nanospheres containing only heparin/gelatin and bovine serum albumin (BSA) were prepared as the control.

4.2.2. Cell isolation, expansion, migration, proliferation, and differentiation *in vitro*.

Rabbit BMSCs were isolated from two-week-old New Zealand White rabbits and collected by flushing of the femoral bone marrow using an 18-gauge syringe needle. 10 ml of marrow was added to 1000 U of heparin-containing maintenance media (high-glucose alpha-MEM (Gibco) containing 10% fetal bovine serum (Gibco) and antibiotics (penicillin G, 100 U/mL; streptomycin,

0.1 mg/mL). The marrow was filtered through a cell strainer to exclude fatty tissues and blood clots, washed with PBS once and fresh media twice, and centrifuged after each wash.[83] Rabbit osteoblasts were obtained by breaking femurs into bone chips and culturing in Dulbecco's Modified Eagle Media (DMEM) supplemented with 10% FBS, 100U/ml penicillin and 100mg/L streptomycin. The primary cells were used for the following studies.

For the colony-forming unit-fibroblast (CFU-F) assay, BMSCs were cultured in six-well-plates at 2×10^5 cells/well in 1mL of the above-mentioned medium, which was changed every 3 days, and cultures were maintained for 10 days. At the end of the culture, the colonies were stained with crystal violet (0.5% w/v in 25% methanol) and the positive colonies were counted using ImageJ software (NIH, Bethesda, MD).

The migration assay was performed in transwell dishes (6.5mm diameter, 8μm pore filters-Corning Costar, Cambridge, MA) as previously described with modification[294]. The upper side of the transwell filter was coated with 100μL 0.1% (w/v) type I collagen solution from rat tail (Sigma; St. Louis, MO) overnight at 4°C. The cells were added to the upper chamber at 2×10^5/well in 100μL serum-free α-MEM after serum starvation for 24h, and 600μL of serum-free α-MEM with different growth factors was added to the bottom chamber. After overnight incubation of the transwells at 37°C, 5% CO_2, the cells on the filters were fixed and mounted on glass slides using mounting medium containing 4'-6-diamidino-2-phenylindole (DAPI) and observed under a fluorescence microscope.

Cell proliferation was measured by a colorimetric method using a 3-(4, 5-dimethylthiazol-2-yl)-5-(3-carboxymethoxyphenyl)-2-(4-sulfonphenyl)-2H-tetrazolium (MTS tetrazolium) compound (Cell-Titer 96 Aqueous One Solution Cell Proliferation Assay; Promega, Madison, WI). The cells were cultured at $2\times10^4/cm^2$ in the α-MEM containing 10% FBS, 100U/mL

penicillin and 100mg/L streptomycin. The absorbance at 490nm was measured by a 96-well spectrophotometer on days 1-5.

To induce osteoblastic differentiation, cells were cultured 2×10^5 at cells/cm^2 in DMEM supplemented with 50μg/mL ascorbic acid, 10mM β-glycerophosphate (Sigma; St. Louis, MO), and specific growth factors (FGF-2/BMP-7). To measure mineralization, calcium deposits were dissolved in 0.5N hydrochloric acid (HCl) overnight on a shaker at 4°C. Calcium content was quantified in the supernatant with Pointe Scientific Calcium Liquid Reagents according to the manufacturer's manual. Total calcium content of each sample was measured by the o-cresolphalein-complexone method. For example, 50 μl of sample was incubated with a 250 μl mixture of the color and base reagents. Absorbance was measured at 570 nm. A calcium standard was used to calculate the content of calcium in each sample.

4.2.3. Subcutaneous implantation and specimen analysis.

The animal procedures were performed according to the guidelines approved by the University of Michigan Committee of Use and Care of Laboratory Animals. Animals were housed in groups and maintained with a normal diet. Male 6-8-week old C57BL/6 mice (Charles River Laboratories International, Inc., Wilmington, MA) were used for the subcutaneous implantation of nanospheres-immobilized PLLA scaffolds study. Surgery was performed under general inhalation anesthesia with isofluorane as previously described[274]. A single midsagittal incision was made on the dorsa, and two subcutaneous pockets were created using blunt dissection. One scaffold was implanted subcutaneously into each pocket and each animal received 2 constructs. The mice were randomly sorted into four groups, corresponding with the dose of FGF-2 loaded into each scaffold. A total of 48 (8 groups, n=3 per group, 2 time points) scaffolds were implanted in 24 mice and evaluated for new bone formation after 3 and 6 weeks. These time points were

found to be suitable to examine the differences in mineralization in our previous studies. Subsequently, a total of 9 constructs (3 groups, n=3 per group) were implanted in 5 mice and evaluated after 1 week for cell infiltration and expression of angiogenic markers. The cell-scaffold constructs were harvested, fixed in 10% buffered formalin, and processed.

The implants at 6 weeks for the dual-release study were analyzed by microcomputed tomography (μCT). The specimens were scanned at a voxel size of 18μm using the μCT scanner (GE Healthcare Pre-Clinical Imaging, London, ON). Micro View software was used to make a three-dimensional reconstruction from the set of scans. A fixed threshold (1,200) was used to extract the mineralized bone phase and the bone volume was calculated. After the X-ray/μCT analysis, each specimen was cut into two equal parts: half was used for the total calcium content detection using the LiquiColor® kit (Stanbio laboratory, TX) after extraction by 0.5N HCl solution[274] and half was paraffin embedded for histology analysis. Five-micrometer sections were cut and stained with hematoxylin and eosin (H & E), von Kossa, or Alcian blue (Sigma; St. Louis, MO), for light microscopic observation. For immunohistochemistry detection, rehydrated sections were pre-treated with pepsin solution for 30min, incubated with CD146 or Factor VIII-related antigen/von Willebrand factor antibody (Thermo Fisher Scientific Inc., Fremont, CA, USA) at 1:100 dilutions at 37°C for 2h and detected by a cell & tissue staining kit (R&D systems Inc., Minneapolis, MN, USA) according to the manual. All sections were counterstained with hematoxylin.

4.2.4. RNA extraction and real-time PCR.

The total RNA was isolated from rabbit BMSCs after 2 weeks of osteogenic induction and distinct growth factor treatments using TRIZOL reagent (Invitrogen, Carlsbad, CA). An equivalent amount of RNA samples (1μg) were initially reverse transcribed for 1st strand cDNA synthesis

(TaqMan® Reverse Transcription Reagents, Applied Biosystems, Foster City, CA). Template DNA was then used in gene-specific amplification. Real-time PCR was performed in a 7500 Real-Time PCR System (Applied Biosystems, Foster City, CA) by using TaqMan Master Mix Reagents (Applied Biosystems, Foster City, CA), to measure Runx2 (5'-ccgcacgacaaccgcaccat-3' and 5'-cgctccggccca- caaatctc-3') expression. The housekeeping gene, glyceraldehyde-3-phosphate dehydrogenase (GAPDH), was used as an endogenous reference gene to normalize the calculation through the Comparative Ct (Cycle of threshold) value method.

4.2.5. Statistical analysis.

For all experiments, values were reported as mean ± SD based on triplicate samples. The experiments were performed at least twice to ensure reproducibility. To test the significance of observed differences between the study groups, an unpaired Student's t-test was applied. A value of $p<0.05$ was considered to be statistically significant.

4.3. Results

4.3.1. Effects of FGF-2 on BMSC proliferation and differentiation *in vitro*

A series of cell culture studies were conducted to define basic parameters for BMP-7 and FGF-2 treatment necessary to stimulate proliferation and osteogenic differentiation of BMSCs. Treatment of cells with FGF-2 alone or in the presence of BMP-7, stimulated proliferation, while BMP-7 by itself was without effect on proliferation**[Figure 4.1.A]**. The addition of FGF-2 also caused a dose-dependent increase in expression of the osteogenic transcription factor, RUNX2, and this response was further stimulated in the presence of BMP-7, as measured by quantitative reverse transcriptase polymerase chain reaction (qRT-PCR) after 2 weeks of osteogenic induction and distinct treatment with growth factors **[Figure 4.1.B]**. Subsequent studies examined effects of

FGF-2 on osteogenic induction of BMSCs with or without 100ng/ml BMP-7. This dose was selected based on previous studies examining BMP-7-induced osteogenesis.[295,296] FGF-2 was added at 2, 5, and 25ng/ml for the first three days of growth in osteogenic medium. Osteoblast differentiation, measured by calcium deposition, was then measured after 2 and 4 weeks **[Figure 4.1.C, 4.1.D]**. Although FGF-2 by itself modestly increased mineralization compared to osteogenic medium alone, in all cases, mineralization was further increased by BMP-7 (2-week time point, Fig. 1c). After 4 weeks, FGF-2 (25 ng/ml) continued to stimulate mineralization above the levels obtained with BMP-7 alone **[Figure 4.1.D]**. The duration of FGF-2 treatment also affected mineralization. BMSCs were grown in osteogenic media with or without BMP-7 and treated with increasing concentrations of FGF-2 for 3, 6, or 14 days **[Figure 4.1.E-G)**. At all FGF-2 concentrations, a short-term treatment with FGF-2 (first 3 days) was most favorable for calcium deposition by BMSCs, while the continued presence of FGF-2 for 6 or 14 days reduced mineralization, though to a lesser degree at 25ng/ml BMP-7 and FGF-2 were then evaluated using simultaneous or sequential treatments **[Figure 4.1.H-J)**. Under sequential treatment, osteogenic media (no added BMP-7) was supplemented with FGF-2 for 3 or 6 days, followed by addition of BMP-7 for the remaining time up to day 14. These data show that simultaneous treatment with BMP-7 and FGF-2 is preferable to sequential treatment, particularly at the lower doses (2ng/ml, 5ng/ml) **[Figure 4.1.H, Figure 4.1.I]**. Although there was no significant difference between sequential or simultaneous delivery of the factors at 25ng/ml of FGF-2 **[Figure 4.1.J]**, the overall mineralization by cells at this dose was greater than mineralization at 2ng/ml and 5ng/ml FGF-2. Together, these data suggest that 25ng/ml of FGF-2 given for three days together with continuous BMP-7 treatment can enhance osteogenic differentiation of BMSCs.

4.3.2. Effects of FGF-2 on maturing BMSCs or mature primary osteoblasts

Some studies reported that FGF-2 has a positive effect on osteoprogenitor cells to enhance mineralization of tissue and expression of pro-osteogenic genes.[297,298] To determine whether BMSCs might be more susceptible to FGF-2 as they mature and undergo osteoblast differentiation, cells were treated with FGF-2 according to a delayed treatment schedule **[Figure 4.2.A]**. After one or two weeks of osteogenic differentiation with BMP-7, BMSCs were treated simultaneously with BMP-7 and FGF-2 at 0, 2, 5, and 25ng/ml. In all three treatment schedules, delayed treatment of BMSCs with FGF-2 resulted in decreased calcium deposition at 2 and 5ng/ml. At 25ng/ml, delayed treatment with FGF-2 resulted in similar amounts of calcium deposition to the positive control (BMP-7 alone) **[Figure 4.2.B-D)**. At low doses, FGF-2 inhibited osteogenic differentiation when treatment was delayed, while delayed treatment of FGF-2 at 25ng/ml was neither beneficial nor detrimental.

To examine effects of BMP-7 and FGF-2 on more mature cells, primary osteoblasts were isolated from rabbit femurs and cultured to passage 3 followed by growth in osteogenic media supplemented with FGF-2 and BMP-7 using the regimen shown **(**i.e. treatment with increasing concentrations of FGF-2 for days 1-4 together with continuous BMP-7 treatment **[Fig.4.2.E]**. After two weeks, treatment of osteoblasts with FGF-2 at all three doses resulted in significantly higher mineralization than treatment with BMP-7 alone **[Figure 4.2.F]**. At the 4-week time point, FGF-2 at 25ng/ml maintained a significantly higher level of mineralization versus untreated control while low doses of FGF-2 did not **[Figure 4.2.G]**. Together, these data suggest that 25ng/ml of FGF-2, administered early during treatment of BMSCs or osteoblasts can enhance mineralization of cells, while delayed treatment with FGF-2 has an inhibitory effect at low doses. These *in vitro* studies provide general parameters for designing treatment profiles for *in vivo* studies.

4.3.3. Dual-release of BMP-7 and FGF-2 on 3D PLLA nanofibrous scaffolds.

Our previous research demonstrated the advantages of porous and nanofibrous 3D PLLA scaffolds for bone tissue engineering[47,299] and controlled release of BMP-7[198]. Based on our *in vitro* observation that early short-term exposure to FGF-2 combined with continuous to BMP-7 treatment gave the strongest osteogenic response, a controlled release system was developed for the simultaneous short-term release of FGF-2 and long-term release of BMP-7. To achieve this, we designed a dual drug delivery system that combines two formulations of drug encapsulated PLGA nanospheres with 3D PLLA scaffolds **[Figure 4.3.A)**. FGF-2 was encapsulated in low molecular weight PLGA nanospheres, designated as PLGA50-6.5k (fast release) and high molecular weight PLGA nanospheres, designated as PLGA50-65k (slow release) nanospheres. BMP-7 was encapsulated in PLGA50-65k nanospheres. Each formulation of PLGA maintained a 50:50 ratio of lactic acid to glycolic acid. The resulting nanospheres were then incorporated onto the 3D PLLA scaffolds. The scaffolds preserved their 3D multi-level porous architecture after nanosphere incorporation **[Figure 4.3.B]** with the spherical macro-pores of 250-425μm in diameter, inter-pore openings of approximately 100μm, and nanofibers of 50-500nm in diameter within the pore wall **[Figure 4.3.C]**. PLGA nanospheres encapsulating FGF-2 and BMP-7 were spherical with an average diameter in the range of 300-600nm. They were attached to the PLLA nanofibers and uniformly distributed throughout the scaffolds.

Figure 4.3.D shows the *in vitro* release profiles of FGF-2 incorporated into fast and slow release nanospheres. PLGA50-6.5k released 550ng of FGF-2 with an initial burst at day 1 (55% of total FGF-2 incorporated) followed by a slow release of 30-40ng at each designated time point within the first two weeks. Approximately 78% of the FGF-2 incorporated into nanospheres was released within the first two weeks. The release rate subsequently slowed to 10-20ng at each

designated time point such that approximately 80% of the total FGF-2 incorporated into the scaffold was released by 60 days. Nanospheres made of PLGA50-64k released FGF-2 at a slower rate. These nanospheres released only 260ng FGF-2 in the initial burst at day 1 (26% of total FGF-2 incorporated), followed by a slow release of 20ng at each designated time point within the first four weeks (47% released within the first 4 weeks). PLGA50-64k nanospheres showed a second fast release on day 35 with 130ng released (13%), which was in accordance with the significant mass loss and disintegration of PLGA nanospheres at that time. They subsequently released 30-40ng at each designated time point until week 9.

4.3.4. Stimulation of BMP-7-induced bone formation by controlled release of FGF-2.

PLLA scaffolds with or without FGF-2 and BMP-7-loaded PLGA nanospheres were subcutaneously implanted into mice and ectopic bone formation was measured after 3 and 6 weeks. Bone formation was assessed by μCT and histological analysis of excised implants. To quantify mineral content, implants were dissolved in 0.5 N HCl for direct measurement of calcium. Total calcium content at 3 weeks in the group treated with BMP-7 + FGF-2 (100ng, fast release) was the highest among all the groups. The total calcium content of in this group was ~3.8, ~2.2 and ~2.1 fold higher than the BMP-7 group, BMP-7 + FGF-2(10 ng, slow release) and BMP-7 + FGF-2 (100ng slow release), respectively. BMP-7-induced calcification in groups with high dose FGF-2 (1000 ng/scaffold) were noticeably reduced when compared to BMP-7 alone. The inhibitory effect of high dose FGF-2 on bone formation was more obvious by analysis of the total calcium content per scaffold after six weeks. At this timepoint, the highest calcium content was observed in the BMP-7 + FGF-2 (10ng, slow release) and BMP-7 + FGF-2 (100ng, slow release) groups, which were significantly higher than the BMP-7 alone group [**Figure 4.4.A**].

The newly formed bone at 3 weeks in all implants was mineralized as observed by von Kossa staining of histological sections **[Figure 4.4.B]**. The positive von Kossa staining consistent with newly formed bone was noted throughout the BMP-7 scaffolds, while bone formation was scant to non-existent in the control group and the high dose FGF-2 groups. Consistent with the radiographic examination and calcium content detection, there was more intense von Kossa-positive mineral in the BMP-7 + FGF-2 (100ng, fast release) group than other groups.

In order to further evaluate the bone formation in the recovered implants, microcomputed tomographic (μCT) analysis was conducted on 6-week samples. Comparing the bone volume fraction of each group, there was a significantly greater volume in the BMP-7 + FGF-2 (10ng, slow release) group than BMP-7 alone (29.6%±6.9% vs. 9.5%±2.3%). A statistically significant difference also was observed between BMP-7 + FGF-2 (100ng, fast release) group and BMP-7 alone (17.3%±2.3% vs. 9.5%±2.3%). However, such differences were not observed in BMP-7 + FGF-2 (10ng, fast release) or BMP-7 + FGF-2 (100ng, slow release) groups compared with BMP-7 alone **[Figure 4.4.C]**. While the BMP-7 + FGF-2 (10ng, slow release) and BMP-7 + FGF-2 (100ng, fast release) groups showed no difference in calcium content, there was a noticeable, but statistically insignificant difference in the bone volume fraction between these groups. We believe that this apparent discrepancy may be attributed to the fact that μCT was conducted on a whole sample, while calcium quantification was conducted on half the sample, as the other half was preserved for histological analysis. The heterogeneity of new bone formation throughout the scaffold, combined with our analytical approach, may have contributed to this observation.

Histological analysis was used to visualize the new bone tissue distribution in the scaffolds. As the images show, no bone was formed in control group or high dose FGF-2 (1,000ng) groups at 3 weeks, although cells and tissue penetrated throughout the scaffolds in all groups **[Figure**

4.4.D]. The cells observed were predominantly fibroblasts with some multinucleated giant cells and adipocytes in the marrow regions. Significant new bone (stained pink with H & E staining) was observed on the scaffold surface of low and medium dose FGF-2 (10ng, 100ng/scaffold) and with BMP-7 alone. Compared with BMP-7 alone, BMP-7 + FGF-2 (10ng, fast release), and BMP-7 + FGF-2 (100ng, slow release), new bone in the BMP-7 + FGF-2 (10ng, slow release) and BMP-7 + FGF-2 (100ng, fast release) displayed more mature structural features including bone marrow like tissue. This suggests that the ectopic bone formation process was accelerated by the administration of FGF-2. It was interesting that fewer hypertrophic chondrocytes were observed by Alcian blue staining in groups with increased bone formation (10 ng/slow release or 100ng/fast release) compared to other groups with significant bone **[Figure 4.4.E]**, which not only indicates that BMP-7-induced bone formation was via endochondral ossification, but also that FGF-2 promoted bone formation by accelerating the ossification of hypertrophic chondrocytes **[Figure 4.4.F]**. The well-developed bone marrow and bone tissue were observed in all these groups, although there was still no bone tissue detected in control, or high dose FGF-2 (1000ng/scaffold) groups. Taken together, these data clearly indicate that BMP-7-induced endochondral ossification can be promoted by FGF-2, but only when it is delivered at a defined dosage and release rate.

4.3.5. Stem cell recruitment and angiogenesis regulated by FGF-2 during the early stage of endochondral ossification.

Due to the pleiotropic effects of FGF-2, we sought to determine whether FGF-2 enhanced cell migration and angiogenesis early in ectopic bone formation. In order to study these phenomena, we selected control, BMP-7 alone and BMP-7 + FGF-2 (100ng/fast release) for further analysis. Scaffolds were retrieved 1 week after subcutaneous implantation and analyzed for cellular penetration of scaffolds and for expression of pro-angiogenic factors. Upon retrieval,

scaffolds were cross-sectioned to visualize penetrating tissue. As the histological analysis shows, the penetrating tissue occupied almost half of the scaffold spaces (~1000μm) in the FGF-2+BMP-7 group, while the tissue penetration was seen only in the superficial regions (~300μm) in the BMP-7 and control group **[Figure 4.5.A**]. This data indicates that FGF-2 can promote tissue in-growth into the scaffold, possibly including increased blood vessels and stem cells. To evaluate new blood vessel formation, immunohistochemical staining was used to visualize Factor VIII-related antigen/von Willebrand factor (vWF) and CD31, which are known as endothelial cell markers. Increased staining of CD31 and vWF in the FGF-2 + BMP-7 group compared to the BMP-7 or control groups **[Figure 4.5.B, middle & lower panels]** indicates enhanced vascularization inside the scaffolds. Similarly, neovascularization was detected by CD146 immunohistochemical staining, which is also believed to be an important marker of vascular endothelial cells and pericytes **[Figure 4.5.B, upper panel]**. Immune positive areas of each marker were quantified using ImageJ **[Figure 4.5.C]**. These data suggest that the early angiogenesis, which is known to precede osteogenesis, is promoted by codelivery of FGF-2 with BMP-7 during ectopic bone formation.

In addition to angiogenesis, recruitment of progenitor/stem cells is also necessary for bone regeneration. BMP-7-induced bone formation was possibly enhanced due to increased stem cell recruitment by FGF-2. We confirmed by *in vitro* migration assay that FGF-2 did have the capability to promote BMSCs migration in a dose dependent manner **[Figure 4.5.D]**. Moreover, the CFU-F of BMSCs was also increased by FGF-2 **[Figure 4.5.E]**. Taken together, these data suggest that BMP-7-induced bone formation was enhanced by FGF-2 possibly because FGF-2 can promote angiogenesis, stem cells recruitment, and proliferation. New blood vessels supply

essential nutrients and also deliver progenitor/stem cells, which are responsible for new bone formation, to the scaffold.

4.4. Discussion

Fracture healing and bone regeneration are coordinated processes that are influenced and directed by inflammatory, angiogenic, and osteogenic factors. The effort to deliver multiple growth factors in distinct spatiotemporal patterns that mimic the natural bone regeneration process can potentially improve bone formation [264,300]. We sought to deliver FGF-2 and BMP-7 to enhance the quality and survival of tissue engineered bone. FGF-2 is one of the most abundant growth factors present in skeletal tissue[301] and it has an important role in bone development[302,303], fracture healing[304], and cranial suture fusion[302]. At the cellular level, FGF-2 is known to regulate osteoblast/osteoprogenitor cell proliferation, differentiation and apoptosis[305]. We found that the proliferation and mineralization of BMSCs and primary osteoblasts can be stimulated by FGF-2 *in vitro* **[Figure 4.1]**. The effect of FGF-2 on BMP-7 induced osteoblastic differentiation was dependent on the dosage, duration, and timing of growth factor treatment of cells. Previously, it was demonstrated that FGF-2 expression increases significantly after skeletal fracture in mice and peaks after 1 day. Subsequently, FGF-2 is highly expressed until post-fracture day 9, at which point expression begins to decline.[14] By comparison, BMP expression also increases significantly at post-fracture day 1. Unlike FGF-2, BMP expression continues to increase after day 9 and remains high during fracture healing.[14] The expression patterns of FGF-2 and BMPs after mouse skeletal fracture provide a guideline as to *when* exogenous growth factors might be appropriate and how to optimally combine FGF-2 with BMP-7. Our *in vitro* findings support early, low dose FGF-2, simultaneous with continuous BMP-7 treatment, which mimics the natural expression patterns in mouse skeletal fracture healing.

These data suggest that exogenous FGF-2 can be used to enhance bone formation and also highlight the importance of a multiphasic controlled delivery system. Prior to this study, a controlled release system capable of locally delivering FGF-2 and BMP-7 in distinct patterns and doses had not been developed. A major limitation of FDA-approved BMP products is the supra-physiological doses required to induce bone formation and the side effects that result from such high doses.[306] An ideal tissue engineering construct would serve as a delivery system for growth factors and provide a 3-dimensional (3D) scaffold for cellular activities [197]. Local delivery of growth factors was previously achieved by simple adsorption of the factors onto natural or synthetic polymeric matrices, but the temporal release kinetics from such a platform is hard to control[307,308]. Other approaches including the use of emulsions or gas foaming techniques are able to achieve slow rates of growth factor release, but these systems are limited by the suboptimal architecture and mechanical properties of the associated scaffolds[309–311].

PLLA and PLGA are biodegradable and biocompatible polymers with great potential as tissue engineering scaffolds and drug carriers. The growth factor release rate can be controlled by adjusting factor loading, polymer molecular weight, lactide/glycolide ratio in the copolymer, and formulation methods[312]. In the current study, the co-delivery of BMP-7 and FGF-2 was achieved on a nanofibrous, porous PLLA scaffold. This highly porous scaffold (98%) favors the diffusion of nutrients and oxygen and the in-growth of cells throughout the scaffold. Its fibrous nanostructure mimics the natural collagenous ECM found in native bone and thus provides as a suitable architecture for cell attachment and differentiation. BMP-7 and FGF-2 were released from PLGA nanospheres immobilized onto the scaffold surface. Different growth factor release rates were obtained by manipulating polymer molecular weight in nanospheres **[Figure 4.2]**. This approach is different from the traditional coating method where the release rate of growth factors

depends on the physio-chemical interactions between the adsorbed growth factors and the scaffold surface[197,200] and from methods that seek to embed growth factors within a scaffold[313]. We found that BMP-7-induced osteogenesis can be promoted by co-delivery of FGF-2 at a defined dosage and release rate **[Figure 4.3**], which can be achieved using a composite PLLA scaffold and PLGA nanospheres.

Angiogenesis is a critical process in bone regeneration that is required for the survival of newly formed bone [314]. Regenerative therapies increasingly seek to modulate and stimulate angiogenesis to enhance bone repair and survival of bone tissue engineering grafts. The major angiogenic factors include FGF-2, PDGF, and VEGF. FGFs and VEGF promote angiogenesis mainly by stimulating endothelial cell proliferation and migration[315]. Several studies have shown that a combination of VEGF with BMPs can augment bone formation[249,316,317]. Our data showed that early angiogenesis was increased by the release of FGF-2 **[Figure 4.5.B]**. The presence of blood vessels are favorable for bone regeneration because they supply nutrients, growth factors, and oxygen[290] and are also a source of mesenchymal stem cells during fracture healing. Blood vessels are also critical to the supply of calcium and phosphate ions for mineralization of tissue during later stages of bone regeneration[285]. The increased expression of CD146 and CD31, markers of vascular endothelial cells and pericytes, was observed due to FGF-2 delivery at 1 week **[Figure 4.5.B]**. FGF-2 also showed the ability to directly promote BMSC recruitment and proliferation *in vitro* **[Figure 4.5.C, D]**. This may be another mechanism where FGF-2 could increase the cell numbers in the scaffolds. This opens a new avenue for understand the contribution of angiogenesis to bone formation triggered by FGF-2. Invasion of blood vessels is known to be necessary for the replacement of hypertrophic chondrocytes with bone during

endochondral ossification via their ability to deliver stem cells and osteoprogenitor cells to the site of bone formation[318].

The subcutaneous ectopic bone formation model used in the present study has certain limitations for bone regeneration studies including the relative low number of mesenchymal progenitor cells in the subcutaneous space and the non-orthotopic location of the ectopic bone formed. However, we chose this model because it allowed us to observe the effect of the controlled release of FGF-2 and BMP-7 from our platform in the absence of osteogenic factors that would be secreted from bone in an orthotopic implant. Moreover, we could observe the angiogenic effect of FGF-2 more prominently, in comparison to a calvarial defect model, where the defect site is already well vascularized.

4.5. Conclusion

We concluded that BMP-7-induced ectopic bone formation can be enhanced by controlled release of FGF-2 at a defined dosage and release rate. FGF-2 showed multiple effects on bone regeneration including enhancement of stem cell migration, proliferation and angiogenesis at an early stage. The local controlled dual-release system not only provides a promising technology for bone regeneration applications, but also helps us understand the possible roles of the growth factors, which will in turn provide more potential treatment strategies.

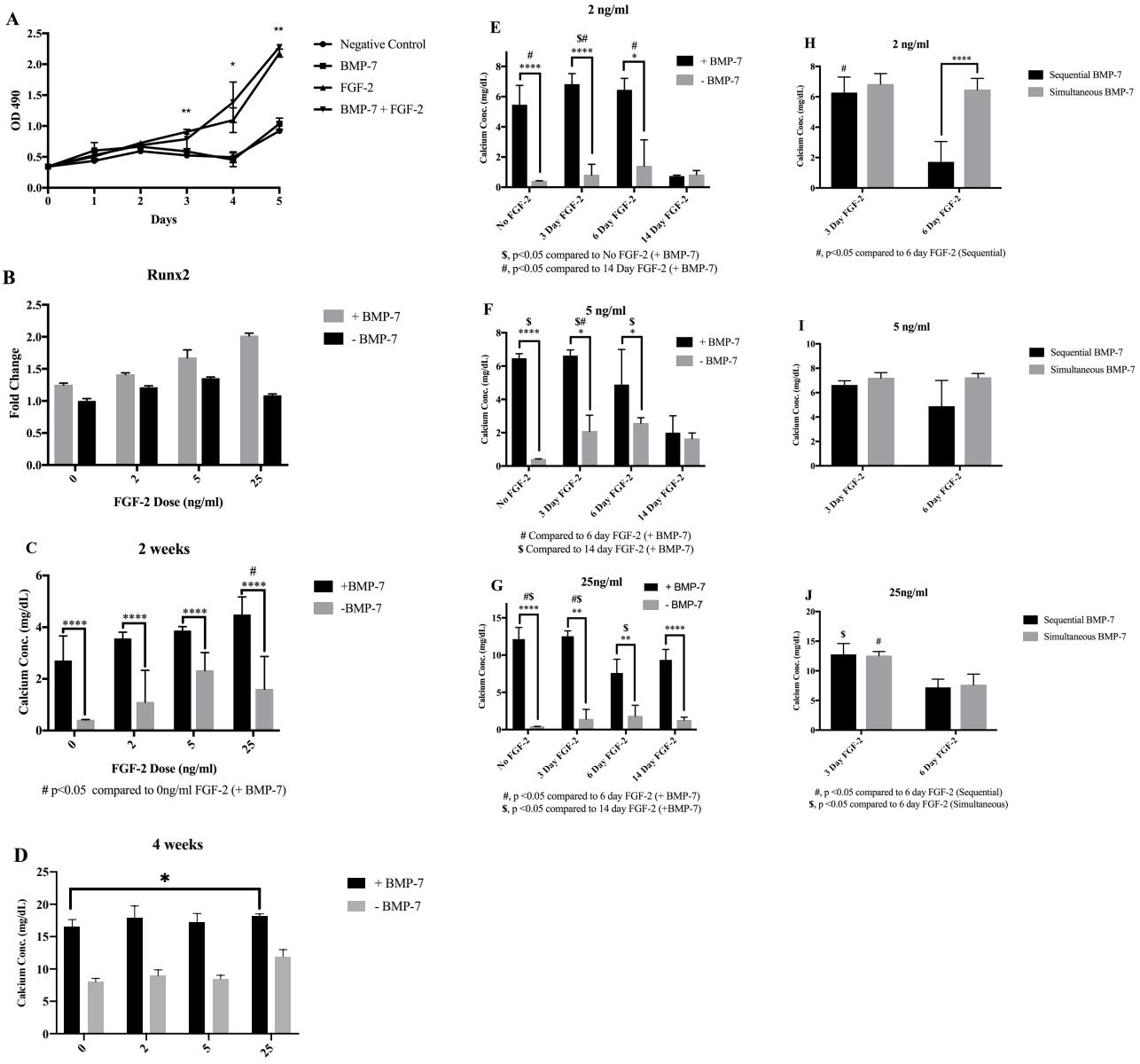
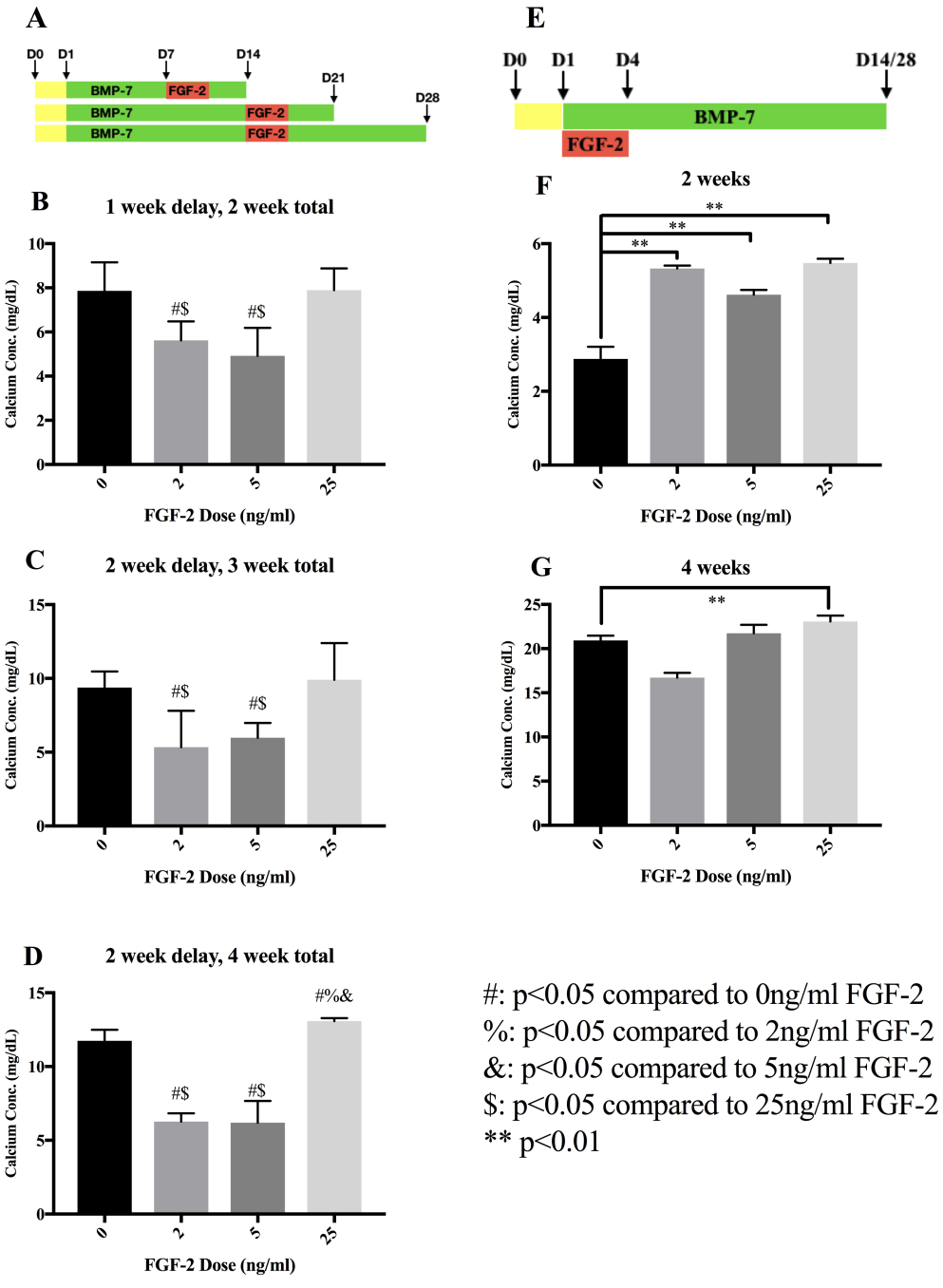


Figure 4.1. FGF-2 and BMP-7 regulation of rabbit BMSC proliferation and differentiation.

(A) Cell proliferation. BMSCs were treated with 100ng/mL BMP-7, 2ng/mL FGF-2, 100ng/mL BMP-7+2ng/mL FGF-2, or no additional growth factors (control). After the times indicated, cell growth was measured using the MTS assay. (B) FGF-2 and BMP-7 regulation of Runx2 expression. BMSCs were grown in osteogenic media +/- 100ng/ml BMP-7 and the indicated concentrations of FGF-2. RNA was isolated after 14 days for measurement of Runx2 mRNA by Q/RT-PCR. (C,D) Mineralization. BMSCs were grown in osteogenic media with or without 100ng/mL BMP-7 and the indicated concentrations of FGF-2 with FGF-2 added only for the first 3 days of the experiment. Mineralization was measured by calcium quantification at 14 (C) and 28 days (D). (E-G) Calcium quantification at 14 days after cells were

treated with osteogenic media supplemented with 2, 5, or 25 ng/ml FGF-2 for 0, 3, 6 or 14 days, +/- 100ng/ml BMP-7. (H-J) Calcium quantification at 14 days after cells were treated with osteogenic media supplemented with FGF-2 and BMP-7 with BMP added either together with FGF-2 (simultaneous) or after FGF-2 (sequential). (* p<.05, **, p < .01, *** p < .001, **** p <.0001)



#: p<0.05 compared to 0ng/ml FGF-2
%: p<0.05 compared to 2ng/ml FGF-2
&: p<0.05 compared to 5ng/ml FGF-2
$: p<0.05 compared to 25ng/ml FGF-2
** p<0.01

Figure 4.2. Effect of FGF-2 on maturing BMSCs or primary osteoblasts.

(A) Schematic of delayed FGF-2 treatment of BMSCs at 0, 2, 5, and 25 ng/ml. (B) Mineralization by BMSCs following induction with BMP-7 at 100ng/ml and 1-week delayed treatment of FGF-2 after 2 weeks. Mineralization by BMSCs following induction with BMP-7 at 100ng/ml and 2-week delayed treatment of FGF-2 after 3 weeks (C) and 4 weeks (D). (E) Schematic of treatment of osteoblasts with FGF-2 at 0, 2, 5, and 25 ng/ml. Mineralization of osteoblasts following induction with BMP-7 at 100ng/ml and FGF-2 at respective doses at 2 weeks (F) and 4 weeks (G).

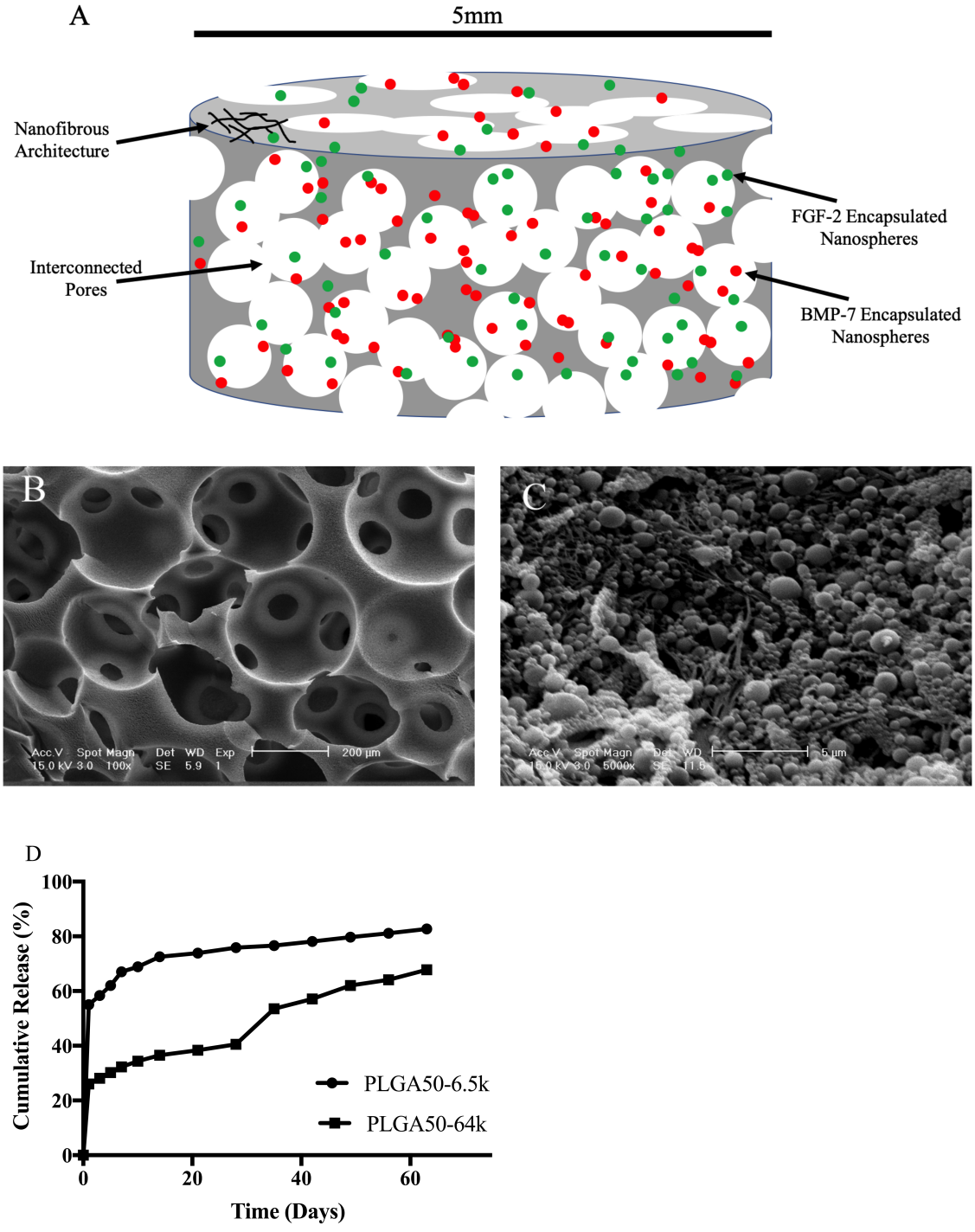
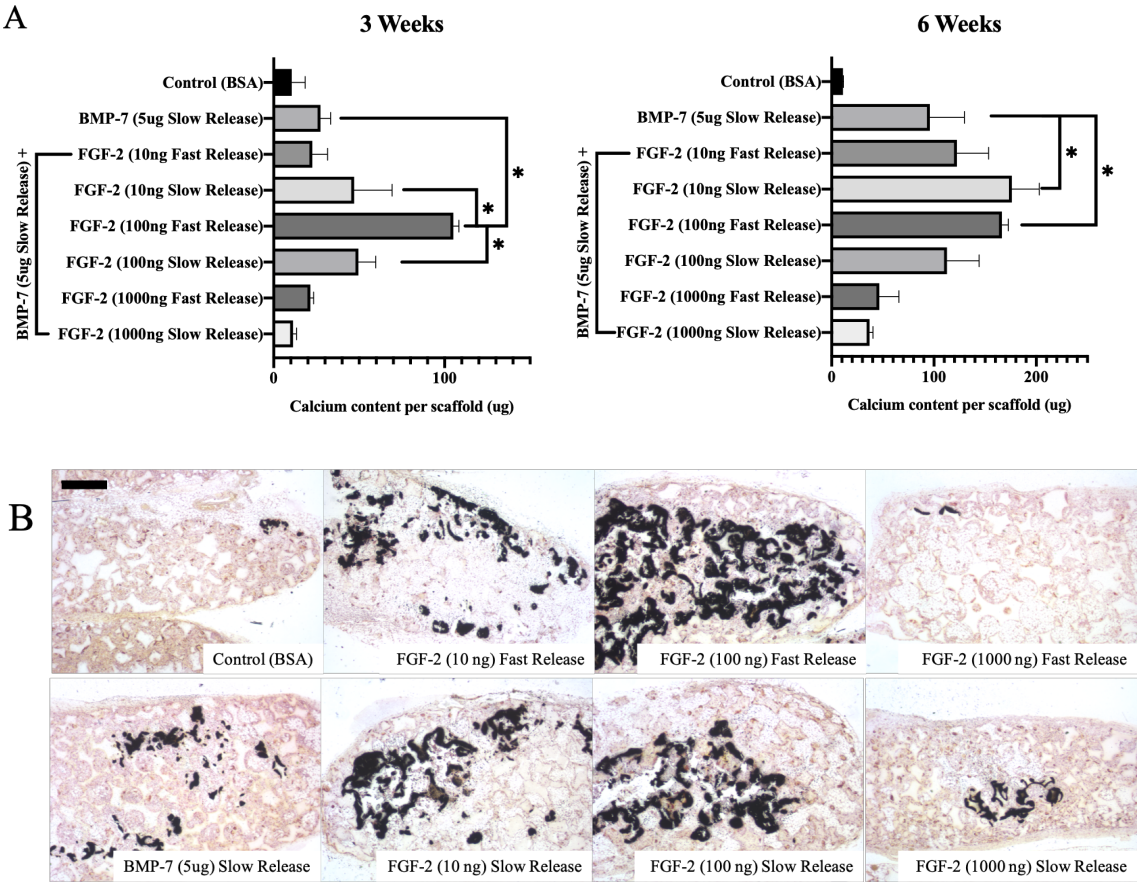
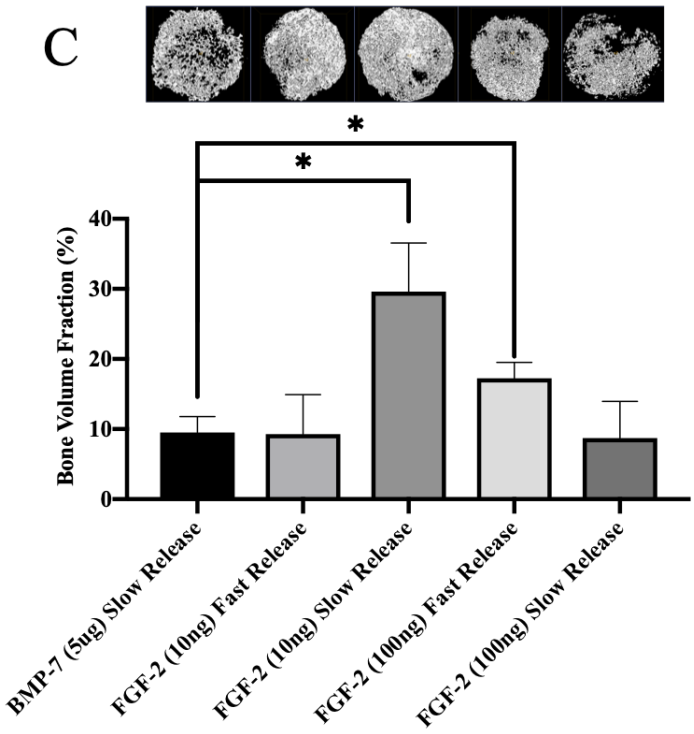


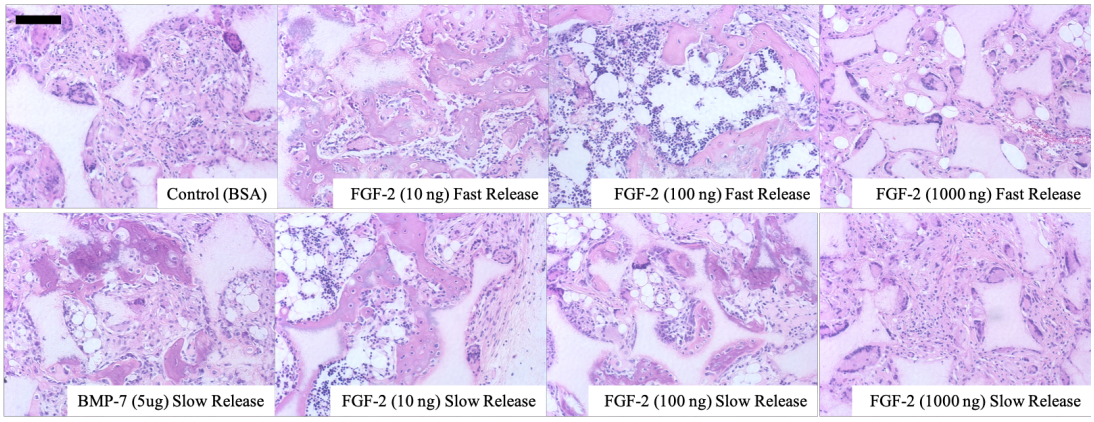
Figure 4.3. Dual-release of BMP-7 and FGF-2 on 3D PLLA nanofibrous scaffolds.
(A) Schematic of FGF-2-PLGA nanospheres and BMP-7-nanospheres immobilized PLLA nanofibrous scaffolds. (B)The morphology of the PLLA nanofibrous scaffold after the incorporation of PLGA nanospheres observed by SEM (low magnification). (C) High magnification of SEM to observe the morphology of PLGA nanospheres immobilized PLLA nanofibrous scaffold. (D) Cumulative release curve for FGF-2 released from low or high molecular weight PLGA nanospheres incorporated into PLLA scaffolds *in vitro*.



C


*
*
Bone Volume Fraction (%)
40
30
20
10
0
BMP-7 (5ug) Slow Release
FGF-2 (10ng) Fast Release
FGF-2 (10ng) Slow Release
FGF-2 (100ng) Fast Release
FGF-2 (100ng) Slow Release

D


Control (BSA)
FGF-2 (10 ng) Fast Release
FGF-2 (100 ng) Fast Release
FGF-2 (1000 ng) Fast Release
BMP-7 (5ug) Slow Release
FGF-2 (10 ng) Slow Release
FGF-2 (100 ng) Slow Release
FGF-2 (1000 ng) Slow Release

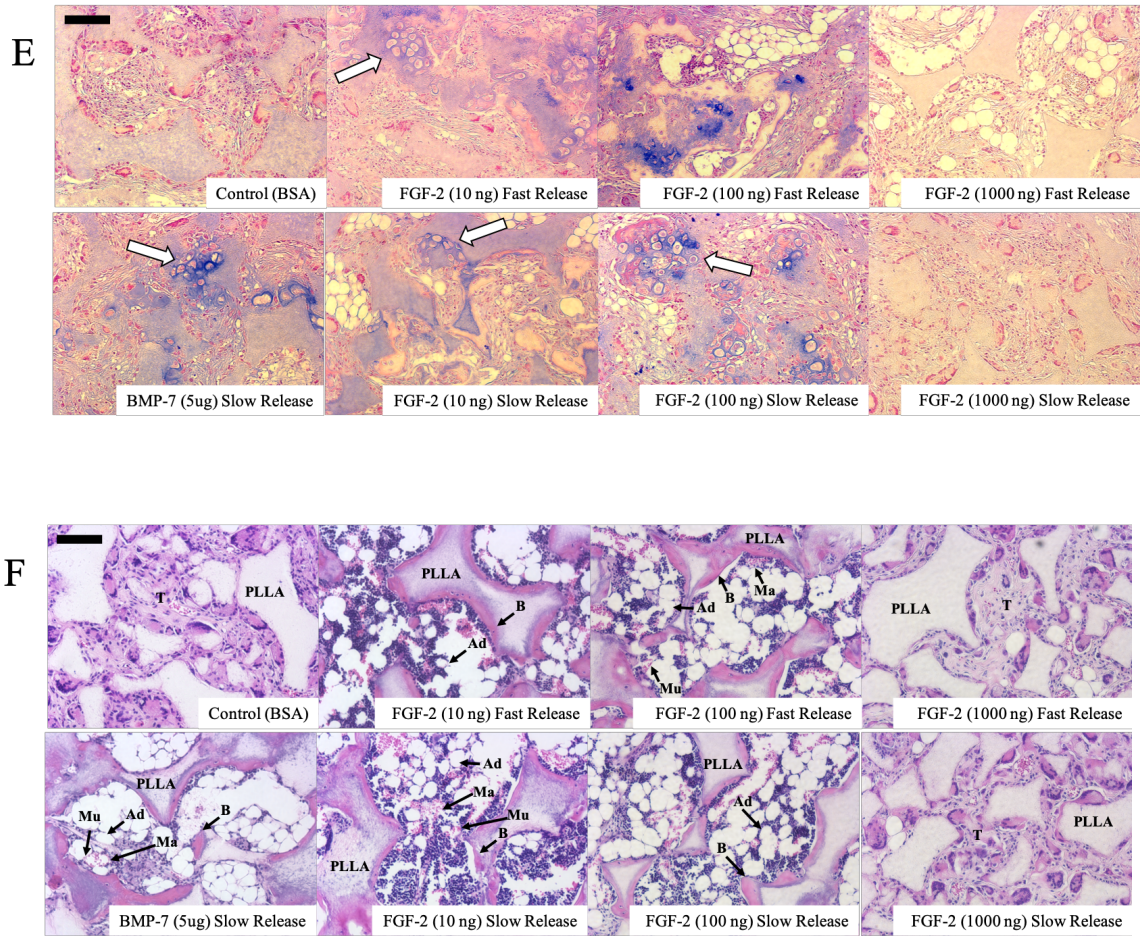
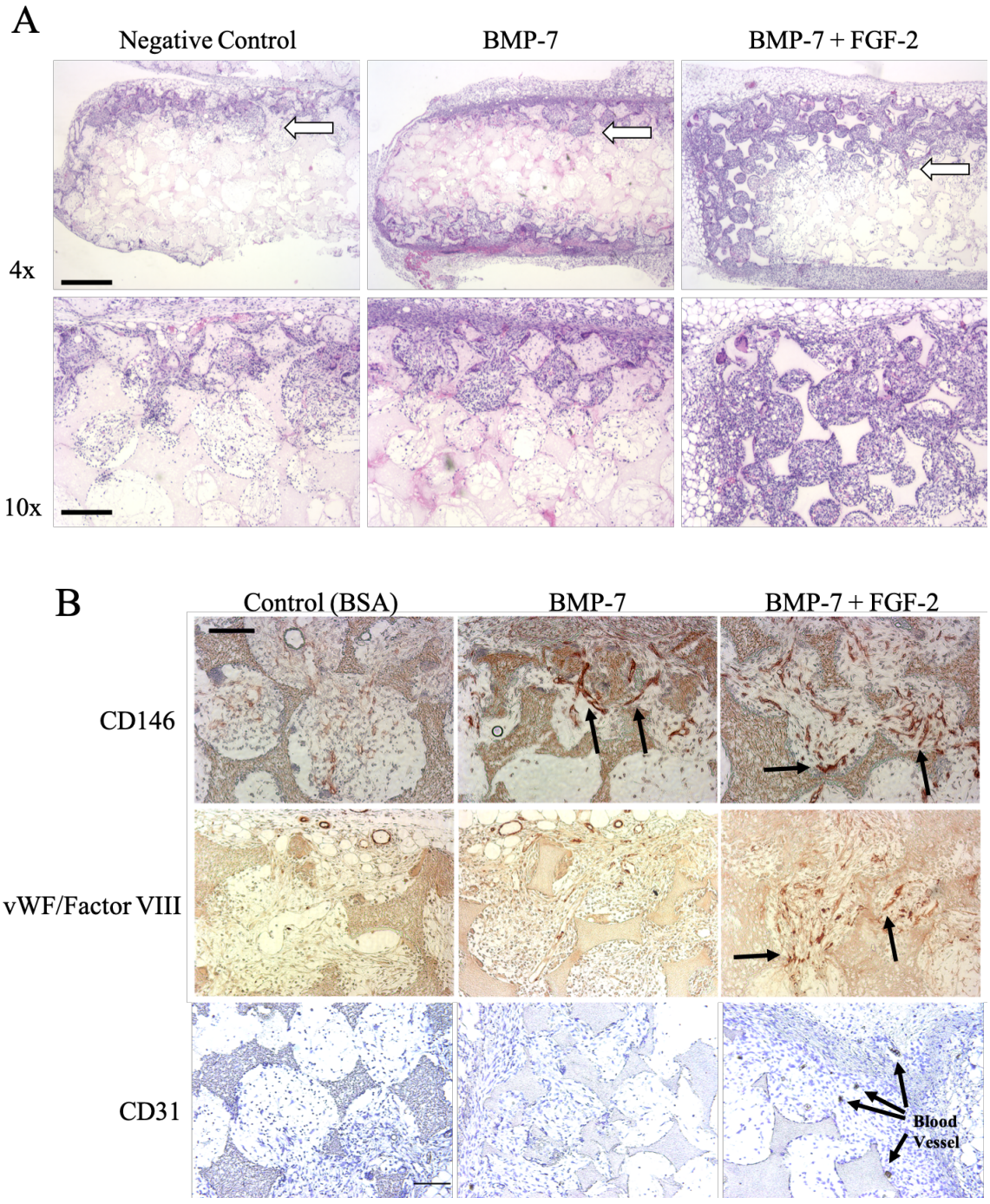
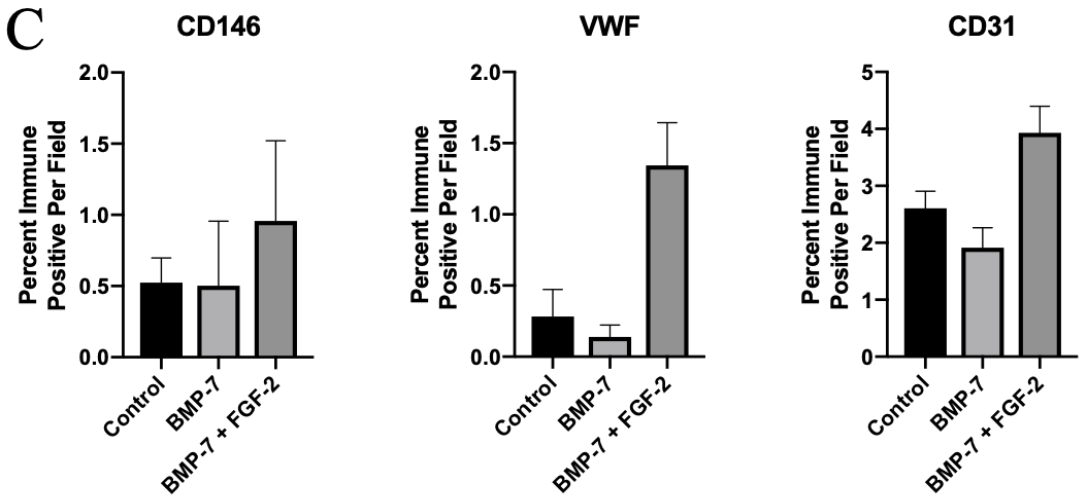
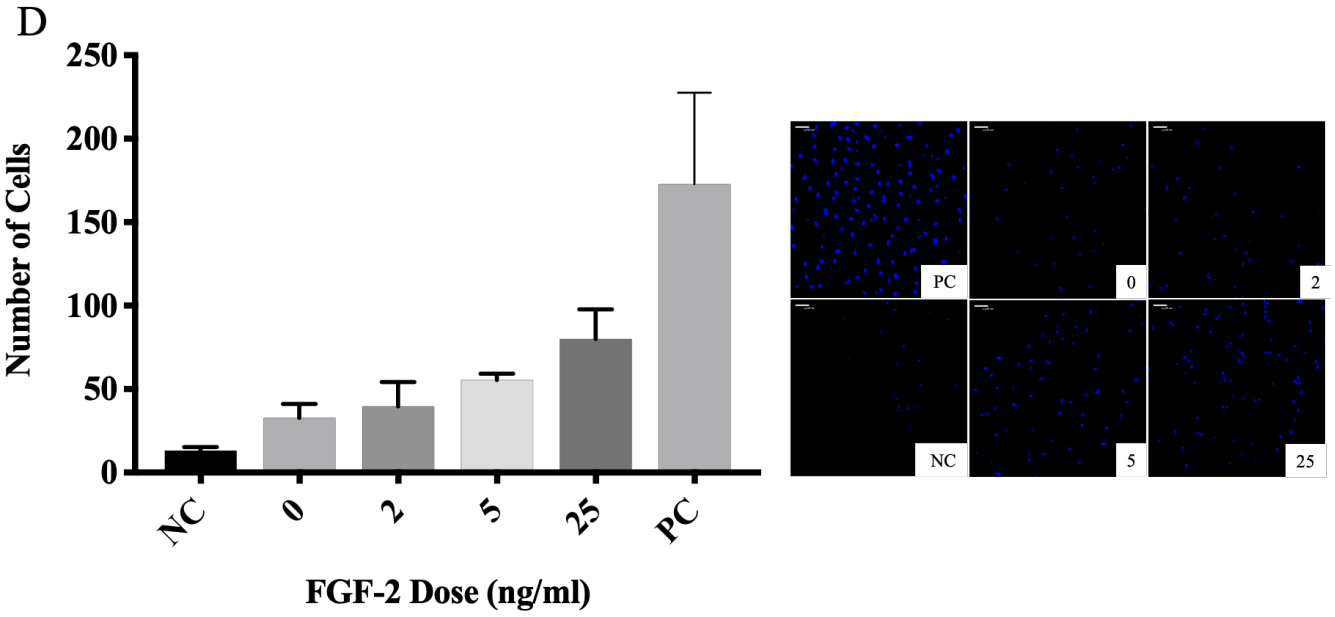


Figure 4.4. Ectopic bone regeneration controlled by dual-release of BMP-7 and FGF-2 on 3D PLLA nanofibrous scaffolds.
(A) The total calcium content in the scaffolds was detected 3 and 6 weeks after implantation (*, $P<0.05$). (B) Mineralization in the scaffolds at 3 weeks was visualized using von Kossa staining (scale bar=500μm). (C) Bone formation in implants at 6 weeks was detected by μCT scanned at a voxel size of 18 μm. The three-dimensional reconstruction was created from the set of scans. A fixed threshold (1,200) was used to extract the mineralized bone phase and bone volume fraction was calculated (*, $P<0.05$). (D) Microscopic observations of the H & E stained tissue sections of scaffolds retrieved 3 weeks after implantation (scale bar=100μm). (E) Microscopic observations of the Alcian blue stained tissue sections of scaffolds retrieved 3 weeks after implantation (scale bar=100μm). (F) Microscopic observations of the H & E stained tissue sections of scaffolds retrieved 6 weeks after implantation (scale bar=100μm).


A
Negative Control
BMP-7
BMP-7 + FGF-2
4x
10x
B
Control (BSA)
BMP-7
BMP-7 + FGF-2
CD146
vWF/Factor VIII
CD31
Blood Vessel


C
CD146
VWF
CD31
Percent Immune Positive Per Field
2.0
1.5
1.0
0.5
0.0
5
4
3
2
1
0
Control
BMP-7
BMP-7 + FGF-2


D
Number of Cells
250
200
150
100
50
0
NC
0
2
5
25
PC
FGF-2 Dose (ng/ml)
PC
0
2
NC
5
25

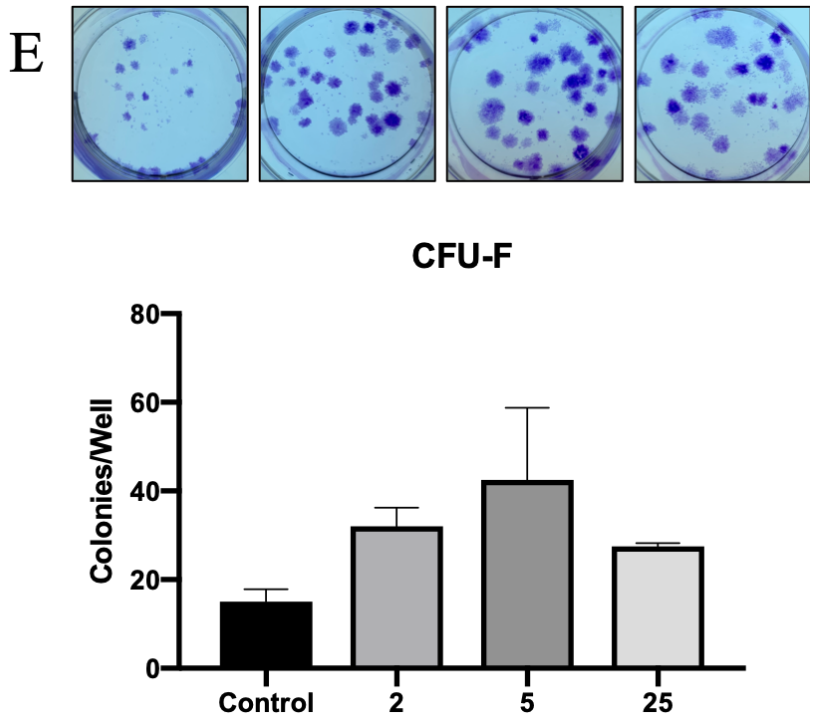


Figure 4.5. Stem cells recruitment and angiogenesis regulated by delivery of FGF-2 during the early stage of BMP-7-induced endochondral ossification.

(A) FGF-2-containing nanospheres in nanofibrous scaffolds stimulates tissue invasion *in vivo*. Upper panel is at low magnification (4X) (scale bar=500μm). Lower panel is at high magnification (10X) (scale bar=200μm). (B) Early vascularization was visualized using CD146 (upper panel), Factor VIII-related antigen/von Willebrand Factor (middle panel), and CD31 (lower panel) immunohistochemical staining (scale bar=50μm). (C) Immunohistochemical stain was quantified using ImageJ. (D) FGF-2 promoted BMSCs migration *in vitro* in a dose dependent manner. Cell nuclei (blue color) were observed and counted under the fluorescence microscope. (E) The CFU-F ability of BMSCs was increased by FGF-2 *in vitro*. BMP-7 at 100ng/mL supplemented with 0 (control), 2, 5, or 25ng/ml of FGF-2.

Chapter 5. Dual Delivery of FGF-2 and BMP-7 from Nanofibrous Spongy Microspheres Platform Enhances Repair of Critical Size Bone Defect

5.1. Introduction

Autologous bone graft procedures are the reference standard for treatment of large volume injuries. Bone tissue engineering seeks to replace the need for autologous bone grafting in the treatment of non-healing or large volume bone injuries. Tissue-engineered scaffolds can be used as cell carriers and combined with controlled release of growth factors to regenerate bone *in situ*. These systems obviate the need for harvesting donor bone from non-injury sites, and thus avoiding risk of donor-site morbidity. Additionally, these platforms do not depend on the limited available quantity of donor-site bone.

5.1.1. Scaffolds for bone tissue engineering

Scaffolds in tissue engineering are widely diverse in their material makeup, physical properties, and clinical applications. The use of biomimetic and biodegradable synthetic scaffolds offers certain advantages in design of an optimal bone tissue engineering scaffold. We previously reported that scaffolds made from poly (l-lactic acid) (PLLA) that possess a porous microstructure and fibrous nanostructure are advantageous for bone tissue engineering compared to solid walled scaffolds.[46] We optimized the pore size and nanofiber diameter to allow for sufficient cell penetration of the scaffold, nutrient and waste exchange, and matched nanofiber diameter with native collagen fiber size to mimic the bone extracellular matrix.[319,320] These 3-dimensional bulk scaffolds have demonstrated both *in vitro* and *in vivo* potential for bone

regeneration.[46,47] The clinical application of bone grafts and their substitutes requires invasive surgical implantation. The development of microspheres and hydrogels that can be delivered by injection offers a potentially non-invasive scaffold for bone repair.[92,321,322] We synthesized an injectable nanofibrous spongy microsphere (NF-SMS) that possesses both the micro-porous and nanofibrous characteristics of the bulky 3D scaffolds, with the added benefit of being an injectable and therefore non-invasive scaffold, for the delivery of cells and PLGA encapsulated growth factors. [82,84,323,324]

5.1.2. Simultaneous growth factor delivery

Local delivery and controlled release of relevant growth factors at physiological doses can aid in the directed differentiation of transplanted or endogenous progenitor cells that are recruited to the site of injury. Combination of a scaffold with a tunable drug delivery system provides both structural and biological cues for cell attachment, proliferation, differentiation and tissue regeneration. We previously demonstrated that recombinant human BMP-7 can be delivered in a continuous and long-term fashion to enhance osteogenic differentiation and ectopic bone formation.[198]

Fracture healing is a complex multi-stage cascade of events. Immediately after injury, an inflammatory response occurs that is followed by callus formation, mineralization of the callus, and bone remodeling.[325] This multi-stage process is modulated by many endogenous growth factors during each phase of healing. In recent years, there has been an increased emphasis on developing drug delivery platforms that incorporate the delivery of multiple factors to better mimic the natural healing process.[326]

One of the challenges associated with autologous bone grafts or bone tissue engineering platforms is the long-term survival of the transplanted graft. Failure of autografts and other bone

healing platforms has often been attributed to insufficient vascularization of the graft.[327] Efforts to support neovascularization and angiogenesis in bone often seek to promote VEGF, PDGF, or FGF-2 expression as these factors are responsible for stimulating endothelial cells (VEGF, FGF-2) or smooth muscle cells (PDGF) to invade the newly forming tissue and promote blood vessel formation. [304,328,329]

Efforts to use FGF-2, with and without BMP, in bone repair have been met with contradictory results, as FGF-2 can both promote and inhibit bone formation *in vivo*.[132,137,291] The dose and temporal release of FGF-2 greatly varied in previous studies, which might explain the lack of consensus with regard to the role of FGF-2 in bone tissue engineering. Upon closer examination, studies with low dose and short-term treatment of FGF-2 were more consistently associated with enhanced bone formation and healing.[135,297] Our previous study also found that low doses and short-term release of FGF-2 from PLGA nanoparticles enhanced BMP-7 directed *in vitro* osteogenic differentiation and ectopic bone formation *in vivo* (Chapter 4). The controlled short-term release of FGF-2 combined with long term release of BMP-7 from distinct formulations of poly (lactic-co-glycolic acid) (PLGA) nanoparticles enhanced cell proliferation, migration, and differentiation.

In this research, we sought to evaluate the potential of FGF-2 to enhance BMP-7 directed osteogenic differentiation (of hiPSC-derived MSCs) and bone regeneration using NF-SMS. We developed a controlled release system for simultaneous release of FGF-2 and BMP-7. Each growth factor was encapsulated in PLGA with specific molecular weight PLGA in order for each factor to achieve distinct release kinetics and to mimic the optimal treatment profile determined by *in vitro* experiments. The PLGA-NS were conjugated onto the NF-SMS and this combination therapy was evaluated in a relevant orthotopic, cranial defect model.

5.2. Materials and methods

5.2.1. NF-SMS fabrication

NF-SMS were produced from poly(2-hydroxyethyl methacrylate)-graft-poly(L-lactic acid) (PHEMA10-g-PLLA5) through an emulsification process followed by thermally induced phase separation (TIPS). Briefly, the polymer was dissolved in tetrahydrofuran at 50°C with a concentration of 2.0% (w/v). The polymer solution was quickly added into glycerol (50°C) under rigorous mechanical stirring (speed 4.5, IKA RW16 basic laboratory stirrer). After 15 seconds, the mixture was quickly poured into liquid nitrogen. After 10 minutes, ice was packed into the beaker for a gradual increase in temperature, and the ice/water mixture (1000 mL) undergoes solvent exchange for 24 hours. The microspheres were then passed through sieves and washed with distilled water to remove residual glycerol. The 60-90μm NF-SMS collected for this work were then lyophilized for two days.

5.2.2. Smooth microsphere fabrication

Smooth (solid) microspheres were prepared using a conventional solvent evaporation method as previously described.[330] Briefly, PLLA was dissolved in dichloromethane and added into an aqueous poly(vinyl alcohol) (PVA, Mw = 89,000–98,000, Sigma–Aldrich) solution. The mixture was then subjected to rigorous stirring for 24 hours. The microspheres were sieved and washed and then lyophilized.

5.2.3. Encapsulation of BMP-7 and FGF-2 and incorporation of PLGA-NS into NF-SMS

Lyophilized rhBMP-7 powder was dissolved in 0.1% trifluoroacetic acid (TFA) with 0.1% bovine serum albumin (BSA). PLGA50–28K was used to encapsulate rhBMP-7 (Stryker)

and PLGA50-7-17K was used to encapsulate rhFGF-2 (Stemgent) via a previously described double emulsion technique.[125]

PLGA-NS were incorporated into NF-SMS using a modified post seeding method previously used in the lab [197,198,331]. For this process, PLGA-NS and NF-SMS were dispersed in hexane with 0.1% span 80 separately at a concentration of 5mg/ml. The two particles were combined and after 2 hours incubation under vacuum, the dried powder was then put into 1 ml of hexane/THF (3% THF by volume) for 30 minutes and placed on a shaker. The PLGA-NS/NF-SMS combinations were then placed on a rotary evaporator to remove solvent and lyophilized for 3 days. Prior to *in vivo* studies, particles were sterilized using ethylene oxide gas.

5.2.4. Cell Culture and osteogenic differentiation

Human iPSC-MSCs (hiPSC-MSCs) were obtained from the Bo Yang lab. Cells are maintained in media containing αMEM, 20% Fetal Bovine Serum (FBS), 100 U/ml penicillin/streptomycin (Gibco), and supplemented with 2mM L-glutamine, 1x non-essential amino acids (NEAA), 1mM 2-mercaptoethanol, and 2 ng/ml FGF-2. These cells were proliferated on 0.1% gelatin coated T75 flasks under normal cell culture conditions (5% CO_2 and 37°C). Media was changed every 48-72 hours.

24 hours after seeding, maintenance medium was replaced with osteogenic medium, consisting of high glucose Dulbecco's Modified Eagle Medium (DMEM) with 10% FBS and 1% penicillin/streptomycin and supplemented with ascorbic acid (50 μg/ml), β glycerophosphate (10mM), and dexamethasone (100nM). Cells were treated with FGF-2, which was prepared in 0.2% sterile filtered bovine serum albumin (BSA), and/or BMP-7.

5.2.5. 3D culture of hiPSCs on NF-SMS

Cells were seeded onto NF-SMS and control, smooth walled and non-porous microspheres (S-MS) as previously described, with modification.[330] Briefly, cells were incubated with microspheres at a 5:1, cell:microsphere ratio in 2ml of growth media in a 15ml conical tube for 4 hours with gentle shaking under normal cell culture conditions. The cell/microsphere slurry was agitated every 30 minutes. Following seeding, the microsphere/cell constructs were cultured in suspension using a magnetic biological stirrer (Techne) for 24 hours. Growth media was then replaced with 40ml osteogenic media and supplemented relevant growth factors. Media was replaced every 3-5 days.

5.2.6. Calcium quantification

Cells were washed 3 times with distilled water and calcium was extracted by incubating cells in 0.5N hydrochloric acid (HCl) overnight on a shaker at 4°C. Calcium quantification was determined with Pointe Scientific Calcium Liquid Reagents according to the manufacturer's manual. Total calcium content of each sample was measured by the o-cresolphalein-complexone method. For example, 50 µl of sample was incubated with a 250 µl mixture of the color and base reagents. Absorbance was measured at 570 nm. A calcium standard was used to calculate the content of calcium in each sample.

5.2.7. Confocal Imaging

After 5 days of 3D culture, NF-SMS and hiPSC-MSCs formed aggregates which were washed with 1x PBS and fixed in 4% paraformaldehyde for 24 hours. After fixation, cells were stained with Phalloidin (Alexa Fluor™ 555) (Invitrogen) and counterstained with 4′,6-diamidino-2-phenylindole (DAPI).

For live/dead staining, NF-SMS-cell aggregates were recovered after 5 days of culture and were stained with a LIVE/DEAD™ Viability/Cytotoxicity Kit (Fisher) following the manufacturer instructions. Briefly, cells on NF-SMS were washed with PBS three times and treated with Ethidium homodimer-1 (0.5 μM) and calcein AM (0.25 μM) (Life technologies) for 45 min.

For immunofluorescent staining, NF-SMS-cell aggregates were recovered after 4 weeks of culture in osteogenic medium + 10- ng/ml BMP-7. Cells were washed with PBS and fixed with 4% paraformaldehyde overnight. Cells were then permeabilized with ice cold methanol and treated with 0.1% Triton-X 100. Nonspecific binding was blocked with goat serum and anti-osteocalcin primary antibody was incubated overnight at 4°C with gentle shaking. FITC labeled secondary goat anti-mouse IgG antibody (1:1000) was incubated for 1 hour at room temperature in the dark, together with Phalloidin (Alexa Fluor™ 555) (Invitrogen) to stain F-actin and DAPI to stain nuclei. NF-SMS-cell aggregates were examined using Confocal Laser Scanning Microscopy (CLSM) (Nikon Eclipse C1).

5.2.8. RNA extraction and RT-qPCR

Total RNA was isolated using TRIzol. A cDNA library was created with SuperScriptII Reverse transcription reagents (Applied Biosystems) and real time qPCR was performed using TaqMan Universal PCR Master Mix (Applied Biosystems). Specific primers for Runx2 (Hs01047973_m1), osteocalcin (BGLAP, Hs00609452_g1), and GAPDH (Hs02786624_g1) were used to measure relative expression. GAPDH was used as a house-keeping gene to normalize gene expression.

5.2.9. Calvarial bone-defect repair model construction

The animal procedures were performed following a protocol approved by the University of Michigan Institutional Animal Care and Use Committee. Animals were housed in groups and maintained with a normal diet. Male 6-8-week-old C57BL/6 mice (Charles River Laboratories International, Inc., Wilmington, MA) were used for the calvarial defect study. Surgery was performed under general inhalation anesthesia with 2% isoflurane as previously described[274]. Mice were randomly divided into 6 groups. A 5 mm craniotomy defect centered on the parietal calvarial bone was created using a trephine. A slurry of NF-SMS with PLGA-NS conjugated to the surface was applied to the defect. Mice were euthanized 8 weeks after implantation and their skulls were harvested for microcomputed tomography (μCT) and histological analysis.

5.2.10. Micro CT analysis

For the calvarial bone analysis, the skulls were scanned with a fixed global threshold of 20%. 3D reconstruction of the skull and quantitative analyses were performed. A 5 mm-circular region of interest centered on the defect was determined and the bone volume (mm^3) (BV) and bone mineral density (BMD) in the defect area were measured using manufacturer's software (Scanco mCT 100).

5.2.11. Histological analysis

3D *in vitro* samples were washed with PBS, fixed in 10% formalin and embedded in paraffin blocks. 5 μm sections were prepared, which were subsequently deparaffinized, rehydrated with a graded series of ethanol, and stained with hematoxylin and eosin (H&E), Alizarin red S, and von Kossa. Alcian blue and trichrome stains were performed by the Histology Core at the University of Michigan School of Dentistry.

The calvarial samples were fixed with 4% paraformaldehyde, decalcified with 10% EDTA for 3 weeks and subsequently embedded in paraffin. H&E staining and trichrome staining of the coronal sections (5 μm thick) were performed by the Histology Core at the University of Michigan School of Dentistry.

5.2.12. Statistical Analyses

At least three replicates of each condition were used for statistical analysis. Values were reported as means and standard deviations. To determine significance of differences in observed and measured values, Student's t-test was performed, with $p<0.05$ as the threshold for statistical significance.

5.3 Results

5.3.1. Fabrication and characterization of NF-SMS

NF-SMS were produced from poly(2-hydroxyethyl methacrylate)-graft-poly(L-lactic acid) (PHEMA10-g-PLLA5) through an emulsification process followed by thermally induced phase separation (TIPS)[332].[Figure 5.1.a] Under SEM observation, we found these microspheres possess nanofibrous and micro-porous characteristics.[Figure 5.1.b] The majority of pores range from 15-18 μm in diameter, allowing for cell infiltration and migration throughout the interconnected pores of the NF-SMS.

5.3.2. *In vitro* 2D evaluation of dose, length, and timing of FGF-2

A series of 2D cell culture studies were conducted to define the basic parameters for BMP-7 and FGF-2 treatment necessary to stimulate osteogenic differentiation of hiPSC-MSCs. FGF-2, in the presence or absence of BMP-7, stimulated proliferation of hiPSC-MSCs, while BMP-7 had no effect on proliferation compared with the control. [Figure 5.2.a] Subsequently, we

studied the effect of FGF-2, with or without 100 ng/ml of BMP-7, on osteogenic induction of hiPSC-MSCs. For *in vitro* osteogenic differentiation, BMP-2 and BMP-7 have been applied in concentrations ranging from 50-100 ng/ml.[24,333] FGF-2 was added at 2, 5, and 25 ng/ml for the first three days of culture in osteogenic medium and differentiation was measured by calcium deposition after 2 and 4 weeks [Figure 5.2.b]. We found that low dose (2 ng/ml) treatment with FGF-2 for the first three days of osteogenic differentiation did not inhibit BMP-7 induced mineralization of cell matrix as measured by calcium content [Figure 5.2.c, 5.2.d]. We determined that higher doses of FGF-2 reduced calcium deposition especially at the earlier time point (2 weeks), though significant mineralization by cells was still observed.

We also tested whether it was favorable to deliver FGF-2 with BMP-7 added sequentially or simultaneously. [Figure 2e] Cells were treated with a dose of 2ng/ml FGF-2 for the first three or six days of osteogenic differentiation. BMP-7 was added at the start of induction of osteogenic differentiation (simultaneously with FGF-2) or after three or six days of osteogenic induction (sequential with FGF-2). Simultaneous or sequential treatment did not significantly affect mineralization by cells after two weeks and four weeks. [Figure 5.2.e, 5.2.f] We then tested the effect of prolonged FGF-2 treatment on osteogenic differentiation of hiPSC-MSCs. [Figure 5.2.h] At four weeks, three-day treatment of FGF-2 appeared to be favorable when compared to six days or 28 days. [Figure 5.2.i] Prolonged treatment with FGF-2 decreased calcium deposition.

To determine whether the presence of FGF-2 may have a stronger effect on hiPSC-MSCs as they mature and undergo osteoblast differentiation, cells were treated with FGF-2 according to a delayed treatment schedule. [Figure 5.3.a] Delaying FGF-2 treatment for one week enhanced calcium deposition after two weeks of osteogenic differentiation of hiPSC-MSCs. [Figure 5.3.b]

A two-week delay of FGF-2 did not result in any significant increase in mineralization by hiPSCs after 3 or 4 weeks of osteogenic induction. [Figure 5.3.c, 5.3.d] Taken together, this suggests that delayed FGF-2 treatment was not superior to early and low dose treatment.

5.3.3. Osteogenic gene expression by qRT-PCR analysis of RUNX2

We performed a series of studies to evaluate the effect of FGF-2 on the expression of the osteogenic transcription factor, RUNX2. Cells were induced with osteogenic medium and treated with FGF-2 for 3 days or for 9 days, with or without 100 ng/ml of BMP-7. After 2 and 4 weeks of osteogenic induction, mRNA was extracted to evaluate gene expression by quantitative reverse transcriptase polymerase chain reaction (qRT-PCR). At two weeks, treatment of cells with 2ng/ml of FGF-2 stimulated the expression of RUNX2, though to a lesser degree than 100 ng/ml BMP-7. The treatment of cells with both BMP-7 and FGF-2 produced an additive effect, enhancing RUNX2 expression over BMP-7 treatment alone. [Figure 5.4.a] When FGF-2 was extended to 9 days, the synergy between FGF-2 and BMP-7 was profound, as RUNX2 expression was nearly 3-fold higher than BMP-7 alone or a 3-day treatment with FGF-2 + BMP-7. [Figure 5.4.b] Addition of increasing doses of FGF-2 stimulated a dose-dependent increase in RUNX2 expression, at both 2 and 4-week time points. [Figure 5.4.c, 5.4.f] Interestingly, after 4 weeks of culture, expression of RUNX2 was increased in the BMP-7 alone groups compared with the FGF-2 + BMP-7 groups. [Figure 5.4.d, 5.4.e]

5.3.4. Evaluation of nanofibrous spongy microsphere platform

NF-SMS were previously shown to be advantageous for regeneration of dental tissue and intervertebral disc.[84,324,331] These injectable particles possess the nanofibrous and porous characteristics that proved to be advantageous for 3D disc-shaped PLLA scaffolds in bone tissue

engineering. We first evaluated the ability of hiPSC-MSCs to attach, survive, and grow on the NF-SMS scaffold.

To evaluate cell attachment, we compared NF-SMS with smooth non-porous microspheres (S-MS), which served as a control scaffold. We found that hiPSC-MSCs attached at a significantly higher rate to NF-SMS (~90%) than to S-MS (~70%).[Figure 5.5.a] To further evaluate NF-SMS, we performed confocal microscopy to examine the morphology and cell survival. Under confocal microscopic observation, hiPSC-MSCs showed could be observed within pores of NF-SMS as well as on the surface of the microspheres. [Figure 5.5.b] By contrast, cells were limited to the outer surface of the solid S-MS control microspheres. Cells were seeded onto NF-SMS or S-MS at a 5:1, cell to microsphere ratio. At this ratio, we identified multiple cells attaching to each individual microsphere. After several days of 3D suspension culture, cells proliferate on the scaffold and tended to form aggregates, with clustering of cells and microspheres. We sought to examine the cytocompatibility of NF-SMS by evaluating hiPSC-MSCs using a live/dead assay 5 days post-seeding. We found abundant living cells with normal cell spreading and morphology as observed by the positive green stain (calcein-AM). Few dead cells were observed as indicated by the positive red stain (ethidium homodimer-1). [Figure 5.5.c] After 4 weeks of osteogenic differentiation, cells on NF-SMS showed substantial osteocalcin expression, further demonstrating the osteoconductive potential of the porous and nanofibrous scaffold. [Figure 5.5.d] We also observed significant increases in relative gene expression of RUNX2 and osteocalcin (BGLAP) after four weeks of osteogenic differentiation on each scaffold. [Figure 5.5.e,5.5.f]

5.3.5. *In vitro* osteogenic differentiation of hiPSC-MSCs on NF-SMS

We then evaluated the effect of FGF-2 with or without BMP-7 on osteogenic differentiation of hiPSC-MSCs seeded on NF-SMS in 3D suspension spinner flask culture. The cell-microsphere cultures were treated with growth factors according to the 2D *in vitro* studies described above. In the FGF-2 only group, cells were induced in osteogenic media, supplemented with 2ng/ml FGF-2 for 3 days, and subsequently induced in osteogenic media, without additional factors, for a total of four weeks. In the BMP-7 only group, cells were induced by osteogenic media supplemented with 100ng/ml BMP-7 for four weeks. The dual treatment group received FGF-2 for the first 3 days only and BMP-7 for the entire four weeks. After osteogenic differentiation for four weeks, increased staining with Alizarin Red S [Figure 5.6.a] and von Kossa [Figure 5.6.b] was observed in the dual treatment group when compared to BMP-7 alone or FGF-2 alone groups. Image analysis for staining intensity of Alizarin Red S and von Kossa was performed in ImageJ [Figure 5.6.g, h]. Further histological analysis by hematoxylin and eosin stain (H&E) [Figure 5.6.c] shows evidence of new bone formation in the dual growth factor group. Alcian blue positive staining areas in the BMP-7 and BMP-7 + FGF-2 treatment groups indicated endochondral-osteoblast transition. [Figure 5.6.d] Immunohistochemical staining for bone sialoprotein (BSP) was strongly positive in the dual treatment group. [Figure 5.6.f] BSP stain was quantified using ImageJ and showed a significant increase in BSP positive stain in groups treated with BMP-7 + FGF-2. [Figure 5.6.k] We also observed a synergistic effect of BMP-7 and FGF-2 on the gene expression of RUNX2 and an additive effect on the expression of osteocalcin (BGLAP) after four weeks. [Figure 5.6.i, 5.6.j]

5.3.6. Controlled release of FGF-2 and BMP-7 from PLGA nanospheres

For the *in vivo* delivery of FGF-2 and BMP-7, we encapsulated the growth factors in poly(D,L-lactide-co-glycolide) PLGA nanospheres (NS) through a standard water/oil/water double emulsification method[197,334]. By encapsulating FGF-2 in nanoparticles with a 50-50 LA:GA ratio (PLGA-50) and with an average molecular weight of 7.0kDa (Resomer RG 502 H), we observed a rapid release of FGF-2 within the first 1-2 weeks. BMP-7 was encapsulated in PLGA-50 (Resomer RG 503 H) with an average molecular weight of 28kDa. The release profile demonstrated a lower burst release, followed by a long-term continuous release of BMP-7. [Figure 5.7.a] Both formulations of PLGA particles were measured out to 5mg and suspended in 1 ml pH 7.4 PBS for the release tests. The supernatant was collected at designated timepoints and resuspended with fresh PBS after collection. Drug loaded PLGA nanoparticles were immobilized onto NF-SMS using a modified post-seeding method.[198,324,334] After incorporation of PLGA-NS, the NF-SMS maintained their porous and nanofibrous characteristics [Figure 5.7.b, 5.7.c].

5.3.7. *In vivo* repair of calvarial defects with NF-SMS and drug-loaded PLGA-NS

We combined fast release FGF-2-loaded PLGA-NS and slow release BMP-7 PLGA-NS with NF-SMS to treat critical size bone defects in C57BL/6 mice. Two doses of FGF-2, 10ng/defect and 100ng/defect were loaded in combination with 5 ug/defect BMP-7. A sham group and a NF-SMS group loaded with blank PLGA-NS served as controls. Combination therapy groups were compared with BMP-7 alone (5ug/defect) and FGF-2 alone (100ng/defect). These doses have been established in previous studies.[295,296] Microcomputed tomography (microCT, μCT) analysis showed that 10ng FGF-2 (low dose) + 5ug BMP-7 regenerated more bone than BMP-7 alone, FGF-2 alone (100 ng/defect), or blank NF-SMS. The higher dose of

FGF-2 (100ng/defect) failed to produce a combinatorial effect with BMP-7 directed bone regeneration. Minimal healing was observed in the peripheral areas of the defect of the NF-SMS + Blank PLGA-NS treatment group. [Figure 5.8.a] Quantitative bone histomorphometry analysis showed that new bone volume was highest in the low dose FGF-2 + BMP-7 group while the high dose FGF-2 + BMP-7 group produced only slightly more bone than non-drug-loaded NF-SMS.[Figure 5.8.h, 5.8.i] Histological evaluation of each group demonstrated that the co-delivery group with low dose FGF-2 and BMP-7 had collagen rich bone-like features as seen by H&E stain [Figure 5.8.b, 5.8.c] and trichrome stain [Figure 5.8.d, 5.8.e].

5.3.8. Radiographic analysis to screen for heterotopic or ectopic bone formation

We conducted x-ray analysis of mouse carcasses to screen for bone formation outside of the calvarial defect site to examine potential NF-SMS migration post-operatively [Figure 5.9]. We found no evidence of their migration or associated heterotopic or ectopic bone in any of the treatment groups.

5.4. Discussion

FGFs and BMPs are ubiquitous in nearly every human tissue, including bone.[335] Due to their important roles in early development, fracture repair, and maintenance of healthy bone, they are attractive candidates for tissue engineering applications. BMP-7 is well established as a potent osteogenic factor, capable of enhancing new bone growth in humans and is included in FDA-approved products indicated for spinal fusion and long bone nonunion.[336] FGF-2 is attractive because of its angiogenic and mitogenic qualities, as well as its ability to potentially produce synergistic effects with BMPs to accelerate and improve bone healing. It has been used to stimulate bone regeneration alone, as well as in combination with other growth factors.[133] Its application in tissue engineering scaffolds has been met with controversial and inconclusive

results to date, warranting additional studies to evaluate its potential for bone regeneration.[337] The lack of consensus on the use of FGF-2 to promote osteogenic differentiation *in vitro* and bone regeneration *in vivo* can partially be attributed to the wide range of doses used in previous studies, from 0.016 ng/ml[291] to 300 ng/ml[338] *in vitro* and up to 200 ug/site *in vivo.*[339] Dose, as well as duration of FGF-2 treatment on progenitor cells and osteoblasts, can influence whether FGF-2 has an anabolic or catabolic effect on osteogenic differentiation or bone formation.

We show that a relatively low dose, 2 ng/ml FGF-2, can stimulate hiPSC-MSCs to proliferate *in vitro* while maintaining their potential for BMP-7 directed osteogenic differentiation if FGF-2 is limited to the first three days of osteogenic induction. To achieve an additive effect between BMP-7 and FGF-2, it is imperative to carefully control the dose and length of treatment with FGF-2 as mentioned above. While easily accomplished *in vitro* during media preparation, reproducing the doses and unique temporal treatment profiles of multiple drugs *in vivo* remains challenging. Typical approaches to adsorb growth factor to scaffold surfaces produce rapid and unreliable release kinetics and rapid clearance from the body.[293,307,308] We sought to develop a system that facilitated the simultaneous release of FGF-2 and BMP-7 and maintained the controlled and unique temporal release of each factor. Early release of FGF-2 and sustained release of BMP-7 were needed to achieve an additive effect between the factors, as determined by *in vitro* studies. By encapsulating each factor in different formulations of PLGA, we achieve unique release profiles by solely by changing the molecular weights of the PLGA polymer. Low molecular weight PLGA degrades faster than high molecular weight PLGA, allowing for controlled but rapid release of FGF-2, while high molecular weight PLGA enabled sustained release of BMP-7. This dual delivery system

represents a possible model for future delivery of two or more growth factors that require unique release profiles. The sequential or simultaneous delivery of multiple factors has received increased attention in recent years as researchers attempt to modulate multiple aspects of tissue healing or regeneration.[340] Our composite PLGA-NS and NF-SMS platform allows for controlled and sustained release of drugs, and supports the proliferative and osteogenic phases of fracture healing and bone regeneration.

Preclinical animal models have advantages and disadvantages for evaluating bone tissue engineering constructs.[341–343] Our previous study demonstrated the ability of FGF-2 and BMP-7 to enhance ectopic bone formation in a subcutaneous mouse model.[Chapter 4, Figure 4.4] We showed that FGF-2 enhanced osteogenesis by contributing to cell migration and early angiogenesis. In the current study, we employed a novel NF-SMS scaffold to support *in situ* bone regeneration in a critical size calvarial defect. This orthotopic model is more clinically relevant as it better reflects a clinical use case for tissue engineering constructs that are meant to replace autologous bone grafts. However, our finding that the defects were not completely healed after 8 weeks led us to consider a number of factors that might influence the completeness of healing of the critical size defect, including the physiological aspects of the orthotopic site, dose of BMP-7, dose of FGF-2, duration of FGF-2.

We found that the additive effect between FGF-2 and BMP-7 is modest, but observable as both factors contribute to both the bone volume and the quality of new bone. Regarding its physiological characteristics, the calvarium is highly vascularized and abundant of progenitor cells are in the surrounding tissue. The effect of FGF-2 as a stimulator of blood vessel growth and cell migration could be less significant in this highly vascularized environment and we can

likely better observe the pro-osteogenic effect of FGF-2 in this orthotopic model compared to an ectopic model.

We demonstrated that 5μg of BMP-7, encapsulated within high molecular weight PLGA, initiated substantial healing of a 5mm murine calvarial defect, though the defect was not totally healed after 8 weeks. Our choice of a dose of 5μg of BMP-7 was based on previous studies that showed 5μg BMP-7 encapsulated in PLGA nanoparticles could stimulate ectopic bone formation on a PLLA scaffold (Chapter 4). The purpose of our controlled drug release system is to achieve local and physiologically relevant doses of BMP, and to avoid the supraphysiological doses used in the current FDA approved BMP products, which use 1.5-12mg BMP-2 or BMP-7. We reduce the amount of BMP-7 by 1,000-fold compared with commercially available products. Though the calvarial defect is not entirely healed after 8 weeks, additional time to heal a large, critical size defect, may have been required. It was important to evaluate whether FGF-2 could enhance BMP-7 induced bone formation, therefore, it was advantageous to develop a system in which our positive control (BMP-7 alone) did not completely heal the defect.

Our study demonstrated that a rapid release of 10ng FGF-2 from PLGA-NS of low molecular weight could enhance continuous release of BMP-7 from high molecular weight PLGA-NS to increase new bone formation. Consistent with the hypothesis that there may be a threshold beyond which the effect of FGF-2 is no longer pro-osteogenic[339], we found that a 10-fold increase the dose of FGF-2 from 10 ng/defect to 100 ng/defect eliminates any combinatorial osteogenic effect with BMP-7 and limits new bone formation. An additional consideration besides the dose of FGF-2 used is its rate of release from low molecular weight PLGA-NS. Our *in vitro* studies showed that the presence of low-dose FGF-2 for 14 days diminishes the osteogenic potential of hiPSC-MSCs. FGF-2 release from low molecular weight

PLGA-NS was measured at ~50% after 7 days and nearly 75% by the end of 14 days. Though we limit the release of FGF-2 to the early part of an 8-week *in vivo* study, its presence for up to 2 weeks may be suboptimal for bone regeneration in this orthotopic site. This may help to explain the disparity in effect between the low dose (10ng/defect) and high dose (100ng/defect) FGF-2 in combination with BMP-7.

Our choice of animal model, dose of BMP-7 and FGF-2, delivery system, and scaffold all may have influenced the rate and completeness of healing. Further optimization of the combined doses and controlled release of FGF-2 and BMP-7 may improve bone formation and better stimulate healing. This should be the focus of future studies.

5.5. Conclusion

We employed the use of a novel NF-SMS scaffold for repair of a critical size mouse calvarial defect. Previous studies with a nanofibrous and porous disc shaped scaffold, coupled with controlled release of pro-osteogenic biological factors (including small molecules, proteins, and nucleotides) have shown regenerative potential in both ectopic and orthotopic models.[343] We demonstrate that an injectable nanofibrous and porous scaffold may result in substantial healing within a calvarial defect model. The presence of BMP-7 and FGF-2 aided in new tissue growth and the combinatorial effect of low dose FGF-2 (10ng/defect) and BMP-7 to enhanced new bone formation. Our study demonstrates the potential of microspheres as a scaffold to fill a critical size defect. Furthermore, locally delivered FGF-2 and BMP-7 can stimulate bone healing without off-target bone formation.

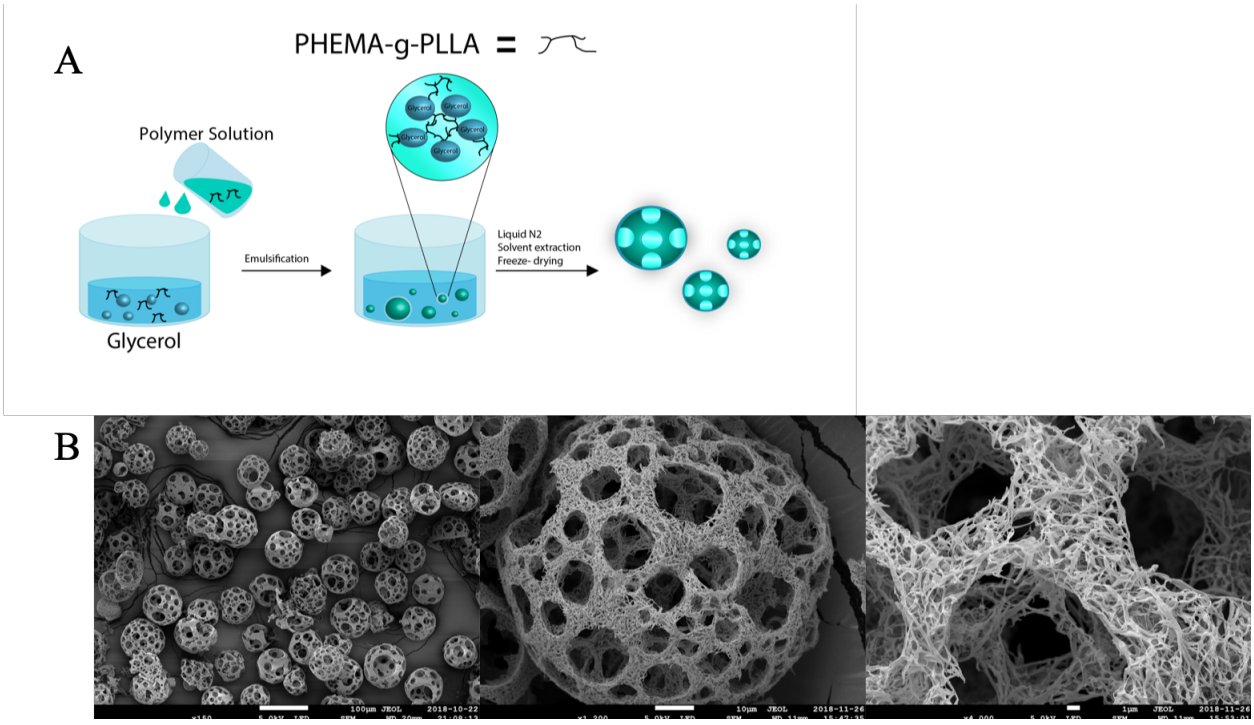


Figure 5.1. Synthesis of nanofibrous spongy microspheres.
(A) Schematic for the synthesis of nanofibrous spongy microspheres (NF-SMS) using a PHEMA-g-PLLA co-polymer. PHEMA-g-PLLA was dissolved in tetrahydrofuran (THF). While mixing, polymer solution was quickly added to spinning glycerol. Liquid nitrogen was used to form the nanofibers while ice was added to extract the solvent and reveal the porous and interconnected microstructure. (B) SEM images of NF-SMS at low magnification (left) showing many spheres, at medium magnification (middle) showing porosity and interconnectedness, and high magnification (right) showing nanofibrous architecture. Scale bar 100 µm (left), 10 µm (middle), 1 µm (right)

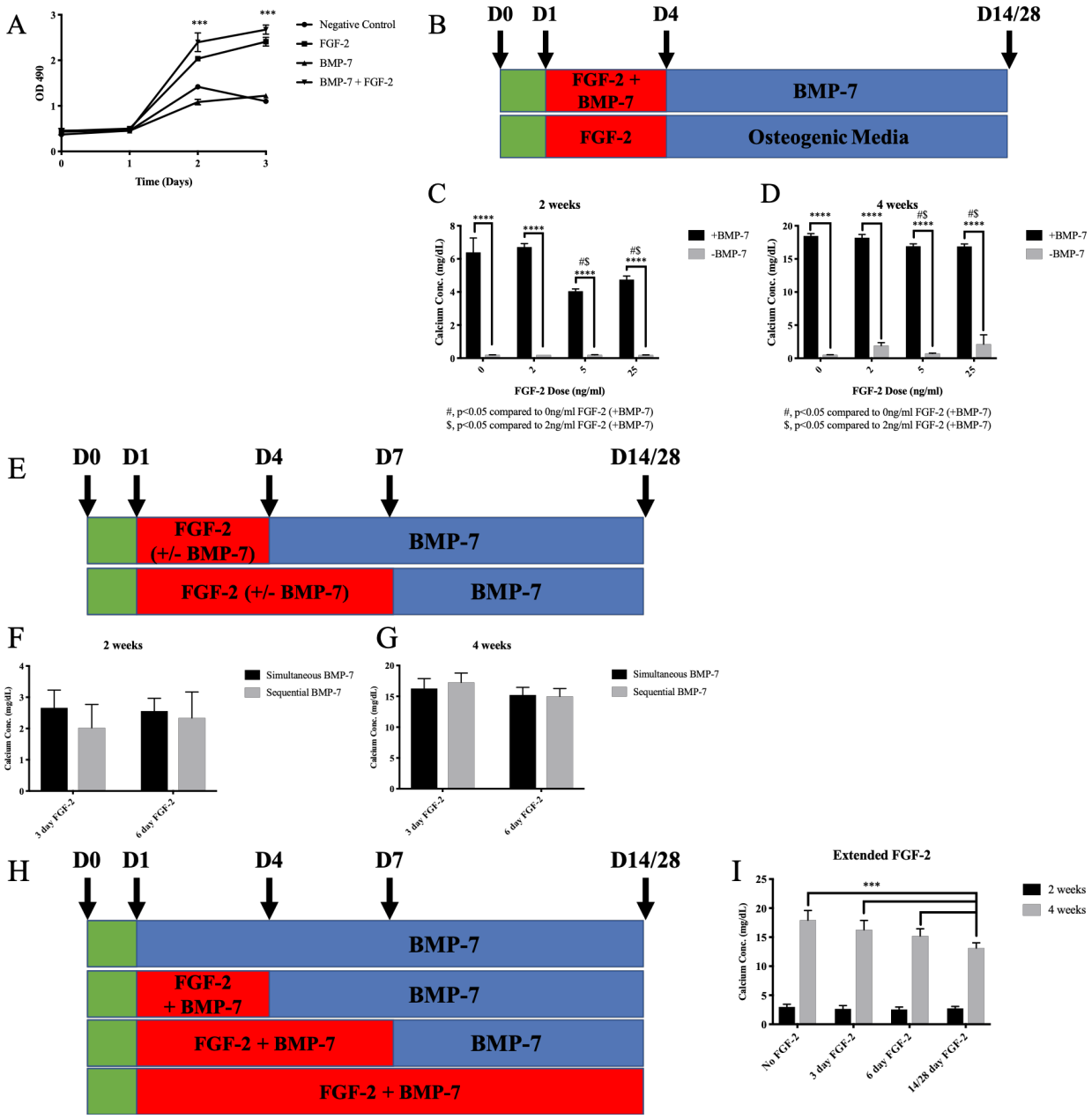


Figure 5.2. FGF-2 and BMP-7 regulation of hiPSC-MSC proliferation and differentiation. (A) Cell Proliferation. HiPSC-MSCs were treated with 2ng/ml FGF-2, 100ng/ml BMP-7, 2ng/ml FGF-2 + 100ng/ml BMP-7, or no additional growth factors (control). After the times indicated, cell growth was measured using the MTS assay. (B) Schematic of mineralization of hiPSC-MSCs at 0, 2, 5, and 25 ng/ml FGF-2 +/- 100 ng/ml BMP-7. (C, D). Mineralization. HiPSC-MSCs were grown in osteogenic media with or without 100ng/ml BMP-7 and the indicated concentrations of FGF-2, with FGF-2 added only for the first 3 days of the experiment. Mineralization was measured by calcium quantification at 14 (C) and 28 days (D). (E) Schematic of simultaneous and sequential treatment of 2 ng/ml FGF-2 and 100 ng/ml BMP-7. Calcium quantification at 14 (F) and 28 days (G) after cells were treated with osteogenic media supplemented with FGF-2 and BMP-7 with BMP added either simultaneously (black) with FGF-

2 or sequentially after FGF-2 (grey). (H) Schematic of extended FGF-2 treatments. (I) Calcium quantification after cells were treated with osteogenic media supplemented with 2 ng/ml FGF-2 for 0, 3, 6, 14 or 28 days + 100ng/ml BMP-7. (* p<.05, ** p < .01, *** p < .001, **** p <.0001)

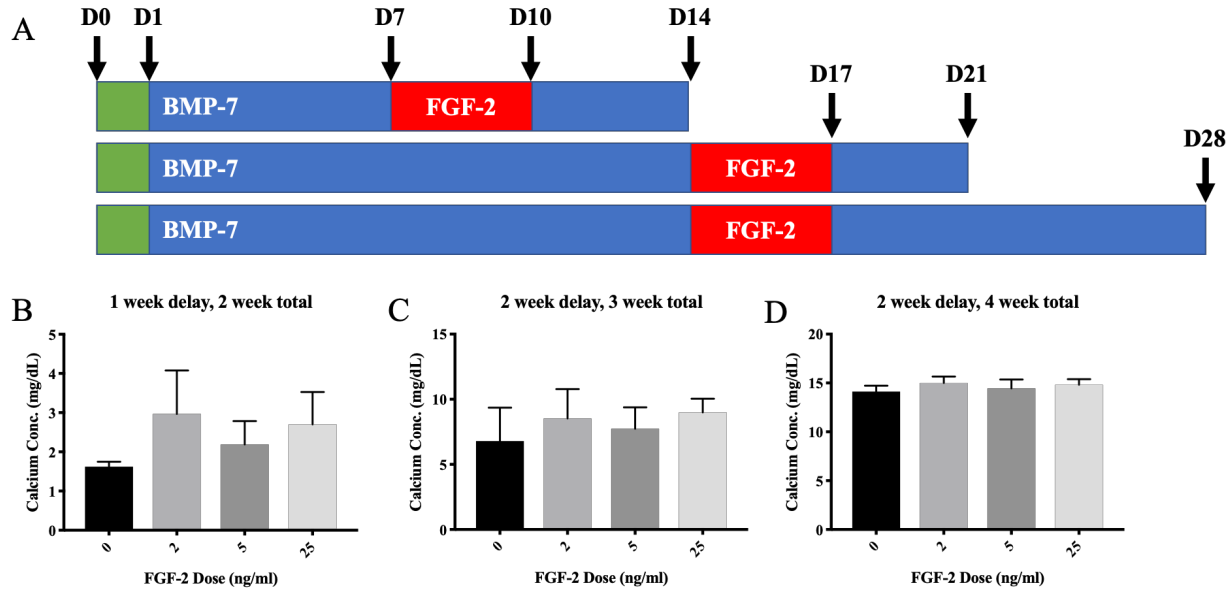


Figure 5.3. Effect of FGF-2 on maturing hiPSC-MSCs.
(A) Schematic of delayed FGF-2 treatment of hiPSC-MSCs at 0, 2, 5, and 25 ng/ml. (B) Mineralization by hiPSC-MSCs following induction with BMP-7 at 100ng/ml and 1-week delayed treatment of FGF-2 after 2 weeks. Mineralization by hiPSC-MSCs following induction with BMP-7 at 100ng/ml and 2-week delayed treatment of FGF-2 after 3 weeks (C) and 4 weeks (D).

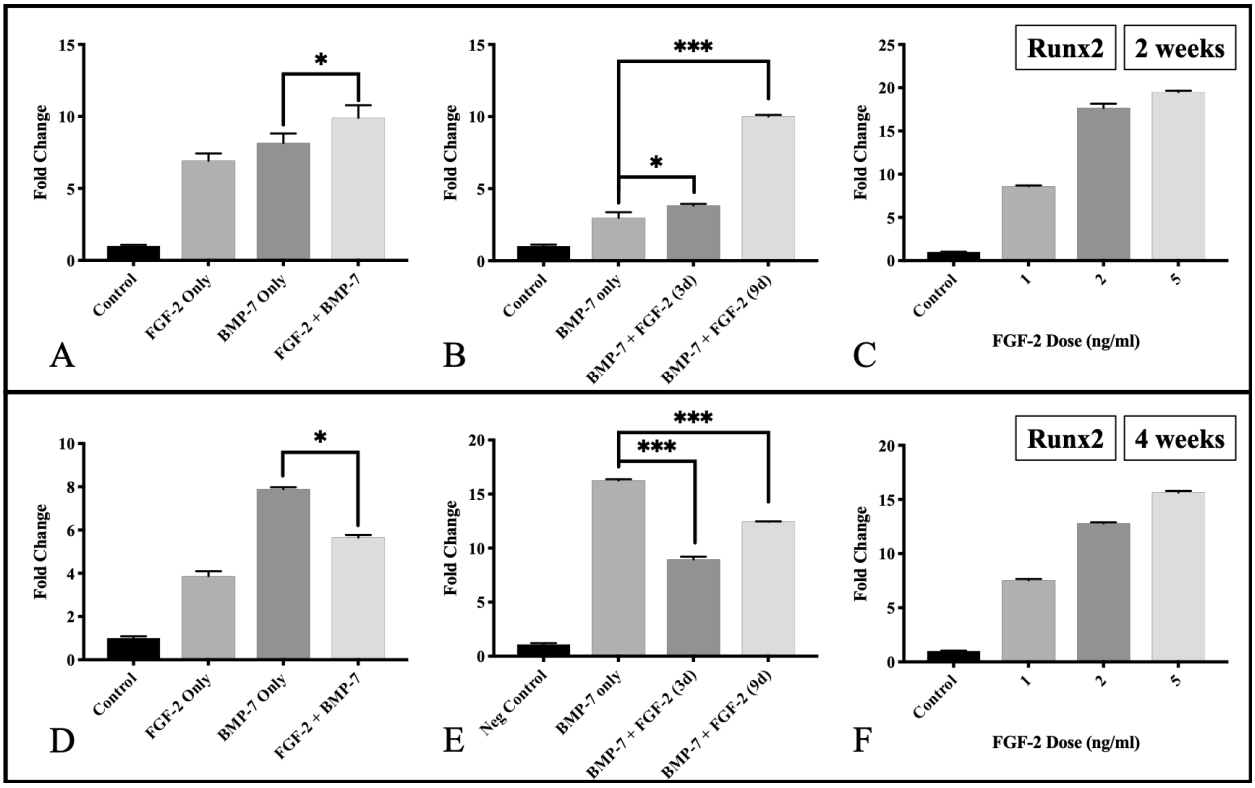


Figure 5.4. FGF-2 and BMP-7 regulation of RUNX2 expression.
(A, D) HiPSC-MSCs were grown in osteogenic media with 2ng/ml FGF-2, 100ng/ml BMP-7, 2ng/ml FGF-2 + 100 ng/ml BMP-7, or no added factors (Control), with FGF-2 added only for the first 3 days of the experiment. RNA was isolated after 14 (A) and 28 days (D) for measurement of RUNX2 mRNA by qRT-PCR. (B,E) HiPSC-MSCs were grown in osteogenic media with 100 ng/ml BMP-7 or 100 ng/ml BMP-7 + 2 ng/ml FGF-2, with FGF-2 added for 3 or 9 days. RNA was isolated after 14 (B) and 28 days (E) for measurement of RUNX2 by qRT-PCR. (C,F) HiPSC-MSCs were grown in osteogenic media with 100ng/ml BMP-7 and the indicated concentrations of FGF-2. RNA was isolated after 14 (C) and 28 (F) days for measurement of RUNX2 mRNA by qRT-PCR. (* $p<.05$, *** $p < .001$)

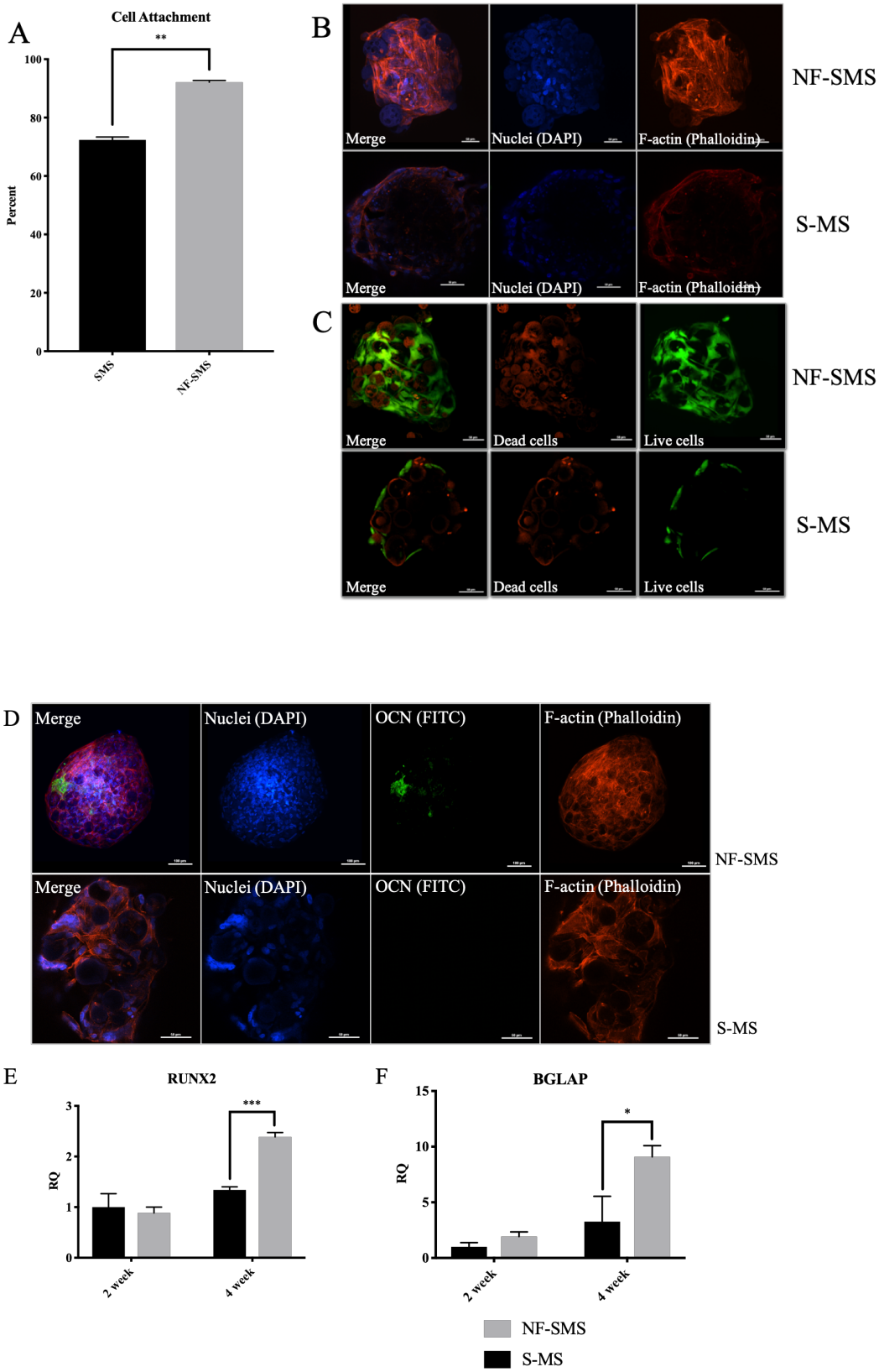

A
Cell Attachment
**
Percent
100
80
60
40
20
0
SMS
NF-SMS
B
Merge
Nuclei (DAPI)
F-actin (Phalloidin)
NF-SMS
S-MS
C
Merge
Dead cells
Live cells
NF-SMS
S-MS
D
Merge
Nuclei (DAPI)
OCN (FITC)
F-actin (Phalloidin)
NF-SMS
S-MS
E
RUNX2
***
RQ
3
2
1
0
2 week
4 week
F
BGLAP
*
RQ
15
10
5
0
2 week
4 week
NF-SMS
S-MS

Figure 5.5. *In vitro* evaluation of NF-SMS compared with S-MS.
(A) Cell attachment. HiPSC-MSCs were mixed with NF-SMS or S-MS at a 5:1 ratio in a 15 ml conical tube and placed on a shaker for 4 hours to allow cells to attach to microspheres. After 4 hours of gentle shaking, unattached cells were counted using a hemocytometer. (B, C) HiPSC-MSCs were seeded onto NF-SMS and S-MS and transferred to spinner flask with growth media for 5 days. Cell-microsphere aggregates were stained with DAPI and phalloidin (B) and evaluated with a live/dead assay (C) and visualized by confocal microscopy. Blue: nuclei, Red: F-actin (B). Green: Calcein-AM (live cells), Red: Ethidium Homodimer (dead cells) (C). Scale bar = 50 µm. (D) HiPSC-MSCs were seeded onto NF-SMS and S-MS and cultured in osteogenic media with 100 ng/ml BMP-7. After 4 weeks, cell-microsphere aggregates were fixed and immunofluorescent staining was used to visualize osteocalcin. Blue: nuclei, Red: F-actin, Green: osteocalcin. Scale bar = 100 µm for NF-SMS (upper panel), 50 µm for S-MS (lower panel). (E, F) Expression of RUNX2 and BGLAP. HiPSC-MSCs were seeded onto NF-SMS and S-MS and transferred to spinner flask for suspension culture with osteogenic media + 100 ng/ml BMP-7. RNA was extracted after 14 and 28 days of culture and RUNX2 (E) and BGLAP (F) and relative gene expression was measured by qRT-PCR.

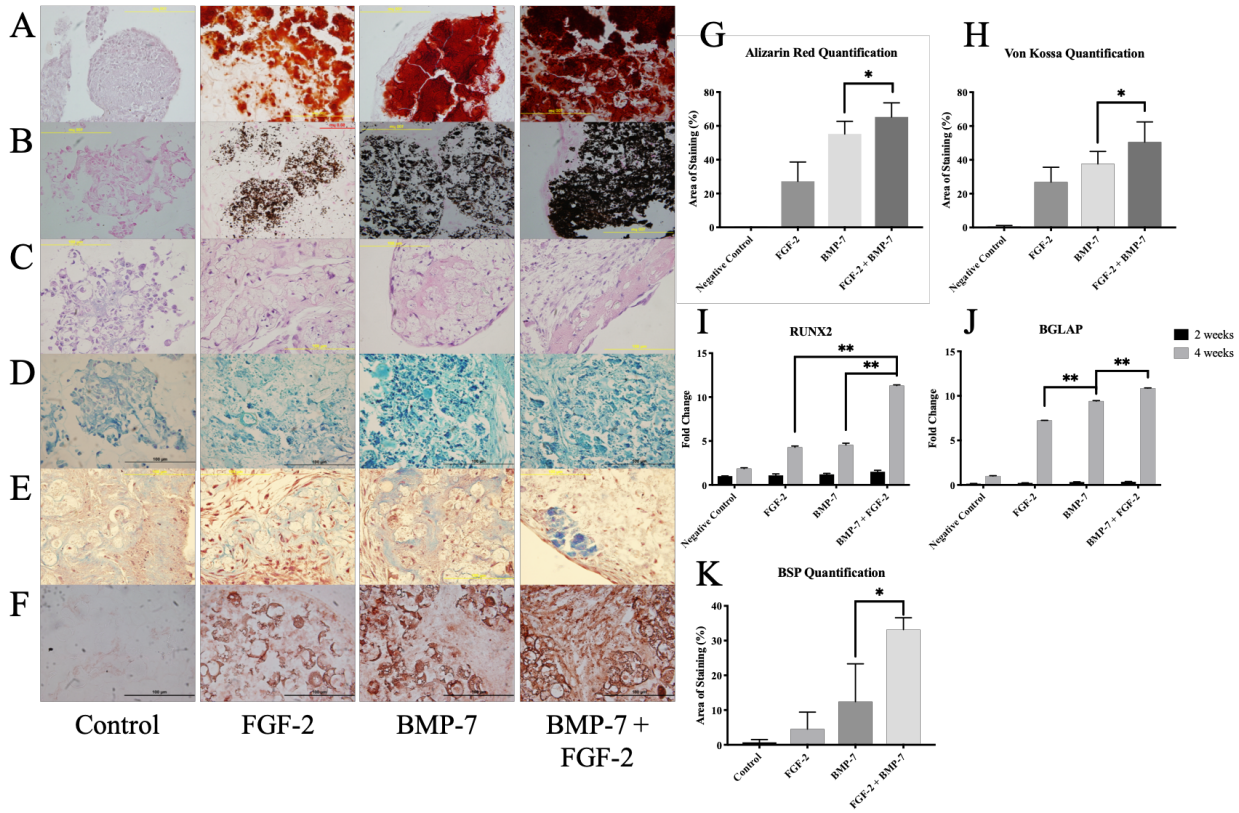


Figure 5.6. Combinatorial effect of FGF-2 and BMP-7 on *in vitro* differentiation of hiPSC-MSCs on NFSMS.
HiPSC-MSCs were seeded onto NF-SMS and transferred to spinner flask for suspension culture with osteogenic media and 2 ng/ml FGF-2, 100 ng/ml BMP-7, 2 ng/ml FGF-2 + 100 ng/ml BMP-7, or no factors added (control), with FGF-2 added only for the first 3 days of the experiment. After 4 weeks, the cell-microsphere aggregates were fixed with 10% buffered

formalin and sectioned. Slides were stained with Alizarin Red S (A), von Kossa (B), hematoxylin and eosin (C), Alcian blue (D), and trichrome (E). Immunohistochemical staining was used to evaluate expression of bone sialoprotein (F). Alizarin Red S and von Kossa staining were quantified (G, H), by ImageJ analysis. RNA was extracted after 2 and 4 weeks of culture and expression of RUNX2 (I) and BLGAP (J) was measured by qRT-PCR. (K) BSP staining was quantified. (* p<.05, ** p < .01)

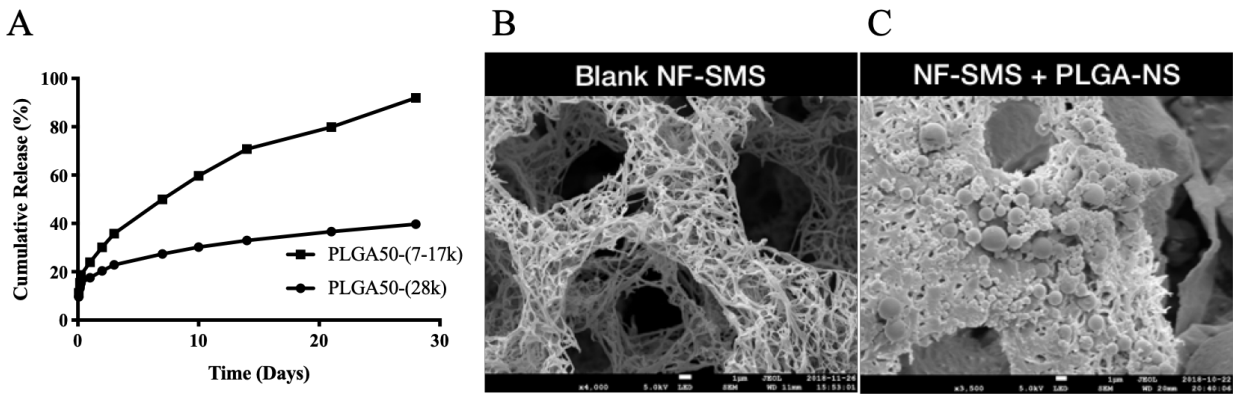


Figure 5.7. Controlled release of FGF-2 and BMP-7 and surgical implantation of NF-SMS in cranial defect.
(A) Cumulative *in vitro* release curves from PLGA nanoparticles of different molecular weight. PLGA50-(7-17k) was used to encapsulate FGF-2 and PLGA50-(28k) Release of factors was measured at 2h, 4h, 8h, 24h, 2d, 3d, 7d, 10d, 14d, 21d, 28d. (B, C) Representative high magnification SEM images of NF-SMS before (B) and after (C) conjugation of PLGA-NS onto the surface (scale bar = 1μm).

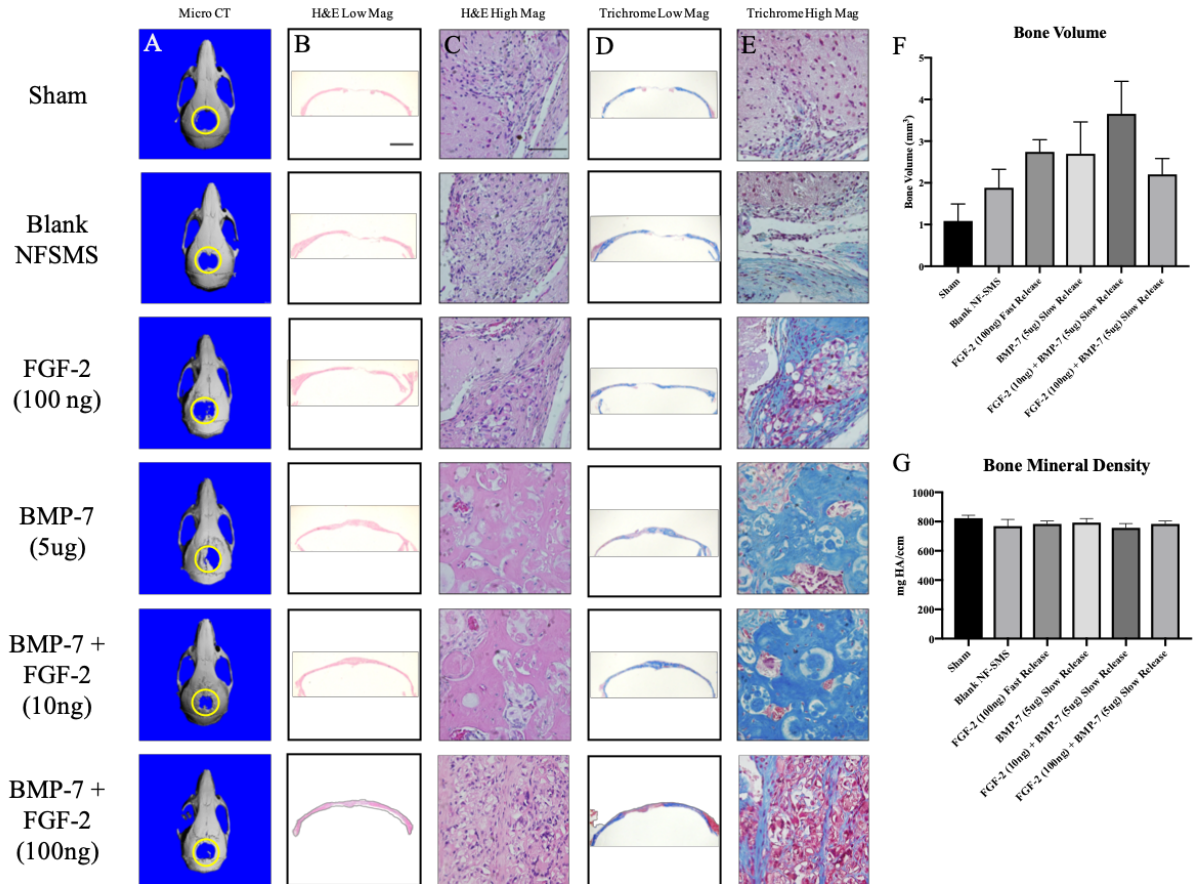


Figure 5.8. µCT and histological characterization of calvarial defect repair after 8 weeks. (A) Representative µCT reconstructions of mouse calvarial defects in different treatment groups. (B, C) Hematoxylin and eosin stain at low (B) and high magnification (C). (D, E) Trichrome stain at low (D) and high (E) magnification. (F) New bone volume and (G) bone mineral density. n = 4-6 per group. (A) circle diameter = 5 mm. Scale bar (B) = 5mm, (C) = 50 µm.

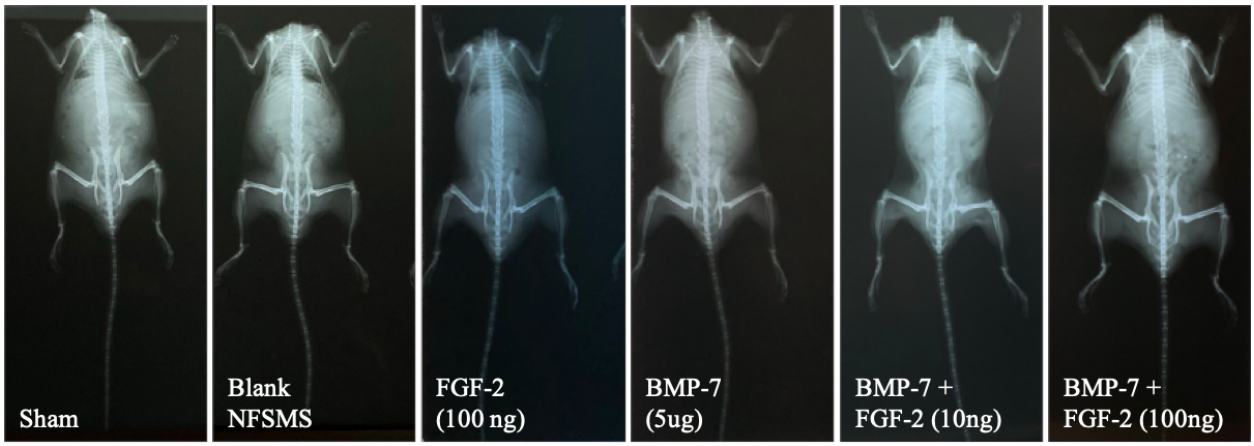


Figure 5.9. Radiological imaging of mouse carcasses for ectopic/heterotopic bone. 25kV for 8 seconds.

Chapter 6. FGF-2 enhances ACVR1 dependent canonical BMP signaling in mouse calvarial osteoblasts

6.1. Introduction

6.1.1. Canonical BMP signaling

Bone morphogenetic proteins (BMPs) are members of the TGF-β family and are known to be essential for bone development. BMP-2, -4, -6, -7, and -9 have demonstrated pro-osteogenic effects through canonical BMP signaling.[344–347] BMPs transduce intracellular signal by binding and activating cell surface BMP receptors. These receptors transfer the signal of bound extracellular ligand via intracellular phosphorylation of a group of R-Smad proteins, known as Smad1, Smad5, and Smad8/9. Phosphorylated Smad proteins (p-Smad1/5/9) form a complex with Smad4, which facilitates translocation of active p-Smad1/5/9 to the nucleus. Upon nuclear localization, p-Smad1/5/9 promotes gene expression including runt related transcription factor 2 (RUNX2), which is considered the master regulator gene for bone formation.[110] This pathway is known as canonical BMP signaling. [Appendix A, Figure A.1] Downstream of RUNX2, pro-osteogenic gene osterix (Osx) is activated and expression of matrix proteins osteocalcin (OCN), bone sialoprotein (BSP), and osteopontin (OSP) is initiated.[348] Canonical BMP signaling is critical to bone development and fracture healing, and often the focus of clinical treatments for bone defects and injuries.

6.1.2. Receptor and ligand specificity

BMPs are found as both homodimers and heterodimers (e.g. BMP-2/7).[349] Upon ligand binding, BMP receptors form a tetramer, consisting of two Type I and two Type II receptors. The presence of bound ligand results in phosphorylation of the Type I receptor by the Type II receptor, activating its kinase activity and subsequent phosphorylation of R-Smad proteins. BMP-2 and BMP-4 signal via the BMPR1A Type I receptor (also known as ALK3), while BMP-7 signals via the ACVR1 Type I receptor (also known as ALK2).[350,351] [Appendix A, Figure A.3.4]

6.1.3. FGF-2 expression during bone development

During initial human bone development, mesenchymal and osteoprogenitor cells are stimulated by several growth factors. As developing tissue matures, expression of these factors changes to help stimulate formation of cancellous and cortical bone with typical features. In addition to the essential role of canonical BMP signaling, bone development and formation is modulated by fibroblast growth factors (FGFs), which can affect cell proliferation, maturation, and fate.[303,352]

FGFs activate four FGF receptors (FGFRs) that in turn produce a cascade of intracellular signaling. Of particular interest is the role of FGF-2, which plays a critical role in endochondral bone formation and cranial suture fusion. FGF-2-deficient mice display phenotypes of improper or incomplete bone development. [302,353] In addition to its critical role in bone formation, FGF-2 has a wide range of effects on various tissue types throughout the body. In particular, it is known as a mitogen and induces proliferation of many cell types, including mesenchymal stem cells and osteoblasts. It is furthermore known to initiate cell migration and stimulate cell

recruitment. FGF-2 is also a pro-angiogenic growth factor, promoting the invasion of endothelial cells and new blood vessel formation. [354]

6.1.4. Crosstalk between BMP and FGF signaling pathways

FGF-2 has been targeted as a potent factor for use in combination with BMP-2, -4, and -7 in regenerative therapies.[132,135,291] FGF-2 has shown potential for the repair of critical size defects in orthotopic models.[339,355] In combination with BMP-2, low dose FGF-2 has a pro-osteogenic effect in mouse osteoblasts[291] and stimulates ectopic bone formation in mice.[135] By contrast, high doses or prolonged exposure to FGF-2 has led to a reduction in BMP-induced mineralization or bone formation.[137,333,356] Their signaling pathways between these factors may be synergistic, additive, or antagonistic, depending on the site and cell type being studied.[335,353] A better understanding of how FGF and BMP signaling pathways interact to enhance or inhibit bone formation is needed for the continued clinical development of combined therapies involving both factors.

Specifically during endochondral ossification in the growth plate, FGFs and BMPs display either synergistic or antagonistic interactions, depending on the region of the growth plate and cell type.[353,357] BMP and FGF signaling can provide transcriptional and post-transcriptional feedback to the opposite signaling pathway.[358,359]

During cranial suture fusion, the interaction of BMP and FGF signaling is notable. FGF-2 causes immature osteoblasts to proliferate and mature osteoblasts to further differentiate.[360] Studies indicate that FGF-2 prevents noggin's ability to inhibit BMP signaling and thus promotes suture fusion (i.e. bone formation).[361] FGF-2 expression is elevated in the mesenchyme/dura of posterity frontal sutures during fusion and FGF-2 induces BMP-2 expression in sagittal and coronal suture cells.[362]

Other studies describe the role FGF-2 has in activation of RUNX2 expression through nuclear localization of p-Smad1/5/9 proteins.[363] The FGF-2 induced activation of RUNX2 was also shown to promote OCN expression.[298] Despite the strong evidence for FGF-2 as a stimulator of RUNX2, the mechanisms by which it upregulates RUNX2 are still not clearly understood. It is evident that a complex relationship between BMP and FGF signaling exists, with multiple nodes of possible interactions, in which duration and intensity of signal can influence the relationship.

Additional studies establish a potential role for FGF signaling in the regulation of BMP receptor expression[364] or Smad phosphorylation [365]. Regulation of BMP receptor activity by FGF-2 is not well described or understood. In this current study, we investigated the interaction of BMP and FGF signaling pathways in neonatal mouse osteoblasts. We hypothesized that FGF signaling may target BMP receptors and tested whether FGF-2 enhances phosphorylation of R-Smad1/5/9 proteins involved in canonical BMP signaling.

6.2. Materials and Methods

6.2.1. Cell Isolation and Culture

Wild-type osteoblasts were isolated from frontal and parietal bone, and suture cells were isolated from surgical suture of mouse calvaria by sequential enzyme digestion. Primary calvarial pre-osteoblasts were isolated from postnatal day 3 mice as reported previously.[366] Cells were cultured in α-MEM supplemented with 10% fetal bovine serum (FBS) and 1% penicillin-streptomycin at 5% CO_2 and 37°C. *Acvr1* floxed and *Bmpr1a* floxed calvarial osteoblast cells were isolated as previously described.[367] Disruption of genes was achieved by activation of *Cre* with incubation of tamoxifen (100 ng/ml) for 72 hours in culture.

Primary mouse bone marrow stromal cells (BMSCs) were isolated from 6-8 week old C57BL/6J mice using a typical method with modification.[368] Briefly, bone marrow was harvested from 6-8-week-old male C57BL/6 mice (Charles River Laboratories International, Inc., Wilmington, MA). Femurs were flushed with Eagle's minimum essential medium (α-MEM, Invitrogen; Carlsbad, CA) containing 10% fetal bovine serum (FBS, Invitrogen; Carlsbad, CA), 100U/mL penicillin and 100 mg/L streptomycin (Invitrogen, Carlsbad, CA). Cells were passed through a 23-gauge needle to create single-cell suspension and resuspended in complete α-MEM and cultured for at least two weeks, removing non-adherent cells and replacing media every 24-48 hours. Cells were used prior to passage 4.

6.2.2. Induction and inhibition of BMP and FGF signaling

Recombinant human BMP-7 (rhBMP-7) was a kind donation from Stryker Biotech (Hopkinton, MA). BMP-2 and BMP-4 were purchased from PeproTech (Rocky Hill, NJ). FGF-2 was purchased from Stemgent (Cambridge, MA). Cells were serum starved for 24 hours prior to growth factor treatment.

LDN-193189 was obtained from Riken Institute (Japan). LDN-212854, U0126, SU5402 and MG132 were purchased from Sigma Aldrich (St. Louis, MO) and used according to the manufacturer's instructions. Cycloheximide, PD184352, and 5z-7-oxozeaenol were purchased from Cell Signaling Technology and used according to the manufacturer's instructions.[Table 6.2]

6.2.3. Protein isolation and western blot analysis

Whole protein isolates were extracted using the EpiQuick Whole Cell Extraction Kit, purchased from EpiGentek (Farmingdale, NY). Halt™ Phosphatase Inhibitor Cocktail (Fisher Scientific, Pittsburgh, PA) was added during protein extraction. Total protein content was

measured with Micro BCA™ Protein Assay Kit purchased from Fisher Scientific (Pittsburgh, PA). 10ug of protein was loaded in NuPAGE™ 4-12% Bis-Tris Protein Gels, 1.5 mm, 10-well, with 4x NuPAGE™ LDS Sample Buffer. Protein was transferred to PVDF membranes (BioRad). Membranes were washed with 1X TBST (BioRad) and blocked using 5% Bovine Serum Albumin (BSA) (Sigma Aldrich) in TBST. Primary antibodies were incubated overnight on a mechanical shaker at 4°C [Table 6.1]. Primary antibodies were purchased from Cell Signaling Technologies. TAK1 antibody was purchased from AbCam. HRP conjugated mouse-anti-rabbit secondary antibody (Santa Cruz) was incubated for one hour at room temperature on a mechanical shaker. Chemiluminescence was activated using BrightStar™ ECL Detection kit (Alkali Scientific) and blots were visualized using BioBlue-MR™ Western Blot Film (Alkali Scientific). Densometric analysis of blot images was conducted using ImageJ software and target protein levels were normalized to endogenous control, b-actin.

6.2.4. Immunohistochemical analysis

Cells were seeded onto sterile glass slides and treated with 100 ng/ml BMP-7 and 2ng/ml FGF-2 for 30 minutes. Samples were then washed with PBS and fixed for 15 minutes with 4% paraformaldehyde (PFA). IHC was conducted with Anti-Rabbit HRP-AEC Cell & Tissue Staining Kit (R&D Systems) according to the manufacturer's instructions. Primary antibody was diluted in 1xPBST at 1:200 dilution. Image analysis to detect staining intensity was conducted with ImageJ and representative images were chosen.

6.3. Results

6.3.1. Activation of canonical BMP and FGF signaling in mouse osteoblasts

Canonical BMP and FGF signaling in mouse osteoblasts were activated when cells were stimulated by 2 ng/ml FGF-2, 100 ng/ml BMP-7, or FGF-2 + BMP-7 for 30 minutes, following 24 hours of serum starvation. Canonical BMP signaling was activated by BMP-7, as a two-fold increase in p-Smad1/5/9 level was observed above control. Addition of 2ng/ml FGF-2 in combination with BMP-7 significantly increased level of p-Smad1/5/9 compared to BMP-7 alone [Figure 6.1.A,B]. Addition of BMP-7 and/or FGF-2 did not change the amount of total Smad1. [Figure 6.1.A] Notably, p-Smad1/5/9 was significantly increased in groups with FGF-2 alone, above control. As anticipated, FGF-2 stimulated phosphorylation of ERK1/2, p38, and JNK, while BMP-7 had no effect on the activation of these mitogen activated protein kinases (MAPK). Non-canonical BMP signaling through TAK1 was not affected by addition of either BMP-7 or FGF-2, as no p-TAK1 (Thr187) was observed in any groups, while p-TAK1(Ser412) remained unchanged from baseline with addition of BMP-7 and/or FGF-2.

We used immunohistochemical staining to observe the intracellular location of activated p-Smad1/5/9 proteins, as activated R-Smad proteins are normally translocated to the nucleus upon phosphorylation. Consistent with the immunoblot assays, we observed that cells treated with BMP-7 or BMP-7 + FGF-2 showed p-Smad1/5/9 protein highly localized to cell nuclei. [Figure 6.1.C] We quantified these results and found a moderate but significant increase in nuclear p-Smad1/5/9 in cells treated with BMP-7 + FGF-2.[Figure 6.1.D] We also found evidence of p-Smad1/5/9 in cells treated with only FGF-2, above the control.

Next, we stimulated mouse calvarial osteoblasts with 100 ng/ml of BMP-2, -4, or -7 with or without 2 ng/ml FGF-2 and measured p-Smad1/5/9. We found that the addition of FGF-2 to

BMP-4 and BMP-7 elevated p-Smad1/5/9 levels, while the presence of FGF-2 reduced BMP-2 induced Smad phosphorylation. [Figure 6.1.E,F]

6.3.2. Pharmacologic suppression of BMP receptor activity

The increase in p-Smad1/5/9 caused by treatment with BMP-7 and FGF-2 and the corresponding lack of an additive effect between BMP-2 and FGF-2 led us to further probe the ligand/receptor specificity of FGF-2 crosstalk with BMP signaling. We used chemical inhibitors LDN-193189 (LDN-19) and LDN-212854 (LDN-21) to pharmacologically inhibit BMP receptor type 1 kinase activity.[Appendix A, Figure A.3] LDN-19 is a derivative of dorsomorphin that is highly selective to BMP type I receptors, while LDN-21 is another dorsomorphin derivative with increased selectivity for ACVR1.[369] Because BMP-2 signals via the BMPR1A receptor and BMP-7 signals via the ACVR1 receptor, we used LDN-19 and LDN-21 to better understand the role of FGF-2 in R-Smad phosphorylation.

In the presence of the LDN-19, p-Smad1/5/9 was not observed when cells were treated with BMP-2, BMP-2 + FGF-2, or BMP-7. However, substantial p-Smad1/5/9 was observed in the group treated with BMP-7 and FGF-2. By contrast, BMP-2 induced p-Smad1/5/9 was still abundant in the presence of LDN-21, while BMP-7-induced Smad1/5/9 phosphorylation was almost entirely inhibited. The addition of FGF-2 to BMP-2 or BMP-7 treated cells in the presence of LDN-21 did not produce or enhance p-Smad1/5/9. [Figure 6.2.A]

After 1, 3, and 5 days of incubation with LDN-19 with BMP-7 +/- FGF-2, pharmacological inhibition of p-Smad1/5/9 was maintained in BMP-7 treated cells, while substantial p-Smad1/5/9 was detected in the BMP-7 + FGF-2 group. Based on these findings, we proposed that ACVR1 was a target for FGF-2 signaling. [Figure 6.2.B]

6.3.3. ACVR1 and BMPR1A receptor deficient cells

To further elucidate the potential role of FGF-2 in modulating BMP type I receptors, we used *Acvr1* floxed or *Bmpr1a* floxed mouse osteoblast cells and induced a conditional knockout by *Cre* activation with Tamoxifen.[Appendix A, Figure A.4] We induced an ACVR1 knockout phenotype and subsequently treated cells with FGF-2, BMP-2 +/- FGF-2, BMP-7 +/- FGF-2, or without additional factor (control) for 30 minutes and measured p-Smad1/5/9 content. In osteoblasts with loss-of-function of ACVR1, p-Smad1/5/9 could not be detected upon treatment with BMP-7 or BMP-7 + FGF-2. ACVR1 cKO cells treated with BMP-2 or BMP-2 + FGF-2 behaved in the same pattern as wild type calvarial osteoblasts. [Figure 6.2.C, upper right panel] Mutant ACVR1 cKO cells were left untreated without Tamoxifen to serve as a control. These cells, in which all BMP type I receptors are left intact, behaved similarly to wild-type calvarial osteoblasts. [Figure 6.2.C, upper left panel]

We induced a BMPR1A knockout phenotype with Tamoxifen and subsequently treated cells under the same conditions as ACVR1 conditional knockout cells, as described above. In cells with loss-of-function of BMPR1A, p-Smad1/5/9 could not be detected after treatment with BMP-2 or BMP-2 + FGF. However, BMP-7 treatment resulted in R-Smad phosphorylation following the same trend as wild-type calvarial osteoblasts. [Figure 6.2.C, lower right panel] FGF-2 mediated increase of BMP-7-induced p-Smad1/5/9 was not significant in these cells. [Figure 6.2.D] Mutant BMPR1A cells were also left untreated with Tamoxifen as a control. In these cells, p-Smad1/5/9 levels followed the same pattern as wide-type calvarial osteoblasts. [Figure 6.2.C, lower left panel]

Together, these data demonstrate that the presence of the BMP type I receptors is essential for p-Smad1/5/9 signaling and FGF-2 enhanced Smad phosphorylation is eliminated in cells with ACVR1 loss-of-function.

6.3.4. Inhibition of FGF receptor and ERK1/2 signaling results in corresponding reduction of p-Smad1/5/9

FGF-2 binds to FGF receptors and activates multiple cascades of signaling, including activation of MAP kinases that can initiate transcriptional regulation of cells.[Appendix A, Figure A.5] Previous studies suggest that FGF-induced MAP kinase activation, specifically ERK1/2 signaling, is responsible for modulating canonical BMP signaling.[370] We therefore sought to interrupt FGF signaling by using selective inhibitors of FGF receptors (SU5402), MEK phosphorylation (PD184352) and ERK1/2 phosphorylation (U0126). We subsequently measured p-Smad1/5/9 after treatment with FGF-2, BMP-7, or BMP-7 + FGF-2. [Appendix A, Figure A.6]

Treatment of cells with SU5402 resulted in total reduction in p-ERK1/2, with substantial reduction of p-JNK and p-p38. Correspondingly, p-Smad1/5/9 was reduced in all groups. [Figure 6.3.A] The inhibition of Smad phosphorylation caused by SU5402 was quantified and compared with control osteoblasts. [Figure 6.3.B]

Treatment of cells with MEK inhibitor PD184352 resulted in a total reduction of p-ERK1/2. In the presence of the MEK inhibitor, BMP-7 induced normal Smad phosphorylation. [Figure 6.3.C] Reduced p-Smad1/5/9 was observed in the combined treatment with BMP-7 and FGF-2, suggesting the importance of the p-ERK1/2 signaling pathway in BMP and FGF signaling crosstalk.[Figure 3d] In cells treated with U0126, there was no change in p-Smad1/5/9 between BMP-7 treated and BMP-7 + FGF-2 treated cells, reinforcing the hypothesis that p-ERK1/2 signaling potentially targets ACVR1 dependent Smad phosphorylation. [Figure 6.3.E,F]

Our previous experiments [Figure 6.2] identified ACVR1 as a potential target of FGF-2 signaling and based on this set of experiments, we propose a mechanism for FGF-2 regulation of Smad signaling via p-ERK1/2.

6.3.5. Non-canonical BMP signaling is unaffected by FGF-2

It is known that TAK1 mediates BMP signaling independently from Smad activity.[371] To evaluate the effect of FGF-2 on noncanonical BMP signaling we measured the level of p-TAK1 and p-Smad1/5/9 in the presence or absence of a TAK1 inhibitor, 5z-7-Oxozeaenol, which prevents TAK1 phosphorylation and its subsequent signaling via p38 and JNK.[Appendix A, Figure A.7] We measured TAK1 phosphorylation at the Serine 412 (Ser412) and Threonine 187 (Thr187) amino acid sites and no observable differences were found among treatment groups. [Figure 6.4.A] Despite successfully inhibiting phosphorylation of JNK and p38 with 5z-7-Oxozeaenol, no changes in p-Smad1/5/9 levels were observed. Importantly, we observed FGF-2 enhanced p-Smad1/5/9 levels in BMP-7 treated cells, which was consistent with our previous findings.[Figure 6.4.B] Taken together, these data suggest that non-canonical BMP signaling activity is not modified by FGF-2 signaling and is not responsible for FGF-2 induced elevated levels of p-Smad1/5/9.

6.3.6. Increased LDN-19 concentration eliminates FGF-2 induced Smad phosphorylation

Above we present evidence that FGF-2 crosstalk with BMP-7 occurs by p-ERK1/2 targeting of ACVR1 receptor kinase activity. To support this proposed mechanism, we found abundant levels of p-Smad1/5/9 when cells were treated with BMP-7 + FGF-2 despite the use of a pan BMP Receptor type 1 inhibitor, LDN-19, which blocks BMP-activated Smad signaling. To better understand the potential role of p-ERK1/2 as it relates to ACVR1, we increased the concentration of LDN-19 from 100nM to 300nM, 1000nM, and 3000nM. While FGF-2

treatment supports Smad phosphorylation at 100 and 300nM LDN-19, p-Smad1/5/9 is not detectable when LDN-19 concentration reaches 1000nM or 3000nM. [Figure 6.5.A] LDN-19 inhibits the kinase domain of BMP type I receptors, thus preventing R-Smad phosphorylation.[372] We propose that p-ERK1/2 targets ACVR1 as a substrate for its enzymatic kinase activity because saturated concentration of inhibitor prevents phosphorylation of R-Smads.

LDN-19 is known to be an ATP-competitive small molecule inhibitor of type I BMP receptors.[373] Its IC_{50} values vary depending on the target receptor, but range from 40-210nM.[373,374] In the presence of an effective concentration of LDN-19 (100 nM), BMP-7 induced Smad1/5/9 phosphorylation was inhibited, but treatment of cells with BMP-7 + FGF-2 maintained substantial Smad1/5/9 phosphorylation. By increasing the concentration of LDN-19 to 1000 nM, we completely blocked ACVR1 kinase activity, even in the presence of FGF-2.

We sought to elucidate whether p-ERK1/2 would act competitively or non-competitively with LDN-19.[Figure A.10] If p-ERK1/2 were to create a conformational change in the ACVR1 kinase domain that lessens the effectiveness of LDN-19, this non-competitive regulatory mechanism might not be affected by an increase in LDN-19 dose. Because an increasing dose of LDN-19 suppresses the Smad1/5/9 phosphorylation attributed to FGF-2, we interpret this finding to suggest that the ACVR1 receptor is still susceptible to LDN-19 inhibition and that p-ERK1/2 and LDN-19 are competitive in their targeting of ACVR1. We therefore hypothesize that p-ERK1/2 does not cause a conformational change to ACVR1 to increase its kinase activity. Rather, we propose that p-ERK1/2 kinase activity targets ACVR1 as a substrate, enhancing its C-terminal phosphorylation and increasing its R-Smad kinase activity. Our findings highlight the importance of p-ERK1/2 signaling as a modulator of BMP signaling.

6.3.7. FGF-2 does not affect Smad1 synthesis or p-Smad degradation

Smad1/5/9 and their activated forms (p-Smad1/5/9) are regulated within the cells in several mechanisms. Their degradation is mediated by Smurf1 and Smurf 2 proteins, which act as E3 ubiquitin ligases to initiate proteolysis of Smad proteins.[375,376] Canonical BMP signaling can be further regulated by phosphatases that target active receptors or active Smad proteins.[377] We sought to evaluate whether FGF-2 interrupted Smad1/5/9 translation or degradation. We used cycloheximide (CHX) to interrupt protein translation and MG132 to interrupt proteasomal degradation to study the potential effects of FGF-2 on p-Smad1/5/9.[Appendix A, Figure A.8,9]

We pretreated cells for 1 hour with CHX, MG132, CHX + MG132 or DMSO as a vehicle control and subsequently added 100 ng/ml BMP-7 +/- 2 ng/ml FGF-2 and incubated cells for an additional 1 hour. We then replaced the media with fresh media including inhibitors, but without the growth factors. Protein was extracted after 1, 24, and 48 hours and subjected to Western blotting, with equal total protein loaded into each lane. Of note, the granularity of the results from these studies is somewhat limited because of the non-specific effects of CHX and MG132. CHX will equally prevent translation of new Smad proteins, as well as the phosphatases that inhibit them. Similarly, MG132 will stabilize Smad and p-Smad1/5/9 proteins, as well as the proteins and phosphatases that regulate them.

In the presence of CHX, MG132, or CHX + MG132, total Smad1 protein level was unchanged in the BMP-7 and BMP-7 + FGF-2 treatment groups at 1, 24, and 48 hours. [Figure 6.6.A,B] We found no evidence that FGF-2 enhanced stabilization of Smad1 against ubiquitination and subsequent degradation. Similarly, we found no evidence that FGF-2 affected

Smad1 half-life. These findings rule out another potential mechanism by which FGF-2 modulates BMP-induced Smad signaling.

6.3.8. BMP and FGF signaling overlap in BMSCs and Suture Cells

In endochondral ossification and in cranial suture fusion, crosstalk between BMP and FGF signaling was found to produce pro-osteogenic effects. To better understand the interplay of these pathways in relevant cell types that exist in these environments, we measured p-Smad1/5/9 in murine suture cells [Figure 6.7.A] and BMSCs [Figure 6.7.B,C] treated with BMP-7 +/- FGF-2. We found that BMSCs were less sensitive to both BMP-7 and FGF-2 after being exposed to the growth factors for 30 minutes, as low levels of p-Smad1/5/9 and p-ERK1/2 were observed.[Figure 6.7.B] When this treatment duration was increased to 24 hours, we observed a notable increase in p-Smad1/5/9 and p-ERK1/2.[Figure 6.7.C] In both BMSCs and suture cells, we observed that BMP-7 + FGF-2 enhanced p-Smad1/5/9 compared with BMP-7 alone, though these changes were not statistically significant. [Figure 6.7.D-F]

6.4. Discussion

We found that treatment of mouse calvarial osteoblasts with BMP-7 + FGF-2 results in elevated p-Smad1/5/9 levels compared to BMP-7 alone.[Figure 6.1] In cells treated with LDN-19, the presence of p-Smad1/5/9 after administration of BMP-7 + FGF-2 highlights the potential importance of the ACVR1 receptor in crosstalk between these two signaling pathways, as p-Smad1/5/9 is not detected under 100nM LDN-19 treatment when only BMP-7 is administered. [Figure 6.2.A] The absence of the ACVR1 receptor in conditional knockout cells completely eliminates BMP-7 induced signaling and the addition of FGF-2 is unable to induce p-Smad1/5/9. This suggests that the ACVR1 receptor must be both present and active for FGF-2 to enhance BMP-7 related Smad phosphorylation. [Figure 6.2] By interrupting FGF receptor, MEK, and

ERK activity and observing a corresponding decline in p-Smad1/5/9 levels upon treatment with BMP-7 +/- FGF-2, we determined that intracellular transduction of FGF-2 signal was necessary to modulate BMP receptor activity and highlight ERK as focal signaling molecule in crosstalk between these pathways.[Figure 6.3] Our data suggest that p-ERK1/2 signaling, not TAK1 or its downstream targets p38 and JNK, is responsible for modulating Smad-dependent BMP signaling in this *in vitro* model. [Figure 6.3]

BMP signaling can be regulated by several modalities, including but not limited to the following: a) control of extracellular BMP ligand concentration and binding; b) cell surface receptor expression and kinase activity; c) p-Smad1/5/9 nuclear translocation; and d) p-Smad1/5/9 stabilization, degradation, and modulation inhibitory Smads.[378] Among these modalities, FGFs have been shown to affect extracellular ligand binding through inhibition of expression of the BMP antagonist noggin [379], BMP receptor expression[364], p-Smad1/5/9 degradation through Smurf1 E3 ligase activity[380], and nuclear translocation and subsequent RUNX2 activation[363]. Our data suggest that FGF-2 can additionally regulate ACVR1 receptor kinase activity, thereby increasing Smad phosphorylation and establishing a positive regulatory relationship between FGF-2 and BMP-7. This finding has not previously been reported and only one previous study establishes a link between FGF signaling and Smad phosphorylation in an osteogenic model.[365]

We further propose that p-ERK1/2 acts to phosphorylate ACVR1 receptor in an enzyme/substrate manner. Typically, BMP type II receptors facilitate extracellular ligand binding and phosphorylate C-terminal serine/threonine (Ser/Thr) residues of the BMP type I receptor to initiate R-Smad phosphorylation and propagate the signal of bound ligand. Like the BMP type II receptor, p-ERK1/2 is also a serine/threonine kinase and can phosphorylate target substrates that

possess a Ser/Thr-Proline (Pro) motif.[381] Evidence that p-ERK1/2 can broadly target a large number of substrates[381,382] is consistent with our proposed mechanism of action, though we acknowledge that our study is limited in that we do not show a direct physical interaction between p-ERK1/2 and ACVR1. Demonstrating a physical interaction between p-ERK1/2 and the ACVR1 receptor would more definitively link these two signaling pathways. Typically, co-immunoprecipitation assays or FLAG-tag assays can be used to establish these physical interactions. However, our studies have found that the commercially available antibodies to ACVR1 are not specific enough to produce reliable results to this end. We therefore rely on indirect evidence that p-ERK leads to C-terminal phosphorylation of ACVR1 to propagate p-Smad1/5/9 signaling. [Figure 6.5.A]

In the absence of a highly specific ACVR1 primary antibody that would be necessary to conduct co-immunoprecipitation or Flag-Tag assays to establish protein-protein interactions, an autokinase assay using gamma labeled ATP may provide additional insights as to the ability of p-ERK1/2 to treat ACVR1 as a substrate. Furthermore, an analysis of the target domain of p-ERK1/2 kinase and comparison between the C-terminal BMPR1A and ACVR1 receptor domains may yield additional theoretical support to the proposed mechanism for p-ERK1/2 targeting of ACVR1 within this work. Future studies should also consider the roles of Smad4, Smad6/7, and Smurf1/2 in the regulation of ACVR1 dependent Smad1/5/9 activation by FGF-2. Additionally, assessing the effect of increasing doses of FGF-2 on Smad1/5/9 phosphorylation would aid in providing mechanistic support for tissue engineering platforms that seek to combine FGF-2 with BMPs. Furthermore, an understanding the influence of various FGFR isoforms on FGF-2 induced Smad1/5/9 phosphorylation may provide additional insight into the complex regulatory mechanisms involved in the crosstalk of these pathways.

6.5. Conclusion

BMP-2 and BMP-7 are FDA approved factors indicated for use in spinal fusion surgery and long bone nonunions as substitutes for autologous bone grafts. There has been an increased interest in developing bone graft substitutes that include multiple growth factors to provide critical biological cues that enhance healing and tissue regeneration. FGF-2 is a particularly attractive target to combine with BMP-7 due to its potent angiogenic, mitogenic, and osteogenic effects, as it has potential to increase rate of healing and to reduce rate of graft failure. Understanding the underlying mechanisms for crosstalk between BMP and FGF signaling pathways is important to support tissue engineering platforms that seek to combine BMPs and FGFs as a combination therapy for repairing large volume bone defects. The crosstalk between BMP and FGF signaling pathways is observed in bone development, particularly during endochondral ossification and cranial suture fusion.[361,383]. We present compelling evidence that FGF-2 signaling can elevate ACVR1-specific Smad phosphorylation via p-ERK1/2. Further validation and exploration of the relationship between p-ERK1/2 and ACVR1 receptor may lead to additional therapeutic approaches to bone regeneration and tissue engineering.

Table 6.1. Antibody Concentrations

Primary Antibody	Dilution
p-Smad1/5/9	1:1,000
Total Smad1	1:1,000
b-actin	1:20,000
p-ERK1/2	1:40,000
Total ERK1/2	1:20,000
pTAK1 (Thr187)	1:1,000
pTAK1 (Ser412)	1:1,000
Total TAK1	1:1,000
p-JNK	1:1,000
Total JNK	1:1,000
p-p38	1:1,000

Total p-38	1:1,000

Table 6.2. Inhibitor Doses and Treatment Times

	Concentration	**Treatment Time**
LDN-193189	100nM – 3000nM	30 min
LDN-212854	100nM	30 min
Cycloheximide	50uM	1 hour-72 hours
U0126	10uM	30 min
SU5402	80uM	30 min
MG132(R)	10uM	1 hour-72 hours
(5Z)-7-Oxozeaenol	20uM	30 min
PD184352	10uM	30 min

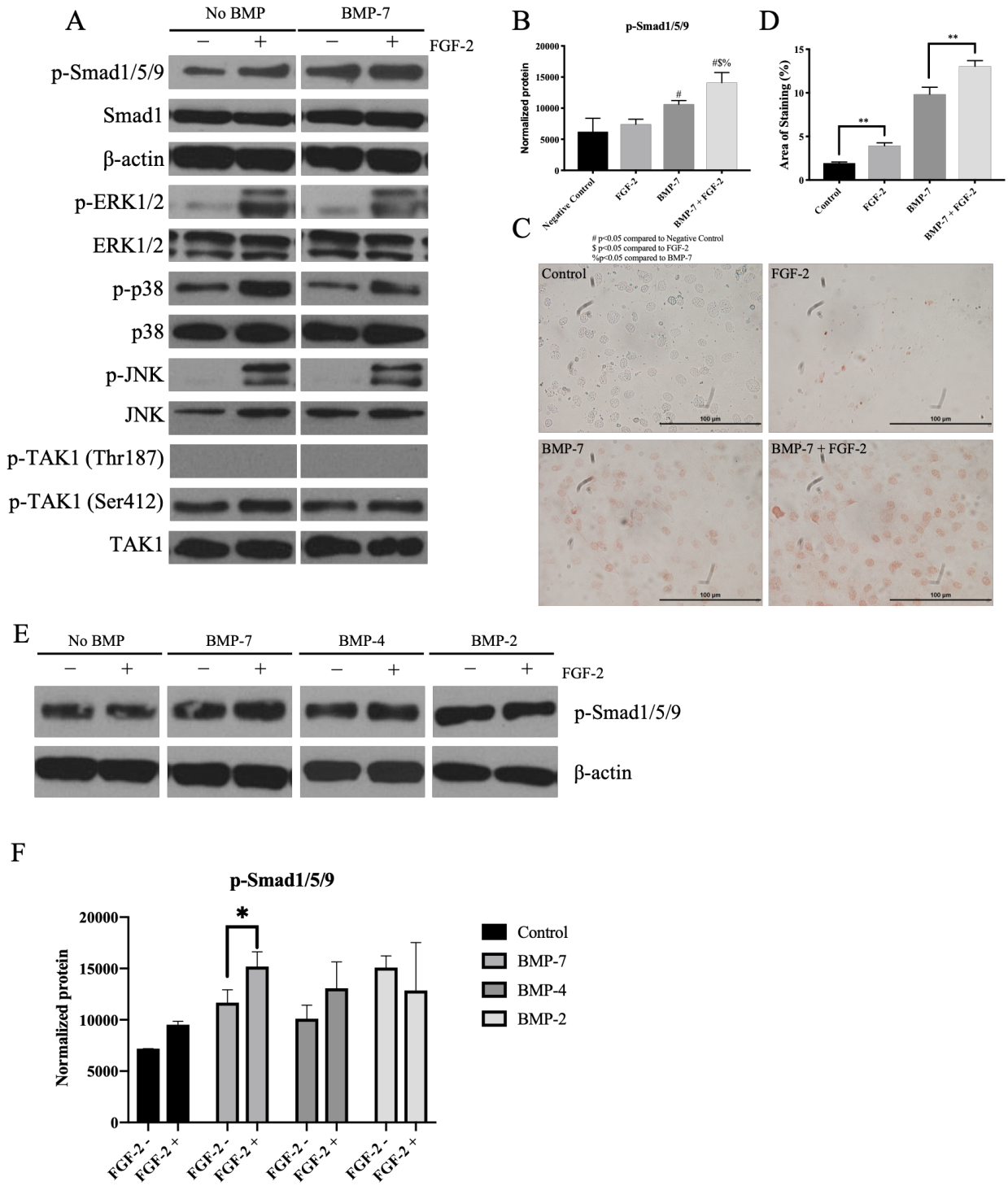
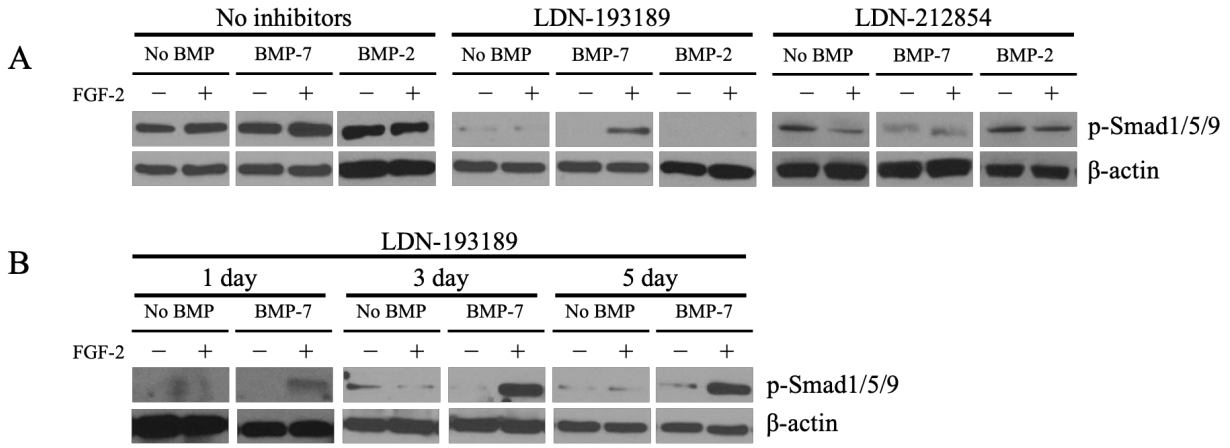


Figure 6.1. Activation of canonical BMP and FGF signaling by BMP-7 and FGF-2

(A) Baseline levels of canonical and non-canonical BMP signaling pathway markers and mitogen activated protein kinase (MAPK) markers in canonical FGF signaling. Mouse calvarial osteoblasts were serum starved for 24 hours before treatment with 2ng/ml FGF-2, 100 ng/ml BMP-7, FGF-2 + BMP-7, or no added factors (Control). Protein isolates were subjected to western blotting and total protein was normalized per lane. (B) Densometric analysis of p-Smad1/5/9 (n=4). P-Smad1/5/9 was normalized to β -actin. (C) Immunohistochemical staining of mouse calvarial osteoblasts after 24 hours of serum starvation and treatment with FGF-2, BMP-7, FGF-2 + BMP-7 or no added factors (control). (D) Image analysis was conducted in ImageJ to obtain percent positive stain for p-Smad1/5/9 (n=3) representative images shown. (E) Comparison of Smad1/5/9 phosphorylation by 100 ng/ml BMP-2, -4, or -7 with or without 2 ng/ml FGF-2. (F) Densometric analysis of p-Smad1/5/9 from (E)(n=4).



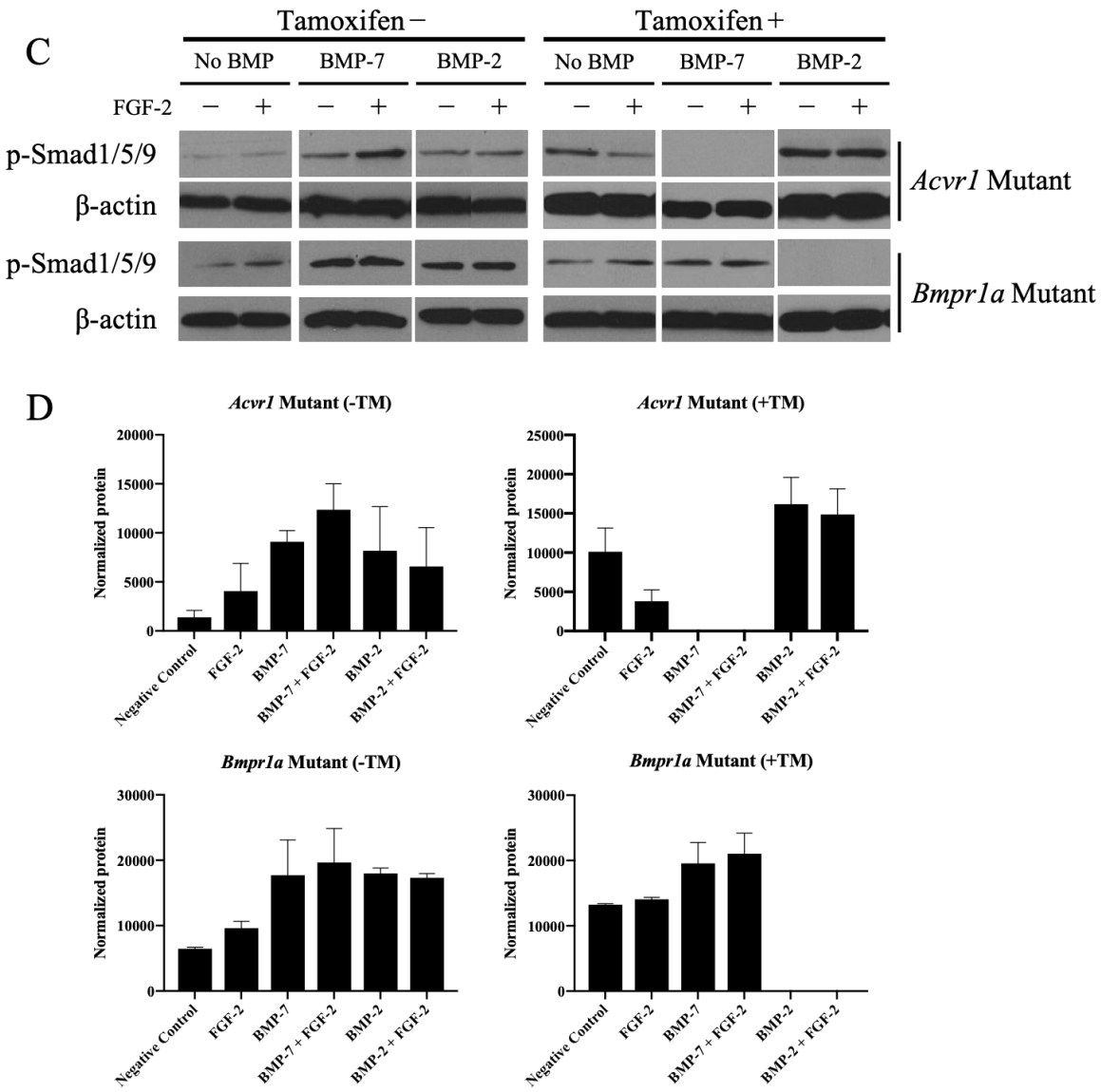


Figure 6.2. Selective inhibition and conditional knockout of ACVR1 and BMPR1A receptor kinases

(A) Comparison of p-Smad1/5/9 in mouse calvarial osteoblasts after pre-treatment with selective inhibitors of BMP Receptor type I, LDN-193189 (100 nM), LDN-212854 (100nM), or no added inhibitors. Cells were serum starved for 24 hours and pre-incubated with inhibitors prior to treatment with +/- 2 ng/ml FGF-2, with or without 100 ng/ml BMP-7 or BMP-2. (B) Prolonged treatment of mouse calvarial osteoblasts with growth factors in the presence of LDN-193189. Cells were serum starved for 24 hours prior to addition of inhibitors and growth factors. Protein lysate was obtained after 24, 72, or 120 hours and subjected to western blotting. (C) Measurement of p-Smad1/5/9 in ACVR1 or BMPR1A conditional knockout cells. Mutant loss-of-function phenotype was induced by tamoxifen (TM) (right panel) or not. Cells were serum starved for 24 hours prior to 30-minute treatment with growth factors as indicated. (D) Densometric analysis of p-Smad1/5/9 in conditional knockout cells (n=4).

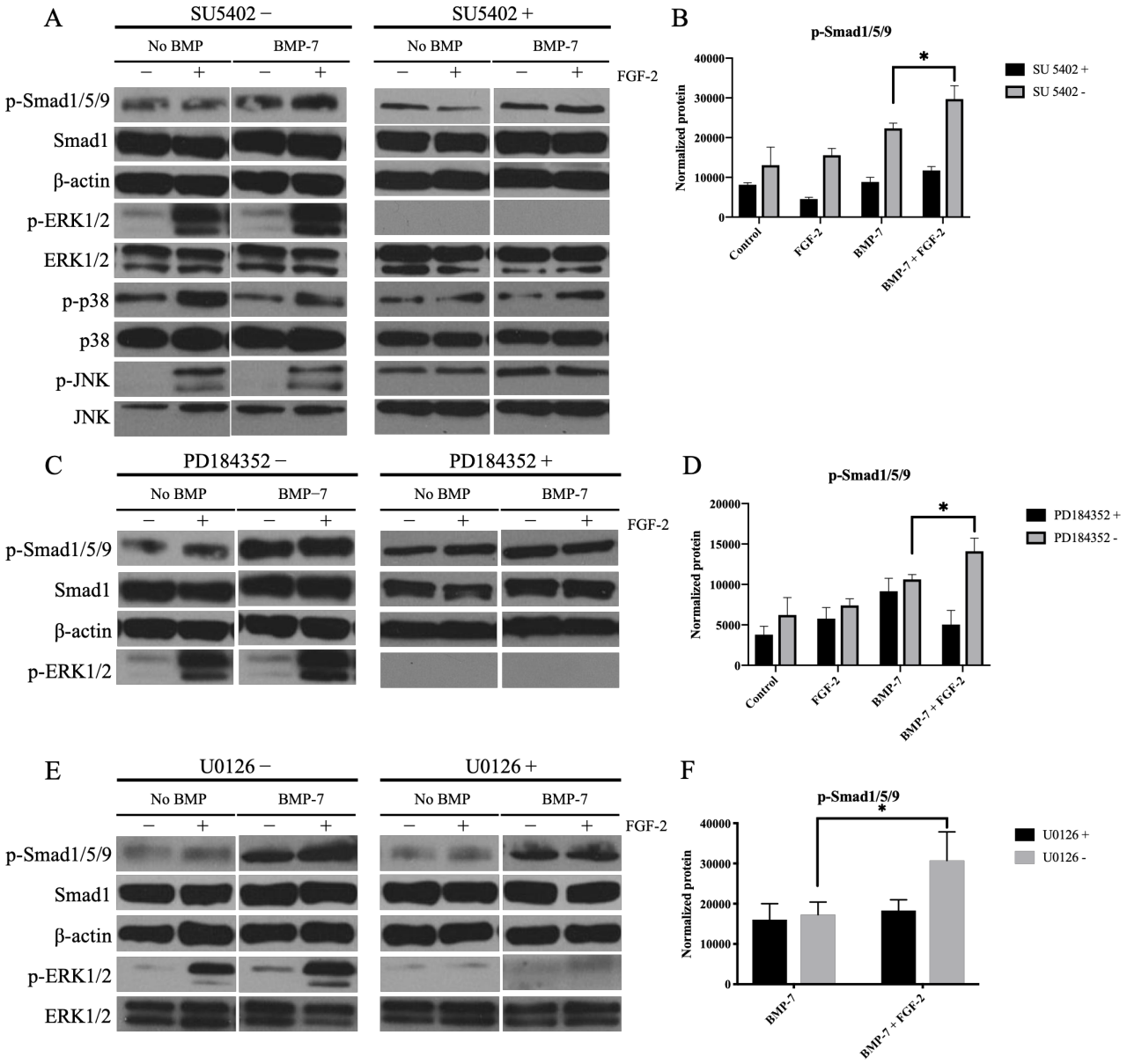


Figure 6.3. Selective inhibition of FGF receptor and MEK/ERK signaling
(A) P-Smad1/5/9 and relevant MAPK signaling molecules after mouse calvarial osteoblasts were pretreated for 30 minutes with 80μM SU5402, a selective inhibitor of FGF receptor tyrosine kinases and with 2 ng/ml FGF-2, 100 ng/ml BMP-7, FGF-2 + BMP-7 or no additional factor (Control) for 30 minutes. (B) Densometric analysis of p-Smad1/5/9 (n=4). (C) P-Smad1/5/9 was evaluated in mouse calvarial osteoblasts following 30-minute pretreatment with 10 μM MEK inhibitor PD184352 and 30-minute treatment with FGF-2, BMP-7, FGF-2 + BMP-7, no additional factor (Control). (D) Densometric analysis of p-Smad1/5/9 (n=4). (E) P-Smad1/5/9 was evaluated in mouse calvarial osteoblasts following 30-minute pretreatment with 10 μM ERK inhibitor U0126 and 30-minute treatment with FGF-2, BMP-7, FGF-2 + BMP-7, no additional factor (Control). (F) Densometric analysis of p-Smad1/5/9 (n=6).

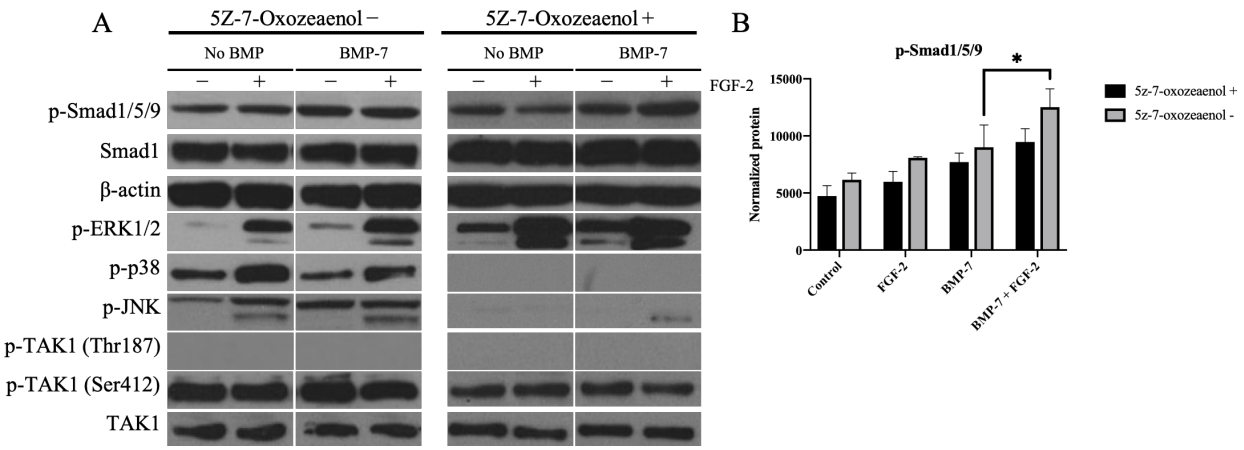


Figure 6.4. Evaluation of non-canonical BMP signaling pathway
(A) Canonical and non canonical BMP and canonical FGF signaling molecules were measured after 30 minute pretreatment with 20 μM TAK1 inhibitor 5z-7-oxozeaenol and 30 minute treatment with 2 ng/ml FGF-2, 100 ng/ml BMP-7, FGF-2 + BMP-7, or no additional factor (Control) (B) Densometric analysis of p-Smad1/5/9 (n=4).

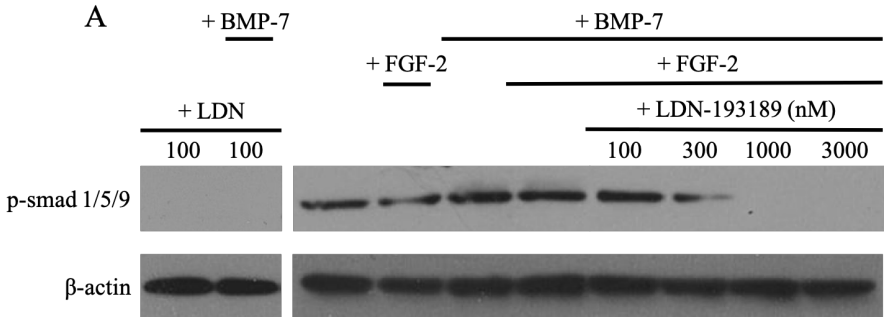


Figure 6.5. Increased LDN-19 concentration inhibits Smad1/5/9 phosphorylation induced by FGF-2
(A) Level of p-Smad1/5/9 was measured after pretreatment of cells with or without LDN-193189 for 30 minutes followed by treatment with 2 ng/ml FGF-2, 100 ng/ml BMP-7, FGF-2 + BMP-7 or no additional factor (control). Concentration of LDN-193189 was increased sequentially (100, 300, 1000, 3000 nM)

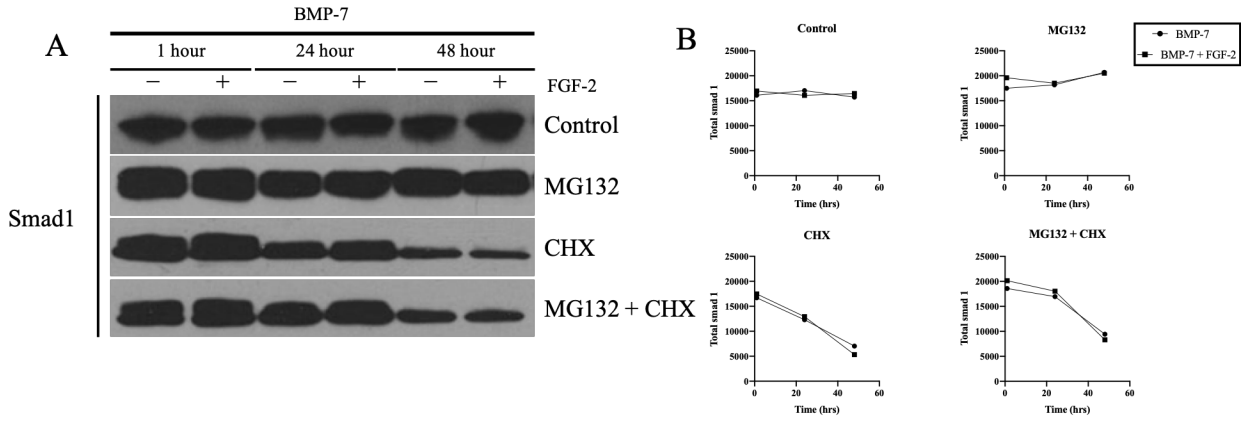


Figure 6.6. Evaluation of FGF-2 effect on Smad1 degradation
(A) Total Smad1 was measured in mouse calvarial osteoblasts after pretreatment of cells for 60 minutes with 50 μM cycloheximide (CHX), 10 μM MG132, CHX + MG132 or DMSO as a vehicle control and subsequent treatment with 100 ng/ml BMP-7 +/- 2 ng/ml FGF-2 for 60 minutes. After incubation with growth factors, cells were given fresh media without factors, but including +/- CHX, +/- MG132. Protein isolates were obtained immediately after 1 hour factor incubation, after 24, and 48 hours of incubation with appropriate inhibitors. Equal amounts of protein were loaded per lane. (B) Densometric analysis of Smad1 (n=2).

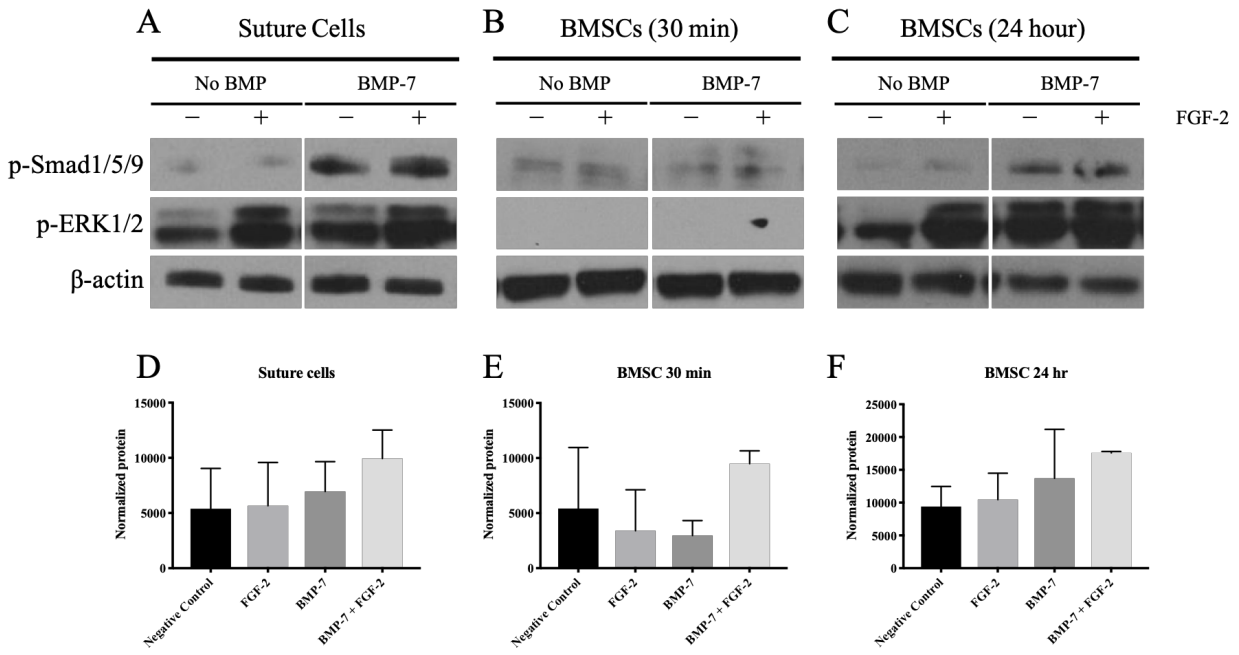


Figure 6.7. Comparison of p-Smad1/5/9 and p-ERK1/2 in murine suture cells and BMSCs
(A) Suture cells or bone marrow stromal cells (BMSCs) were serum starved for 24 hours prior to treatment with 2 ng/ml FGF-2, 100 ng/ml BMP-7, FGF-2 + BMP-7, or no additional factors (Control). Factors were incubated for 30 minutes (A, B) or 24 hours (C). P-Smad1/5/9 and p-ERK1/2 levels were discerned by western blotting. (D-F) Densometric analysis of p-Smad1/5/9 (n=2).

Chapter 7. Conclusions

This thesis focused on investigating the combined effect of two growth factors, BMP-7 and FGF-2, to support and enhance bone tissue engineering. Importantly, FGF-2 has been reported to both synergize with and antagonize BMP signaling in bony and non-bony tissue. It was therefore important to establish an *in vitro* model that allowed us to characterize, define, and understand the conditions under which these two factors can be combined to enhance their pro-osteogenic effect. Through extensive *in vitro* experiments, we first identified the dose and treatment schedule required to achieve an additive effect between these two factors in the osteogenic differentiation of mesenchymal progenitor cells. We showed that FGF-2 stimulated proliferation of BMSCs and enhanced their osteogenic potential when cells were treated with short term, low doses of FGF-2 in combination with continuous BMP-7 treatment. We then built a drug delivery system for the spatiotemporal release of each factor, based on the optimal conditions we determined from our *in vitro* model. We encapsulated each factor into high and low molecular weight PLGA nanoparticles. By controlling the molecular weight of PLGA, we controlled the rate of release of encapsulated FGF-2 and BMP-7. We applied this drug delivery system to a nanofibrous PLLA 3D scaffold that served as a biomimetic surface on which cells could attach, proliferate, and differentiate. We tested our system using a cell-free ectopic bone model, evaluating new bone formation after 3 and 6 weeks of subcutaneous implantation. Our findings support the use of FGF-2 to enhance bone formation in a dose and spatiotemporally controlled manner, providing additional evidence that FGF-2 can enhance BMP-7-directed bone

formation. Importantly, we demonstrated that low doses (10ng, 100ng) of FGF-2 can produce an additive effect with BMP-7, while a high dose (1000ng) of FGF-2 inhibits new bone formation. These findings are important to bone tissue engineering because we developed a delivery system capable of finely tuning the release of multiple growth factors from a single construct. By choosing to deliver FGF-2 with BMP-7, we promote angiogenesis, a critical step in bone regeneration and in ensuring successful integration with surrounding tissue. This research can help to support the development of translational products designed to deliver multiple growth factors to enhance bone healing and reduce the serious clinical risk of graft failure.

Our success in developing an ectopic model for new bone formation using both FGF-2 and BMP-7 led us to the work in Chapter 5, where advanced our approach to achieve a more clinically relevant treatment for large volume bone defects. We built on our ectopic model from Chapter 4 by evaluating bone formation in an orthotopic, calvarial defect model. Additionally, we evaluated our dual factor delivery system on an injectable NF-SMS scaffold, which maintains the porosity and nanofibrous architecture of our disc-shaped 3D PLLA scaffold used in Chapter 4 but has the additional advantage non-invasive administration. At 8 weeks, we used microCT and histological staining to observe significant healing in the group that received BMP-7 + low dose FGF-2 (10ng). In these studies, the difference in new bone volume between the BMP-7 + FGF-2 (10ng) compared with the BMP-7 alone group was significant, although not as pronounced as our findings in the ectopic model. As we determined in our ectopic study, FGF-2 can affect cell migration, proliferation, and blood vessel formation, as well as osteogenic differentiation of BMSCs. In an ectopic model, cell migration and blood vessel formation are very important as the subcutaneous environment lacks large quantities of progenitor cells. In the cranial defect model, progenitor cells are more plentiful, and the injury site is highly

vascularized. As a result, the contributions of FGF-2 are more limited to its pro-osteogenic effect. Based on our *in vitro* work, we know that FGF-2 can enhance mineralization by BMSCs and osteoblasts, but that its pro-osteogenic effect is small in comparison with BMP-7. Our findings are important because they establish that FGF-2 can have a pro-osteogenic effect in an orthotopic model and that our NF-SMS platform can be effectively used to support healing of a critical size orthotopic defect.

Due to the complex signaling relationship between BMPs and FGFs we sought to elucidate the interactions between FGF-2 and BMP-7 in bone-forming osteoblasts to better understand how and why an additive effect between these factors could be achieved. We used neonatal calvarial osteoblasts to establish an *in vitro* model to study the interactions of BMP and FGF signaling pathways. While previous studies primarily focused on the effect that FGF-2 can have on RUNX2 expression and downstream pro-osteogenic gene expression, we focused on the potential upstream interactions, specifically whether FGF-2 could stimulate phosphorylation of Smad1/5/9 proteins and thereby enhance BMP signaling. Importantly, we found that FGF-2 could enhance BMP-7 induced p-Smad1/5/9 signaling but did not enhance Smad phosphorylation when combined with BMP-2. Because BMP-7 and BMP-2 transduce their signal by activation of distinct BMP receptors, we probed this further by implementing selective inhibitors of the BMPR1a and ACVR1a receptors, namely LDN-19 and LDN-21. We found that in the presence of LDN-19, FGF-2 could maintain significant levels of p-Smad1/5/9 while BMP-7 alone could not, leading us to focus on the ACVR1a receptor as a potential specific target of FGF-2. This important and new observation led us to use ACVR1 and BMPR1A conditional knockout cells to demonstrate that the presence of the BMP receptors was critical to maintaining p-Smad1/5/9 levels and that receptor kinase activity was potentially the target of FGF-2

signaling. We then identified the ERK1/2 signaling arm of FGF-2 signaling as the potential pathway by which FGF-2 can enhance p-Smad1/5/9 signaling. We also ruled out the possibility that TAK1 signaling was responsible for increased p-Smad1/5/9 by treating cells with or without the TAK1 inhibitor 5z-7-oxozeaenol. This work identifies a potentially new mechanism by which the FGF pathway can regulate canonical BMP signaling. Because of the novelty of our discovery that FGF-2 can potentially modulate kinase activity of ACVR1 receptor, we acknowledge the need for further studies to confirm this enzyme/substrate relationship and to show a direct physical interaction between p-ERK1/2 and ACVR1. Nevertheless, this finding is important as it elucidates a critical aspect of the pro-osteogenic properties of FGF-2.

Together, these results advance the fields of bone tissue engineering, drug delivery, and bone biology. Both the ectopic and orthotopic models used in these studies provide evidence for the additive effect of FGF-2 and BMP-7 and valuable insights as to how to combine growth factors to enhance the quality of engineered tissue. Combined with our novel microsphere platform and enhanced understanding of BMP and FGF signaling pathways, there is significant promise in using this work to translate bone tissue engineering technology clinically and potentially advance fundamental understanding of bone biology.

Chapter 8. Future Work

One of the main accomplishments of this work was to establish the simultaneous delivery of FGF-2 and BMP-7, each with distinct release patterns, to stimulate bone regeneration. While our success in developing ectopic and orthotopic *in vivo* models provides a strong foundation for advancing preclinical studies, the need to further validate and develop these models is necessary. In each model, we implanted cell-free scaffolds into subcutaneous pockets or calvarial defects of mice. While cell-free scaffolds were effective in producing bone, using a cell-seeded scaffold with hiPSC-MSCs could further demonstrate the effect of FGF-2 as a pro-osteogenic factor. Furthermore, by implanting cells, the healing of a critical size defect may be enhanced due to the paracrine effect that cells have on the microenvironment in which they are implanted. The use of a human cell source would be particularly relevant to the clinical utility of a cell-seeded scaffold based on this platform. While we saw significant healing at 8 weeks in the calvarial defects using cell free NF-SMS scaffold, a higher goal would be to see more complete healing of the defect by this time point. In addition to the calvarial defect, other orthotopic defects may be appropriate to evaluate our NF-SMS and dual drug delivery platform. For example, a tibial or femoral defect in rabbits or femoral defect in rodents may be useful to evaluate bone regeneration in a mechanically stimulated bone site.[384]

More work can also be done to improve upon the NF-SMS scaffold that we used in this thesis. Our lab's previous work with 3D disc shaped scaffolds showed that a larger pore size was more conducive to bone regeneration.[319] We selected a 60-90 um NF-SMS, with pore sizes

that mirrored previous work with 3D disc shaped scaffolds. It would be valuable to evaluate and compare NF-SMS of variable sizes, 30-60 um, 60-90 um, and 90-120 um, with respect to their pore size and subsequently their osteogenic potential. A logical next step towards the clinical development of NF-SMS as a tissue engineering scaffold would be to develop a hydrogel that contains NF-SMS. A NF-SMS-based hydrogel would maintain their advantage as an injectable scaffold with porous and nanofibrous features, while also improving upon the ability to fill a defect geometry and maintain the scaffold within the defect, which is important to alleviating the risk of off-target bone growth.

Our ectopic and orthotopic drug delivery models took advantage of different molecular weight PLGA to achieve distinct release profiles. In our ectopic model, we found that a low dose (10ng), slow release FGF-2 enhanced bone regeneration in a similar fashion to a medium dose (100ng), fast release FGF-2. These results point to the importance of local dose and rate of FGF-2 release. More work can be done to further optimize both the dose and release rate of FGF-2 in this platform. According to our release studies, low molecular weight PLGA-NS released 55% of total loaded FGF-2 in a burst release on Day 1. For the low dose (10ng), this would correspond with 5.5ng of FGF-2. Similarly, high molecular weight PLGA released 26% of total FGF-2 loaded on Day 1. For the medium dose (100ng), this would correspond with 26ng of FGF-2. Each of these conditions enhanced ectopic bone formation. These approximations correspond well with our *in vitro* findings that 5ng/ml and 25ng/ml of FGF-2 early in treatment of BMSCs can enhance their osteogenic differentiation. We relied on *in vitro* release kinetics to model our *in vivo* doses and release rates. Studies that elucidate the *in vivo* release kinetics of our growth factors would be valuable to improve the precision of dose and spatiotemporal release of factors from various PLGA formulations.

Finally, the observations we made relating to the crosstalk between FGF-2 and BMP-7 represent a potentially novel signaling mechanism. While this is a promising first step in elucidating this pathway, additional work should to be done to establish a definitive link between p-ERK1/2 and the ACVR receptor. Co-immunoprecipitation assays or FLAG-tag assays may be helpful to determine the direct protein-protein interaction between ERK and ACVR. One of the main challenges of this work is the lack of a truly specific antibody for the ACVR receptor as commercially available products tend to cross-react with other BMP receptors. Due to this limitation, other biochemical assays might be more appropriate. For example, an auto-kinase assay can be used to detect whether enzymatic kinase activity of p-ERK1/2 targets the ACVR receptor. This can be accomplished by mixing purified ACVR and p-ERK1/2 proteins with a radiolabeled ATP (e.g. [γ-32P]ATP). After incubation, the mixture can be subjected to SDS page electrophoresis and phosphorylation can be detected by autoradiography. If p-ERK1/2 is able to phosphorylate ACVR, then a band can be observed by exposing the gel to x-ray film. The band would be observed on the gel at the depth corresponding with the molecular weight of the ACVR protein, as the radiolabeled phosphate would have been transferred to the ACVR protein.

FGF signaling has been shown to also interact with WNT signaling, PTH, and other signaling mechanisms.[303,385] Exploration of these alternative pathways may further clarify the links between FGF signaling and canonical BMP signaling. Furthermore, we gathered preliminary evidence that FGF-2 could enhance p-Smad1/5/9 signaling in BMSCs and suture cells. Characterization of FGF-2 and BMP signaling in these cell types, specifically to evaluate whether or not FGF-2 enhances ACVR1 activity, would further clarify the role of FGF-2 in bone regeneration. It would also be important to examine the crosstalk of the BMP and FGF pathway in BMSCs and calvarial osteoblasts in a 3D *in vitro* system and in an *in vivo* setting. Of

particular interest would be to study whether endogenous calvarial osteoblasts, suture cells, BMSCs, and other cell types, *in vivo,* show increased Smad1/5/9 phosphorylation when exposed to exogenous FGF-2, with or without BMP-7. Immunohistochemistry or immunofluorescent staining of p-Smad1/5/9 in tissue sections from mice treated with FGF-2 +/- BMP-7 could yield interesting information regarding the variable effect of FGF-2 on Smad1/5/9 phosphorylation in different cell types.

While we focused on the upstream phosphorylation of the r-Smad proteins, additional studies that focus on downstream effects of combined FGF-2 and BMP-7 treatment would provide additional information regarding the potential transcriptional implications of using both growth factors together in tissue engineering platforms. These pathway crosstalk studies may also benefit from a proteomic approach to better understand the changes caused by FGF-2 and BMP-7 in gene expression, protein translation, and post-translational modifications of relevant signaling molecules in each pathway.

The persistent clinical need for bone graft substitutes, and particularly to enhance the survival of synthetic grafts by inducing vascularization of tissue engineered bone, make this work an important contribution. Ultimately these technologies will be evaluated in large animal and human clinical trials.

Appendix A. Diagrams of BMP and FGF signaling pathways

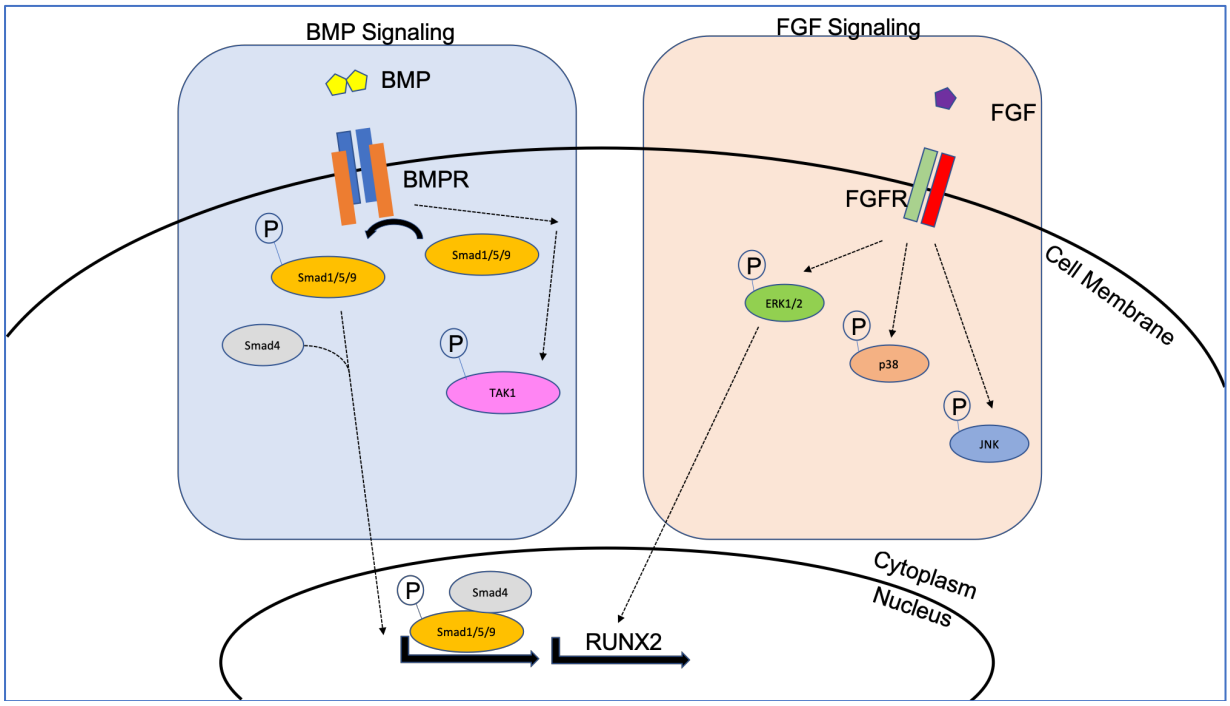


Figure A.1. Overview of BMP and FGF signaling pathways.
In canonical BMP signaling, a BMP dimer, typically a homodimer, binds to a BMP type I receptor, causing a hetero-tetramer receptor-ligand complex to form. Activation of type I receptor by type II receptor leads to Smad1/5/9 phosphorylation. P-Smad1/5/9 forms a complex with Smad4 and translocates to the nucleus, activating RUNX2. During canonical FGF signaling, an FGF monomer binds to a cell surface FGF receptor, activating a multitude of downstream activity. Highlighted here is a simplified depiction of the mitogen-activated protein kinase (MAPK) signaling molecules activated by FGFR. Of particular interest, p-ERK1/2 is known to enhance RUNX2 expression.

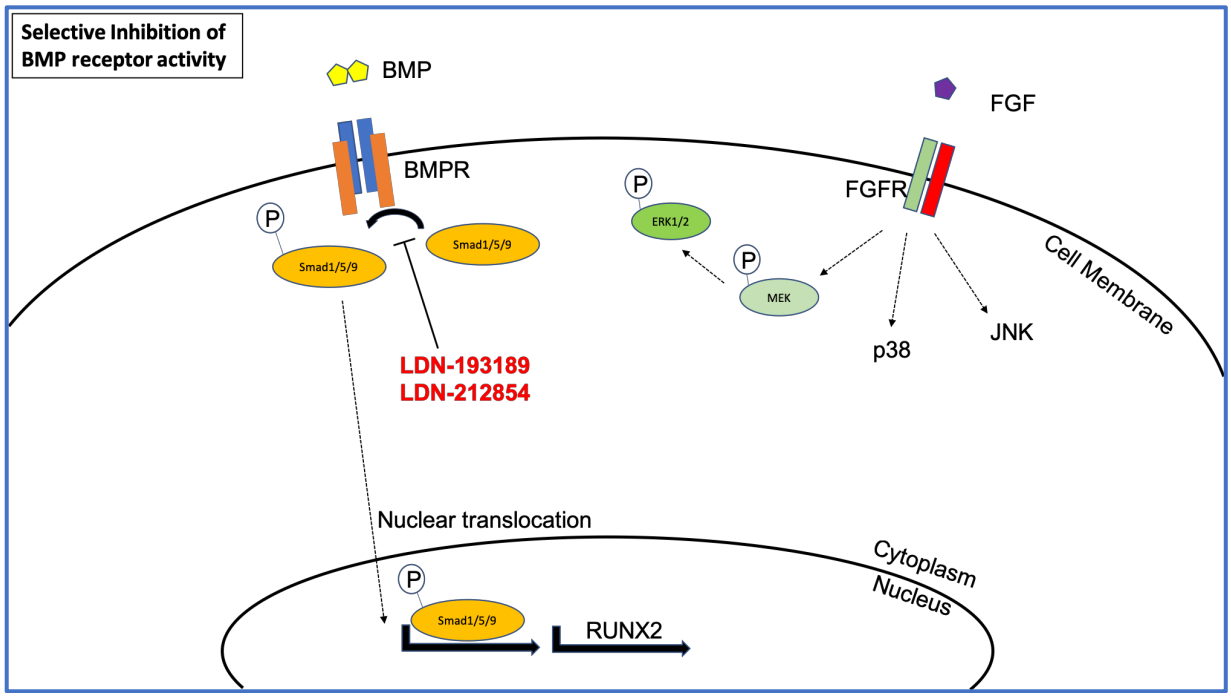


Figure A.2. Selective inhibition of BMP receptor kinase activity.
Chemical inhibitors can be used to inhibit Smad1/5/9 phosphorylation. LDN-193189 and LDN-212854 are dorsomorphin derivatives specific for BMP receptors that inhibit Smad1/5/9 phosphorylation by competitively preventing ATP from accessing kinase domain.

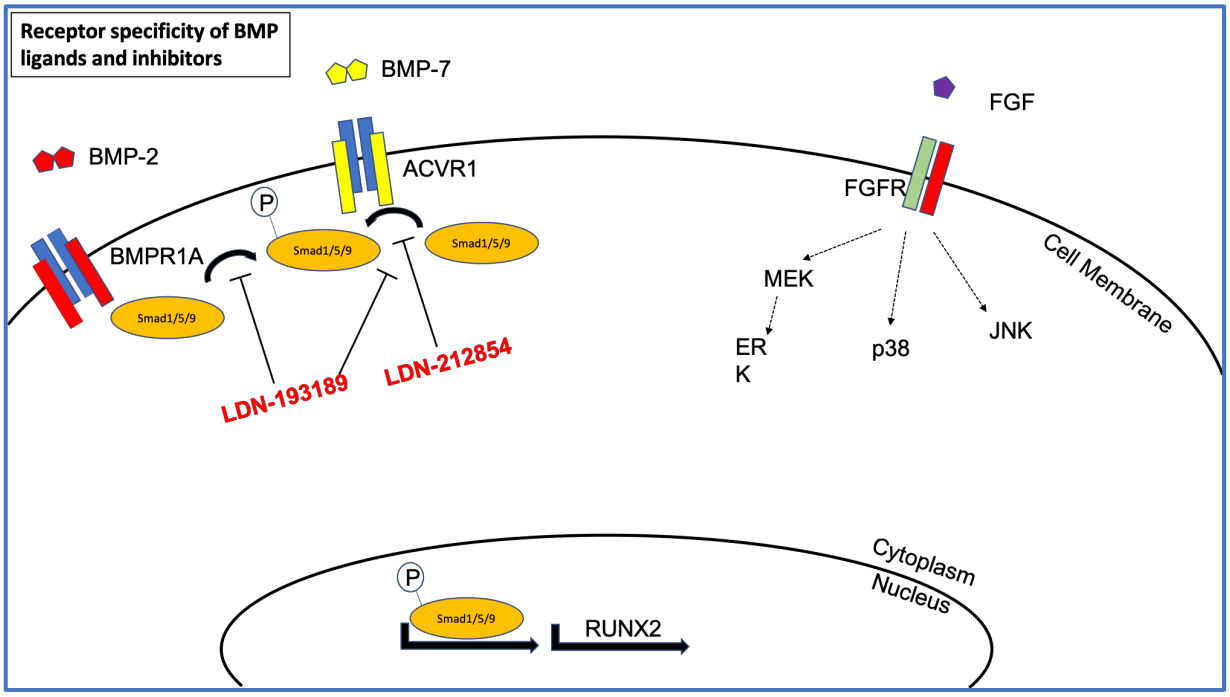


Figure A.3. BMP ligand and receptor specificity.
LDN-193189 is known as a pan-BMP receptor type I inhibitor, preventing Smad1/5/9 phosphorylation associated with both BMPR1A and ACVR1. LDN-212854 is highly specific for ACVR1 receptor and does not inhibit BMPR1A associated Smad1/5/9 phosphorylation.

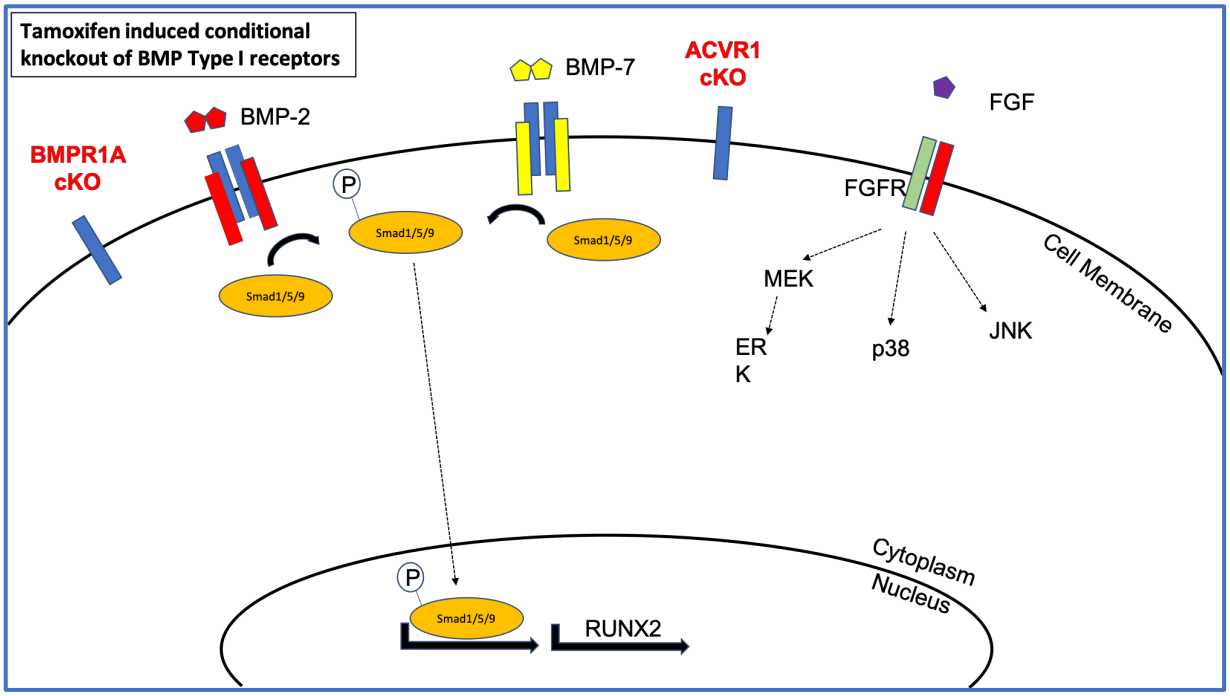


Figure A.4. Induction of mutant BMPR1A or ACVR1 deficient phenotype by Tamoxifen activation of *Cre.*
BMP type I receptors are activated preferentially by different BMP ligands. BMP-2 and BMP-4 signal via the BMPR1A receptor, while BMP-7 signals via the ACVR1 receptor. Conditional knockout of a single receptor is achieved via cre-lox recombination. Cells with BMPR1A cKO maintain ACVR1 signaling activity and vice-versa. Smad1/5/9 phosphorylation can be measured in cKO cells (Tamoxifen induced) and wildtype cells (untreated) after exposure to BMP and/or FGF.

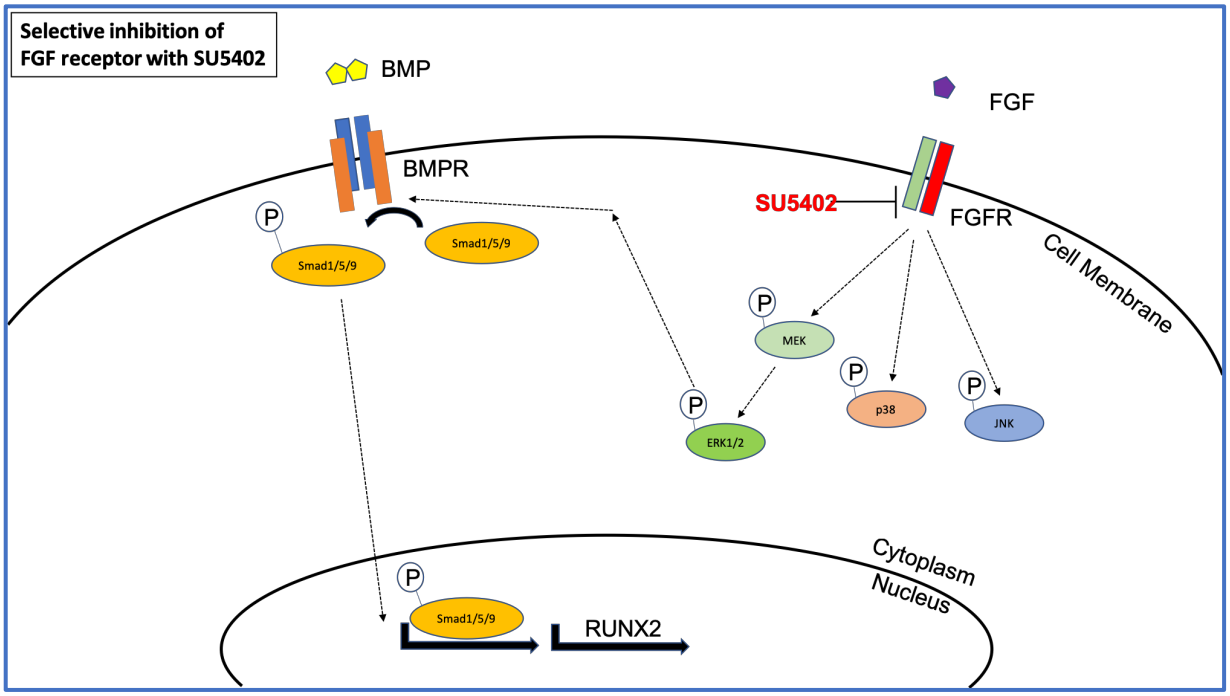


Figure A.5. Pharmacological inhibition of FGF receptor kinase activity.
FGF receptor activity can be specifically inhibited by a chemical inhibitor SU5402 that prevents downstream MAPK activation and their intracellular signaling cascades. Levels of p-Smad1/5/9 can be measured in cells pre-treated with SU5402 or DMSO (control) for 30 minutes and subsequently treated with BMP-7 +/- FGF-2.

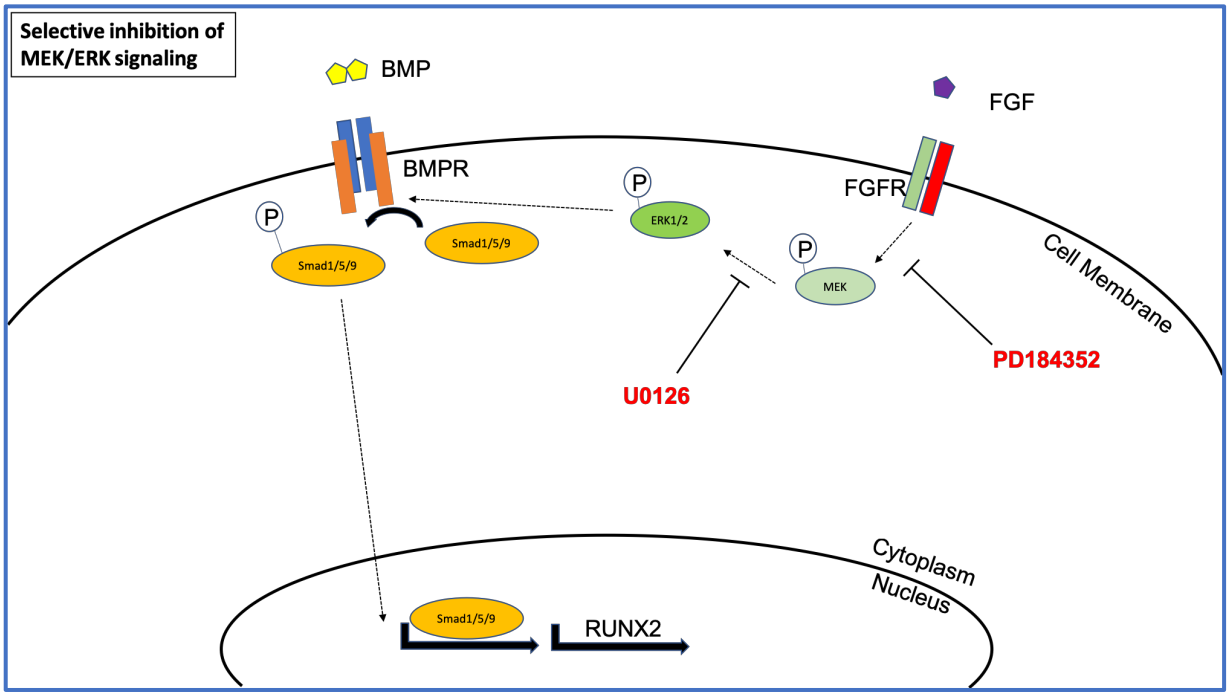


Figure A.6. Selective inhibition of p-ERK1/2 with pharmacological inhibitors.
ERK1/2 activation can be specifically inhibited using MEK-inhibitor PD184352 or U0126, which prevent phosphorylation of ERK1/2. To evaluate the proposed mechanism of action of p-ERK1/2 targeting of ACVR1, Smad1/5/9 phosphorylation can be measured in cells pre-treated with PD184352 or U0126 or DMSO (control).

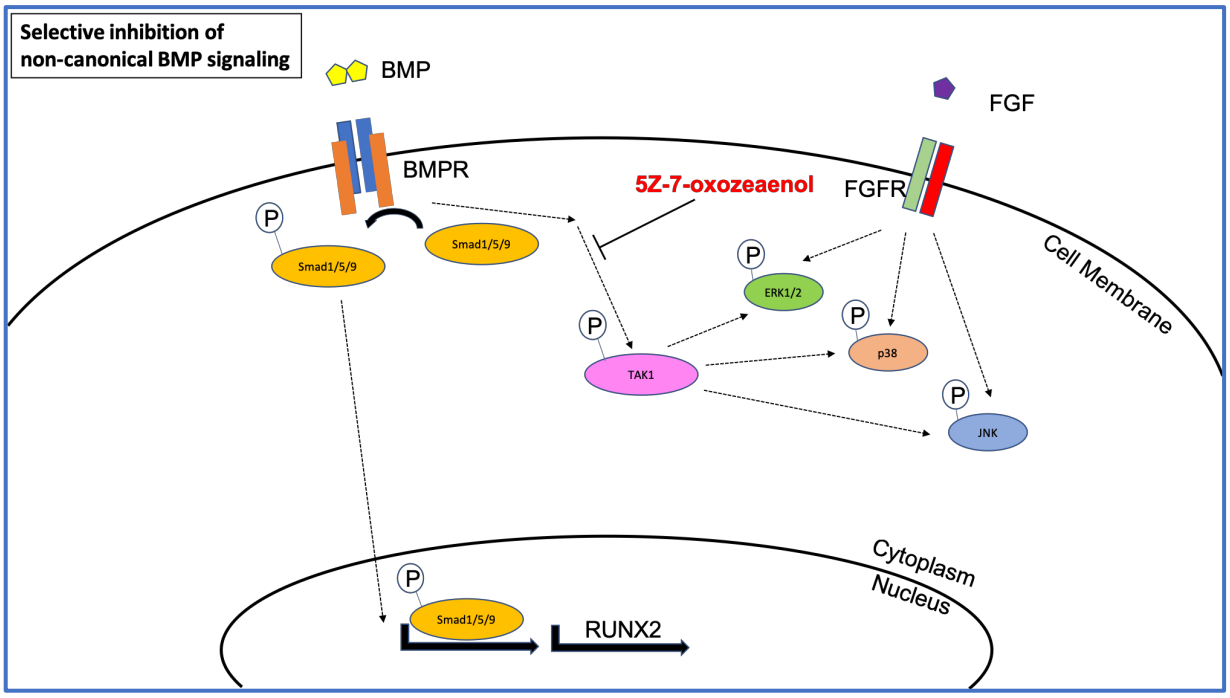


Figure A.7. Inhibition of non-canonical BMP signaling pathway.
In addition to Smad1/5/9 phosphorylation, the BMP/BMPR complex activates phosphorylation of TAK1, which subsequently activates a MAPK signaling cascade. 5Z-7-oxozeaenol can be used to inhibit activation of TAK1 and level of p-Smad1/5/9 can be measured to probe the effect of non-canonical BMP signaling on canonical BMP signaling in the presence or absence of FGF-2.

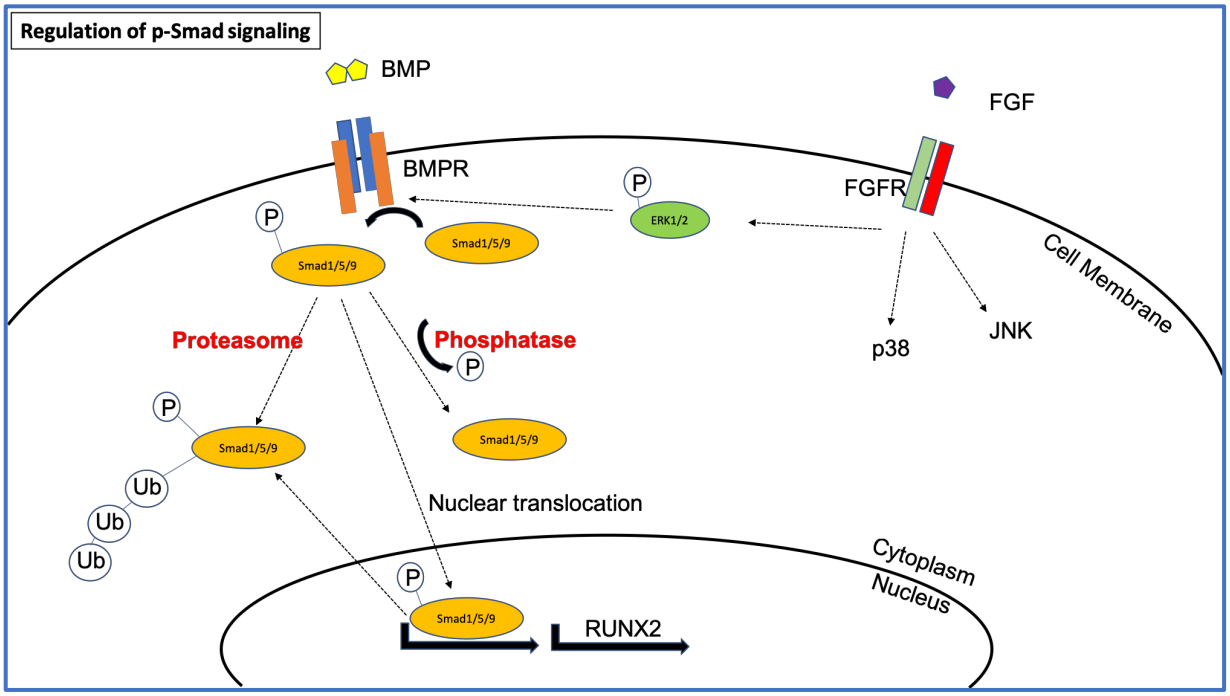


Figure A.8. Common regulatory mechanisms of Smad-dependent signaling. Intracellular concentration of Smad1/5/9 and p-Smad1/5/9 proteins are regulated by several mechanisms, including nuclear translocation, proteasomal degradation and deactivation of p-Smad1/5/9 via phosphatase enzymes. Degradation of p-Smad1/5/9 is directed by its ubiquitination. Both specific and nonspecific phosphatases can play a role in deactivation of Smad1/5/9 signaling.

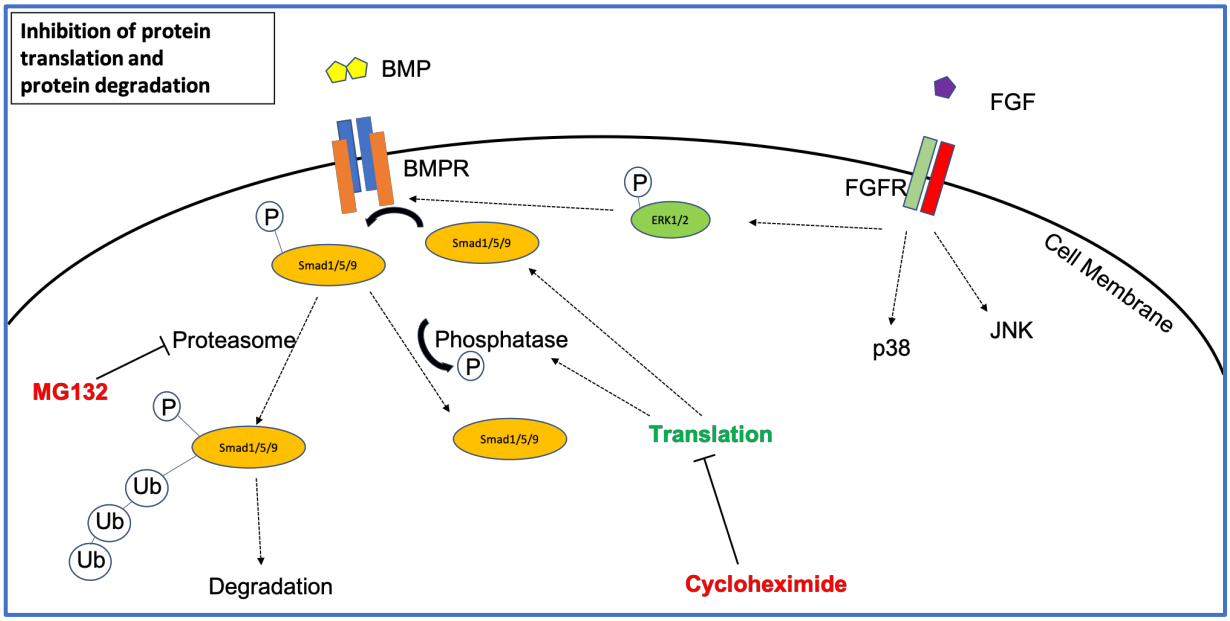


Figure A.9. Inhibition of translation and proteasomal degradation of Smad and p-Smad proteins.

MG132 is a reversible and cell-permeable inhibitor that reduces degradation of ubiquitin-conjugated proteins, thereby blocking proteasomal activity. We use MG132 to better understand whether FGF-2 elevates intracellular levels of p-Smad1/5/9 by interrupting Smad1/5/9 degradation. Cycloheximide is a reversible inhibitor of protein translation. It is nonspecific and therefore affects Smad1/5/9, as well as the regulatory proteases and phosphatases that may influence the total Smad1/5/9 level within a cell. We use it in combination with MG132 to understand the effect of FGF-2 on Smad1/5/9 translation and stability.

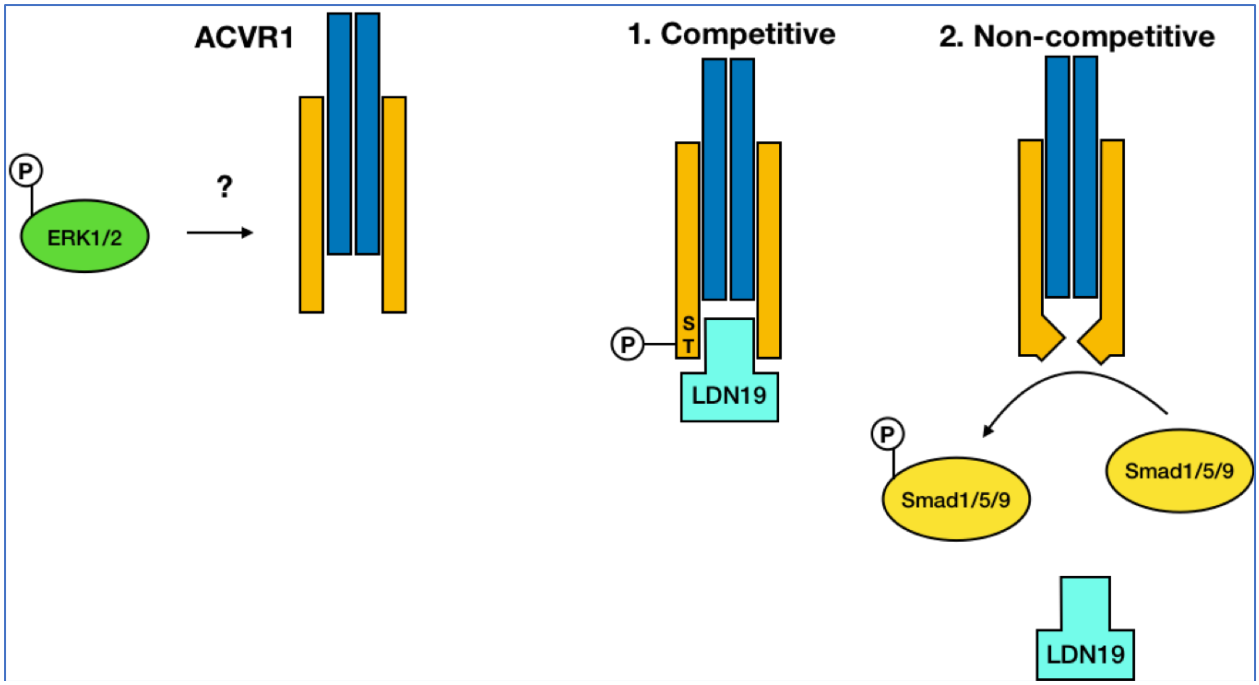


Figure A.10. Possible mechanisms for p-ERK1/2 targeting of ACVR1.
LDN-193189 is a competitive inhibitor of BMP type I receptors, which acts to block access of ATP to kinase domains of the receptor. We sought to increase the dose of LDN-19 to understand whether p-ERK1/2 targets ACVR1 through competitive of non-competitive means with LDN-19. This would help elucidate the nature of p-ERK1/2 and ACVR1 interaction.

Bibliography

[1] G. Victoria, B. Petrisor, B. Drew, D. Dick, Bone stimulation for fracture healing: What's all the fuss?, Indian J. Orthop. 43 (2009) 117–20. doi:10.4103/0019-5413.50844.

[2] R. Dimitriou, E. Jones, D. McGonagle, P. V Giannoudis, Bone regeneration: current concepts and future directions., BMC Med. 9 (2011) 66. doi:10.1186/1741-7015-9-66.

[3] D. Deluiz, L. Oliveira, P. Fletcher, F.R. Pires, M.A. Nunes, E.M.B. Tinoco, Fresh-Frozen Bone Allografts in Maxillary Alveolar Augmentation: Analysis of the Complications, Adverse Outcomes and Implant Survival., J. Periodontol. (2016) 1–13. doi:10.1902/jop.2016.160155.

[4] M.A. Ayerza, N.S. Piuzzi, L.A. Aponte-Tinao, G.L. Farfalli, D.L. Muscolo, Structural allograft reconstruction of the foot and ankle after tumor resections, Musculoskelet. Surg. (2016) 1–8. doi:10.1007/s12306-016-0413-4.

[5] A. Faundez, C. Tournier, M. Garcia, S. Aunoble, J.C. Le Huec, Bone morphogenetic protein use in spine surgery—complications and outcomes: a systematic review, Int. Orthop. 40 (2016) 1309–1319. doi:10.1007/s00264-016-3149-8.

[6] A. Sakkas, F. Wilde, M. Heufelder, K. Winter, A. Schramm, Autogenous bone grafts in oral implantology—is it still a "gold standard"? A consecutive review of 279 patients with 456 clinical procedures, Int. J. Implant Dent. 3 (2017) 23. doi:10.1186/s40729-017-0084-4.

[7] S.R. Shin, P. Tornetta, Donor site morbidity after anterior iliac bone graft harvesting, J. Orthop. Trauma. 30 (2016) 340–343. doi:10.1097/BOT.0000000000000551.

[8] A.W. James, G. LaChaud, J. Shen, G. Asatrian, V. Nguyen, X. Zhang, et al., A Review of the Clinical Side Effects of Bone Morphogenetic Protein-2, Tissue Eng. Part B Rev. 22 (2016) 284–297. doi:10.1089/ten.teb.2015.0357.

[9] A.C. Karaplis, Embryonic Development of Bone and Regulation of Intramembranous and Endochondral Bone Formation, in: Princ. Bone Biol. Two-Volume Set, 2008: pp. 53–84. doi:10.1016/B978-0-12-373884-4.00025-2.

[10] C.J. Percival, J.T. Richtsmeier, Angiogenesis and intramembranous osteogenesis, Dev. Dyn. 242 (2013) 909–922. doi:10.1002/dvdy.23992.

[11] Y. Mishina, T.N. Snider, Neural crest cell signaling pathways critical to cranial bone development and pathology, Exp. Cell Res. 325 (2014) 138–147. doi:10.1016/j.yexcr.2014.01.019.

[12] E.M. Thompson, A. Matsiko, E. Farrell, D.J. Kelly, F.J. O'Brien, Recapitulating endochondral ossification: a promising route to in vivo bone regeneration, J. Tissue Eng. Regen. Med. 9 (2015) 889–902. doi:10.1002/term.1918.

[13] L.C. Gerstenfeld, D.M. Cullinane, G.L. Barnes, D.T. Graves, T.A. Einhorn, Fracture healing as a post-natal developmental process: Molecular, spatial, and temporal aspects of its regulation, J. Cell. Biochem. 88 (2003) 873–884. doi:10.1002/jcb.10435.

[14] G.J. Schmid, C. Kobayashi, L.J. Sandell, D.M. Ornitz, Fibroblast growth factor expression during skeletal fracture healing in mice, Dev. Dyn. 238 (2009) 766–774. doi:10.1002/dvdy.21882.
[15] G.M. Cooper, M.P. Mooney, A.K. Gosain, P.G. Campbell, J.E. Losee, J. Huard, Testing the critical size in calvarial bone defects: revisiting the concept of a critical-size defect., Plast. Reconstr. Surg. 125 (2010) 1685–92. doi:10.1097/PRS.0b013e3181cb63a3.
[16] J. Hu, X. Liu, P.X. Ma, Biomineralization and Bone Regeneration, in: A. Atala, R. Lanza, J.A. Thomson, R. Nerem (Eds.), Princ. Regen. Med., Elsevier Inc., 2011: pp. 733–745. doi:10.1016/B978-0-12-381422-7.10040-9.
[17] X. Liu, P.X. Ma, Polymeric scaffolds for bone tissue engineering, Ann. Biomed. Eng. 32 (2004) 477–486. doi:10.1023/B:ABME.0000017544.36001.8e.
[18] C.H. Evans, Gene delivery to bone, Adv. Drug Deliv. Rev. 64 (2012) 1331–1340. doi:10.1016/j.addr.2012.03.013.
[19] F. Loi, L.A. Córdova, R. Zhang, J. Pajarinen, T. Lin, S.B. Goodman, et al., The effects of immunomodulation by macrophage subsets on osteogenesis in vitro, Stem Cell Res. Ther. 7 (2016) 15. doi:10.1186/s13287-016-0276-5.
[20] A.J. Wagers, I.L. Weissman, Plasticity of adult stem cells, Cell. 116 (2004) 639–648. doi:10.1016/S0092-8674(04)00208-9.
[21] L. Peng, Z. Jia, X. Yin, X. Zhang, Y. Liu, P. Chen, et al., Comparative Analysis of Mesenchymal Stem Cells from Bone Marrow, Cartilage, and Adipose Tissue, Stem Cells Dev. 17 (2008) 761–774. doi:10.1089/scd.2007.0217.
[22] A. Shafiee, E. Seyedjafari, M. Soleimani, N. Ahmadbeigi, P. Dinarvand, N. Ghaemi, A comparison between osteogenic differentiation of human unrestricted somatic stem cells and mesenchymal stem cells from bone marrow and adipose tissue, Biotechnol. Lett. 33 (2011) 1257–1264. doi:10.1007/s10529-011-0541-8.
[23] S. Rumiński, B. Ostrowska, J. Jaroszewicz, T. Skirecki, K. Włodarski, W. Święszkowski, et al., Three-dimensional printed polycaprolactone-based scaffolds provide an advantageous environment for osteogenic differentiation of human adipose-derived stem cells, J. Tissue Eng. Regen. Med. 12 (2018) e473–e485. doi:10.1002/term.2310.
[24] J. Hu, L.A. Smith, K. Feng, X. Liu, H. Sun, P.X. Ma, Response of human embryonic stem cell-derived mesenchymal stem cells to osteogenic factors and architectures of materials during in vitro osteogenesis., Tissue Eng. Part A. 16 (2010) 3507–14. doi:10.1089/ten.TEA.2010.0097.
[25] L.A. Smith, X. Liu, J. Hu, P.X. Ma, The Enhancement of human embryonic stem cell osteogenic differentiation with nano-fibrous scaffolding, Biomaterials. 31 (2010) 5526–5535. doi:10.1016/j.biomaterials.2010.03.065.
[26] K. Takahashi, S. Yamanaka, Induction of pluripotent stem cells from mouse embryonic and adult fibroblast cultures by defined factors., Cell. 126 (2006) 663–76. doi:10.1016/j.cell.2006.07.024.
[27] N. Malik, M.S. Rao, A review of the methods for human iPSC derivation, in: Methods Mol. Biol., 2013: pp. 23–33. doi:10.1007/978-1-62703-348-0_3.
[28] G. Chen, D.R. Gulbranson, Z. Hou, J.M. Bolin, V. Ruotti, M.D. Probasco, et al., Chemically defined conditions for human iPSC derivation and culture, Nat Meth. 8 (2011) 424–429.
[29] S. Menendez, S. Camus, A. Herreria, I. Paramonov, L.B. Morera, M. Collado, et al., Increased dosage of tumor suppressors limits the tumorigenicity of iPS cells without

affecting their pluripotency, Aging Cell. 11 (2012) 41–50. doi:10.1111/j.1474-9726.2011.00754.x.
[30] O. Habib, G. Habib, H.W. Choi, K.-S. Hong, J. Tae Do, S.-H. Moon, et al., An improved method for the derivation of high quality iPSCs in the absence of c-Myc, Exp. Cell Res. 319 (2013) 3190–3200. doi:10.1016/j.yexcr.2013.09.014.
[31] D. Paull, A. Sevilla, H. Zhou, A.K. Hahn, H. Kim, C. Napolitano, et al., Automated, high-throughput derivation, characterization and differentiation of induced pluripotent stem cells, Nat. Methods. 12 (2015) 885–892. doi:10.1038/nmeth.3507.
[32] Y. Kishino, T. Seki, J. Fujita, S. Yuasa, S. Tohyama, A. Kunitomi, et al., Derivation of Transgene-Free Human Induced Pluripotent Stem Cells from Human Peripheral T Cells in Defined Culture Conditions, PLoS One. 9 (2014) e97397. doi:10.1371/journal.pone.0097397.
[33] T. Seki, K. Fukuda, Methods of induced pluripotent stem cells for clinical application., World J. Stem Cells. 7 (2015) 116–25. doi:10.4252/wjsc.v7.i1.116.
[34] R. Kang, Y. Zhou, S. Tan, G. Zhou, L. Aagaard, L. Xie, et al., Mesenchymal stem cells derived from human induced pluripotent stem cells retain adequate osteogenicity and chondrogenicity but less adipogenicity., Stem Cell Res. Ther. 6 (2015) 144. doi:10.1186/s13287-015-0137-7.
[35] M.D. Phillips, S.A. Kuznetsov, N. Cherman, K. Park, K.G. Chen, B.N. McClendon, et al., Directed differentiation of human induced pluripotent stem cells toward bone and cartilage: in vitro versus in vivo assays., Stem Cells Transl. Med. 3 (2014) 867–78. doi:10.5966/sctm.2013-0154.
[36] F. Li, C. Niyibizi, Cells derived from murine induced pluripotent stem cells (iPSC) by treatment with members of TGF-beta family give rise to osteoblasts differentiation and form bone in vivo., BMC Cell Biol. 13 (2012) 35. doi:10.1186/1471-2121-13-35.
[37] J. Liu, W. Chen, Z. Zhao, H.H.K. Xu, Reprogramming of mesenchymal stem cells derived from iPSCs seeded on biofunctionalized calcium phosphate scaffold for bone engineering, Biomaterials. 34 (2013) 7862–7872. doi:10.1016/j.biomaterials.2013.07.029.
[38] M. Tang, W. Chen, J. Liu, M.D. Weir, L. Cheng, H.H.K. Xu, Human induced pluripotent stem cell-derived mesenchymal stem cell seeding on calcium phosphate scaffold for bone regeneration., Tissue Eng. Part A. 20 (2014) 1295–1305. doi:10.1089/ten.TEA.2013.0211.
[39] S. Teng, C. Liu, C. Krettek, M. Jagodzinski, The application of induced pluripotent stem cells for bone regeneration: current progress and prospects., Tissue Eng. Part B. Rev. 20 (2014) 328–339. doi:10.1089/ten.TEB.2013.0301.
[40] A. Ardeshirylajimi, P. Dinarvand, E. Seyedjafari, L. Langroudi, F.J. Adegani, M. Soleimani, Enhanced reconstruction of rat calvarial defects achieved by plasma-treated electrospun scaffolds and induced pluripotent stem cells., Cell Tissue Res. 354 (2013) 849–860. doi:10.1007/s00441-013-1693-8.
[41] O.H. Jeon, L.M. Panicker, Q. Lu, J.J. Chae, R.A. Feldman, J.H. Elisseeff, Human iPSC-derived osteoblasts and osteoclasts together promote bone regeneration in 3D biomaterials, Sci. Rep. 6 (2016) 26761. doi:10.1038/srep26761.
[42] K. Gooch, Tissue engineering/Biomaterials, in: Ann. Biomed. Eng., John Wiley & Sons, Inc., 2007: p. S-42. doi:10.1007/bf02647371.
[43] P.X. Ma, Scaffolds for tissue fabrication, Mater. Today. 7 (2004) 30–40. doi:10.1016/S1369-7021(04)00233-0.
[44] L.A. Smith, P.X. Ma, Nano-fibrous scaffolds for tissue engineering, Colloids Surfaces B

Biointerfaces. 39 (2004) 125–131. doi:10.1016/j.colsurfb.2003.12.004.
[45] J.M. Holzwarth, P.X. Ma, Biomimetic nanofibrous scaffolds for bone tissue engineering, Biomaterials. 32 (2011) 9622–9629. doi:10.1016/j.biomaterials.2011.09.009.
[46] K.M. Woo, V.J. Chen, H.-M. Jung, T.-I. Kim, H.-I. Shin, J.-H. Baek, et al., Comparative evaluation of nanofibrous scaffolding for bone regeneration in critical-size calvarial defects., Tissue Eng. Part A. 15 (2009) 2155–62. doi:10.1089/ten.tea.2008.0433.
[47] K.M. Woo, J.H. Jun, V.J. Chen, J. Seo, J.H. Baek, H.M. Ryoo, et al., Nano-fibrous scaffolding promotes osteoblast differentiation and biomineralization, Biomaterials. 28 (2007) 335–343. doi:10.1016/j.biomaterials.2006.06.013.
[48] A.G. Mikos, A.J. Thorsen, L.A. Czerwonka, Y. Bao, R. Langer, D.N. Winslow, et al., Preparation and characterization of poly(l-lactic acid) foams, Polymer (Guildf). 35 (1994) 1068–1077. doi:10.1016/0032-3861(94)90953-9.
[49] R.C. Thomson, M.J. Yaszemski, J.M. Powers, A.G. Mikos, Fabrication of biodegradable polymer scaffolds to engineer trabecular bone, J. Biomater. Sci. Polym. Ed. 7 (1996) 23–38. doi:10.1163/156856295X00805.
[50] D.J. Mooney, D.F. Baldwin, N.P. Suh, J.P. Vacanti, R. Langer, Novel approach to fabricate porous sponges of poly(D,L-lactic-co-glycolic acid) without the use of organic solvents, Biomaterials. 17 (1996) 1417–1422. doi:10.1016/0142-9612(96)87284-X.
[51] D.D. Hile, M.L. Amirpour, A. Akgerman, M. V. Pishko, Active growth factor delivery from poly(D,L-lactide-co-glycolide) foams prepared in supercritical CO2, J. Control. Release. 66 (2000) 177–185. doi:10.1016/S0168-3659(99)00268-0.
[52] K. Whang, C.H. Thomas, K.E. Healy, G. Nuber, A novel method to fabricate bioabsorbable scaffolds, Polymer (Guildf). 36 (1995) 837–842. doi:10.1016/0032-3861(95)93115-3.
[53] W.J. Li, C.T. Laurencin, E.J. Caterson, R.S. Tuan, F.K. Ko, Electrospun nanofibrous structure: A novel scaffold for tissue engineering, J. Biomed. Mater. Res. 60 (2002) 613–621. doi:10.1002/jbm.10167.
[54] J.A. Matthews, G.E. Wnek, D.G. Simpson, G.L. Bowlin, Electrospinning of collagen nanofibers, Biomacromolecules. 3 (2002) 232–238. doi:10.1021/bm015533u.
[55] R.A. Giordano, B.M. Wu, S.W. Borland, L.G. Cima, E.M. Sachs, M.J. Cima, Mechanical properties of dense polylactic acid structures fabricated by three dimensional printing, J. Biomater. Sci. Polym. Ed. 8 (1997) 63–75. doi:10.1163/156856297X00588.
[56] W. Sun, A. Darling, B. Starly, J. Nam, Computer-aided tissue engineering: overview, scope and challenges, Biotechnol. Appl. Biochem. 39 (2004) 29. doi:10.1042/BA20030108.
[57] Y.S. Nam, T.G. Park, Porous biodegradable polymeric scaffolds prepared by thermally induced phase separation, J. Biomed. Mater. Res. 47 (1999) 8–17. doi:10.1002/(SICI)1097-4636(199910)47:1<8::AID-JBM2>3.0.CO;2-L.
[58] R. Zhang, P.X. Ma, Poly(alpha-hydroxyl acids)/hydroxyapatite porous composites for bone-tissue engineering. I. Preparation and morphology., J. Biomed. Mater. Res. 44 (1999) 446–455.
[59] P.X. Ma, R. Zhang, Microtubular architecture of biodegradable polymer scaffolds, J. Biomed. Mater. Res. 56 (2001) 469–477. doi:10.1002/1097-4636(20010915)56:4<469::AID-JBM1118>3.0.CO;2-H.
[60] D.W. Hutmacher, Scaffolds in tissue engineering bone and cartilage, Biomaterials. 21 (2000) 2529–2543. doi:10.1016/S0142-9612(00)00121-6.

[61] E.L. Chaikof, H. Matthew, J. Kohn, A.G. Mikos, G.D. Prestwich, C.M. Yip, Biomaterials and scaffolds in reparative medicine., Ann. N. Y. Acad. Sci. 961 (2002) 96–105. doi:10.1111/j.1749-6632.2002.tb03057.x.
[62] X. Liu, P.X. Ma, Polymeric Scaffolds for Bone Tissue Engineering, Ann. Biomed. Eng. 32 (2004) 477–486. doi:10.1023/B:ABME.0000017544.36001.8e.
[63] F. Sun, H. Zhou, J. Lee, Various preparation methods of highly porous hydroxyapatite/polymer nanoscale biocomposites for bone regeneration, Acta Biomater. 7 (2011) 3813–3828. doi:10.1016/j.actbio.2011.07.002.
[64] P.X. Ma, J.-W. Choi, Biodegradable Polymer Scaffolds with Well-Defined Interconnected Spherical Pore Network, Tissue Eng. 7 (2001) 23–33. doi:10.1089/107632701300003269.
[65] G. Wei, P.X. Ma, Partially nanofibrous architecture of 3D tissue engineering scaffolds., Biomaterials. 30 (2009) 6426–34. doi:10.1016/j.biomaterials.2009.08.012.
[66] A.I. Alford, K.M. Kozloff, K.D. Hankenson, Extracellular matrix networks in bone remodeling, Int. J. Biochem. Cell Biol. 65 (2015) 20–31. doi:10.1016/j.biocel.2015.05.008.
[67] J.D. Hartgerink, E. Beniash, S.I. Stupp, Self-Assembly and Mineralization of Peptide-Amphiphile Nanofibers, Science (80-.). 294 (2001).
[68] R. Zhang, P.X. Ma, Synthetic nano-fibrillar extracellular matrices with predesigned macroporous architectures., J. Biomed. Mater. Res. 52 (2000) 430–8.
[69] G. Wei, P.X. Ma, 2 – Polymeric biomaterials, in: Tissue Eng. Using Ceram. Polym., 2007: pp. 32–51. doi:10.1533/9781845693817.1.32.
[70] P.X. Ma, R. Zhang, G. Xiao, R. Franceschi, Engineering new bone tissue in vitro on highly porous poly(alpha-hydroxyl acids)/hydroxyapatite composite scaffolds., J. Biomed. Mater. Res. 54 (2001) 284–293.
[71] H. Yoshimoto, Y.M. Shin, H. Terai, J.P. Vacanti, A biodegradable nanofiber scaffold by electrospinning and its potential for bone tissue engineering., Biomaterials. 24 (2003) 2077–82.
[72] K. Fujihara, M. Kotaki, S. Ramakrishna, Guided bone regeneration membrane made of polycaprolactone/calcium carbonate composite nano-fibers, Biomaterials. 26 (2005) 4139–4147. doi:10.1016/j.biomaterials.2004.09.014.
[73] Y. Zhang, H. Ouyang, C.T. Lim, S. Ramakrishna, Z.-M. Huang, Electrospinning of gelatin fibers and gelatin/PCL composite fibrous scaffolds, J. Biomed. Mater. Res. 72B (2005) 156–165. doi:10.1002/jbm.b.30128.
[74] C.L. He, G.Y. Xiao, X.B. Jin, C.H. Sun, P.X. Ma, Electrodeposition on Nanofibrous Polymer Scaffolds: Rapid Mineralization, Tunable Calcium Phosphate Composition and Topography, Adv. Funct. Mater. 20 (2010) 3568–3576.
[75] C. He, X. Jin, P.X. Ma, Calcium phosphate deposition rate, structure and osteoconductivity on electrospun poly(l-lactic acid) matrix using electrodeposition or simulated body fluid incubation, Acta Biomater. 10 (2014) 419–427. doi:10.1016/j.actbio.2013.08.041.
[76] P.X. Ma, R. Zhang, Synthetic nano-scale fibrous extracellular matrix, J. Biomed. Mater. Res. 46 (1999) 60–72. doi:10.1002/(SICI)1097-4636(199907)46:1<60::AID-JBM7>3.0.CO;2-H.
[77] R. Zhang, P.X. Ma, Biomimetic polymer/apatite composite scaffolds for mineralized tissue engineering, Macromol. Biosci. 4 (2004) 100–111. doi:10.1002/mabi.200300017.
[78] G. Wei, P.X. Ma, Structure and properties of nano-hydroxyapatite/polymer composite

scaffolds for bone tissue engineering, Biomaterials. 25 (2004) 4749–4757. doi:10.1016/j.biomaterials.2003.12.005.
[79] J. Li, B.A. Baker, X. Mou, N. Ren, J. Qiu, R.I. Boughton, et al., Biopolymer/Calcium Phosphate Scaffolds for Bone Tissue Engineering, Adv. Healthc. Mater. 3 (2014) 469–484. doi:10.1002/adhm.201300562.
[80] V. Mourino, J.P. Cattalini, J.A. Roether, P. Dubey, I. Roy, A.R. Boccaccini, Composite polymer-bioceramic scaffolds with drug delivery capability for bone tissue engineering, Expert Opin. Drug Deliv. 10 (2013) 1353–1365. doi:10.1517/17425247.2013.808183.
[81] J. Venkatesan, I. Bhatnagar, P. Manivasagan, K.-H. Kang, S.-K. Kim, Alginate composites for bone tissue engineering: A review, Int. J. Biol. Macromol. 72 (2015) 269–281. doi:10.1016/j.ijbiomac.2014.07.008.
[82] X. Liu, X. Jin, P.X. Ma, Nanofibrous hollow microspheres self-assembled from star-shaped polymers as injectable cell carriers for knee repair., Nat. Mater. 10 (2011) 398–406. doi:10.1038/nmat2999.
[83] Z. Zhang, M.J. Gupte, X. Jin, P.X. Ma, Injectable Peptide Decorated Functional Nanofibrous Hollow Microspheres to Direct Stem Cell Differentiation and Tissue Regeneration, Adv. Funct. Mater. 25 (2015) 350–360. doi:10.1002/adfm.201402618.
[84] R. Kuang, Z. Zhang, X. Jin, J. Hu, M.J. Gupte, L. Ni, et al., Nanofibrous Spongy Microspheres Enhance Odontogenic Differentiation of Human Dental Pulp Stem Cells, Adv. Healthc. Mater. 4 (2015) 1993–2000. doi:10.1002/adhm.201500308.
[85] R.A. Perez, A. El-Fiqi, J.-H. Park, T.-H. Kim, J.-H. Kim, H.-W. Kim, Therapeutic bioactive microcarriers: co-delivery of growth factors and stem cells for bone tissue engineering., Acta Biomater. 10 (2014) 520–530. doi:10.1016/j.actbio.2013.09.042.
[86] J.-H. Park, R.A. Pérez, G.-Z. Jin, S.-J. Choi, H.-W. Kim, I.B. Wall, Microcarriers Designed for Cell Culture and Tissue Engineering of Bone, Tissue Eng. Part B Rev. 19 (2013) 172–190. doi:10.1089/ten.teb.2012.0432.
[87] M. Kucharska, K. Walenko, M. Lewandowska-Szumieł, T. Brynk, J. Jaroszewicz, T. Ciach, Chitosan and composite microsphere-based scaffold for bone tissue engineering: evaluation of tricalcium phosphate content influence on physical and biological properties, J. Mater. Sci. Mater. Med. 26 (2015) 143. doi:10.1007/s10856-015-5464-9.
[88] S. Bagheri-Khoulenjani, H. Mirzadeh, M. Etrati-Khosroshahi, M. Ali Shokrgozar, Particle size modeling and morphology study of chitosan/gelatin/nanohydroxyapatite nanocomposite microspheres for bone tissue engineering, J. Biomed. Mater. Res. Part A. 101A (2013) 1758–1767. doi:10.1002/jbm.a.34481.
[89] S. Shen, D. Fu, F. Xu, T. Long, F. Hong, J. Wang, The design and features of apatite-coated chitosan microspheres as injectable scaffold for bone tissue engineering, Biomed. Mater. 8 (2013) 025007. doi:10.1088/1748-6041/8/2/025007.
[90] C. Tao, J. Huang, Y. Lu, H. Zou, X. He, Y. Chen, et al., Development and characterization of GRGDSPC-modified poly(lactide-co-glycolide acid) porous microspheres incorporated with protein-loaded chitosan microspheres for bone tissue engineering, Colloids Surfaces B Biointerfaces. 122 (2014) 439–446. doi:10.1016/j.colsurfb.2014.04.024.
[91] G.-Z. Jin, J.-H. Park, S.-J. Seo, H.-W. Kim, Dynamic cell culture on porous biopolymer microcarriers in a spinner flask for bone tissue engineering: a feasibility study, Biotechnol. Lett. 36 (2014) 1539–1548. doi:10.1007/s10529-014-1513-6.
[92] D.M.R. Gibbs, C.R.M. Black, J.I. Dawson, R.O.C. Oreffo, A review of hydrogel use in fracture healing and bone regeneration, J. Tissue Eng. Regen. Med. 10 (2016) 187–198.

doi:10.1002/term.1968.
[93] W. Liu, J. Zhan, Y. Su, T. Wu, S. Ramakrishna, S. Liao, et al., Injectable hydrogel incorporating with nanoyarn for bone regeneration, J. Biomater. Sci. Polym. Ed. 25 (2014) 168–180. doi:10.1080/09205063.2013.848326.
[94] Q. Zeng, Y. Han, H. Li, J. Chang, Bioglass/alginate composite hydrogel beads as cell carriers for bone regeneration, J. Biomed. Mater. Res. Part B Appl. Biomater. 102 (2014) 42–51. doi:10.1002/jbm.b.32978.
[95] S. Dhivya, S. Saravanan, T.P. Sastry, N. Selvamurugan, Nanohydroxyapatite-reinforced chitosan composite hydrogel for bone tissue repair in vitro and in vivo, J. Nanobiotechnology. 13 (2015) 40. doi:10.1186/s12951-015-0099-z.
[96] X.H. Liu, J.M. Holzwarth, P.X. Ma, Functionalized Synthetic Biodegradable Polymer Scaffolds for Tissue Engineering, Macromol. Biosci. 12 (2012) 911–919.
[97] X. Liu, Y. Won, P.X. Ma, Porogen-induced surface modification of nano-fibrous poly(l-lactic acid) scaffolds for tissue engineering, Biomaterials. 27 (2006) 3980–3987. doi:10.1016/j.biomaterials.2006.03.008.
[98] X. Liu, Y. Won, P.X. Ma, Surface modification of interconnected porous scaffolds, J. Biomed. Mater. Res. Part A. 74A (2005) 84–91. doi:10.1002/jbm.a.30367.
[99] J.R. García, A.Y. Clark, A.J. García, Integrin-specific hydrogels functionalized with VEGF for vascularization and bone regeneration of critical-size bone defects, J. Biomed. Mater. Res. Part A. 104 (2016) 889–900. doi:10.1002/jbm.a.35626.
[100] M.A. Yassin, K. Mustafa, Z. Xing, Y. Sun, K.E. Fasmer, T. Waag, et al., A Copolymer Scaffold Functionalized with Nanodiamond Particles Enhances Osteogenic Metabolic Activity and Bone Regeneration, Macromol. Biosci. (2017) 1600427. doi:10.1002/mabi.201600427.
[101] S.R. Motamedian, S. Hosseinpour, M.G. Ahsaie, A. Khojasteh, Smart scaffolds in bone tissue engineering : A systematic review of literature, World J. Stem Cells. 7 (2015) 657–668. doi:10.4252/wjsc.v7.i3.657.
[102] N.A. Sears, D.R. Seshadri, P.S. Dhavalikar, E. Cosgriff-Hernandez, A Review of Three-Dimensional Printing in Tissue Engineering., Tissue Eng. Part B. Rev. 22 (2016) 298–310. doi:10.1089/ten.TEB.2015.0464.
[103] M.O. Wang, C.E. Vorwald, M.L. Dreher, E.J. Mott, M.-H. Cheng, A. Cinar, et al., Evaluating 3D-printed biomaterials as scaffolds for vascularized bone tissue engineering., Adv. Mater. 27 (2015) 138–44. doi:10.1002/adma.201403943.
[104] G. Fielding, S. Bose, SiO2 and ZnO dopants in three-dimensionally printed tricalcium phosphate bone tissue engineering scaffolds enhance osteogenesis and angiogenesis in vivo, Acta Biomater. 9 (2013) 9137–9148. doi:10.1016/j.actbio.2013.07.009.
[105] G.D.G. Barabaschi, V. Manoharan, Q. Li, L.E. Bertassoni, Engineering Pre-vascularized Scaffolds for Bone Regeneration, in: Adv. Exp. Med. Biol., 2015: pp. 79–94. doi:10.1007/978-3-319-22345-2_5.
[106] J.P. Temple, D.L. Hutton, B.P. Hung, P.Y. Huri, C.A. Cook, R. Kondragunta, et al., Engineering anatomically shaped vascularized bone grafts with hASCs and 3D-printed PCL scaffolds, J. Biomed. Mater. Res. Part A. 102 (2014) n/a-n/a. doi:10.1002/jbm.a.35107.
[107] C.G. Jeong, A. Atala, 3D Printing and Biofabrication for Load Bearing Tissue Engineering, in: Adv. Exp. Med. Biol., 2015: pp. 3–14. doi:10.1007/978-3-319-22345-2_1.

[108] G. Brunello, S. Sivolella, R. Meneghello, L. Ferroni, C. Gardin, A. Piattelli, et al., Powder-based 3D printing for bone tissue engineering, Biotechnol. Adv. 34 (2016) 740–753. doi:10.1016/j.biotechadv.2016.03.009.
[109] S. Shaunak, B. Dhinsa, W. Khan, The Role of 3D Modelling and Printing in Orthopaedic Tissue Engineering: A Review of the Current Literature, Curr. Stem Cell Res. Ther. 12 (2017) 225–232. doi:10.2174/1574888X11666160429122238.
[110] G. Chen, C. Deng, Y.-P. Li, TGF-β and BMP Signaling in Osteoblast Differentiation and Bone Formation, Int. J. Biol. Sci. 8 (2012) 272–288. doi:10.7150/ijbs.2929.
[111] T. Morimoto, T. Kaito, Y. Matsuo, T. Sugiura, M. Kashii, T. Makino, et al., The bone morphogenetic protein-2/7 heterodimer is a stronger inducer of bone regeneration than the individual homodimers in a rat spinal fusion model, Spine J. 15 (2015) 1379–1390. doi:10.1016/j.spinee.2015.02.034.
[112] P. Sun, J. Wang, Y. Zheng, Y. Fan, Z. Gu, BMP2/7 heterodimer is a stronger inducer of bone regeneration in peri-implant bone defects model than BMP2 or BMP7 homodimer, Dent. Mater. J. 31 (2012) 239–248. doi:10.4012/dmj.2011-191.
[113] K. Sagomonyants, M. Mina, Biphasic effects of FGF2 on odontoblast differentiation involve changes in the BMP and Wnt signaling pathways, Connect. Tissue Res. 55 (2014) 53–56. doi:10.3109/03008207.2014.923867.
[114] K.L. Ong, M.L. Villarraga, E. Lau, L.Y. Carreon, S.M. Kurtz, S.D. Glassman, Off-label use of bone morphogenetic proteins in the United States using administrative data, Spine (Phila. Pa. 1976). 35 (2010) 1794–1800. doi:10.1097/BRS.0b013e3181ecf6e4.
[115] J.D. Smucker, J.M. Rhee, K. Singh, S.T. Yoon, J.G. Heller, Increased Swelling Complications Associated With Off-Label Usage of rhBMP-2 in the Anterior Cervical Spine, Spine (Phila. Pa. 1976). 31 (2006) 2813–2819. doi:10.1097/01.brs.0000245863.52371.c2.
[116] S.A. Mindea, P. Shih, J.K. Song, Recombinant Human Bone Morphogenetic Protein-2-Induced Radiculitis in Elective Minimally Invasive Transforaminal Lumbar Interbody Fusions, Spine (Phila. Pa. 1976). 34 (2009) 1480–1484. doi:10.1097/BRS.0b013e3181a396a1.
[117] H. Deutsch, High-dose bone morphogenetic protein–induced ectopic abdomen bone growth, Spine J. 10 (2010) e1–e4. doi:10.1016/j.spinee.2009.10.016.
[118] N.-F. Chen, Z.A. Smith, E. Stiner, S. Armin, H. Sheikh, L.T. Khoo, Symptomatic ectopic bone formation after off-label use of recombinant human bone morphogenetic protein-2 in transforaminal lumbar interbody fusion., J. Neurosurg. Spine. 12 (2010) 40–6. doi:10.3171/2009.4.SPINE0876.
[119] J.W. McClellan, D.S. Mulconrey, R.J. Forbes, N. Fullmer, Vertebral Bone Resorption After Transforaminal Lumbar Interbody Fusion With Bone Morphogenetic Protein (rhBMP-2), J. Spinal Disord. Tech. 19 (2006) 483–486. doi:10.1097/01.bsd.0000211231.83716.4b.
[120] R. Vaidya, A. Sethi, S. Bartol, M. Jacobson, C. Coe, J.G. Craig, Complications in the Use of rhBMP-2 in PEEK Cages for Interbody Spinal Fusions, J. Spinal Disord. Tech. 21 (2008) 557–562. doi:10.1097/BSD.0b013e31815ea897.
[121] E.J. Carragee, K.A. Mitsunaga, E.L. Hurwitz, G.J. Scuderi, Retrograde ejaculation after anterior lumbar interbody fusion using rhBMP-2: a cohort controlled study, Spine J. 11 (2011) 511–516. doi:10.1016/j.spinee.2011.02.013.
[122] J. Leach, R.G. Bittar, BMP-7 (OP-1®) Safety in anterior cervical fusion surgery, J. Clin.

Neurosci. 16 (2009) 1417–1420. doi:10.1016/j.jocn.2009.02.012.
[123] B. Dohin, N. Dahan-Oliel, F. Fassier, R. Hamdy, Enhancement of Difficult Nonunion in Children with Osteogenic Protein-1 (OP-1): Early Experience, Clin. Orthop. Relat. Res. 467 (2009) 3230–3238. doi:10.1007/s11999-009-0967-7.
[124] W.F. McKay, S.M. Peckham, J.M. Badura, A comprehensive clinical review of recombinant human bone morphogenetic protein-2 (INFUSE® Bone Graft), Int. Orthop. 31 (2007) 729–734. doi:10.1007/s00264-007-0418-6.
[125] G. Wei, Q. Jin, W. V Giannobile, P.X. Ma, The enhancement of osteogenesis by nano-fibrous scaffolds incorporating rhBMP-7 nanospheres, Biomaterials. 28 (2007) 2087–2096. doi:10.1016/j.biomaterials.2006.12.028.
[126] C. V Rahman, D. Ben-David, A. Dhillon, G. Kuhn, T.W. A Gould, R. Müller, et al., Controlled release of BMP-2 from a sintered polymer scaffold enhances bone repair in a mouse calvarial defect model, (2012). doi:10.1002/term.1497.
[127] E.R. Luvizuto, S. Tangl, G. Zanoni, T. Okamoto, C.K. Sonoda, R. Gruber, et al., The effect of BMP-2 on the osteoconductive properties of β-tricalcium phosphate in rat calvaria defects, Biomaterials. 32 (2011) 3855–3861. doi:10.1016/j.biomaterials.2011.01.076.
[128] D.J. Baylink, R.D. Finkelman, S. Mohan, Growth factors to stimulate bone formation, J. Bone Miner. Res. 8 (2009) S565–S572. doi:10.1002/jbmr.5650081326.
[129] N. Hansen-Algenstaedt, C. Joscheck, L. Wolfram, C. Schaefer, I. Müller, A. Böttcher, et al., Sequential changes in vessel formation and micro-vascular function during bone repair, Acta Orthop. 77 (2006) 429–439. doi:10.1080/17453670610046361.
[130] Y. Zhang, N. Cheng, R. Miron, B. Shi, X. Cheng, Delivery of PDGF-B and BMP-7 by mesoporous bioglass/silk fibrin scaffolds for the repair of osteoporotic defects, Biomaterials. 33 (2012) 6698–6708. doi:10.1016/J.BIOMATERIALS.2012.06.021.
[131] D.H.R. Kempen, L. Lu, A. Heijink, T.E. Hefferan, L.B. Creemers, A. Maran, et al., Effect of local sequential VEGF and BMP-2 delivery on ectopic and orthotopic bone regeneration, Biomaterials. 30 (2009) 2816–2825. doi:10.1016/J.BIOMATERIALS.2009.01.031.
[132] G. Gronowicz, E. Jacobs, T. Peng, L. Zhu, M. Hurley, L.T. Kuhn, Calvarial Bone Regeneration Is Enhanced by Sequential Delivery of FGF-2 and BMP-2 from Layer-by-Layer Coatings with a Biomimetic Calcium Phosphate Barrier Layer., Tissue Eng. Part A. 23 (2017) 1490–1501. doi:10.1089/ten.TEA.2017.0111.
[133] L. Lei, S. Wang, H. Wu, W. Ju, J. Peng, A.S.A. Qahtan, et al., Optimization of release pattern of FGF-2 and BMP-2 for osteogenic differentiation of low-population density hMSCs., J. Biomed. Mater. Res. A. 103 (2015) 252–261. doi:10.1002/jbm.a.35168.
[134] M.G. Sabbieti, D. Agas, L. Marchetti, J.D. Coffin, L. Xiao, M.M. Hurley, BMP-2 differentially modulates FGF-2 isoform effects in osteoblasts from newborn transgenic mice., Endocrinology. 154 (2013) 2723–33. doi:10.1210/en.2013-1025.
[135] Y. Nakamura, K. Tensho, H. Nakaya, M. Nawata, T. Okabe, S. Wakitani, Low dose fibroblast growth factor-2 (FGF-2) enhances bone morphogenetic protein-2 (BMP-2)-induced ectopic bone formation in mice., Bone. 36 (2005) 399–407. doi:10.1016/j.bone.2004.11.010.
[136] J. Yin, S. Qiu, B. Shi, X. Xu, Y. Zhao, J. Gao, et al., Controlled release of FGF-2 and BMP-2 in tissue engineered periosteum promotes bone repair in rats, Biomed. Mater. 13 (2018) 025001. doi:10.1088/1748-605X/aa93c0.

[137] H. Wang, Q. Zou, O.C. Boerman, A.W.G. Nijhuis, J.A. Jansen, Y. Li, et al., Combined delivery of BMP-2 and bFGF from nanostructured colloidal gelatin gels and its effect on bone regeneration in vivo, J. Control. Release. 166 (2013) 172–181. doi:10.1016/j.jconrel.2012.12.015.
[138] Y. Tabata, K. Yamada, L. Hong, S. Miyamoto, N. Hashimoto, Y. Ikada, Skull bone regeneration in primates in response to basic fibroblast growth factor, J. Neurosurg. 91 (1999) 851–856. doi:10.3171/jns.1999.91.5.0851.
[139] A. Khojasteh, H. Behnia, N. Naghdi, M. Esmaeelinejad, Z. Alikhassy, M. Stevens, Effects of different growth factors and carriers on bone regeneration: A systematic review, Oral Surg. Oral Med. Oral Pathol. Oral Radiol. 116 (2013) e405–e423. doi:10.1016/j.oooo.2012.01.044.
[140] T. Cheng, C. Yang, N. Weber, H.T. Kim, A.C. Kuo, Fibroblast growth factor 2 enhances the kinetics of mesenchymal stem cell chondrogenesis, Biochem. Biophys. Res. Commun. 426 (2012) 544–550. doi:10.1016/J.BBRC.2012.08.124.
[141] R.A. Cornell, T.J. Musci, D. Kimelman, FGF is a prospective competence factor for early activin-type signals in Xenopus mesoderm induction, Development. 121 (1995).
[142] T.-H. Lee, W.-T. Kim, C.J. Ryu, Y.-J. Jang, Optimization of treatment with recombinant FGF-2 for proliferation and differentiation of human dental stem cells, mesenchymal stem cells, and osteoblasts., Biochem. Cell Biol. (2015) 1–8. doi:10.1139/bcb-2014-0140.
[143] Y.W. Eom, J.-E. Oh, J.I. Lee, S.K. Baik, K.-J. Rhee, H.C. Shin, et al., The role of growth factors in maintenance of stemness in bone marrow-derived mesenchymal stem cells, Biochem. Biophys. Res. Commun. 445 (2014) 16–22. doi:10.1016/J.BBRC.2014.01.084.
[144] L. Eiselleova, K. Matulka, V. Kriz, M. Kunova, Z. Schmidtova, J. Neradil, et al., A Complex Role for FGF-2 in Self-Renewal, Survival, and Adhesion of Human Embryonic Stem Cells, Stem Cells. 27 (2009) 1847–1857. doi:10.1002/stem.128.
[145] A.T. Dudley, R.E. Godin, E.J. Robertson, Interaction between FGF and BMP signaling pathways regulates development of metanephric mesenchyme, Genes Dev. 13 (1999) 1601–1613. doi:10.1101/gad.13.12.1601.
[146] J. Karbanova, T.T.T. Soukup, J. Suchanek, J. Mokry, J. Karbanová, T.T.T. Soukup, et al., Osteogenic differentiation of human dental pulp-derived stem cells under various ex-vivo culture conditions., Acta Medica (Hradec Kralove). 53 (2010) 79–84.
[147] K. Hanada, J.E. Dennis, A.I. Caplan, Stimulatory Effects of Basic Fibroblast Growth Factor and Bone Morphogenetic Protein-2 on Osteogenic Differentiation of Rat Bone Marrow-Derived Mesenchymal Stem Cells, J. Bone Miner. Res. 12 (1997) 1606–1614. doi:10.1359/jbmr.1997.12.10.1606.
[148] E.E. Golub, K. Boesze-Battaglia, The role of alkaline phosphatase in mineralization, Curr Opin Orthop Curr. Opin. Orthop. 18 (2007).
[149] T. Komori, Runx2, A multifunctional transcription factor in skeletal development, J. Cell. Biochem. 87 (2002) 1–8. doi:10.1002/jcb.10276.
[150] X. Zhou, Z. Zhang, J.Q. Feng, V.M. Dusevich, K. Sinha, H. Zhang, et al., Multiple functions of Osterix are required for bone growth and homeostasis in postnatal mice, Proc. Natl. Acad. Sci. 107 (2010) 12919–12924. doi:10.1073/pnas.0912855107.
[151] J. Wei, G. Karsenty, An overview of the metabolic functions of osteocalcin, Rev. Endocr. Metab. Disord. 16 (2015) 93–98. doi:10.1007/s11154-014-9307-7.
[152] R. neves Granito, W. Bouleftour, O. Sabido, C. Lescale, M. Thomas, J.E. Aubin, et al., Absence of Bone Sialoprotein (BSP) Alters Profoundly Hematopoiesis and Upregulates

Osteopontin, J. Cell. Physiol. 230 (2015) 1342–1351. doi:10.1002/jcp.24877.
[153] P.J. Thurner, C.G. Chen, S. Ionova-Martin, L. Sun, A. Harman, A. Porter, et al., Osteopontin deficiency increases bone fragility but preserves bone mass, Bone. 46 (2010) 1564–1573. doi:10.1016/j.bone.2010.02.014.
[154] J. Hu, P.X. Ma, Nano-fibrous tissue engineering scaffolds capable of growth factor delivery, Pharm. Res. 28 (2011) 1273–1281. doi:10.1007/s11095-011-0367-z.
[155] G. Ma, Microencapsulation of protein drugs for drug delivery: strategy, preparation, and applications., J. Control. Release. 193 (2014) 324–340. doi:10.1016/j.jconrel.2014.09.003.
[156] J. Li, L. Xu, H. Liu, Y. Wang, Q. Wang, H. Chen, et al., Biomimetic synthesized nanoporous silica@poly(ethyleneimine)s xerogel as drug carrier: Characteristics and controlled release effect, Int. J. Pharm. 467 (2014) 9–18. doi:10.1016/j.ijpharm.2014.03.045.
[157] W. Mulyasasmita, L. Cai, R.E. Dewi, A. Jha, S.D. Ullmann, R.H. Luong, et al., Avidity-controlled hydrogels for injectable co-delivery of induced pluripotent stem cell-derived endothelial cells and growth factors, J. Control. Release. 191 (2014) 71–81. doi:10.1016/j.jconrel.2014.05.015.
[158] M. Montiel-Herrera, A. Gandini, F.M. Goycoolea, N.E. Jacobsen, J. Lizardi-mendoza, M. Recillas-mota, et al., N-(furfural) chitosan hydrogels based on Diels–Alder cycloadditions and application as microspheres for controlled drug release, Carbohydr. Polym. 128 (2015) 220–227. doi:10.1016/j.carbpol.2015.03.052.
[159] J.L. Holloway, H. Ma, R. Rai, J.A. Burdick, Modulating hydrogel crosslink density and degradation to control bone morphogenetic protein delivery and in vivo bone formation, J. Control. Release. 191 (2014) 63–70. doi:10.1016/j.jconrel.2014.05.053.
[160] J. Zhao, X. Zhao, B. Guo, P.X. Ma, Multi-functional Interpenetrating Polymer Network Hydrogels Based on Methacrylated Alginate for Delivery of Small Molecule Drugs and Sustained Protein Release., Biomacromolecules. (2014). doi:10.1021/bm5006257.
[161] Y. Nagai, L.D. Unsworth, S. Koutsopoulos, S. Zhang, Slow release of molecules in self-assembling peptide nanofiber scaffold, J. Control. Release. 115 (2006) 18–25. doi:10.1016/j.jconrel.2006.06.031.
[162] F. Gelain, L.D. Unsworth, S. Zhang, Slow and sustained release of active cytokines from self-assembling peptide scaffolds, J. Control. Release. 145 (2010) 231–239. doi:10.1016/j.jconrel.2010.04.026.
[163] K. Saiga, T. Furumatsu, A. Yoshida, S. Masuda, S. Takihira, N. Abe, Biochemical and Biophysical Research Communications Combined use of bFGF and GDF-5 enhances the healing of medial collateral ligament injury, Biochem. Biophys. Res. Commun. 402 (2010) 329–334. doi:10.1016/j.bbrc.2010.10.026.
[164] J. Elisseeff, W. Mcintosh, K. Fu, T. Blunk, R. Langer, P. Technology, et al., Controlled-release of IGF-I and TGF-P 1 in a photopolymerizing hydrogel for cartilage tissue engineering, J. Orthop. Res. 19 (2001) 1098–1104.
[165] J.-P. Karam, C. Muscari, L. Sindji, G. Bastiat, F. Bonafè, M. Venier-Julienne, et al., Pharmacologically active microcarriers associated with thermosensitive hydrogel as a growth factor releasing biomimetic 3D scaffold for cardiac tissue-engineering, J. Control. Release. 192 (2014) 82–94. doi:10.1016/j.jconrel.2014.06.052.
[166] D. Dyondi, T.J. Webster, R. Banerjee, A nanoparticulate injectable hydrogel as a tissue engineering scaffold for multiple growth factor delivery for bone regeneration, Int. J. Nanomedicine. 8 (2012) 47–59. doi:10.2147/IJN.S37953.

[167] S. Ansboro, J.S. Hayes, V. Barron, S. Browne, L. Howard, U. Greiser, et al., A chondromimetic microsphere for in situ spatially controlled chondrogenic differentiation of human mesenchymal stem cells, J. Control. Release. 179 (2014) 42–51. doi:10.1016/j.jconrel.2014.01.023.
[168] M.M. Hasani-Sadrabadi, S.P. Hajrezaei, S.H. Emami, G. Bahlakeh, L. Daneshmandi, E. Dashtimoghadam, et al., Enhanced osteogenic differentiation of stem cells via microfluidics synthesized nanoparticles, Nanomedicine Nanotechnology, Biol. Med. (2015) 1–11. doi:10.1016/j.nano.2015.04.005.
[169] E. Quinlan, E.M. Thompson, A. Matsiko, F.J.O. Brien, A. López-noriega, Long-term controlled delivery of rhBMP-2 from collagen – hydroxyapatite scaffolds for superior bone tissue regeneration, J. Control. Release. 207 (2015) 112–119. doi:10.1016/j.jconrel.2015.03.028.
[170] R. Raftery, F.J. O'Brien, S.A. Cryan, Chitosan for gene delivery and orthopedic tissue engineering applications, Molecules. 18 (2013) 5611–5647. doi:10.3390/molecules18055611.
[171] T.C. Santos, B. Hoering, K. Reise, A. Marques, S.S. Silva, J.M. Oliveira, et al., In vivo performance of chitosan/soy-based membranes as wound dressing devices for acute skin wounds, Tissue Eng. Part A. 19 (2012) 860–869. doi:10.1089/ten.TEA.2011.0651.
[172] A. Rahmanian-Schwarz, M. Held, T. Knoeller, S. Stachon, T. Schmidt, H.E. Schaller, et al., In vivo biocompatibility and biodegradation of a novel thin and mechanically stable collagen scaffold, J. Biomed. Mater. Res. - Part A. 102 (2014) 1173–1179. doi:10.1002/jbm.a.34793.
[173] S. Daneshmandi, S.P. Dibazar, S. Fateh, Effects of 3-dimensional culture conditions (collagen-chitosan nano-scaffolds) on maturation of dendritic cells and their capacity to interact with T-lymphocytes., J. Immunotoxicol. (2015) 1–8. doi:10.3109/1547691X.2015.1045636.
[174] R.M. Desai, S.T. Koshy, S.A. Hilderbrand, D.J. Mooney, N.S. Joshi, Versatile click alginate hydrogels crosslinked via tetrazine–norbornene chemistry, Biomaterials. 50 (2015) 30–37. doi:10.1016/j.biomaterials.2015.01.048.
[175] M.P. Lutolf, J.A. Hubbell, Synthetic biomaterials as instructive extracellular microenvironments for morphogenesis in tissue engineering., Nat. Biotechnol. 23 (2005) 47–55. doi:10.1038/nbt1055.
[176] J. Wang, H. Ma, X. Jin, J. Hu, X. Liu, L. Ni, et al., The effect of scaffold architecture on odontogenic differentiation of human dental pulp stem cells, Biomaterials. 32 (2011) 7822–7830. doi:10.1016/j.biotechadv.2011.08.021.Secreted.
[177] Y. Yu, J. Chen, R. Chen, L. Cao, W. Tang, D. Lin, et al., Enhancement of VEGF-Mediated Angiogenesis by 2-N, 6-O-Sulfated Chitosan-Coated Hierarchical PLGA Scaffolds, ACS Appl. Mater. Interfaces. 7 (2015) 9982–9990. doi:10.1021/acsami.5b02324.
[178] L.C. Ionescu, G.C. Lee, B.J. Sennett, J.A. Burdick, R.L. Mauck, An anisotropic nanofiber/microsphere composite with controlled release of biomolecules for fibrous tissue engineering., Biomaterials. 31 (2010) 4113–4120. doi:10.1016/j.biomaterials.2010.01.098.
[179] P.S. Gungor-Ozkerim, T. Balkan, G.T. Kose, A.S. Sarac, F.N. Kok, Incorporation of growth factor loaded microspheres into polymeric electrospun nanofibers for tissue engineering applications., J. Biomed. Mater. Res. A. 102 (2014) 1897–1908.

doi:10.1002/jbm.a.34857.
[180] G. Feng, X. Jin, J. Hu, H. Ma, M.J. Gupte, H. Liu, et al., Effects of hypoxias and scaffold architecture on rabbit mesenchymal stem cell differentiation towards a nucleus pulposus-like phenotype, Biomaterials. 32 (2011) 8182–8189. doi:10.1016/j.biomaterials.2011.07.049.
[181] P.X. Ma, Biomimetic Materials for Tissue Engineering, Adv. Drug Deliv. Rev. 60 (2008) 184–198. doi:10.1016/j.addr.2007.08.041.
[182] Z. Zhang, J. Hu, P.X. Ma, Nanofiber-based delivery of bioactive agents and stem cells to bone sites, Adv. Drug Deliv. Rev. 64 (2012) 1129–1141. doi:10.1016/j.addr.2012.04.008.Nanofiber-based.
[183] M.J. Gupte, P.X. Ma, Nanofibrous Scaffolds for Dental and Craniofacial Applications, J. Dent. Res. 91 (2012) 227–234. doi:10.1177/0022034511417441.
[184] W. Ji, Y. Sun, F. Yang, J.J.P. Jeroen, Bioactive Electrospun Scaffolds Delivering Growth Factors and Genes for Tissue Engineering Applications, Pharm. Res. 28 (2011) 1259–1272. doi:10.1007/s11095-010-0320-6.
[185] J. Pelipenko, P. Kocbek, J. Kristl, Critical attributes of nanofibers : Preparation, drug loading, and tissue regeneration, Int. J. Pharm. 484 (2015) 57–74. doi:10.1016/j.ijpharm.2015.02.043.
[186] E. Amler, E. Filova, M. Buzgo, E. Prosecka, M. Rampichova, A. Necas, et al., Functionalized nanofibers as drug-delivery systems for osteochondral regeneration., Nanomedicine. 9 (2014) 1083–1094. doi:10.2217/nnm.14.57.
[187] J. Joshi, C.R. Kothapalli, Nanofibers based tissue engineering and drug delivery approaches for myocardial regeneration., Curr. Pharm. Des. 21 (2015) 2006–2020.
[188] D. Puppi, X. Zhang, L. Yang, F. Chiellini, X. Sun, E. Chiellini, Nano/microfibrous polymeric constructs loaded with bioactive agents and designed for tissue engineering applications: a review., J. Biomed. Mater. Res. B. Appl. Biomater. 102 (2014) 1562–1579. doi:10.1002/jbm.b.33144.
[189] Y. Mu, F. Wu, Y. Lu, L. Wei, W. Yuan, Progress of electrospun fibers as nerve conduits for neural tissue repair., Nanomedicine. 9 (2014) 1869–1883. doi:10.2217/nnm.14.70.
[190] R. Sridhar, R. Lakshminarayanan, K. Madhaiyan, V. Amutha Barathi, K.H.C. Lim, S. Ramakrishna, Electrosprayed nanoparticles and electrospun nanofibers based on natural materials: applications in tissue regeneration, drug delivery and pharmaceuticals., Chem. Soc. Rev. 44 (2015) 790–814. doi:10.1039/c4cs00226a.
[191] R.B. Montero, X. Vial, D.T. Nguyen, S. Farhand, M. Reardon, S.M. Pham, et al., bFGF-containing electrospun gelatin scaffolds with controlled nano-architectural features for directed angiogenesis., Acta Biomater. 8 (2012) 1778–1791. doi:10.1016/j.actbio.2011.12.008.
[192] H.-J. Lai, C.-H. Kuan, H.-C. Wu, J.-C. Tsai, T.-M. Chen, D.-J. Hsieh, et al., Tailored design of electrospun composite nanofibers with staged release of multiple angiogenic growth factors for chronic wound healing., Acta Biomater. 10 (2014) 4156–4166. doi:10.1016/j.actbio.2014.05.001.
[193] C. Gandhimathi, J.R. Venugopal, V. Bhaarathy, S. Ramakrishna, S.D. Kumar, Biocomposite nanofibrous strategies for the controlled release of biomolecules for skin tissue regeneration., Int. J. Nanomedicine. 9 (2014) 4709–4722. doi:10.2147/IJN.S65335.
[194] L. Tian, M.P. Prabhakaran, X. Ding, D. Kai, S. Ramakrishna, Emulsion electrospun vascular endothelial growth factor encapsulated poly(l-lactic acid-co-ε-caprolactone)

nanofibers for sustained release in cardiac tissue engineering, J. Mater. Sci. 47 (2011) 3272–3281. doi:10.1007/s10853-011-6166-4.
[195] J. Xue, M. He, H. Liu, Y. Niu, A. Crawford, P.D. Coates, et al., Drug loaded homogeneous electrospun PCL/gelatin hybrid nanofiber structures for anti-infective tissue regeneration membranes., Biomaterials. 35 (2014) 9395–9405. doi:10.1016/j.biomaterials.2014.07.060.
[196] L. Li, H. Li, Y. Qian, X. Li, G.K. Singh, L. Zhong, et al., Electrospun poly (varepsilon-caprolactone)/silk fibroin core-sheath nanofibers and their potential applications in tissue engineering and drug release., Int. J. Biol. Macromol. 49 (2011) 223–232. doi:10.1016/j.ijbiomac.2011.04.018.
[197] G. Wei, Q. Jin, W. V. Giannobile, P.X. Ma, Nano-fibrous scaffold for controlled delivery of recombinant human PDGF-BB, J. Control. Release. 112 (2006) 103–110. doi:10.1016/j.jconrel.2006.01.011.
[198] G. Wei, Q. Jin, W. V. Giannobile, P.X. Ma, The enhancement of osteogenesis by nano-fibrous scaffolds incorporating rhBMP-7 nanospheres, Biomaterials. 28 (2007) 2087–2096. doi:10.1016/j.biomaterials.2006.12.028.
[199] Q. Jin, P.X. Ma, W. V. Giannobile, Platelet-Derived Growth Factor Delivery via Nanofibrous Scaffolds for Soft-Tissue Repair, Adv. Skin Wound Care. 1 (2010) 375–381. doi:10.1016/j.biotechadv.2011.08.021.Secreted.
[200] Q. Jin, G. Wei, Z. Lin, J. V Sugai, S.E. Lynch, P.X. Ma, et al., Nanofibrous Scaffolds Incorporating PDGF-BB Microspheres Induce Chemokine Expression and Tissue Neogenesis In Vivo, PLoS One. 3 (2008) 1–9. doi:10.1371/journal.pone.0001729.
[201] K. Feng, H. Sun, M.A. Bradley, E.J. Dupler, W. V. Giannobile, P.X. Ma, Novel antibacterial nanofibrous PLLA scaffolds, J. Control. Release. 146 (2010) 363–369. doi:10.1016/j.jconrel.2010.05.035.
[202] M. Kawalec, A. Sitkowska, M. Sobota, A.L. Sieron, P. Komar, P. Kurcok, Human procollagen type I surface-modified PHB-based non-woven textile scaffolds for cell growth: preparation and short-term biological tests., Biomed. Mater. 9 (2014) 65005. doi:10.1088/1748-6041/9/6/065005.
[203] C.-H. Chen, M.-Y. Lee, V.B.-H. Shyu, Y.-C. Chen, C.-T. Chen, J.-P. Chen, Surface modification of polycaprolactone scaffolds fabricated via selective laser sintering for cartilage tissue engineering., Mater. Sci. Eng. C. Mater. Biol. Appl. 40 (2014) 389–397. doi:10.1016/j.msec.2014.04.029.
[204] Y. Cheng, D. Ramos, P. Lee, D. Liang, X. Yu, S.G. Kumbar, Collagen functionalized bioactive nanofiber matrices for osteogenic differentiation of mesenchymal stem cells: bone tissue engineering., J. Biomed. Nanotechnol. 10 (2014) 287–298.
[205] E. Rosellini, C. Cristallini, G.D. Guerra, N. Barbani, Surface chemical immobilization of bioactive peptides on synthetic polymers for cardiac tissue engineering., J. Biomater. Sci. Polym. Ed. 26 (2015) 515–533. doi:10.1080/09205063.2015.1030991.
[206] M. Mashhadikhan, M. Soleimani, K. Parivar, P. Yaghmaei, ADSCs on PLLA/PCL Hybrid Nanoscaffold and Gelatin Modification: Cytocompatibility and Mechanical Properties., Avicenna J. Med. Biotechnol. 7 (2015) 32–38.
[207] T.H. Kim, J.J. Kim, H.W. Kim, Basic fibroblast growth factor-loaded, mineralized biopolymer-nanofiber scaffold improves adhesion and proliferation of rat mesenchymal stem cells, Biotechnol. Lett. 36 (2014) 383–390. doi:10.1007/s10529-013-1366-4.
[208] M. Tallawi, E. Rosellini, N. Barbani, M.G. Cascone, R. Rai, G. Saint-Pierre, et al.,

Strategies for the chemical and biological functionalization of scaffolds for cardiac tissue engineering: a review., J. R. Soc. Interface. 12 (2015) 20150254. doi:10.1098/rsif.2015.0254.
[209] M. Gu, Y. Liu, T. Chen, F. Du, X. Zhao, C. Xiong, et al., Is graphene a promising nano-material for promoting surface modification of implants or scaffold materials in bone tissue engineering?, Tissue Eng. Part B. Rev. 20 (2014) 477–491. doi:10.1089/ten.TEB.2013.0638.
[210] Z. Shao, X. Zhang, Y. Pi, L. Yin, L. Li, H. Chen, et al., Surface modification on polycaprolactone electrospun mesh and human decalcified bone scaffold with synovium-derived mesenchymal stem cells-affinity peptide for tissue engineering., J. Biomed. Mater. Res. A. 103 (2015) 318–329. doi:10.1002/jbm.a.35177.
[211] H. Pan, Q. Zheng, S. Yang, X. Guo, Effects of functionalization of PLGA-[Asp-PEG]n copolymer surfaces with Arg-Gly-Asp peptides, hydroxyapatite nanoparticles, and BMP-2-derived peptides on cell behavior in vitro., J. Biomed. Mater. Res. A. 102 (2014) 4526–4535. doi:10.1002/jbm.a.35129.
[212] J. Svobodova, V. Proks, O. Karabiyik, A.C. Calikoglu Koyuncu, G. Torun Kose, F. Rypacek, et al., Poly(amino acid)-based fibrous scaffolds modified with surface-pendant peptides for cartilage tissue engineering., J. Tissue Eng. Regen. Med. (2015). doi:10.1002/term.1982.
[213] C. Zanden, N. Hellstrom Erkenstam, T. Padel, J. Wittgenstein, J. Liu, H.G. Kuhn, Stem cell responses to plasma surface modified electrospun polyurethane scaffolds., Nanomedicine. 10 (2014) 949–958. doi:10.1016/j.nano.2014.01.010.
[214] H. Mahjoubi, J.M. Kinsella, M. Murshed, M. Cerruti, Surface modification of poly(D,L-lactic acid) scaffolds for orthopedic applications: a biocompatible, nondestructive route via diazonium chemistry., ACS Appl. Mater. Interfaces. 6 (2014) 9975–9987. doi:10.1021/am502752j.
[215] M. Wang, X. Cheng, W. Zhu, B. Holmes, M. Keidar, L.G. Zhang, Design of biomimetic and bioactive cold plasma-modified nanostructured scaffolds for enhanced osteogenic differentiation of bone marrow-derived mesenchymal stem cells., Tissue Eng. Part A. 20 (2014) 1060–1071. doi:10.1089/ten.TEA.2013.0235.
[216] X. Kong, J. Wang, L. Cao, Y. Yu, C. Liu, Enhanced osteogenesis of bone morphology protein-2 in 2-N,6-O-sulfated chitosan immobilized PLGA scaffolds., Colloids Surf. B. Biointerfaces. 122 (2014) 359–367. doi:10.1016/j.colsurfb.2014.07.012.
[217] B.Y. Kim, J.W. Bae, K.D. Park, Enzymatically in situ shell cross-linked micelles composed of 4-arm PPO-PEO and heparin for controlled dual drug delivery, J. Control. Release. 172 (2013) 535–540. doi:10.1016/j.jconrel.2013.05.003.
[218] S. Knaack, A. Lode, B. Hoyer, A. Rösen-Wolff, A. Gabrielyan, I. Roeder, et al., Heparin modification of a biomimetic bone matrix for controlled release of VEGF, J. Biomed. Mater. Res. - Part A. 102 (2014) 3500–3511. doi:10.1002/jbm.a.35020.
[219] S.E. Sakiyama-Elbert, J.A. Hubbell, Controlled release of nerve growth factor from a heparin-containing fibrin-based cell ingrowth matrix, J. Control. Release. 69 (2000) 149–158.
[220] C.N. Manning, H.M. Kim, S. Sakiyama-elbert, L.M. Galatz, N. Havlioglu, S. Thomopoulos, Sustained Delivery of Transforming Growth Factor Beta Three Enhances Tendon-to-Bone Healing in a Rat Model, J. Orthop. Res. 3 (2011) 1099–1105. doi:10.1002/jor.21301.

[221] N.X. Wang, H.A. von Recum, Affinity-based drug delivery., Macromol. Biosci. 11 (2011) 321–32. doi:10.1002/mabi.201000206.
[222] K. Vulic, M.S. Shoichet, Affinity-based drug delivery systems for tissue repair and regeneration., Biomacromolecules. 15 (2014) 3867–80. doi:10.1021/bm501084u.
[223] T.R. Thatiparti, A.J. Shoffstall, H.A. von Recum, Cyclodextrin-based device coatings for affinity-based release of antibiotics., Biomaterials. 31 (2010) 2335–47. doi:10.1016/j.biomaterials.2009.11.087.
[224] M.R. Battig, B. Soontornworajit, Y. Wang, Programmable release of multiple protein drugs from aptamer-functionalized hydrogels via nucleic acid hybridization., J. Am. Chem. Soc. 134 (2012) 12410–3. doi:10.1021/ja305238a.
[225] C.-C. Lin, K.S. Anseth, Controlling Affinity Binding with Peptide-Functionalized Poly(ethylene glycol) Hydrogels., Adv. Funct. Mater. 19 (2009) 2325. doi:10.1002/adfm.200900107.
[226] N.A. Impellitteri, M.W. Toepke, S.K. Lan Levengood, W.L. Murphy, Specific VEGF sequestering and release using peptide-functionalized hydrogel microspheres., Biomaterials. 33 (2012) 3475–84. doi:10.1016/j.biomaterials.2012.01.032.
[227] G.J. Pettway, J.A. Meganck, A.J. Koh, E.T. Keller, S.A. Goldstein, L.K. McCauley, Parathyroid hormone mediates bone growth through the regulation of osteoblast proliferation and differentiation, Bone. 42 (2008) 806–818. doi:10.1016/j.bone.2007.11.017.
[228] X. Liu, G.J. Pettway, L.K. McCauley, P.X. Ma, Pulsatile release of parathyroid hormone from an implantable delivery system, Biomaterials. 28 (2007) 4124–4131. doi:10.1016/j.biomaterials.2007.05.034.
[229] J. Min, R.D. Braatz, P.T. Hammond, Biomaterials Tunable staged release of therapeutics from layer-by-layer coatings with clay interlayer barrier, Biomaterials. 35 (2014) 2507–2517. doi:10.1016/j.biomaterials.2013.12.009.
[230] F. Reyes-Ortega, A. Cifuentes, G. Rodríguez, M. Rosa, Á. González-gómez, R. Solis, et al., Acta Biomaterialia Bioactive bilayered dressing for compromised epidermal tissue regeneration with sequential activity of complementary agents, Acta Biomater. (2015). doi:10.1016/j.actbio.2015.05.012.
[231] N. Garcia-Honduvilla, A. Cifuentes, J. Bellon, J. Bujan, A. Martinez, The angiogenesis promoter, proadrenomedullin N-terminal 20 peptide (PAMP), improves healing in both normoxic and ischemic wounds either alone or in combination with autologous stem/progenitor cells, Histol Histopathol. 28 (2013) 115–125.
[232] S. Azodi-Deilami, M. Abdouss, D. Kordestani, Synthesis and Characterization of the Magnetic Molecularly Imprinted Polymer Nanoparticles Using N , N -bis Methacryloyl Ethylenediamine as a New Cross-linking Agent for Controlled Release of Meloxicam, Appl Biochem Biotechnol. 172 (2014) 3271–3286. doi:10.1007/s12010-014-0769-6.
[233] A. Cittadini, M.G. Monti, V. Petrillo, G. Esposito, G. Imparato, A. Luciani, et al., Complementary therapeutic effects of dual delivery of insulin-like growth factor-1 and vascular endothelial growth factor by gelatin microspheres in experimental heart failure., Eur. J. Heart Fail. 13 (2011) 1264–1274. doi:10.1093/eurjhf/hfr143.
[234] I. Freeman, S. Cohen, The influence of the sequential delivery of angiogenic factors from affinity-binding alginate scaffolds on vascularization., Biomaterials. 30 (2009) 2122–31. doi:10.1016/j.biomaterials.2008.12.057.
[235] X. Hao, E.A. Silva, A. Mansson-Broberg, K.-H. Grinnemo, A.J. Siddiqui, G. Dellgren, et

al., Angiogenic effects of sequential release of VEGF-A165 and PDGF-BB with alginate hydrogels after myocardial infarction., Cardiovasc. Res. 75 (2007) 178–185. doi:10.1016/j.cardiores.2007.03.028.
[236] H.K. Awada, N.R. Johnson, Y. Wang, Sequential delivery of angiogenic growth factors improves revascularization and heart function after myocardial infarction., J. Control. Release. 207 (2015) 7–17. doi:10.1016/j.jconrel.2015.03.034.
[237] R.R. Chen, E.A. Silva, W.W. Yuen, D.J. Mooney, Spatio-temporal VEGF and PDGF delivery patterns blood vessel formation and maturation., Pharm. Res. 24 (2007) 258–264. doi:10.1007/s11095-006-9173-4.
[238] Q. Sun, E. a. Silva, A. Wang, J.C. Fritton, D.J. Mooney, M.B. Schaffler, et al., Sustained release of multiple growth factors from injectable polymeric system as a novel therapeutic approach towards angiogenesis, Pharm. Res. 27 (2010) 264–271. doi:10.1007/s11095-009-0014-0.
[239] H. Layman, X. Li, E. Nagar, X. Vial, S.M. Pham, F.M. Andreopoulos, Enhanced angiogenic efficacy through controlled and sustained delivery of FGF-2 and G-CSF from fibrin hydrogels containing ionic-albumin microspheres., J. Biomater. Sci. Polym. Ed. 23 (2012) 185–206. doi:10.1163/092050610X546417.
[240] E. Ruvinov, J. Leor, S. Cohen, The promotion of myocardial repair by the sequential delivery of IGF-1 and HGF from an injectable alginate biomaterial in a model of acute myocardial infarction., Biomaterials. 32 (2011) 565–578. doi:10.1016/j.biomaterials.2010.08.097.
[241] J. Sung, P.W. Barone, H. Kong, M.S. Strano, Sequential delivery of dexamethasone and VEGF to control local tissue response for carbon nanotube fluorescence based micro-capillary implantable sensors., Biomaterials. 30 (2009) 622–631. doi:10.1016/j.biomaterials.2008.09.052.
[242] J.E. Tengood, R. Ridenour, R. Brodsky, A.J. Russell, S.R. Little, Sequential delivery of basic fibroblast growth factor and platelet-derived growth factor for angiogenesis., Tissue Eng. Part A. 17 (2011) 1181–1189. doi:10.1089/ten.TEA.2010.0551.
[243] F.B. Basmanav, G.T. Kose, V. Hasirci, Biomaterials Sequential growth factor delivery from complexed microspheres for bone tissue engineering, Biomaterials. 29 (2008) 4195–4204. doi:10.1016/j.biomaterials.2008.07.017.
[244] P. Yilgor, G. Huri, U. Yasar, Y. Ucar, N. Dikmen, N. Hasirci, et al., A biomimetic growth factor delivery strategy for enhanced regeneration of iliac crest defects., Biomed. Mater. 8 (2013) 45009. doi:10.1088/1748-6041/8/4/045009.
[245] P. Yilgor, N. Hasirci, V. Hasirci, Sequential BMP-2/BMP-7 delivery from polyester nanocapsules, J. Biomed. Mater. Res. - Part A. 93 (2010) 528–536. doi:10.1002/jbm.a.32520.
[246] Y. Zou, J.L. Brooks, V. Talwalkar, T.A. Milbrandt, D.A. Puleo, Development of an injectable two-phase drug delivery system for sequential release of antiresorptive and osteogenic drugs., J. Biomed. Mater. Res. B. Appl. Biomater. 100 (2012) 155–162. doi:10.1002/jbm.b.31933.
[247] P.-C. Chang, L.Y. Chong, A.S.M. Dovban, L.P. Lim, J.C. Lim, M.Y.-P. Kuo, et al., Sequential platelet-derived growth factor-simvastatin release promotes dentoalveolar regeneration., Tissue Eng. Part A. 20 (2014) 356–364. doi:10.1089/ten.TEA.2012.0687.
[248] M.S. Kang, J.-H. Kim, R.K. Singh, J.-H. Jang, H.-W. Kim, Therapeutic-designed electrospun bone scaffolds: mesoporous bioactive nanocarriers in hollow fiber composites

to sequentially deliver dual growth factors., Acta Biomater. 16 (2015) 103–16. doi:10.1016/j.actbio.2014.12.028.
[249] D.H.R. Kempen, L. Lu, A. Heijink, T.E. Hefferan, L.B. Creemers, A. Maran, et al., Effect of local sequential VEGF and BMP-2 delivery on ectopic and orthotopic bone regeneration., Biomaterials. 30 (2009) 2816–25. doi:10.1016/j.biomaterials.2009.01.031.
[250] S. Kim, Y. Kang, C.A. Krueger, M. Sen, J.B. Holcomb, D. Chen, et al., Sequential delivery of BMP-2 and IGF-1 using a chitosan gel with gelatin microspheres enhances early osteoblastic differentiation., Acta Biomater. 8 (2012) 1768–1777. doi:10.1016/j.actbio.2012.01.009.
[251] H. Pacheco, K. Vedantham, Aniket, A. Young, I. Marriott, A. El-Ghannam, Tissue engineering scaffold for sequential release of vancomycin and rhBMP2 to treat bone infections., J. Biomed. Mater. Res. A. 102 (2014) 4213–4223. doi:10.1002/jbm.a.35092.
[252] L. Li, G. Zhou, Y. Wang, G. Yang, S. Ding, S. Zhou, Controlled dual delivery of BMP-2 and dexamethasone by nanoparticle-embedded electrospun nanofibers for the efficient repair of critical-sized rat calvarial defect., Biomaterials. 37 (2015) 218–229. doi:10.1016/j.biomaterials.2014.10.015.
[253] K. Song, N.J. Rao, M.L. Chen, Z.J. Huang, Y.G. Cao, Enhanced bone regeneration with sequential delivery of basic fibroblast growth factor and sonic hedgehog, Injury. 42 (2011) 796–802. doi:10.1016/j.injury.2011.02.003.
[254] P. Yilgor, K. Tuzlakoglu, R.L. Reis, N. Hasirci, V. Hasirci, Incorporation of a sequential BMP-2/BMP-7 delivery system into chitosan-based scaffolds for bone tissue engineering., Biomaterials. 30 (2009) 3551–3559. doi:10.1016/j.biomaterials.2009.03.024.
[255] Y. Wang, M.J. Cooke, N. Sachewsky, C.M. Morshead, M.S. Shoichet, Bioengineered sequential growth factor delivery stimulates brain tissue regeneration after stroke., J. Control. Release. 172 (2013) 1–11. doi:10.1016/j.jconrel.2013.07.032.
[256] J.K. Sabo, T.D. Aumann, T.J. Kilpatrick, H.S. Cate, Investigation of sequential growth factor delivery during cuprizone challenge in mice aimed to enhance oligodendrogliogenesis and myelin repair., PLoS One. 8 (2013) e63415. doi:10.1371/journal.pone.0063415.
[257] A. Jaklenec, A. Hinckfuss, B. Bilgen, D.M. Ciombor, R. Aaron, E. Mathiowitz, Sequential release of bioactive IGF-I and TGF-beta 1 from PLGA microsphere-based scaffolds., Biomaterials. 29 (2008) 1518–25. doi:10.1016/j.biomaterials.2007.12.004.
[258] D.M. Nelson, Z. Ma, C.E. Leeson, W.R. Wagner, Extended and sequential delivery of protein from injectable thermoresponsive hydrogels., J. Biomed. Mater. Res. A. 100 (2012) 776–85. doi:10.1002/jbm.a.34015.
[259] G. Tang, H. Zhang, Y. Zhao, X. Li, X. Yuan, M. Wang, Prolonged release from PLGA/HAp scaffolds containing drug-loaded PLGA/gelatin composite microspheres., J. Mater. Sci. Mater. Med. 23 (2012) 419–429. doi:10.1007/s10856-011-4493-2.
[260] A. Ozkizilcik, K. Tuzlakoglu, A new method for the production of gelatin microparticles for controlled protein release from porous polymeric scaffolds, J. Tissue Eng. Regen. Med. 8 (2014) 242–247. doi:10.1002/term.
[261] O. Mirdailami, M. Soleimani, R. Dinarvand, M. Reza, Controlled release of rhEGF and rhbFGF from electrospun scaffolds for skin regeneration (Accepted article), J. Biomed. Mater. Res. - Part A. (2015) 1–38.
[262] Q. Li, G. Zhou, X. Yu, T. Wang, Y. Xi, Z. Tang, Porous deproteinized bovine bone scaffold with three-dimensional localized drug delivery system using chitosan

microspheres Porous deproteinized bovine bone scaffold with three-dimensional localized drug delivery system using chitosan microspheres, Biomed. Eng. Online. 14 (2015) 1–14. doi:10.1186/s12938-015-0028-2.
[263] J.L. Paris, J. Román, M. Manzano, M. V Cabañas, M. Vallet-regí, Tuning dual-drug release from composite scaffolds for bone regeneration, Int. J. Pharm. 486 (2015) 30–37. doi:10.1016/j.ijpharm.2015.03.048.
[264] B.R. Orellana, D. a. Puleo, Tailored sequential drug release from bilayered calcium sulfate composites, Mater. Sci. Eng. C. 43 (2014) 243–252. doi:10.1016/j.msec.2014.06.044.
[265] R.A. Perez, H.W. Kim, Core-shell designed scaffolds for drug delivery and tissue engineering, Acta Biomater. 21 (2015) 2–19. doi:10.1016/j.actbio.2015.03.013.
[266] R.A. Perez, J.-E. Won, J.C. Knowles, H.-W. Kim, Naturally and synthetic smart composite biomaterials for tissue regeneration., Adv. Drug Deliv. Rev. 65 (2013) 471–496. doi:10.1016/j.addr.2012.03.009.
[267] S.C. Sundararaj, M. V. Thomas, T.D. Dziubla, D.A. Puleo, Bioerodible system for sequential release of multiple drugs, Acta Biomater. 10 (2014) 115–125. doi:10.1016/j.actbio.2013.09.031.
[268] S.C. Sundararaj, M. Al-Sabbagh, C.L. Rabek, T.D. Dziubla, M. V Thomas, D.A. Puleo, Comparison of sequential drug release in vitro and in vivo., J. Biomed. Mater. Res. B. Appl. Biomater. (2015). doi:10.1002/jbm.b.33472.
[269] N.A. Dzhoyashvili, S. Shen, Y.A. Rochev, Natural and Synthetic Materials for Self-Renewal, Long-Term Maintenance, and Differentiation of Induced Pluripotent Stem Cells, Adv. Healthc. Mater. (2015) n/a-n/a. doi:10.1002/adhm.201400798.
[270] M. Bouyer, R. Guillot, J. Lavaud, C. Plettinx, C. Olivier, V. Curry, et al., Surface delivery of tunable doses of BMP-2 from an adaptable polymeric scaffold induces volumetric bone regeneration, Biomaterials. 104 (2016) 168–181. doi:10.1016/j.biomaterials.2016.06.001.
[271] C. Laurencin, Y. Khan, S.F. El-Amin, Bone graft substitutes, Expert Rev. Med. Devices. 3 (2006) 49–57. doi:10.1586/17434440.3.1.49.
[272] S.M. Graham, A. Leonidou, N. Aslam-Pervez, A. Hamza, P. Panteliadis, M. Heliotis, et al., Biological therapy of bone defects: the immunology of bone allo-transplantation, Expert Opin. Biol. Ther. 10 (2010) 885–901. doi:10.1517/14712598.2010.481669.
[273] C.-Y. Ang, A.K.-S. Yew, D.K.-J. Tay, S.-L. Chia, S.-J. Yeo, N.-N. Lo, et al., Reducing allograft contamination and disease transmission: intraosseous temperatures of femoral head allografts during autoclaving., Singapore Med. J. 55 (2014) 526–8. doi:10.11622/SMEDJ.2014135.
[274] H. Sun, K. Feng, J. Hu, S. Soker, A. Atala, P.X. Ma, Osteogenic differentiation of human amniotic fluid-derived stem cells induced by bone morphogenetic protein-7 and enhanced by nanofibrous scaffolds, Biomaterials. 31 (2010) 1133–1139. doi:10.1016/j.biomaterials.2009.10.030.
[275] R.E. Guldberg, Spatiotemporal Delivery Strategies for Promoting Musculoskeletal Tissue Regeneration, J. Bone Miner. Res. 24 (2009) 1507–1511. doi:10.1359/jbmr.090801.
[276] N. Saito, N. Murakami, J. Takahashi, H. Horiuchi, H. Ota, H. Kato, et al., Synthetic biodegradable polymers as drug delivery systems for bone morphogenetic proteins, Adv. Drug Deliv. Rev. 57 (2005) 1037–1048. doi:10.1016/J.ADDR.2004.12.016.
[277] K.S. Cahill, J.H. Chi, A. Day, E.B. Claus, Prevalence, Complications, and Hospital Charges Associated With Use of Bone-Morphogenetic Proteins in Spinal Fusion Procedures, JAMA. 302 (2009) 58. doi:10.1001/jama.2009.956.

[278] O.P. Gautschi, S.P. Frey, R. Zellweger, Bone morphogenetic proteins in clinical applications, ANZ J. Surg. 77 (2007) 626–631. doi:10.1111/j.1445-2197.2007.04175.x.
[279] D.C. Wan, J.H. Pomerantz, L.J. Brunet, J.-B. Kim, Y.-F. Chou, B.M. Wu, et al., Noggin suppression enhances in vitro osteogenesis and accelerates in vivo bone formation., J. Biol. Chem. 282 (2007) 26450–9. doi:10.1074/jbc.M703282200.
[280] T.A. Einhorn, Clinical applications of recombinant human BMPs: early experience and future development., J. Bone Joint Surg. Am. 85-A Suppl 3 (2003) 82–8.
[281] K. Takayama, A. Suzuki, T. Manaka, S. Taguchi, Y. Hashimoto, Y. Imai, et al., RNA interference for noggin enhances the biological activity of bone morphogenetic proteins in vivo and in vitro, J. Bone Miner. Metab. 27 (2009) 402–411. doi:10.1007/s00774-009-0054-x.
[282] M. Klagsbrun, The fibroblast growth factor family: structural and biological properties., Prog. Growth Factor Res. 1 (1989) 207–35. doi:10.1016/0955-2235(89)90012-4.
[283] M.A. Dupree, S.R. Pollack, E.M. Levine, C.T. Laurencin, Fibroblast Growth Factor 2 Induced Proliferation in Osteoblasts and Bone Marrow Stromal Cells: A Whole Cell Model, Biophys. J. 91 (2006) 3097–3112. doi:10.1529/BIOPHYSJ.106.087098.
[284] Y. Liu, J.K.Y. Chan, S.-H. Teoh, Review of vascularised bone tissue-engineering strategies with a focus on co-culture systems, J. Tissue Eng. Regen. Med. 9 (2015) 85–105. doi:10.1002/term.1617.
[285] S. Stegen, N. van Gastel, G. Carmeliet, Bringing new life to damaged bone: The importance of angiogenesis in bone repair and regeneration, Bone. 70 (2015) 19–27. doi:10.1016/J.BONE.2014.09.017.
[286] T.H. Kim, F. Browne, J. Upton, J.P. Vacanti, C.A. Vacanti, Enhanced Induction of Engineered Bone with Basic Fibroblast Growth Factor, Tissue Eng. 3 (1997) 303–308. doi:10.1089/ten.1997.3.303.
[287] B.L. Eppley, M. Doucet, D.T. Connolly, J. Feder, Enhancement of angiogenesis by bFGF in mandibular bone graft healing in the rabbit., J. Oral Maxillofac. Surg. 46 (1988) 391–8. doi:10.1016/0278-2391(88)90223-6.
[288] N. Kakudo, K. Kusumoto, A. Kuro, Y. Ogawa, Effect of recombinant human fibroblast growth factor-2 on intramuscular ectopic osteoinduction by recombinant human bone morphogenetic protein-2 in rats, Wound Repair Regen. 14 (2006) 336–342. doi:10.1111/j.1743-6109.2006.00129.x.
[289] E. Tanaka, Y. Ishino, A. Sasaki, T. Hasegawa, M. Watanabe, D.A. Dalla-Bona, et al., Fibroblast Growth Factor-2 Augments Recombinant Human Bone Morphogenetic Protein-2-Induced Osteoinductive Activity, Ann. Biomed. Eng. 34 (2006) 717–725. doi:10.1007/s10439-006-9092-x.
[290] K. Fujimura, K. Bessho, Y. Okubo, K. Kusumoto, N. Segami, T. Iizuka, The effect of fibroblast growth factor-2 on the osteoinductive activity of recombinant human bone morphogenetic protein-2 in rat muscle, Arch. Oral Biol. 47 (2002) 577–584. doi:10.1016/S0003-9969(02)00046-8.
[291] L.T. Kuhn, G. Ou, L. Charles, M.M. Hurley, C.M. Rodner, G. Gronowicz, Fibroblast growth factor-2 and bone morphogenetic protein-2 have a synergistic stimulatory effect on bone formation in cell cultures from elderly mouse and human bone., J. Gerontol. A. Biol. Sci. Med. Sci. 68 (2013) 1170–80. doi:10.1093/gerona/glt018.
[292] L. Xiao, S. Catros, D. Ueno, C. Homer-Bouthiette, L. Charles, L. Kuhn, et al., BMP-2 synergizes the bone healing effect of fgf-2 on calvarial defects in mice, J. Investig. Med.

61 (2013) 668–669.
[293] E.R. Edelman, M.A. Nugent, M.J. Karnovsky, Perivascular and intravenous administration of basic fibroblast growth factor: vascular and solid organ deposition., Proc. Natl. Acad. Sci. U. S. A. 90 (1993) 1513–7. doi:10.1073/PNAS.90.4.1513.
[294] A.L. Ponte, E. Marais, N. Gallay, A. Langonné, B. Delorme, O. Hérault, et al., The In Vitro Migration Capacity of Human Bone Marrow Mesenchymal Stem Cells: Comparison of Chemokine and Growth Factor Chemotactic Activities, Stem Cells. 25 (2007) 1737–1745. doi:10.1634/stemcells.2007-0054.
[295] T. Schwarting, M. Benölken, S. Ruchholtz, M. Frink, P. Lechler, Bone morphogenetic protein-7 enhances bone-tendon integration in a murine in vitro co-culture model, Int. Orthop. 39 (2015) 799–805. doi:10.1007/s00264-015-2688-8.
[296] B. Shen, A. Wei, S. Whittaker, L.A. Williams, H. Tao, D.D.F. Ma, et al., The role of BMP-7 in chondrogenic and osteogenic differentiation of human bone marrow multipotent mesenchymal stromal cells in vitro, J. Cell. Biochem. 109 (2009) n/a-n/a. doi:10.1002/jcb.22412.
[297] M. Hughes-Fulford, C.-F. Li, The role of FGF-2 and BMP-2 in regulation of gene induction, cell proliferation and mineralization., J. Orthop. Surg. Res. 6 (2011) 8. doi:10.1186/1749-799X-6-8.
[298] G. Xiao, D. Jiang, R. Gopalakrishnan, R.T. Franceschi, Fibroblast Growth Factor 2 Induction of the Osteocalcin Gene Requires MAPK Activity and Phosphorylation of the Osteoblast Transcription Factor, Cbfa1/Runx2, J. Biol. Chem. 277 (2002) 36181–36187. doi:10.1074/jbc.M206057200.
[299] J. Hu, K. Feng, X. Liu, P.X. Ma, Chondrogenic and osteogenic differentiations of human bone marrow-derived mesenchymal stem cells on a nanofibrous scaffold with designed pore network., Biomaterials. 30 (2009) 5061–7. doi:10.1016/j.biomaterials.2009.06.013.
[300] K.J. Rambhia, P.X. Ma, Controlled drug release for tissue engineering, J. Control. Release. (2015). doi:10.1016/j.jconrel.2015.08.049.
[301] P. Hauschka, A. Mavrakos, M. Iafrati, S. Doleman, M. Klagsbrun, Growth factors in bone matrix. Isolation of multiple types by affinity chromatography on heparin-Sepharose, J. Biol. Chem. 261 (1986) 12665–12674.
[302] D.M. Ornitz, P.J. Marie, FGF signaling pathways in endochondral and intramembranous bone development and human genetic disease., Genes Dev. 16 (2002) 1446–65. doi:10.1101/gad.990702.
[303] N. Su, M. Jin, L. Chen, Role of FGF/FGFR signaling in skeletal development and homeostasis: Learning from mouse models, Bone Res. 2 (2014) 14003. doi:10.1038/boneres.2014.3.
[304] K.D. Hankenson, K. Gagne, M. Shaughnessy, Extracellular signaling molecules to promote fracture healing and bone regeneration, Adv. Drug Deliv. Rev. 94 (2015) 3–12. doi:10.1016/j.addr.2015.09.008.
[305] P.J. Marie, Fibroblast growth factor signaling controlling osteoblast differentiation, Gene. 316 (2003) 23–32. doi:10.1016/S0378-1119(03)00748-0.
[306] K. Schmidt-Bleek, B.M. Willie, P. Schwabe, P. Seemann, G.N. Duda, BMPs in bone regeneration: Less is more effective, a paradigm-shift., Cytokine Growth Factor Rev. (2015). doi:10.1016/j.cytogfr.2015.11.006.
[307] S. Tamura, H. Kataoka, Y. Matsui, Y. Shionoya, K. Ohno, K.I. Michi, et al., The effects of transplantation of osteoblastic cells with bone morphogenetic protein (BMP)/carrier

complex on bone repair., Bone. 29 (2001) 169–75. doi:10.1016/S8756-3282(01)00498-7.
[308] M. Yamamoto, Y. Tabata, L. Hong, S. Miyamoto, N. Hashimoto, Y. Ikada, Bone regeneration by transforming growth factor β1 released from a biodegradable hydrogel, J. Control. Release. 64 (2000) 133–142. doi:10.1016/S0168-3659(99)00129-7.
[309] J. Sohier, R.E. Haan, K. de Groot, J.M. Bezemer, A novel method to obtain protein release from porous polymer scaffolds: emulsion coating, J. Control. Release. 87 (2003) 57–68. doi:10.1016/S0168-3659(02)00350-4.
[310] K. Whang, T.K. Goldstick, K.E. Healy, A biodegradable polymer scaffold for delivery of osteotropic factors, Biomaterials. 21 (2000) 2545–2551. doi:10.1016/S0142-9612(00)00122-8.
[311] T.P. Richardson, M.C. Peters, A.B. Ennett, D.J. Mooney, Polymeric system for dual growth factor delivery, Nat. Biotechnol. 19 (2001) 1029–1034. doi:10.1038/nbt1101-1029.
[312] A.C.R. Grayson, G. Voskerician, A. Lynn, J.M. Anderson, M.J. Cima, R. Langer, Differential degradation rates in vivo and in vitro of biocompatible poly(lactic acid) and poly(glycolic acid) homo- and co-polymers for a polymeric drug-delivery microchip, J. Biomater. Sci. Polym. Ed. 15 (2004) 1281–1304. doi:10.1163/1568562041959991.
[313] X. Shen, Y. Zhang, Y. Gu, Y. Xu, Y. Liu, B. Li, et al., Sequential and sustained release of SDF-1 and BMP-2 from silk fibroin-nanohydroxyapatite scaffold for the enhancement of bone regeneration, Biomaterials. 106 (2016) 205–216. doi:10.1016/j.biomaterials.2016.08.023.
[314] C. Wan, S.R. Gilbert, Y. Wang, X. Cao, X. Shen, G. Ramaswamy, et al., Activation of the hypoxia-inducible factor-1α pathway accelerates bone regeneration, Proc. Natl. Acad. Sci. 105 (2008) 686 LP – 691.
[315] M.J. Cross, L. Claesson-Welsh, FGF and VEGF function in angiogenesis: signalling pathways, biological responses and therapeutic inhibition, Trends Pharmacol. Sci. 22 (2001) 201–207. doi:10.1016/S0165-6147(00)01676-X.
[316] G. Li, K. Corsi-Payne, B. Zheng, A. Usas, H. Peng, J. Huard, The Dose of Growth Factors Influences the Synergistic Effect of Vascular Endothelial Growth Factor on Bone Morphogenetic Protein 4–Induced Ectopic Bone Formation, Tissue Eng. Part A. 15 (2009) 2123–2133. doi:10.1089/ten.tea.2008.0214.
[317] H. Peng, A. Usas, A. Olshanski, A.M. Ho, B. Gearhart, G.M. Cooper, et al., VEGF Improves, Whereas sFlt1 Inhibits, BMP2-Induced Bone Formation and Bone Healing Through Modulation of Angiogenesis, J. Bone Miner. Res. 20 (2005) 2017–2027. doi:10.1359/JBMR.050708.
[318] E.J. Mackie, Y.A. Ahmed, L. Tatarczuch, K.-S. Chen, M. Mirams, Endochondral ossification: How cartilage is converted into bone in the developing skeleton, Int. J. Biochem. Cell Biol. 40 (2008) 46–62. doi:10.1016/J.BIOCEL.2007.06.009.
[319] M.J. Gupte, W.B. Swanson, J. Hu, X. Jin, H. Ma, Z. Zhang, et al., Pore Size Directs Bone Marrow Stromal Cell Fate and Tissue Regeneration in Nanofibrous Macroporous Scaffolds by Mediating Vascularization, Acta Biomater. (2018). doi:10.1016/J.ACTBIO.2018.10.016.
[320] K. Kadler, D. Holmes, J. Trotter, J. Chapman, Collagen fibril formation, J. Biochem. 316 (1996) 1–11. doi:10.1042/bj3160001.
[321] M. Borden, M. Attawia, Y. Khan, C.T. Laurencin, Tissue engineered microsphere-based matrices for bone repair:: design and evaluation, Biomaterials. 23 (2002) 551–559.

doi:10.1016/S0142-9612(01)00137-5.
[322] T. Jiang, S.P. Nukavarapu, M. Deng, E. Jabbarzadeh, M.D. Kofron, S.B. Doty, et al., Chitosan–poly(lactide-co-glycolide) microsphere-based scaffolds for bone tissue engineering: In vitro degradation and in vivo bone regeneration studies, Acta Biomater. 6 (2010) 3457–3470. doi:10.1016/J.ACTBIO.2010.03.023.
[323] Z. Zhang, R.L. Marson, Z. Ge, S.C. Glotzer, P.X. Ma, Simultaneous Nano- and Microscale Control of Nanofi brous Microspheres Self-Assembled from Star-Shaped Polymers, Adv. Mater. (2015) 1–6. doi:10.1002/adma.201501329.
[324] G. Feng, Z. Zhang, M. Dang, X. Zhang, Y. Doleyres, Y. Song, et al., Injectable nanofibrous spongy microspheres for NR4A1 plasmid DNA transfection to reverse fibrotic degeneration and support disc regeneration, Biomaterials. 131 (2017) 86–97. doi:10.1016/j.biomaterials.2017.03.029.
[325] K.J. Rambhia, P.X. Ma, Biomineralization and Bone Regeneration, in: A. Atala, R. Lanza, T. Mikos (Eds.), Princ. Regen. Med., 3rd ed., ELSEVIER ACADEMIC PRESS, 2018.
[326] K.J. Rambhia, P.X. Ma, Controlled drug release for tissue engineering, J. Control. Release. 219 (2015) 119–128. doi:10.1016/j.jconrel.2015.08.049.
[327] S. Almubarak, H. Nethercott, M. Freeberg, C. Beaudon, A. Jha, W. Jackson, et al., Tissue engineering strategies for promoting vascularized bone regeneration, Bone. 83 (2016) 197–209. doi:10.1016/J.BONE.2015.11.011.
[328] R. Subbiah, M.P. Hwang, S.Y. Van, S.H. Do, H. Park, K. Lee, et al., Osteogenic/Angiogenic Dual Growth Factor Delivery Microcapsules for Regeneration of Vascularized Bone Tissue., Adv. Healthc. Mater. (2015). doi:10.1002/adhm.201500341.
[329] T.C. Santos, T.J. Morton, M. Moritz, S. Pfeifer, K. Reise, A.P. Marques, et al., Vascular endothelial growth factor and fibroblast growth factor-2 incorporation in starch-based bone tissue-engineered constructs promote the in vivo expression of neovascularization mediators., Tissue Eng. Part A. 19 (2013) 834–48. doi:10.1089/ten.TEA.2010.0741.
[330] R. Kuang, Z. Zhang, X. Jin, J. Hu, S. Shi, L. Ni, et al., Nanofibrous spongy microspheres for the delivery of hypoxia-primed human dental pulp stem cells to regenerate vascularized dental pulp, Acta Biomater. 33 (2016) 225–234. doi:10.1016/J.ACTBIO.2016.01.032.
[331] Z. Liu, X. Chen, Z. Zhang, X. Zhang, L. Saunders, Y. Zhou, et al., Nanofibrous Spongy Microspheres to Distinctly Release miRNA and Growth Factors to Enrich Regulatory T Cells and Rescue Periodontal Bone Loss, ACS Nano. (2018) acsnano.7b08976. doi:10.1021/acsnano.7b08976.
[332] X. Liu, P.X. Ma, The nanofibrous architecture of poly(l-lactic acid)-based functional copolymers, Biomaterials. 31 (2010) 259–269. doi:10.1016/j.biomaterials.2009.09.046.
[333] L. Wang, Y. Huang, K. Pan, X. Jiang, C. Liu, Osteogenic responses to different concentrations/ratios of BMP-2 and bFGF in bone formation, Ann. Biomed. Eng. 38 (2010) 77–87. doi:10.1007/s10439-009-9841-8.
[334] X. Zhang, Y. Li, Y.E. Chen, J. Chen, P.X. Ma, Cell-free 3D scaffold with two-stage delivery of miRNA-26a to regenerate critical-sized bone defects, Nat. Commun. 7 (2016) 1–15. doi:10.1038/ncomms10376.
[335] A. Schliermann, J. Nickel, Unraveling the Connection between Fibroblast Growth Factor and Bone Morphogenetic Protein Signaling, Int. J. Mol. Sci. 19 (2018) 3220. doi:10.3390/ijms19103220.
[336] T. Barr, A.J.A. McNamara, G.K.B. Sándor, C.M.L. Clokie, S.A.F. Peel, Comparison of

the osteoinductivity of bioimplants containing recombinant human bone morphogenetic proteins 2 (Infuse) and 7 (OP-1), Oral Surgery, Oral Med. Oral Pathol. Oral Radiol. Endodontology. 109 (2010) 531–540. doi:10.1016/j.tripleo.2009.10.027.
[337] V. Khoshkam, H.L. Chan, G.H. Lin, J. Mailoa, W. V. Giannobile, H.L. Wang, et al., Outcomes of regenerative treatment with rhPDGF-BB and rhFGF-2 for periodontal intra-bony defects: A systematic review and meta-analysis, J. Clin. Periodontol. 42 (2015) 272–280. doi:10.1111/jcpe.12354.
[338] Z. Huang, P.G. Ren, T. Ma, R.L. Smith, S.B. Goodman, Modulating osteogenesis of mesenchymal stem cells by modifying growth factor availability, Cytokine. 51 (2010) 305–310. doi:10.1016/j.cyto.2010.06.002.
[339] H. Kawaguchi, K. Nakamura, Y. Tabata, Y. Ikada, I. Aoyama, J. Anzai, et al., Acceleration of fracture healing in nonhuman primates by fibroblast growth factor-2., J. Clin. Endocrinol. Metab. 86 (2001) 875–880. doi:10.1210/jcem.86.2.7199.
[340] F.M. Chen, M. Zhang, Z.F. Wu, Toward delivery of multiple growth factors in tissue engineering, Biomaterials. 31 (2010) 6279–6308. doi:10.1016/j.biomaterials.2010.04.053.
[341] E.L. Francois, M.J. Yaszemski, Preclinical Bone Repair Models in Regenerative Medicine, Princ. Regen. Med. (2019) 761–767. doi:10.1016/B978-0-12-809880-6.00043-6.
[342] M.A. Scott, B. Levi, A. Askarinam, A. Nguyen, T. Rackohn, K. Ting, et al., Brief review of models of ectopic bone formation., Stem Cells Dev. 21 (2012) 655–67. doi:10.1089/scd.2011.0517.
[343] A. Stavropoulos, A. Sculean, D.D. Bosshardt, D. Buser, B. Klinge, Pre-clinical *in vivo* models for the screening of bone biomaterials for oral/craniofacial indications: focus on small-animal models, Periodontol. 2000. 68 (2015) 55–65. doi:10.1111/prd.12065.
[344] V. Rosen, BMP and BMP Inhibitors in Bone, Ann. N. Y. Acad. Sci. 1068 (2006) 19–25. doi:10.1196/annals.1346.005.
[345] M.V. Bais, N. Wigner, M. Young, R. Toholka, D.T. Graves, E.F. Morgan, et al., BMP2 is essential for post natal osteogenesis but not for recruitment of osteogenic stem cells, Bone. 45 (2009) 254–266. doi:10.1016/J.BONE.2009.04.239.
[346] J.A. Jane, B.A. Dunford, A. Kron, D.D. Pittman, T. Sasaki, J.Z. Li, et al., Ectopic Osteogenesis Using Adenoviral Bone Morphogenetic Protein (BMP)-4 and BMP-6 Gene Transfer, Mol. Ther. 6 (2002) 464–470. doi:10.1006/MTHE.2002.0691.
[347] A.W. James, Review of Signaling Pathways Governing MSC Osteogenic and Adipogenic Differentiation., Scientifica (Cairo). 2013 (2013) 684736. doi:10.1155/2013/684736.
[348] M. Bruderer, R. Richards, M. Alini, M.J. Stoddart, Role and Regulation of RUNX2 in Osteogenesis, Eur. Cells Mater. 28 (2014) 269–286. doi:10.22203/eCM.v028a19.
[349] S.C. Little, M.C. Mullins, Bone morphogenetic protein heterodimers assemble heteromeric type I receptor complexes to pattern the dorsoventral axis, Nat. Cell Biol. 11 (2009) 637–643. doi:10.1038/ncb1870.
[350] S. Kishigami, Y. Mishina, BMP signaling and early embryonic patterning, Cytokine Growth Factor Rev. 16 (2005) 265–278. doi:10.1016/j.cytogfr.2005.04.002.
[351] K. Lavery, P. Swain, D. Falb, M.H. Alaoui-Ismaili, BMP-2/4 and BMP-6/7 differentially utilize cell surface receptors to induce osteoblastic differentiation of human bone marrow-derived mesenchymal stem cells., J. Biol. Chem. 283 (2008) 20948–58. doi:10.1074/jbc.M800850200.
[352] D.M. Ornitz, N. Itoh, The Fibroblast Growth Factor signaling pathway, Wiley Interdiscip.

Rev. Dev. Biol. 4 (2015) 215–266. doi:10.1002/wdev.176.
[353] D.M. Ornitz, FGF signaling in the developing endochondral skeleton, Cytokine Growth Factor Rev. 16 (2005) 205–213. doi:10.1016/j.cytogfr.2005.02.003.
[354] M. Okada-Ban, J.P. Thiery, J. Jouanneau, Fibroblast growth factor-2, Int. J. Biochem. Cell Biol. 32 (2000) 263–267. doi:10.1016/S1357-2725(99)00133-8.
[355] Y. Tabata, K. Yamada, S. Miyamoto, I. Nagata, H. Kikuchi, I. Aoyama, et al., Bone regeneration by basic fibroblast growth factor complexed with biodegradable hydrogels, Biomaterials. 19 (1998) 807–815. doi:10.1016/S0142-9612(98)00233-6.
[356] T. Haque, H. Uludag, R.F. Zernicke, S.R. Winn, W. Sebald, Bone marrow cells from normal and ovariectomized rats respond differently to basic fibroblast growth factor and bone morphogenetic protein 2 treatment in vitro., Tissue Eng. 11 (2005) 634–644. doi:10.1089/ten.2005.11.634.
[357] A. Montero, Y. Okada, M. Tomita, M. Ito, H. Tsurukami, T. Nakamura, et al., Disruption of the fibroblast growth factor-2 gene results in decreased bone mass and bone formation, J. Clin. Invest. 105 (2000) 1085–1093. doi:10.1172/JCI8641.
[358] K.N. Retting, B. Song, B.S. Yoon, K.M. Lyons, BMP canonical Smad signaling through Smad1 and Smad5 is required for endochondral bone formation, Development. 136 (2009) 1093–1104. doi:10.1242/dev.029926.
[359] B.S. Yoon, R. Pogue, D.A. Ovchinnikov, I. Yoshii, Y. Mishina, R.R. Behringer, et al., BMPs regulate multiple aspects of growth-plate chondrogenesis through opposing actions on FGF pathways, Development. (2006). doi:10.1242/dev.02680.
[360] A.M. Moursi, P.L. Winnard, A. V Winnard, J.M. Rubenstrunk, M.P. Mooney, Fibroblast growth factor 2 induces increased calvarial osteoblast proliferation and cranial suture fusion, Cleft Palate-Craniofacial J. 39 (2002) 487–496. doi:10.1597/1545-1569(2002)039<0487:FGFIIC>2.0.CO;2.
[361] T. Jiang, S. Ge, Y.H. Shim, C. Zhang, D. Cao, Bone morphogenetic protein is required for fibroblast growth factor 2-dependent later-stage osteoblastic differentiation in cranial suture cells, Int. J. Clin. Exp. Pathol. 8 (2015) 2946–54.
[362] A.K. Gosain, R.F. Recinos, M. Agresti, A.K. Khanna, TGF-beta1, FGF-2, and receptor mRNA expression in suture mesenchyme and dura versus underlying brain in fusing and nonfusing mouse cranial sutures., Plast. Reconstr. Surg. 113 (2004) 1675–84.
[363] D. Agas, M.G. Sabbieti, L. Marchetti, L. Xiao, M.M. Hurley, FGF-2 enhances Runx-2/Smads nuclear localization in BMP-2 canonical signaling in osteoblasts, J. Cell. Physiol. 228 (2013) 2149–2158. doi:10.1002/jcp.24382.
[364] H. Qi, M. Jin, Y. Duan, X. Du, Y. Zhang, F. Ren, et al., FGFR3 induces degradation of BMP type I receptor to regulate skeletal development, Biochim. Biophys. Acta - Mol. Cell Res. 1843 (2014) 1237–1247. doi:10.1016/j.bbamcr.2014.03.011.
[365] K. Ishida, D.R. Haudenschild, Interactions between FGF21 and BMP-2 in osteogenesis, Biochem. Biophys. Res. Commun. 432 (2013) 677–682. doi:10.1016/j.bbrc.2013.02.019.
[366] F. Liu, F. Fang, H. Yuan, D. Yang, Y. Chen, L. Williams, et al., Suppression of autophagy by FIP200 deletion leads to osteopenia in mice through the inhibition of osteoblast terminal differentiation, J. Bone Miner. Res. 28 (2013) 2414–2430. doi:10.1002/jbmr.1971.
[367] H. Pan, H. Zhang, P. Abraham, Y. Komatsu, K. Lyons, V. Kaartinen, et al., BmpR1A is a major type 1 BMP receptor for BMP-Smad signaling during skull development, Dev. Biol. 429 (2017) 260–270. doi:10.1016/J.YDBIO.2017.06.020.

[368] H. Sun, K. Dai, T. Tang, X. Zhang, Regulation of osteoblast differentiation by slit2 in osteoblastic cells., Cells. Tissues. Organs. 190 (2009) 69–80. doi:10.1159/000178020.
[369] E. Williams, A.N. Bullock, Structural basis for the potent and selective binding of LDN-212854 to the BMP receptor kinase ALK2, Bone. 109 (2018) 251–258. doi:10.1016/J.BONE.2017.09.004.
[370] T. Song, W. Wang, J. Xu, D. Zhao, Q. Dong, L. Li, et al., Fibroblast growth factor 2 inhibits bone morphogenetic protein 9-induced osteogenic differentiation of mesenchymal stem cells by repressing Smads signaling and subsequently reducing Smads dependent up-regulation of ALK1 and ALK2, Int. J. Biochem. Cell Biol. 45 (2013) 1639–1646. doi:10.1016/J.BIOCEL.2013.05.005.
[371] M. Wu, G. Chen, Y.P. Li, TGF-β and BMP signaling in osteoblast, skeletal development, and bone formation, homeostasis and disease, Bone Res. 4 (2016) 16009. doi:10.1038/boneres.2016.9.
[372] J.H. Boergermann, J. Kopf, P.B. Yu, P. Knaus, Dorsomorphin and LDN-193189 inhibit BMP-mediated Smad, p38 and Akt signalling in C2C12 cells, Int. J. Biochem. Cell Biol. 42 (2010) 1802–1807. doi:10.1016/j.biocel.2010.07.018.
[373] D. Horbelt, J.H. Boergermann, A. Chaikuad, I. Alfano, E. Williams, I. Lukonin, et al., Small molecules dorsomorphin and LDN-193189 inhibit myostatin/GDF8 signaling and promote functional myoblast differentiation., J. Biol. Chem. 290 (2015) 3390–404. doi:10.1074/jbc.M114.604397.
[374] J. Hao, J.N. Ho, J.A. Lewis, K.A. Karim, R. Nathan Daniels, P.R. Gentry, et al., In Vivo StructureActivity Relationship Study of Dorsomorphin Analogues Identifies Selective VEGF and BMP Inhibitors, Veterans Adm. TVHS. (2010) 37212. doi:10.1021/cb9002865.
[375] G. Murakami, Cooperative Inhibition of Bone Morphogenetic Protein Signaling by Smurf1 and Inhibitory Smads, Mol. Biol. Cell. 14 (2003) 2809–2817. doi:10.1091/mbc.e02-07-0441.
[376] Y. Zhang, C. Chang, D.J. Gehling, A. Hemmati-Brivanlou, R. Derynck, Regulation of Smad degradation and activity by Smurf2, an E3 ubiquitin ligase, Proc. Natl. Acad. Sci. 98 (2002) 974–979. doi:10.1073/pnas.98.3.974.
[377] R.N. Wang, J. Green, Z. Wang, Y. Deng, M. Qiao, M. Peabody, et al., Bone Morphogenetic Protein (BMP) signaling in development and human diseases, Genes Dis. 1 (2014) 87–105. doi:10.1016/J.GENDIS.2014.07.005.
[378] M. Shaifur Rahman, N. Akhtar, H. Mohammad Jamil, R. Suvra Banik, S.M. Asaduzzaman, TGF-b/BMP signaling and other molecular events: regulation of osteoblastogenesis and bone formation, Bone Res. 3 (2015). doi:10.1038/boneres.2015.5.
[379] A. Fakhry, C. Ratisoontorn, C. Vedhachalam, I. Salhab, E. Koyama, P. Leboy, et al., Effects of FGF-2/-9 in calvarial bone cell cultures: Differentiation stage-dependent mitogenic effect, inverse regulation of BMP-2 and noggin, and enhancement of osteogenic potential, Bone. 36 (2005) 254–266. doi:10.1016/j.bone.2004.10.003.
[380] G. Sapkota, C. Alarcón, F.M. Spagnoli, A.H. Brivanlou, J. Massagué, Balancing BMP Signaling through Integrated Inputs into the Smad1 Linker, Mol. Cell. 25 (2007) 441–454. doi:10.1016/j.molcel.2007.01.006.
[381] M. Courcelles, C. Fremin, L. Voisin, S. Lemieux, S. Meloche, P. Thibault, Phosphoproteome dynamics reveal novel ERK1/2 MAP kinase substrates with broad spectrum of functions, Mol. Syst. Biol. 9 (2014) 669–669. doi:10.1038/msb.2013.25.

[382] Z. Lu, S. Xu, ERK1/2 MAP kinases in cell survival and apoptosis, IUBMB Life. 58 (2006) 621–631. doi:10.1080/15216540600957438.
[383] L.F. Mendes, H. Katagiri, W.L. Tam, Y.C. Chai, L. Geris, S.J. Roberts, et al., Advancing osteochondral tissue engineering: bone morphogenetic protein, transforming growth factor, and fibroblast growth factor signaling drive ordered differentiation of periosteal cells resulting in stable cartilage and bone formation in vivo, Stem Cell Res. Ther. 9 (2018) 42. doi:10.1186/s13287-018-0787-3.
[384] Y. Li, S.-K. Chen, L. Li, L. Qin, X.-L. Wang, Y.-X. Lai, Bone defect animal models for testing efficacy of bone substitute biomaterials, J. Orthop. Transl. 3 (2015) 95–104. doi:10.1016/J.JOT.2015.05.002.
[385] Y. Fei, L. Xiao, T. Doetschman, D.J. Coffin, M.M. Hurley, Fibroblast growth factor 2 stimulation of osteoblast differentiation and bone formation is mediated by modulation of the Wnt signaling pathway., J. Biol. Chem. 286 (2011) 40575–83. doi:10.1074/jbc.M111.274910.